Development of Chemical Sensors for Rapid Identification of Amphetamine-Related New Psychoactive Substances

Kathryn Emily Kellett

Submitted to the University of Hertfordshire in partial fulfilment of the requirements of the degree of Doctor of Philosophy.

Supervisors: Dr. Jacqueline L. Stair, Dr. Suzanne Fergus, Dr. Stewart B. Kirton and Prof. Andrew J. Hutt

Department of Pharmacy, School of Life and Medical Sciences, University of Hertfordshire

November 2016

Abstract

A molecular receptor for mephedrone, an amphetamine-like NPS, was developed using host-guest chemistry and pharmacophoric design. The in-field detection of new psychoactive substances (NPS) is an area that has garnered considerable attention in the last few years. With the continuously expanding number of NPS on the market, traditional detection mechanisms lack the selectivity needed. In this project a new methodology has been developed for the design of host molecules for use in in-field detection, based on biomimetic design.

To understand what a sensory molecular needs to be selective against, GC-MS and HPLC analysis were employed to identify and quantify thirteen aminoindane internet samples. It was found that the composition of internet samples varies greatly in terms of concentration of active ingredient, with a range of 17-95 % w/w of active ingredient identified. It was also found that caffeine was the most common cutting agent with a range of 27.7-30.2 % w/w identified. This highlights the need for both selectivity and sensitivity in detection mechanisms.

Using the principles of biomimetic design, a methodology for the treatment of protein-ligand interactions was developed. Protein-ligand binding data collected from the Protein Databank was analysed for mephedrone related structures and common cutting agents, identified through aminoindane internet sample analysis and literature sources. From this work a three-point pharmacophoric model was developed, upon which two host molecules were considered, macrocyclic calixarenes and acyclic anthraquinones. Both contained the three binding interactions deduced from the pharmacophore design; two π-stacking interactions and one hydrogen bond acceptor.

The final host molecule taken forward for testing was 1,8-dibenzylthiourea anthracene (Probe 1). The binding affinity of Probe 1 to mephedrone was tested using ^{1}H-NMR. An estimated association constant of 104 M^{-1} was calculated, with a 1:1 binding stoichiometry. Along with ESI-MS and DFT calculations, it was found that mephedrone binds to Probe 1 in a concerted fashion with a three-point binding geometry, with two hydrogen bonds and one π-stacking interaction. A modest optical response using fluorescence spectroscopy was also observed between mephedrone and Probe 1 at high molar concentrations. A more pronounced response was observed upon addition of high molar concentrations of flephedrone.

^{1}H-NMR showed that Probe 1 selectively bound mephedrone over methamphetamine as well as the four most common cutting agents identified from literature: lidocaine, caffeine, paracetamol and benzocaine, which have been shown to cause false positives in previous studies. Probe 1 showed significant selectivity for the β-ketoamine arrangement. This is supported by the systematic analysis

of mephedrone, methamphetamine, mephedrone precursor and flephedrone. This is the first time this has been achieved using host-guest chemistry. A protocol was developed to successfully detect mephedrone *via* Probe 1 using NMR spectroscopy in a simulated street sample containing two of the most common cutting agents, benzocaine and caffeine. To further aid future design of small host molecules a methodology for the *in silico* analysis of small molecule host-guest binding using metadynamics was explored. Solvent interactions with the host and guest molecules were observed, highlighting the importance of solvent choice in binding studies. Metadynamics shows potential to be used in further work for improving the approach in which host molecules are designed in future.

Acknowledgements

First and foremost I must thank my principal supervisor, Dr. Jacqueline Stair. It goes without saying that without her I could never have got through the last 5 years. She has gone above and beyond the role of a supervisor time and time again, and I will be forever grateful for her guidance and support. I would also like thank the rest of my supervisory team, Dr. Suzanne Fergus, Dr. Stewart Kirton and Prof. Andrew Hutt for their patience and help throughout my PhD.

To Prof. Karl Wallace, who welcomed me into his group at USM, I am very grateful for your time and support. I learnt so much from you in such a short time, which has helped me find new areas of chemistry that I truly love. I would also like to thank the Winston Churchill Memorial Trust for giving me this opportunity to learn. Dr. Hugh Broome I am incredibly grateful for your friendship and support during and after my time at USM, and I look forward to the many adventures still to come.

To all the chemistry lecturers at UH, thank you for always allowing me to call on your expertise. In particular Dr. Ute Gerhard for her guidance on everything NMR! Also Prof. Mire Zloh for all your help with the metadynamics and inspiring me every day, and for all the DFT calculations you performed for the sensor work.

I would like to thank all my colleagues at UH who have made my experience one to remember; in particular my office mates Andy, Hassan, Amira and Dhruv.

I would like to thank all the technical staff at UH. Especially Dr. Mark Scott, without whom none of the instruments would work, and I would have no data. You have continuously gone above and beyond your role and I am very grateful for all you have taught me.

I would like to thank all my family; Mum, Dad, Jenny, Naomi and Mick for your unwavering support for all my crazy plans. To Dad, thank you for everything. To my extremely patient Fiancé Ruan, thank you for your patience, support, love and the countless Ryanair flights.

List of Abbreviations

Abbreviation	Definition
ΔE	Change in Energy
2-AI	2-Aminoindane
5-IAI	5-Iodo-2-aminoindane
Å	Angstroms
ACMD	Advisory Council for the Misuse of Drugs
ACN	Acetonitrile
ADHD	Attention deficit hyperactivity disorder
$AlCl_3$	Aluminium Chloride
BZP	Benzylpiperazine
CAS	Chemical Abstract Service
$CDCl_3$	Chloroform
Cl	Chloride
CNS	Central nervous system
CPU	Central processing unit
CV	Collective Variable
DCM	Dichloromethane
DFT	Density functional theory
DMSO	Dimethyl sulfoxide
DXM	Dextromethorphan
EI	Electron ionisation
EMCDDA	European Monitoring Centre for Drugs and Drug Addiction
eq.	Equivalence

ESI	Electrospray ionisation
EtOAc	Ethyl acetate
FT-IR	Fourier transform infrared spectroscopy
GC-MS	Gas chromatography mass spectrometry
HCl	Hydrochloride
HOMO	Highest occupied molecular orbital
HPLC	High performance liquid chromatography
Hz	Hertz
ICH	International Council for Harmonisation
ICP-AES	Inductively coupled plasma atomic emission spectroscopy
ICP-MS	Inductively coupled plasma mass spectrometry
ICT	Intermolecular charge transfer
IPA	Isopropyl alcohol
IR	Infrared
K	Kelvin
K_a	Association constant
K_d	Dissociation constant
LC-MS	Liquid chromatography mass spectrometry
LC-MS-MS	Liquid chromatography tandem mass spectrometry
LGC	Laboratory of the Government Chemist
LLOQ	Lower limit of quantification
LOD	Limit of detection
LOQ	Limit of quantification
LSD	Lysergic acid diethylamide

LUMO	Lowest unoccupied molecular orbital
m/z	Mass to charge ratio
MCMM	Monte Carlo molecular modelling
MDAI	5,6-Methylenedioxy-2-aminoindane
MDMA	3,4-Methylenedioxymethamphetamine
$MgSO_4$	Magnesium Sulphate
MMAI	5-Methoxy-6-methyl-2-aminoidane
m.p.	Melting Point
MPA	Methiopropamine
MS	Mass spectrometry
MXE	Methoxetamine
NIST	National Institute of Standards and Technology
NMR	Nuclear magnetic resonance
NPS	New psychoactive substance
OPLS	Optimized Potentials for Liquid Simulations
Pd/C	Palladium on Carbon
PDA	Photodiode array
PDB	Protein DataBank
pKa	Acid dissociation constant
ppm	Parts per Million
PRCG	Polak-Ribière conjugate gradient
PTFE	Polytetrafluoroethylene
RMS	Root mean square
RMSD	Root mean square deviation

SA	Simulated annealing
SWGDRUG	Scientific Working Group Drug
TBACl	Tetrabutylammonium chloride
TLC	Thin layer chromatography
TMS	Tetramethylsilane
UNODC	United Nations Office on Drugs and Crime
UV/Vis	Ultraviolet and visible spectroscopy
λ_{max}	Maximum wavelength
λ_{ex}	Excitation wavelength
mg	Milligrams
μg	Microgram

Table of Contents

Table of Figures

Table of Tables

Chapter 1   General Introduction

1.1   History of Psychoactive Substances

Psychoactive drugs have the ability to change people's states of consciousness making them popular for use recreationally, with reports of abuse from as far back as 1300 BC[1]. This is despite the known dangers associated with psychoactive drug use. Psychoactive substances are defined by the World Health Organisation (WHO) as "any substance that, when taken in or administered into one's system, affect mental processes, e.g. cognition or affect"[2]. The total annual worldwide market for medicines is approximately $250 billion, yet the market for recreational drugs is estimated to be at least ten times greater[3]. The culture of taking psychoactive drugs is not new, what changes are the drugs that are abused, and the effects that they have on the body[4]. Psychoactive substances are utilised in the area of psychotherapy and mental illness, but despite in-depth research into their clinical uses from leading scientists such as Alexander Shulgin, these substances are primarily used as "party drugs"[5].

Psychoactive drugs fall into three categories based on their pharmacological effects: stimulants such as amphetamine and caffeine, hallucinogens such as lysergic acid diethylamide (LSD) and psilocybin, and depressants for example benzodiazepines and opioids (Table 1.1). However, it is not uncommon for these drugs to fall into multiple categories. These different effects occur depending on how the drug interacts with the body, especially their effects on the central nervous system (CNS). Psychoactive drugs pass through the blood brain barrier and compete with natural substrates such as serotonin, dopamine and noradrenaline acting primarily on the monoamine transporter proteins.

Table 1.1 - Timeline of common drugs of abuse and their relative pharmacodynamic effects.

Drug Of Abuse	Abuse First Reported	Effect
Cocaine	1884	Stimulant
Marijuana	1920	Depressant
Lysergic acid diethylamide (LSD)	1943	Hallucinogen
Amphetamine	1960	Stimulant
3,4-Methylenedioxymethamphetamine (MDMA)	1970	Stimulant
Crack Cocaine	1985	Stimulant
Diacetylmorphine (Heroin)	1890	Depressant
Mephedrone	2003	Stimulant
Aminoindanes	2005	Stimulant
Methylenedioxypyrovalerone (MDPV)	2014	Stimulant

LSD is seen as the first synthetic psychoactive drug that was abused on a large scale. Its psychedelic effects were discovered inadvertently by Albert Hoffman in 1943 while researching into medically useful ergot alkaloid derivatives. This brought about its use in psychiatry[6]. LSD started to become prevalent on the recreational drug scene in the 1960s; it was seen as the drug at the centre of the counterculture. It quickly became illegal in both the UK and the USA instigating the constant search for alternative legal forms that would induce similar effects. A number of drugs have followed on from LSD, including 3,4-methylenedioxy-*N*-methylamphetamine also known as MDMA (Figure 1.1).
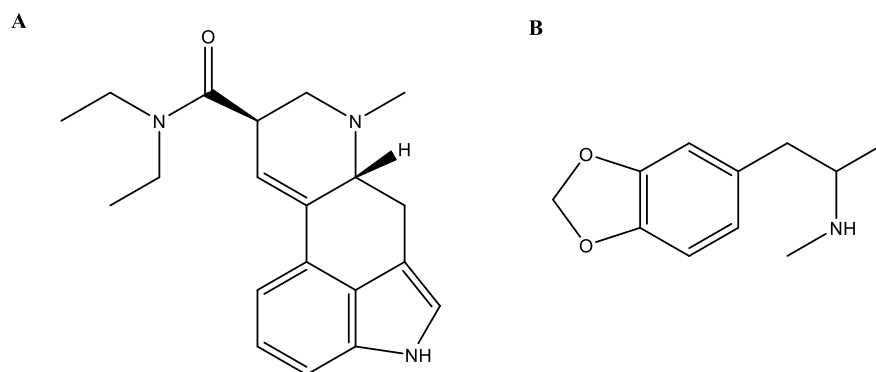
Figure 1.1 - Chemical structure of A. lysergic acid diethylamide (LSD) and B. 3,4-methylenedioxy-*N*-methamphetamine (MDMA).

The emergence of new recreational drugs has increased rapidly over the last 10 years, which has led to the term "new psychoactive substances" or NPS. These are compounds that are chemically altered from government controlled substances to sidestep regulations, yet still have potent effects that rival banned substances. NPS are primarily abused for their stimulant and hallucinogenic effects and are designed to mimic the effects of popular drugs of abuse such as MDMA and LSD. Among other effects

these drugs are seen to induce extreme mood lifts accompanying euphoria and a subjective alteration of consciousness[7,8]. NPS have also been found to improve self-confidence[9]. NPS contain chemicals that in most cases have not been tested in man, and the pharmacology behind such drugs is relatively unknown. Users can therefore not be certain what they are taking and what the effects might be.

The rapidly expanding NPS market has primarily been blamed on the internet and the ease of acquiring them[10]. The speed at which new drugs are introduced is an ever expanding problem[11]. The internet plays a pivotal role in the marketing of these drugs, especially to the younger population[12]. In May 2016 the UK government made the decision to impose a blanket ban on all psychoactive substances. Under this classification importation, exportation, production and supply are prohibited without lawful authority[13]. The psychoactive substances act was brought in to protect the public, especially young people and target suppliers and manufacturers who advertise harmful substances as legal and safe.

1.1.1 Emergence of New Psychoactive Substances (NPS)

The main classes of NPS that are monitored by the European Monitoring Council for Drug and Drug Addition (EMCDDA) include: synthetic cannabinoids, synthetic cathinones, phenethylamines, opioids, tryptamines and benzodiazepines (Figure 1.2). These groups of compounds all have one thing in common, they are relatively small amine-containing, hydrophobic molecules, which have the ability to cross the blood-brain barrier and exhibit psychoactive effects in the CNS. While many fall into multiple categories they can generally be classed as stimulants, inhibitors or hallucinogenic substances[14].
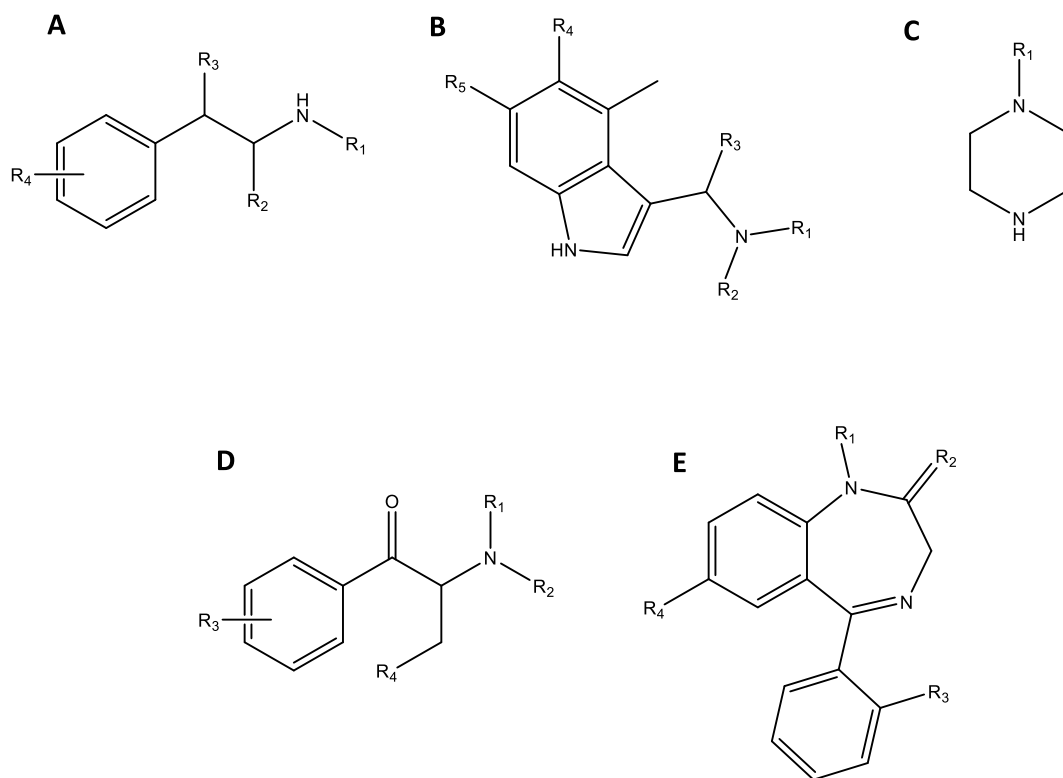
Figure 1.2 - Generic structure for A. phenethylamines, B. tryptamines, C. piperazines, D. cathinones and E. benzodiazepines. Cannabinoids are not classed based on their structure but their action on cannabinoid receptor type one (CB1), and therefore no generic structure of this class is available.

These products are sold under attractive names such as 'sparkle' (mephedrone) and 'ivory wave' (desoxypipradrol) and are presented in striking packaging. They are also relatively cheap in comparison to the illegal alternatives, such as MDMA. A survey conducted in 2010 showed that the average price of a NPS in the UK was £9.69 per tablet[7], compared to between £30-50 for ecstasy[15].

It was reported in 2015 that there were over 560 NPS being monitored by the EMCDDA, 380 of which have come onto the market in the last 5 years (Figure 1.3)[10]. One changing aspect over the years is the class of NPS that are being abused, and to what extent. This highlights the changeability of the NPS market. The UK government has been failing to keep up with the growing number of NPS inundating the market and therefore, have been failing to effectively control these substances, or understand their potential health implications[16]. While new NPS come onto the market continuously, the number of classes does not change as readily, with most falling into one of the already established classes.
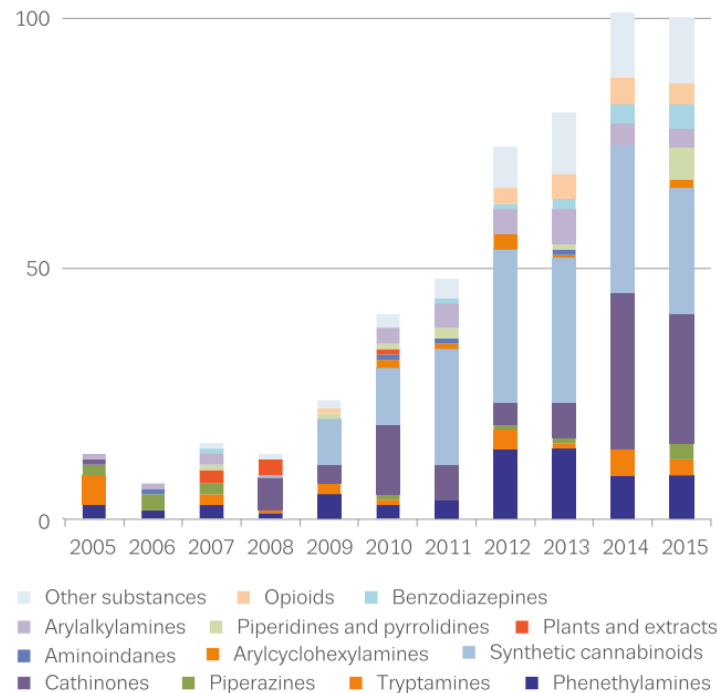
Figure 1.3 - The number of new psychoactive substances notified from 2005–15 in Europe[10].

Stimulant drugs with amphetamine-like structures have long been a popular choice as recreational drugs. This is due to the complex pharmacological profile that is observed from these structures. Figure 1.3 shows thirteen different classes of NPS monitored by the EMCDDA since 2005. Of which, four are deemed to have amphetamine-like structures, including: arylalkylamines, aminoindanes, cathinones and phenethylamines. Of these, cathinones have remained the most prevalent since 2008.

Based on United Nations Office on Drugs and Crime (UNODC) reports, cathinones are the second highest NPS class at 15 % of the reported values. The "original NPS" is often reported to be mephedrone, a synthetic cathinone that was developed as the legal alternative to methamphetamine[17]. Cathinones have been found to exhibit similar psychoactive effects to the amphetamine class. Since their introduction onto the 'drugs market' in 2007 the popularity of cathinones has remained stable, with a peak seen in 2014; by 2015 there were 103 cathinone analogues on the market[18]. Their popularity is thought to have risen due to law enforcement agencies increasing controls over MDMA as well as its precursors. This change lead to an overall decrease in the amount of MDMA available, which subsequently increased the market price. Therefore, paving the way for a cheaper alternative with the same stimulant effects.

Figure 1.3 also shows the emergence of another amphetamine-like class, the aminoindanes, which came onto the market in 2010, with their popularity peaking in 2011, the same year the cathinones were controlled, with 12 main seizures reported in the UK[19]. Aminoindanes were developed to try and

mimic the action of amphetamine, while sufficiently differing in their chemical structure so as to remain uncontrolled. They were advertised as the next legal alternative to mephedrone and became popular as a way to circumvent the new legislation with legal analogues, but with the same reported stimulant effects; showing potent effects on serotonin release and reuptake.

1.1.2 Cathinones

Cathinones are related to the parent compound and ring substituted analogues of the psychoactive cathinone (Figure 1.4), an alkaloid derived from the Khat plant. In the 2000s, many synthetic cathinones received renewed popularity as new drugs of abuse, due to their amphetamine and cocaine like effects[20], cathinones have remained popular ever since their introduction onto the drug scene in 2008.
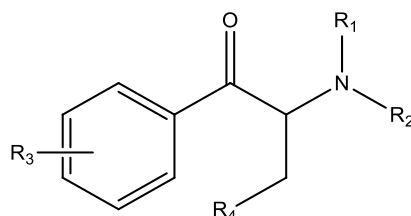
Figure 1.4 - Generic structure for cathinone analogues where R_1= H or alkyl group; R_2= H or alkyl; R_3= H, alkyl or alkoxy; R_4= alkyl group, as stated in the Misuse of Drugs Act 1971[21]. For the natural product cathinone R_1, R_2, R_3 and R_4 = H.

The most prevalent of the natural cathinones present in Khat is cathinone. Cathinone is a beta-keto analogue of amphetamine (Figure 1.4) and is very labile in the presence of oxygen and quickly decomposes to cathine once isolated[22]. This has brought about the production of synthetic cathinones, which as salts are considerably more stable in a solid crystalline state. It is from this that the emergence of substituted cathinone analogues arose. As of 2015, the UNODC has reported that there are now over 103 synthetic cathinones available[10]. In the UK the number of synthetic cathinone seizures has increased 60-fold between 2008 and 2013[23]. This is also reflected in the fatality statistics with just nine deaths from cathinone use in 2007 compared to 60 deaths in 2013[24].

Mephedrone is one of the most popular synthetic cathinones[10] (Figure 1.5). Currently, there are 46 countries that are reporting mephedrone use, thereby establishing its presence worldwide on the illicit drug market. Since 2012 the single most commonly named NPS in drug-related deaths is mephedrone. With the number of deaths involving mephedrone doubling from 22 in 2014 to 44 in 2015, the highest on record[25].
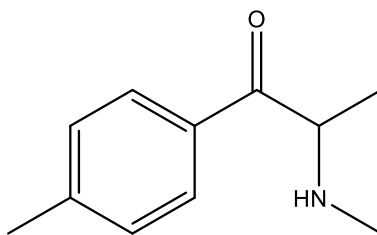
Figure 1.5 - Chemical structure of *para*-methylmethcathinone (mephedrone).

The pharmacology of mephedrone was originally associated with drugs such as amphetamine and MDMA in relation to its behavioural effects[26], including stimulated mood and an increased sex drive. It also mimics the negative side effects of these drugs such as increased heart rate and body temperature, full body convulsions and addictiveness. These effects are associated with mephedrone acting on a number of different monoamine transporters. It was found to be a potent inhibitor of the uptake of all three monoamine transporters: dopamine, serotonin and noradrenaline, comparable to the potency of MDMA[27]. This interaction with the monoamine transporters causes a release of dopamine and 5-HT, with 5-HT release being greater than that of dopamine[28]. The release of dopamine has been found to link the psychostimulant effects of mephedrone to MDMA. Interestingly mephedrone has been shown to substitute for cocaine in drug discrimination studies on rats, which could explain its levels of dependence reported, due to their similar serotonergic responses[27]. The complex pharmacological profile of mephedrone could help to explain why mephedrone is so popular. It is for these reasons that mephedrone is seen as such a large risk to public health, leading to it becoming controlled in the UK in 2011[29]. However, this has not diminished its popularity as expected, with 46 countries currently reporting use of mephedrone[18]. In Europe, mephedrone still accounts for 20 % of all seized cathinone analogues[23]. It is widely believed that the popularity of mephedrone was not associated with its legal status[10,26].

1.1.3 Aminoindanes

Aminoindanes came onto the market in 2010 around the time that cathinones became controlled. At the instigation of this project in 2011 aminoindanes were believed to be the "next big wave" in NPS[30], as a legal alternative to synthetic cathinones. They are conformationally rigid analogues of amphetamines (Figure 1.6). The general structure of aminoindanes can be altered in a number of ways; such as substitution of the aromatic ring with a number of functional groups or through addition of a methylenedioxy bridge. They are primarily prepared using indanone, indene or through intramolecular cyclisation of acyl chloride derivatives of 3-phenyl-2-propenoic acid[31].
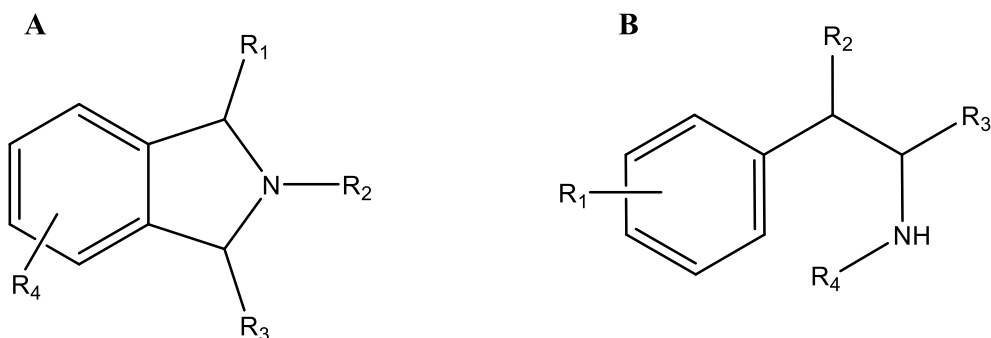
Figure 1.6 - Generic chemical structure for A. aminoindanes and B. amphetamines.

At the commencement of this project, aminoindanes were not covered by legislation and therefore could be easily purchased over the internet. The most prevalent aminoindane analogues sold as research chemicals were: 5,6-methylenedioxy-1-aminoindane (MDAI), 5-iodo-2-aminoindane (5-IAI), 2-aminoindane (2-AI) and 4-methoxy-6-methyl-2-aminoindane (MMAI)[32].

In 2011 a total of 12 aminoindane seizures were reported in the UK by the Laboratory of the Government Chemist (LGC). This number rose to 16 in 2012 with the majority corresponding to MDAI. By 2013 the UNODC showed aminoindanes corresponded to only 1 % of all NPS reports worldwide, and there were no reports of aminoindane seizures in the UK[19,33–35]. Their popularity have not risen to the suggested levels, with seizures significantly lower than those of the cathinones, even once cathinones were controlled. Aminoindanes have been reported to have a reduced potency compared to cathinones and amphetamines such as MDMA. They have been shown to produce a primarily serotonergic response in animal and *in vitro* studies[36], which is unlikely to lead to the combination of neurological effects found desirable in cathinones or the stimulant effects found in amphetamines. This could account for the lack of popularity after 2012 compared to the amphetamine and cathinone classes[30].

1.1.4 Constituents in 'Marketed' Products

The problem with NPS is not limited to the drug itself, but also the formulation of the products sold[37]. There are no regulations enforced to ensure the safety of the NPS and therefore any number of active ingredients and excipients can be found in the purchased products[32]. As well as finding a varying concentration of active ingredient in products bought over the internet, a number of excipients have also been identified as cutting agents. Cutting agents are chemicals used to dilute the NPS with something less expensive than the compound itself. When choosing a cutting agent illicit drug manufacturers or dealers would ideally attempt to find a chemical that is inexpensive, easy to obtain, relatively non-toxic and that mimics the physical attributes of the psychoactive substance used. Common cutting agents range from compounds of no potential abuse such as lactose and mannitol to

common pharmaceuticals such as paracetamol (analgesic), lidocaine (local anaesthetic) and procaine (local anaesthetic). The latter cutting agents can lead the user to think that the product is having an effect, when in fact, it actually contains no active psychoactive ingredient. Sometimes cutting agents used can cause greater side effects than the active substance[38]. For example, a common cutting agent is caffeine; in large quantities (0.5-1 g) caffeine can have similar effects to other stimulant drugs, and can be fatal at doses as low as 5 g[39].

There remains considerable uncertainty into the composition of products, and the extent to which label claims can be accepted as written[26]. For example Baron *et al.* conducted a study analysing seven NPS products, and concluded that six out of the seven products did not contain the advertised active ingredient and that six contained high quantities of caffeine[40].

This mixture of different compounds in products not only has health implications, it also complicates the detection of active ingredients. This is for two reasons, the first being that a large number of cutting agents have similar chemical structures to the active ingredients, the second is that the active ingredient becomes diluted when mixed with a number of cutting agents. This means that there are both selectivity and sensitivity issues relating to the detection of the NPS due to the complex composition of these samples.

Given the rapidly evolving nature of the NPS market, there is a need for more effective analysis of NPS. This has been well documented by UNODC in their yearly World Drug Reports[18,41]. A review by Banks *et al.* highlighted the future challenges with the forensic testing of NPS. They state that one of the main challenges facing the analysis of NPS is that of in-field detection. In particular developing fully validated, simple, selective and sensitive detection mechanisms[42].

1.2   Current Detection of New Psychoactive Substances

Studies of NPS are usually divided into three categories; analysis of pure substances, analysis of NPS products and analysis of NPS in bodily fluids, such as blood or urine. A number of studies have investigated the analysis and characterisation of aminoindanes, specifically MDAI and 5-IAI using nuclear magnetic resonance (NMR), mass spectrometry (MS) and infra-red (IR) spectroscopy [43,44]. Such techniques have also been adopted for the analysis of cathinones[37,45,46]. Gas chromatography-mass spectrometry (GC-MS) is a common technique adopted for the analysis of volatile components of both pure substances and NPS products. The high throughput, ease of sample preparation and high sensitivity makes it a popular means of analysing NPS products. Amphetamine-like substances are small volatile molecules, and therefore GC-MS is an ideal technique for analysis. Baron *et al*. carried out multiple studies into NPS products using GC-MS as well as a broader study into twenty-three NPS in thirty-five internet purchased products including methoxetamine (MXE), mephedrone and 1-

benzylpiperazine (BZP) (Figure 1.7)[47]. GC-MS has also been widely applied to the analysis of NPS reference standards[47–49].

Benzylpiperazine   Methoxetamine
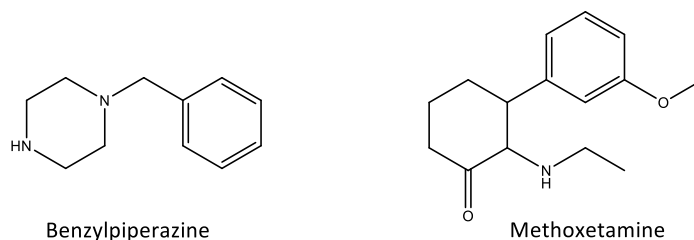
Figure 1.7 - Chemical structures of benzylpiperazine and methoxetamine

High-performance liquid chromatography (HPLC) is another common technique for the analysis of NPS products, as it allows for identification and quantification of both volatile and non-volatile organic compounds. Validated HPLC methodologies have been well established for the analysis of traditional amphetamine-related substances[50,51]. There are also a number of studies that have developed HPLC methodologies for cathinones[52]. Given its prevalence, specific methodology for mephedrone has also been established. Sutcliffe *et al*. published the first validated HPLC analytical method for the identification and quantification of mephedrone[37]. Additionally, they analysed mephedrone in the presence of common adulterants: caffeine, benzocaine, sucrose, mannitol and lactose. They reported limits of detection down to 0.03 μg mL^{-1} for mephedrone. This highlights the advantage of using a separation technique for analysis, as it reduces any interference that could occur from the presence of cutting agents.

Due to the complexity of identifying and quantifying NPS in bodily fluids more advanced techniques are often implemented. Beyer *et al*. conducted two studies using liquid chromatography-tandem mass spectrometry (LC-MS-MS), one examined cathinones found in blood samples[18], the other examined cannabinoids,[19]. Lower limit of quantification (LLOQ) values were determined to be 10 ng mL^{-1} for all compounds analysed.

All of the techniques mentioned above, once validated, can produce consistent and reliable results for the detection of NPS. However, they are all laboratory-based techniques that require a certain level of sample preparation, as well as expertise in the use of the instrumentation and data interpretation, which cannot be used rapidly in the field for identification of NPS samples.

In order to tackle the problem of NPS detection, rapid in-field detection devices are necessary. In-field detection devices for drugs of abuse are utilised in many different ways, from paramedics at the site of a drug overdose, to police and customs officers who can test potentially illegal drugs on site. To be used in situations such as these the methodology needs to be rapid, easy to perform and the results

should be easy to interpret. In the past traditional drugs of abuse have been tackled with using simple in-field tests to allow for rapid positive identification, usually through a visual colour change. However, NPS numbers are growing so rapidly that law enforcement agencies cannot keep up and therefore they are currently very limited in techniques available for in-field detection.

Given their similar structures the NPS classes highlighed above, aminoindanes and cathinones, can be detected using similar detection devices to those used for MDMA, e.g. colourmetric tests, although with poor selectivity. Their predominance in society and the health and safety risks associated with them means that effective laboratory-based detection techniques have been established[42]. These methods however are time-consuming, expensive and require a considerable amount of expertise to analyse the results obtained[45]. There currently remains a lack of in-field detection mechanisms for new amphetamine-like substances, which allows for the rapid identification, with high selectivity, sensitivity and low sample volumes.

1.2.1 Colourmetric Tests for Illicit Drugs

A highly desired form of detection is direct detection, whereby a visual change can be observed upon positive identification. This would allow for simple, inexpensive detection on site. An example of this is a colourmetric test, where the sample is reacted with reagents that change colour depending on the analyte they react with[54].

There are a number of advantages to using colourmetric sensing mechanisms, for example components needed for analyses are typically inexpensive and easy to understand, which means that they do not require highly trained personnel to analyse results. They can be adapted to be made even easier by designing a sensor that changes colour in the visible region to give the desired results[55].

There are a number of simple colourmetric tests for illicit drugs. A popular one that is often used is the Marquis Field Test, which is a simple test to detect MDMA, amphetamine and alkaloids[56]. The test reagent is composed of a mixture of formaldehyde and concentrated sulphuric acid, which produces different coloured products depending on the compound it interacts with. It is the colour change as well as the length of time taken for the colour to become apparent which is noted. For example, MDMA will turn dark purple within 5 s (Figure 1.8) whereas another substance, dextromethorphan (DXM) will turn the solution black within 15-30 s. Methanol is sometimes added to the solution in order to slow the colour change down, making it easier to visualise. The test is extremely sensitive and as with most colour tests, an estimate can be easily made as to the quantity of the drug present, based on the intensity of the colour observed. The Marquis Test has been found to identify a number of

substances but produces no reaction for mephedrone or other synthetic cathinones, due to the *para* substitution preventing the formation of a stable carbocation needed for identification.

Figure 1.8 - Marquis reagent colour change in the presence of 3,4-methylenedioxy-*N*-methylamphetamine (MDMA).

Interpretation of the results obtained can be seen to be subjective and further analysis is needed for definitive identification of compounds, particularly in a legal context. This is also true for another common colourmetric test called the Scott Test. For this test, a small amount of suspected cocaine (2-4 mg) is dissolved in cobalt thiocyanate solution with the addition of concentrated hydrochloric acid. In the presence of cocaine hydrochloride the solution turns bright blue. There are a number of other colourmetric tests that are utilised for drug detection as highlighted in Toole *et al.*[57].

For colourmetric analysis, there are two general signal motifs to consider; change in intensity at a certain wavelength, therefore, seeing the intensity of a colour response change and monitoring a change in maximum wavelength which means a change in colour. Colour changes may not necessarily be visible to the naked eye but through spectroscopic techniques such as fluorescence and ultraviolet and visible spectroscopy (UV/Vis).

A recent study has examined colourmetric tests currently available for preliminary identification of mephedrone and its analogues[57]. Through examination of all the substances against eight different colour tests; including Marquis Reagent and the Scott Test, drugs could be positively identified by means of referring to the appropriate results run from standards. Such simple tests allow for rapid, cheap and easy determination of substances, but are known to have low precision and accuracy and are only qualitative, they also lead to sample destruction in large quantities. This is a problem with the ever-expanding number of NPS coming onto the market that have similar chemical structures.

There are more sophisticated detection devices such as microfluidic affinity sensors, for the detection of cocaine[58]. This device consists of a microchamber packed with aptamer-functionalised microbeads. These act as a sensing surface which has been integrated with an on-chip heater and temperature sensors. These sensors use a Förster resonance energy transfer system, which generates a signal in

response to the drug binding to the sensor, with detection limits as low as 1 nM. However, this technique is still very complex to interpret for a non-expert and expensive to manufacture.

1.2.2 Current In-Field Detection Mechanisms for Amphetamine-Like Substances

The growing complexity of selective in-field detection due to the expanding NPS market, means that more sophisticated detection mechanisms need to be established. Masseroni *et al.* developed a probe that utilises pyrene-derivatized cavitands bound to fluorescent nanoparticles to detect MDMA[59]. Notably, both amphetamine and fluoromethamphetamine showed no fluorescent response. This level of selectivity has not been shown for traditional optical techniques. This highlights the growing need for more sophisticated mechanisms in order to achieve selectivity.

While there are currently no in-field detection mechanisms for aminoindanes, the development of selective detection mechanisms for cathinones (specifically mephedrone), has been of considerable focus. There are currently only a small number of successful novel direct detection mechanisms available for the detection of mephedrone that does not involve large laboratory-based equipment. Sutcliffe *et al.* developed an electrochemical sensor that can detect mephedrone and a number of other analogues through the reduction of the amine functionality to a secondary amine by interactions with the sulfonimide mediator[60]. Electrochemical sensors such as these are ideal for in-field devices exhibiting good sensitivity. However, as these sensors interact with amine groups they show poor selectivity between amphetamines, other cathinone analogues and common cutting agents such as benzocaine[61].

Krishnaiah *et al.* developed another electrochemical detection mechanism for mephedrone in urine that utilised a dropping mercury electrode[62]. Through reduction of the carbonyl functional group, detection limits of 12.5 pM were achieved in universal buffer. However, no selectivity testing was conducted in this experiment against other drugs of abuse or common cutting agents.

A study conducted by Baron *et al.* used direct detection through the incorporation of aqueous mercury chloride solutions to form unique drug related crystals. It has been applied to the detection of mephedrone, BZP and MDAI[63]. Each of these compounds form specific drug-reagent crystals within minutes of exposure, which can be visualised under high magnification using transmitted light microscopy and phase contrast microscopy set. The uniqueness of the test carried out has been confirmed by comparison to the microcrystalline response to that of other psychoactive stimulants and common cutting agents such as caffeine, lactose and magnesium sulphate. The limits of detection vary depending on the drug analysed. These limits were found to be 5 gL^{-1} for mephedrone, 0.5 gL^{-1} for MDAI and 0.3 gL^{-1} for BZP. It was found that there were limitations in the results when the ratio of

the drug to cutting agent was too low. BZP could be detected alongside caffeine from as low as 20 % (v/v), MDAI from 40 % (v/v) and mephedrone was higher at 50 % (v/v), all dissolved in methanol. It is common for tablets and capsules that are analysed to contain much lower concentrations of drugs than those seen here and this would be hard to detect amongst the number of excipients that have been known to be present in these products[32]. It is the low sensitivity and selectivity of this detection mechanism that makes it a poor working model for mephedrone detection.

One traditional in-field detection mechanism that is popular are immunoassay tests, in part due to their selectivity. Randox Laboratories currently have a commercially available immunoassay for synthetic cathinones, which shows limits of detection between 0.18 and 9.2 μgL^{-1}. However, independent validation of this test by Ellefsen *et al.* showed that there was a large negative bias observed, leading to a large number of false positives between cathinone analogues[64].

All of these in-field detection mechanisms successfully detect mephedrone, and in some cases with low limits of detection, and selectivity. However, to achieve an effective in-field detection device it needs to have low limits of detection, selectivity, ease of interpretation, and reliability as well as rapid identification. Currently, there is no working in-field detection mechanism that incorporates all of these characteristics.

1.3   Analysis of New Psychoactive Substances Using Host-Guest Design

Using the principles of host-guest design it may be possible to rationally develop a mechanism that has the ease of colourmetric detection, which has the ability to address all the above criteria, but with increased selectivity[65,66]. As shown above, there are a number of advantages to using colourmetric sensing tests as the components and analyses are typically inexpensive and easy to understand, which means that they do not require highly trained personnel to analyse the results. They have the potential to be adapted to be made even easier by using host-guest chemistry to design a sensor that binds to cause a colour change in the visible region. The ease of visual detection experienced with colourmetric sensing leads to poor sensitivity, which in turn means there are higher limits of detection than other techniques. Colourmetric tests have been shown to be useful working models in the past; however, they now lack selectivity due to the number of structurally similar NPS available. The principle of a colourmetric test is still good, it is the mechanism of the current devices that lacks selectivity as they focus on detection of a single functional group, e.g. amine. If the mechanism of detection is based on reaction with multiple functional groups in a pre-determined geometrical orientation it could be possible to develop a selective colourmetric test[67]. Such mechanisms are often referred to as ligand sensors.

1.3.1 Ligand Sensors

Synthetic ligands are molecules that are developed with specific binding sites in order to coordinate to particular molecules[65,68]. This selectivity makes them a very popular method of detection for molecular recognition. They work as probe molecules by binding to drug molecules by which a positive identification can be made, either through a visible colour change or use of a transducer. They have as yet not been utilised in the area of NPS detection; however, they have been known to be useful in the detection of performance enhancing drugs in athletes[69].

Ligands can be designed in one of two ways; to bind to known drugs to allow for identification of the ligand-drug complexes, or by binding to the matrix, leaving ligand-free drugs in a system. Both can be confirmed through common spectroscopic techniques. The same principles used for detection of traditional drugs can be applied to NPS. By designing sensor ligands with binding sites that correspond to specified drugs, ligand-drug complexes will be formed and this complex can be detected using a chosen transducer mechanism. An ideal mechanism for in-field drug detection is a visible colour change which can be quantified using optical spectroscopy, specifically fluorescence and UV/Vis spectroscopy. It is also possible to investigate the binding between a host and guest system using a number of NMR and mass spectrometry techniques.

As with most chemical tests, selective ligand-host molecules can be time-consuming to develop and synthesise, with large amounts of testing and validation necessary in order to prove selectivity. When developing sensors, the excipients in the formulations, as mentioned in Section 2, have to be considered to ensure there are no false negatives or positives due to drug-sensor and excipient-sensor interactions occurring concurrently, thereby masking the intended response.

One of the most selective interactions in chemistry occurs in nature, between proteins and ligands. Proteins have very high specificity for their target guest despite complex matrixes. Proteins however, are only stable at physiological pH and can be unpractical as in-field detection probes. It may be possible to develop a small molecule ligand sensor that mimics the selectivity of proteins, by extracting the binding data from protein-ligand interactions. The idea of rationally designing a biomimetic sensor based on protein-ligand binding could help to overcome the problems associated with complex mixtures found in samples, by ensuring both selectivity and sensitivity[67,70].

Known databases such as the Brookhaven Protein DataBank[71] can be utilised to help find ligand interactions that afford good relationships with selected drug molecules[71]. This has the possibility to also be used to help minimise the interactions with competing substances in the samples, thereby reducing the amount of time and money spent designing, synthesising and testing ligands that consequently have poor ligand-drug interactions. Currently, *in silico* evaluation of protein-ligand

interactions is commonly utilised in drug design. By understanding the protein-ligand interactions that are observed experimentally, drug molecules can be designed that selectively bind in the protein cavities to induce a physiological response[72]. This is achieved by mapping the binding features (also known as pharmacophoric features) that are necessary for the host molecule to bind to the protein. The developed map is known as a pharmacophore model. If it is possible to experimentally design the guest molecules (drug) by developing a pharmacophore model of the protein binding features, then given the same principles it could theoretically be possible to map the binding features of the proposed guest molecules to rationally design selective host molecules, i.e. reverse the current procedure for pharmacophore design. This is a method for host design that has not yet been reported in the literature. In order to achieve this, it is necessary to have an in-depth understanding of how the guest molecule e.g. a cathinone or aminoindane analogue, interacts with a protein selectively, and then develop a pharmacophore model based on these interactions.

The Brookhaven Protein DataBank contains a number of high-quality protein–ligand complexes which can be examined in order to find a suitable protein-ligand complex, which may then be used to study receptor interactions with drugs of abuse/common adulterants/endogenous psychoactive substances (i.e. dopamine and serotonin). This information could then be used to develop a consensus pharmacophore of protein-ligand binding to support host molecule selection.

1.4 Pharmacophore

A pharmacophore is an abstraction of the molecular features (often referred to as pharmacophoric features) that are necessary for molecular recognition of a ligand by a protein (or a guest molecule by a host molecule)[73]. The pharmacophore summarises the key groups that are required for binding and their relative positions in space with respect to one another (Figure 1.9)[74]. In order to develop a structure-based pharmacophore, a detailed understanding of the dimensions of the binding site is required. Once a pharmacophore model has been developed computationally from a host protein it if often used to screen for potential guest molecules[75].
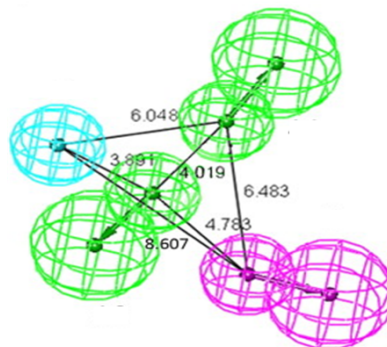
Figure 1.9 - Example of a serotonin pharmacophore. The different colours represent different pharmacophoric features; H-bonding accepting green, hydrophobic pink, and π-stacking in blue. The radius of the spheres shows the distances from a central point, over which it is feasible for the interactions to occur. Distances between the key features identified by the pharmacophore shown are reported in Angströms (Å).

By understanding the interactions involved in protein-ligand binding it is possible to use molecular modelling techniques to design molecules with the potential to fit inside and bind to sites of interest. For example, by using computational techniques to screen potential drugs against therapeutic protein targets it is possible to identify favourable protein-drug interactions, which can be used to prioritise potential lead molecules for further investigation such as initial biological testing[76]. This helps to reduce the number of potential compounds that have to be tested. In this instance, we can categorise the binding site of the protein of interest as a host molecule, and the potential drug molecule that binds to the site as a guest molecule.

Instead of developing a model to describe the drug molecule that fits in the protein cavity, it could be possible to apply the same techniques to modelling the binding site of the protein. This model can then be used to mimic the binding site of the protein and synthesise a small molecule host that encompasses the key binding features of the desired protein, and selectively bind the analyte e.g. a cathinone. Producing a small molecule sensor that mimics the selectivity of proteins can help to overcome the disadvantages of using proteins, such as their relative instabilities when not in a controlled environment[77].

When analysing these proteins and their binding computationally, it is first important to understand how protein structures and binding interactions have been derived. Only fully validated experimental data should be used in order to develop a robust pharmacophore model.

1.4.1 Protein-ligand Pharmacophore Design

Proteins are large macromolecules that consist of one or more chains made up from different permutations of the 20 naturally occurring amino acids linked together *via* peptide bonds. The unique

way in which proteins are sequenced determines their tertiary structure, which in turn determines their function. Protein functionality is diverse; proteins that have functions ranging from transport, through to storage and movement in a biological system have all been observed[78]. The vast number of roles proteins play in the body account for the considerable diversity and complexity of their structures.

All 20 naturally occurring alpha amino acids contain both a carboxylic acid and an amino group (Figure 1.10). They are distinct from one another due to differences in their side chains, which can differ with respect to physicochemical properties such as acidity/basicity and steric bulk.
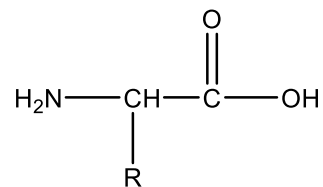
Figure 1.10 - Generalised chemical structure for an alpha amino acid, with variables occurring at the R group.

Protein structure can be described in four levels: primary, secondary, tertiary and quaternary structures (Figure 1.11). The primary structure is the unique sequence of amino acids, secondary structure is the folding or coiling of the polypeptide chains to form recognisable motifs in the protein such as alpha-helices and beta pleated sheets, tertiary structure arises *via* interactions between side chains of the amino acids, such as hydrogen bonding, van der Waals and disulphide bridges. Finally, the quaternary structure is the assembly of multiple polypeptide subunits, producing an overall functional complex, such as triosephosphate isomerase (TIM) barrel folding.
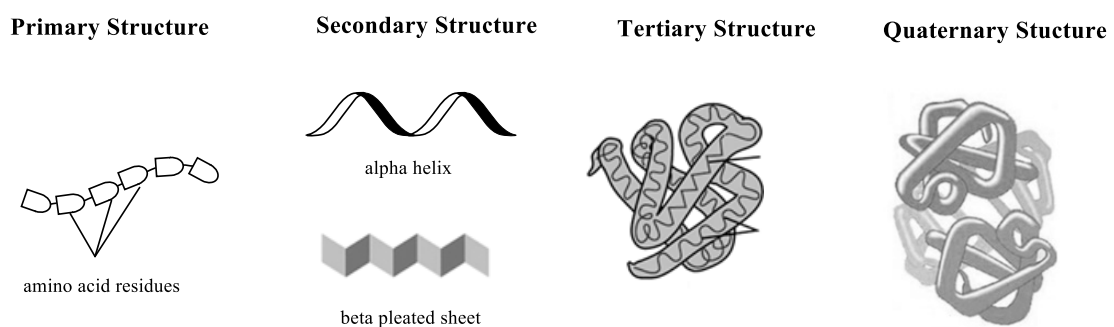
Figure 1.11 - Four structural levels of protein structure (adapted from[79]).

Their complex shapes can give rise to pockets and cavities. It is in such cavities that protein-ligand binding interactions occur. The shape, size and chemical nature of these cavities determines which ligands can bind, based on the potential interactions that can take place[80]. This concept is described by the theory of induced fit[74]. This theory is modified from Fisher's theory of the lock and key

mechanism of enzymes[14] and differs as it does not assume the protein is static. It assumes that the ligand plays a role in determining the final shape of the protein and only the suitable ligand is capable of inducing an appropriate alignment of the active site[74].

The notion of induced fit has long aided drug discovery, to help with the rational design of drug molecules that selectively fit into specific disease-implicated receptors. It is, therefore, important to understand the different types of interactions that can occur to form these complexes in order to fully exploit the theory of induced fit, and develop a robust pharmacophore model for the chosen analyte.

1.4.2   Interactions

Protein–ligand binding interactions are crucial to almost all processes that occur in nature[80]. These chemical interactions occur at a molecular level with a high degree of selectivity and sensitivity[81]. It is important to understand how proteins and ligands interact for two main reasons. Firstly, to understand how a ligand will bind to a protein requires knowledge of how the structure of the ligand affects the binding affinity, and how small structural modification can affect the predicted outcome. Secondly, identifying the forces involved in protein-ligand binding is fundamental to understanding and exploiting molecular recognition.

Proteins and ligands mainly interact through four non-covalent interaction types; hydrogen bonding, π-π interactions, ionic interactions and hydrophobic interactions[82]. Hydrogen bonding occurs *via* electromagnetic attractions between ionisable molecules in which hydrogen atoms interact with a highly electronegative atom (e.g. N, O or F). They are one of the strongest non-covalent interactions ranging in bond strength from 4.2 - 25 kJ mol^{-1} [83]. The relative strength of a hydrogen bond depends on bond length, bond angle, temperature, pressure and environment. These five conditions account for the large range of energies that have been observed. Hydrogen bonds are directional, with an optimum angle of interaction at 180 degrees.

π-surface interactions are attractive, non-covalent interactions between aromatic rings. They can be either offset face-face or edge-face interactions (Figure 1.12), where the p-orbitals overlap to form π bonds. Their strength ranges from 6.7 - 10 kJ mol^{-1} [84]. The type of π-stacking interaction that takes place can be determined by a number of factors. Two such factors are the groups involved in the interaction and the orientation of the two aromatic rings may favour one type over the other[85]. In general, the edge/face orientation maximises the interaction between positive and negative electrostatic potentials between two aromatic rings and therefore, it is usually a more favourable interaction[86]. However, it is not possible to utilise this interaction in all cases.
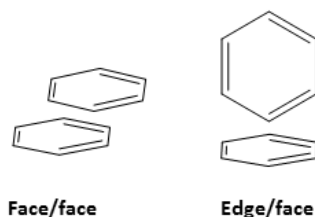
Figure 1.12 - Illustration of face/face vs. edge/face π-stacking interactions.

Ionic interactions can occur between charged ligands and amino acid residues with polar side chains such as aspartic acid. They are the strongest non-covalent bonds found within proteins, with strengths between 20 - 40 kJ mol^{-1}. Their strength is proportional to the distance between two charged interacting funtionalities[74].

Hydrophobic interactions are spatial interactions caused by the aggregation of hydrophobic molecules; they are the sum of the attractive and repulsive forces between these molecules. Van der Waals interactions are one type of hydrophobic interaction. Keesom, Debye and London dispersion forces are the three main contributors to van der Waals interactions. Van der Waals interactions are weak interactions ranging in strength between 2 - 4 kJ mol^{-1}. They are transient interactions that occur between two dipole moments and therefore it is often hard to discriminate between the different interactions leading to them all being labelled as hydrophobic interactions. Despite the relative weakness of van der Waals interactions they are extremely important in protein-ligand binding, due to the sheer number of them. This effect is hard to mimic in a small molecule host.

By understanding how all these forces work together to produce selective protein-ligand interactions, it is possible to rationally design molecules that will only bind at specific complementary binding sites. It could therefore be possible to utilise protein-ligand interactions to develop a small molecule sensor that will capture the type of interactions that make proteins selective for a given molecule of interest. Protein-ligand interactions can be analysed *in silico* based on experimentally derived structures and the binding data extracted in order to develop a pharmacophore model.

1.4.3 Experimental Determination of Protein-Ligand Interactions

Protein-ligand interactions can be studied using the Protein DataBank (PDB; www.rcsb.org)[71]. The PDB is an online repository for three-dimensional structural data of large molecules. Experimentally derived data is used to design a host molecule for specific compounds of interest. There are two main ways to collect experimental data on protein structures: X-ray crystallography and NMR spectroscopy[87].

1.4.3.1   X-ray Crystallography

Over 80 % of the protein structures in the PDB are obtained from X-ray crystallography[88]. It is based on the diffraction of X-rays by a crystalline material, producing an electron density map. Regions of electron density represent atoms and the bonds between atoms. A map of these features allows for the determination of the 3D structure of proteins.

There are several experimental hurdles that need to be overcome in order to obtain a 3D protein structure using X-ray crystallography. Firstly, the protein needs to be in a crystalline state, which is not always possible. For example, transmembrane proteins are very hydrophobic so when they are isolated, as is necessary to obtain crystals for X-ray crystallography, they often form aggregates as the hydrophobic regions try to escape energetically disfavoured aqueous environments. Aggregation of this kind is not compatible with crystallisation.

In order to aid crystallisation of protein structures, it is common for proteins to be altered, or mutated. Mutations are often deliberately applied to amino acid residues in a protein sequence when attempting to obtain an experimental structure. One of the reasons for this is to aid the isolation or crystallisation of the protein and/or prevent aggregate formation. One example of such mutations is to prevent the formation of disulphide bridges between residues. Disulphide bridges have been found to accelerate the formation of aggregates[89]; this hinders the ability to form a crystal structure for analysis. It is believed to be Derewenda who first introduced the concept of mutating protein surfaces in order to increase their suitability for crystallography[90]. Mutations can also be introduced in order to increase the solubility of proteins to aid in crystallisation. Waldo *et al*. suggested that by decreasing the entropic barrier to crystallisation this would aid in crystal formation. One way of doing this is to reduce the flexibility of loops or end termini[91]. It is essential to understand where such mutations have been introduced into a protein sequence as small changes can affect all levels of protein structure, which may impact on binding sites. Any impact on the binding site needs to be taken into consideration when extracting binding data for the pharmacophore model.

Once a crystal is produced and X-ray crystallography has been carried out, there are several important properties of the final model that must be taken into consideration when analysing the data. It is important to ensure that the binding data extracted from the proteins to build the pharmacophore model is fully validated.

The location of a binding site in the protein is important, especially when trying to rule out artefacts of crystallisation as it is possible to observe surface binding of a ligand to a protein, and binding of a ligand in a buried cavity. The binding of a ligand in a buried cavity tends to cause less concern when considering artefacts of crystallisation as binding in a buried site is unlikely to lead to stabilisation

between two unit cell interfaces in the crystal form, and generate misleading information with respect to the nature of protein-ligand binding. However, binding at the surface of a protein requires the investigator to be much more sceptical when considering whether or not the interactions observed are real or the result of artefacts introduced because of the experimental methods used to obtain a crystal structure.

Artefacts of crystallisation are fundamentally interactions or properties that occur due to the protein being in crystal form. Solvation in a cavity does not necessarily mean that interactions are occurring with the water. It may mean that the entire cavity is largely solvated in crystal form; this can prevent interactions occurring, such as π-stacking or hydrophobic interactions, as the water may not be easily displaced by the ligand to allow for binding. This is again dependent on the thermodynamic stability of the water molecules. However, with water present in the crystal structure it is not possible to know whether interactions would occur without water present, and therefore highly solvated cavities need to be considered on a case-by-case basis in relation to the thermodynamic stability of each of the water molecules in the binding cavity. Another example of an artefact of crystallisation is binding occurring between protein interfaces in the crystal form as shown in Figure 1.13 with caffeine.
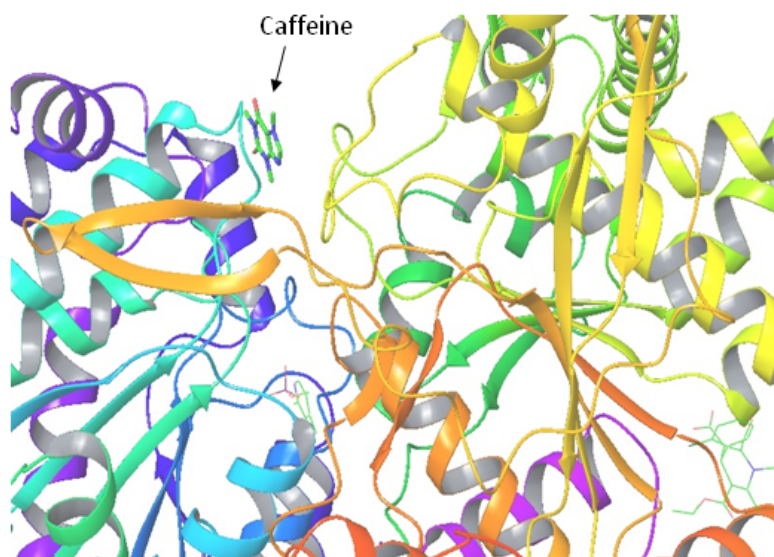
Figure 1.13 - An image showing caffeine binding between two protein subunits in 1C8L.

Another factor to be taken into consideration when looking at electron density maps is resolution. Resolution is defined as the measure of how easy it is to differentiate two adjacent spots in an electron density map and is commonly measured in ångströms (Å)[92]. Resolution is important when looking at interactions between proteins and ligands. As seen in Figure 1.14 the hydrogen bonding interaction occurs at 1.66 Å, if the resolution value of the X-ray crystal structure was greater than this distance then it could not be claimed with complete certainty that the interaction was occurring.
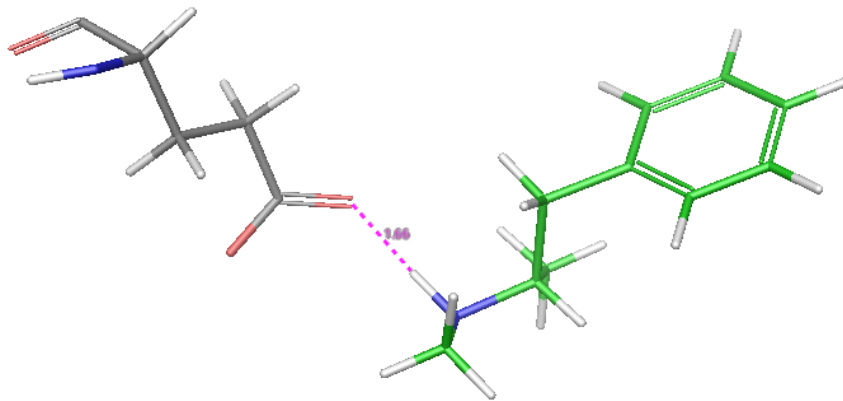
Figure 1.14 - Hydrogen bond between glutamic acid residue and methamphetamine at a distance of 1.66 Å.

Another validation criterion when establishing crystal structure quality is occupancy. Occupancy is associated with the electron density map produced during the X-ray crystallography experiment (Figure 1.15). It is related to units cells i.e. if all molecules in the crystal are precisely identical then the occupancy for all atoms is one[93]. If the occupancy is not one this would indicate that not all the unit cells in the crystal are identical. This may be caused by different conformations of amino acid side chains in different unit cells. These small differences may cause different protein-ligand interactions in different unit cells.
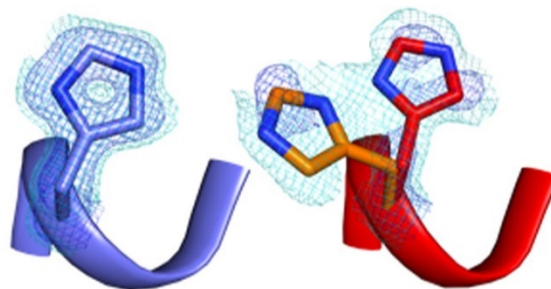
Figure 1.15 - Electron density map showing the possibility of two rotamers for a histidine residue giving an occupancy of less than 1 (taken from[94]).

An additional factor to be taken into account when validating protein binding data is B factors. B factors are values given to denote the thermodynamic stability of atoms in the X-ray crystallographic representation of a protein structure. They give an indication as to the level of thermal motion that is likely to be observed for a given atom[95]. An atom with a high relative B factor in comparison to the overall B factor of the protein suggests they are thermally labile and therefore interactions observed

45

between them and a ligand in the X-ray crystal structure complex may not actually occur in reality. All of these parameters need to be considered for validation of potential binding sites.

1.4.3.2   NMR Spectroscopy

NMR protein structures account for about 16 % of all structures in the PDB[88]. NMR spectroscopy is usually carried out in an aqueous media using highly purified proteins. In aqueous media, the proteins tumble and vibrate allowing for determination of the 1D and 2D structures. For analysis of proteins, ^{1}H-NMR is employed, as hydrogen is the most abundant naturally occurring element in proteins that can be visualised using NMR. Both 1D and 2D experiments are carried out which allows for analysis of bonded and non-bonded interactions between protons.

One of the reasons there is less NMR data in the PDB is because it can only be carried out on small proteins or protein domains (50–60 kDa), due in part to the complexity of analysing spectra of large proteins[96].

As with crystallographic techniques, there are a number of criterion that need to be taken into account when analysing NMR derived protein structures and binding data. Mutations can also occur in proteins that are analysed using NMR; however, they are present for different reasons. One example is to stabilise the helixes in proteins. This can help to rigidify the protein to prevent fast destabilisation, which can occur within the time frame of an NMR scan[97]. As with X-ray crystallography any mutation can affect the binding site, and therefore needs to be taken into account when bound to the ligand of interest.

The geometrical quality of the derived structures is an important factor that needs to be considered when looking at NMR data. It is essential for the NMR structure to be carefully examined for any abnormalities that may arise. For example, the bond lengths and angles should be checked as they can sometimes be incorrect due to non-bonded interactions or strain depending on the NMR restraints[98]. Bond lengths and angles are largely known from analysis of small molecules. For example, if a carbon has a tetrahedral geometry, the angle should not vary significantly from 109.5 degrees or this would be a cause for concern. However, certain atoms in many protein structures are known to exhibit bond angles that would indicate significant strain.

1.4.3.3   Comparison of Experimental Techniques

Data in the PDB is collected primarily from either X-ray crystallography or NMR experimental data. Both of these techniques allow for in-depth analysis not only of the full protein structure but also the binding of ligands in cavities.

The advantage of NMR spectroscopy is that there is no need for a protein crystal to be formed, as analysis is carried out in aqueous media. However, NMR spectroscopy has one major limitation, only proteins less than 60 kDa can be studied. The average protein in the PDB is 107 kDa and therefore NMR is unsuitable for a large number of proteins[99]. X-ray crystallography on the other hand is not limited by size, assuming that a crystal can be isolated. The results of NMR spectroscopy analysis is not as detailed and accurate as those obtained for crystallography[100].

Both techniques have their own advantages and disadvantages when studying protein structures and ligand binding. With validated methodology for both techniques, useful binding information could be extracted and taken forward to build a pharmacophore model for the chosen analyte. With this in mind, a molecular probe (i.e., host molecule) will be designed based on this pharmacophore model that will utilise these interactions to selectively bind the analyte. One way of designing host molecules is through supramolecular chemistry.

1.5 Supramolecular Design and Testing

Supramolecular chemistry is a term coined by Jean-Marie Lehn[101] meaning 'chemistry beyond the molecule'[102]. Individual molecules consist of atoms joined by intramolecular forces such as covalent bonds; however, supramolecular chemistry makes use of intermolecular interactions such as π-stacking, hydrogen bonding and electrostatic forces to bring molecules together. Aromatic molecules can stack together by virtue of π-π interactions, while hydrogen bonding allows for electronegative atoms in molecules to form strong bonds with protons in neighbouring molecules. Electrostatic interactions are individually weaker interactions; however, they can allow for further interactions between molecules. Supramolecular chemistry encompasses all of these interactions making them perfect candidates for use as sensing molecules. A number of different macrocyclic molecules have been designed containing functional groups that aim to enhance these intermolecular interactions and thereby act as 'host molecules' to optimise potential interactions with 'guest molecules', this is known as complementarity i.e. where both the host and guest molecule have mutual spatially and electronically complementary binding sites so as to allow a 'supermolecule' to form[103]. One example of these is protein-ligand interactions.

Host-guest chemistry is used for the detection of guest molecules using rationally designed host molecules. The binding site in the host molecule is designed to selectively attract the guest molecule of interest, using intermolecular interactions. These interactions can be incorporated into the design of a host molecule to allow it to be selective towards a target guest molecule.

Supramolecular host molecules form host-guest complexes based on the principles of molecular complementarity[102]. According to Fisher's lock-and-key theory, complementarity is the most

important factor to consider when designing potential host molecules. The more interactions that make up the binding between a host and guest the stronger the complementarity for the complex, and therefore the stronger the binding constant[104]. This is why using protein-ligand interactions is ideal, as they often involve a large array of binding interactions to provide the selectivity observed.

Macrocycles are host systems that are pre-organised into cyclic shapes and are normally designed with a selection of aromatic functionalities and strongly electronegative atoms such as O, N and S. Electronegative atoms such as nitrogen and oxygen can provide good hydrogen bonding groups, while other atoms such as sulphur can induce intermolecular dipole-dipole interactions which aid in host-guest interactions. Some of the most utilised macrocycles for molecular recognition include cyclodextrins, crown ethers and calixarenes (Figure 1.16)[68,103]. For example Kubo *et al.* used functionalised calixarenes to discriminate between different enantiomers of amine derivatives, *via* an array of hydrogen bonding interactions[105]. This study shows that through rational design even enantioselective molecular recognition can be achieved using ligand sensors.
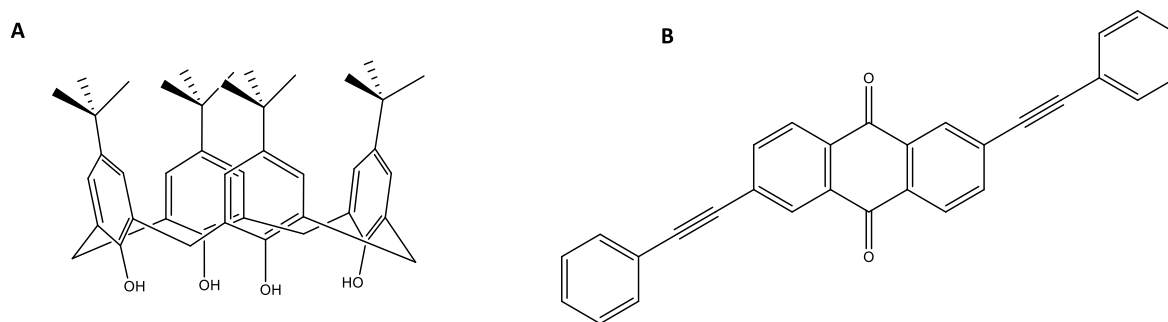
Figure 1.16 - An example of A. calixarene macrocyclic host molecule and B. an anthraquinone based acyclic host molecule.

The advantage of macrocycles is that there may be no energetically unfavourable change in conformation of the host upon binding of the guest[106]. In contrast, acyclic hosts also known as podands are not pre-organised and are more flexible in nature[103]. Anthraquinone derivatives are sometimes utilised as acyclic host molecules due to their flexibility and conjugated ring system (Figure 1.16)[107]. They are therefore capable of 'wrapping around' a guest molecule. This change in conformation requires more energy and therefore the host-guest complex needs to be more energetically favourable. This can sometimes allow for a more selective host molecule as they can be designed around specific guest molecules[103], such as through the use of a pharmacophore model.

There are multiple ways in which to determine binding constants of host-guest interactions. Ideally to determine the mechanism of binding an instrument that is sensitive, enabling reduced sample volumes and has fast analysis times is required. Typically spectroscopic techniques are used for

determining binding constants, including NMR, UV/Vis, fluorescence spectroscopy and mass spectrometry. However, not all of them are capable of identifying the mechanism of binding.

1.5.1 Detection Mechanisms for Binding

Upon binding, the host and guest molecules undergo a physicochemical change, due to the intermolecular interactions taking place. It is this physical change that can be detected. For example, NMR identifies changes in chemical resonance, UV/Vis changes in absorption bands and fluorescence changes in the excited state emission. The information gathered from this can then be compared and fitted to binding models in order to obtain information such as stoichiometry, energetics (enthalpy and entropy) and binding constants (Ka) (Equation 1.1)[108].

$$Ka = \frac{[HG]}{[H][G]} \qquad \textbf{Equation 1.1}$$

Where:

H is the concentration (M) of the host molecule,

G is the concentration (M) of the guest molecule in its free state, and

HG is the concentration (M) of the host/guest complex.

Equation 1.1 assumes a stoichiometry of 1:1 in the bound state. This, of course, may not be true and calculations must be adjusted accordingly[108].

1.5.1.1   NMR

NMR binding studies have long been established for quantitative determination of host-guest binding[109,110]. It works on the principle that, upon binding, the chemical environment of the atoms involved will alter, and these changes can be detected and used to calculate binding constants.

There are two types of exchanges that can occur on examination of a binding system in NMR; slow and fast exchange. Slow exchange is normally seen for large molecules such as protein-ligand binding[110] due to protein–ligand systems exhibiting high binding affinity and low dissociation constants. This would mean that signals would be visible for both the bound and free state of the protein and ligand respectively. However, for small molecule systems that will be used in this project, binding affinity is lower, and fast exchange is normally observed. For a system in fast exchange the chemical shift observed is a mole fraction weighted average of the free and bound states together, i.e. only one peak is observed and its chemical shift will alter depending on the equilibrium state (Equation 1.2).

$$M_{obs} = X_{L(free)}M_{L(free)} + X_{L(bound)}M_{L(bound)} \quad \textbf{Equation 1.2}$$

Where:

M_{obs} is the chemical shift observed by the system (ppm),

$X_{L(bound)}$ and $X_{L(free)}$ are the mole fraction of the bound and free ligand, and

$M_{L(free)}$ and $M_{L(bound)}$ are the chemical shifts for the ligand in its free and bound state (ppm)[110].

By plotting the observed change in chemical shift over a number of molar ratios of host and guest a binding curve can be fitted that will not only allow for association constants to be calculated but can also provide valuable information regarding the stoichiometry of binding. Such experiments are known as NMR titrations.

The advantage of NMR over optical spectroscopy for determination of binding constants is that valuable information as to which groups are involved in the binding interaction may be obtained. This is important when looking at sensors that have been designed to selectively bind host molecules. Knowing the groups that are involved in binding means that the types of intermolecular interactions can be deduced. Another notable advantage over optical spectroscopy is that all organic ligands can be detected through NMR analysis, and therefore it does not require there to be a chromophore or fluorophore present in the ligand. Despite all these advantages, NMR is not as sensitive as other spectroscopic techniques, and larger sample concentrations are required to obtain binding constant values.

1.5.1.2   UV/Vis Detection

The visible and ultraviolet absorption spectra of organic compounds are associated with transitions between electronic energy levels in the ground state. The energy transitions normally occur between bonding or lone-pair orbitals and the unfilled non-bonding orbitals due to a pulse of electromagnetic energy from the spectrometer (Figure 1.17).
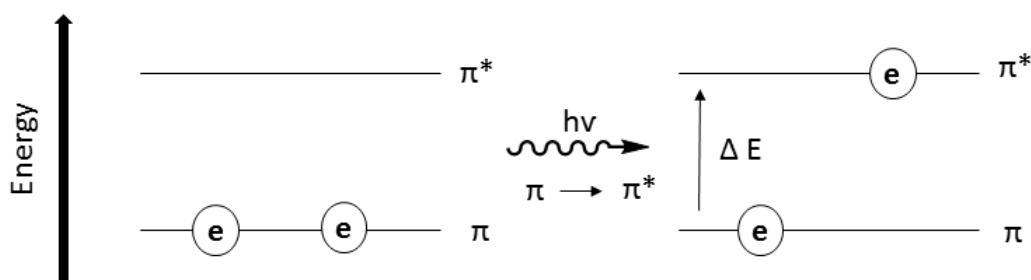
Figure 1.17 - A schematic showing the promotion of an electron from a bonded (π) to non-bonded (π*) orbital due to the absorption of electromagnetic energy (hv).

The energy supplied by the source in a spectrometer promotes electrons from their ground state to an excited state orbital or antibonding orbital. There are three types of orbitals in the ground state that may be involved in this process; sigma bonds (σ), pi-bonds (π) and non-bonding atomic orbitals (n). There are also antibonding orbitals involved in transitions, σ* and π*. The amount of energy absorbed dictates which transition will be brought about.

When these transitions occur there is an increase in energy of the promoted electron and this corresponds to a wavelength of an absorption spectrum. This wavelength is inversely proportional to the change in energy of the orbitals involved (Equation 1.3), where energy (E) is in kJ mol^{-1} and wavelength (λ) in nm.

$$E = \frac{1.19 \times 10^5}{\lambda} \qquad \text{Equation 1.3}$$

Another equation that relates to UV/Vis analysis is the Beer-Lambert Law. This is particularly important when using this technique for quantitative binding studies. Beer's law states that the absorption is proportional to the number of absorbing molecules[111].

$$log_{10}\frac{I_o}{I} = \epsilon.l.c \qquad \text{Equation 1.4}$$

Where:

I_o and I are the intensities of the incident and transmitted light,

l the path length of the solution (cm),

c is the concentration (M) and

ε is molar absorptivity (M^{-1} cm^{-1})

51

The function Log_{10} (I_0/I) is also known as the absorbance or optical density of a given solution. This is important when comparing optical spectroscopy techniques and quantifying binding.

In order to have a UV/Vis active molecule, there must be a chromophore present. A chromophore is a functional group that exhibits a characteristic absorption spectrum. For host-guest binding to be quantified using UV/Vis the chromophore in the host molecule needs to be involved in the binding with the guest. For example, the lone pair on an amine functionality in a chromophore such as thiourea can act as a hydrogen bond donor, upon binding the absorption spectrum of the thiourea will be affected. This is because the energy of electronic transitions is increased when a molecule is hydrogen bonding. This will bring about a change in either the intensity of absorption or red shift of the absorption band, i.e. longer wavelengths (Figure 1.18). It is this change in the absorption of light that can be quantified and used to determine binding constants.
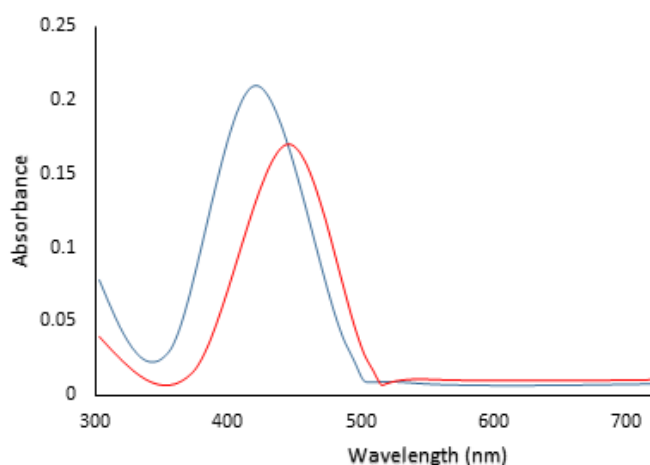
Figure 1.18 - Schematic showing the red shift caused by hydrogen bonding. The blue line indicates an absorption spectrum before hydrogen bonding complexation, the red line indicated the same compound that is taking part in a hydrogen bonding interaction.

Spectrophotometric measurements involve low sample volumes and are simple to carry out, therefore, they are ideal for measuring host-guest interactions. The host molecules, however, must be carefully designed to incorporate a chromophore that is directly involved in binding in order to monitor these interactions.

1.5.1.3   Fluorescent Detection

Fluorescence spectroscopy can be used for determining binding between a host and guest molecule based on the change in the emission spectra of the host molecule. Unlike NMR it is very sensitive and it is possible to use concentrations in the nanomolar range. For this reason, fluorescence is often seen as an ideal signal transduction mechanism in sensing applications.

There are two main components necessary for the design of a fluorescence sensor; a signal moiety (the fluorophore) and a recognition moiety (the receptor). The signal moiety acts as the signal transducer, converting information into an optical response. The recognition moiety is responsible for binding to the analyte in a selective and efficient manner.

It is important to take into account the solvent system when using fluorescence sensors. Such sensors are easily affected by solvent effects such as pH, ionic strength, concentration and polarity. The concentration in particular can play an important role in fluorescence emission. If a sample is highly concentrated then self-quenching or self-absorption can occur. Highly polar solvents can also lead to a decrease in fluorescence as they have the ability to hydrogen bond to the substrates. The pH of the solution when working with acidic or basic compounds can have a significant effect. For example, protonated acids are poor fluorophores and therefore, a weak emission signal will be observed. There needs to be an active communication pathway between signalling and recognition moieties which allows for the photo-physical properties of the fluorophore[112].

In the case of fluorescence, the emission arises from a singlet excited state (in a fluorophore). This is achieved by promoting an electron from a ground state orbital or the highest occupied molecular orbital (HOMO) to a higher energy orbital i.e. the lowest unoccupied molecular orbital (LUMO) through light irradiation. It is the electron returning from the excited state back to the ground state that emits energy of a given wavelength which leads to fluorescence (Figure 1.19).
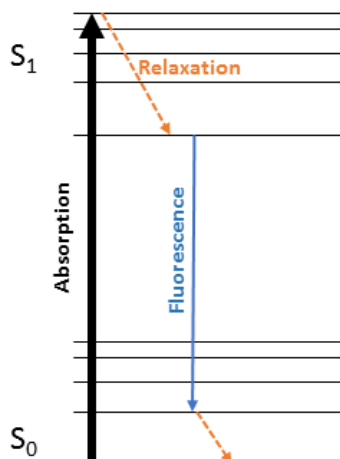
Figure 1.19 - Absorption of light leading to promotion of an electron from the ground state to the excited state. Fluorescence is emitted when the excited electron returns to the ground state. The energy of the emitted light is often less than the absorbed light due to relaxation in the system.

There are a number of different mechanisms through which a change in fluorescence emission can occur in order to be able to visualise binding. One common mechanism is internal charge transfer (ICT). This works on the principle of two components (the host and the guest) connected through π-π or n-π conjugation i.e. hydrogen bonding or π-stacking interactions. A common example of this type of fluorophore is illustrated in Figure 1.20. The crown ether moiety binds to the analyte selectively through electron donor/acceptor interactions between the analyte and receptor.
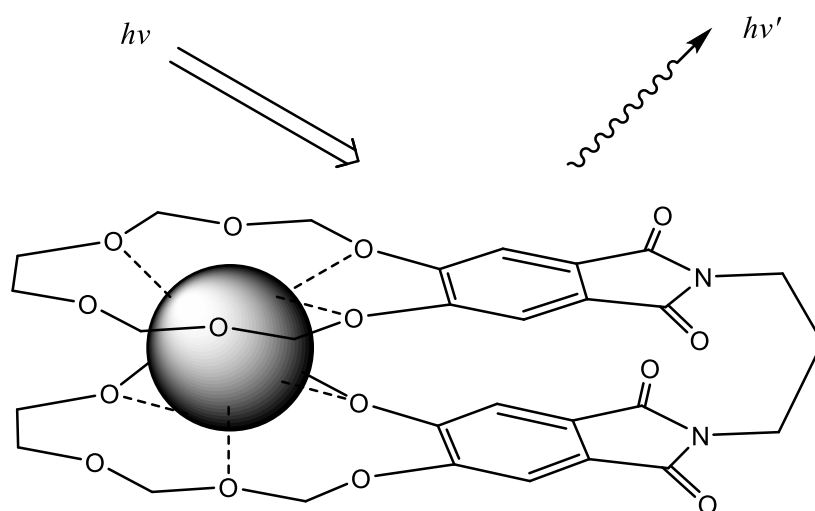
Figure 1.20 - Example of crown ether ligand sensor with a fluorophore. The dashed lines represent the hydrogen bonding between donor and acceptor that occur upon binding. hv is incident light and hv' is the emitted light of lower energy due to internal charge transfer.

The mechanism of energy transfer is achieved by means of modulating energy and electron transfer process between an energy accepting and energy donating moiety or electron donating and electron accepting moiety, most commonly hydrogen bonding. It is the coming together of occupied and unoccupied orbitals between the two components which leads to an energy transfer and it is this that can be detected as an observable energy release through an increase in the intensity of the emission spectrum. Fluorescence is a highly versatile technique that can be applied in real time, using low concentrations of the sensor, and fluorescence emission can be easily detected using inexpensive instruments.

Synthesising and validating the binding of host-guest molecules can be very time-consuming, especially if the host molecules synthesised result in poor binding with the target. It may be possible to minimise the chance of unsuccessful host molecules, by applying the concept of *in silico* molecular dynamics.

1.6 Metadynamics Analysis of Host-Guest Interactions

1.6.1 Molecular Dynamics

Molecular dynamics is a rapidly growing field, providing a link between the microscopic nature of molecular interactions and the macroscopic world of laboratory-based reactions[113]. Ultimately, the aim is to draw links between *in silico* studies and experimental studies in order to develop a greater understanding of how chemical systems work. Applications range from fundamental studies such as equilibria to more complex biomolecular systems[114].

Molecular dynamics can be used to study host-guest binding in a system and to predict the position and movement of these molecules to study potential binding sites. Understanding complex laws of motion and how they can be applied in bulk chemical systems makes molecular dynamics a powerful tool. In order to draw direct links between experimental work and *in silico* simulations the physics applied to the system must be ideal. There are number of factors that need to be taken into account when applying such algorithms. Molecular structures are complex and require a deep understanding of the constraints and interactions that can occur, namely bonding and non-bonding interactions. In a molecule there are a number of degrees of freedom, with rotational and intramolecular potentials being important. For example, every molecule will have a set torsional angle, which is the angle of the atoms in relation to the plane of the molecule (Figure 1.21). The flexibility of each atom from the plane of the molecule will be different and therefore, the constraints associated with each potential angle must be explored in the algorithms applied to the system. The same is true for the electronic effects between molecules. It is for this reason that appropriate application of force fields and constraints are

vital to producing reliable data that is comparable to experimental data. A good force field underpins all modelling and molecular dynamic investigations.
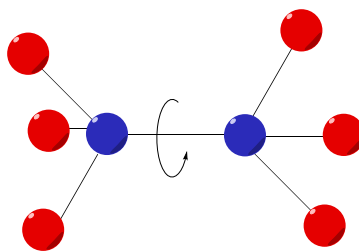
Figure 1.21 - The torsion angle shown in the plane of the molecule is the twist seen along a bond in a molecule.

When studying host-guest interactions the free energy of the system is an important factor to evaluate, as it allows for quantification of the energy of complexation at any given point in a simulation. One of the limitations associated with traditional molecular dynamics is that it cannot predict the free energy of a system, as it would take an infinite amount of time to sample the entire system. In order to predict free energy, mapping of the entire energy profile is required as opposed to taking averages over a set timescale. This is nearly impossible due to the large computational cost involved. The recent branch of molecular dynamics, metadynamics, has been applied to this area due to its less computationally expensive sampling approach to study chemical systems.

1.6.2 Metadynamics

Metadynamics is less computationally expensive than molecular dynamics. It allows for the acceleration of rare occurrences in a system, as described by complex Hamiltonians, which takes into account both the sum of the kinetic energy and the potential energy of the particles[115]. Metadynamic systems are described by a few collective variables (CV), also known as degrees of freedom. During a simulation, the location of the system is determined by the pre-set CVs. The CVs and the free energy at any given point of the system during a simulation are used to produce a positive Gaussian potential which is added to the real energy of the system (Figure 1.22). By doing this it prevents the system from returning to a position it has previously explored. This is repeated throughout the simulation, forcing the system to explore the full energy landscape, at a much lower computational cost than that of traditional molecular dynamics. Once produced the energy profile is the reverse of the sum of applied Gaussians.
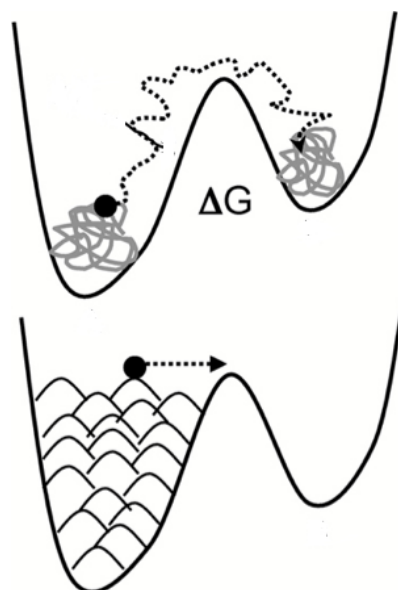
Figure 1.22 - Representation of the addition of Gaussians potentials to escape free energy minima, to overcome ΔG, to explore the entire energy landscape of the system. Each hump in the lower energy potential represents the addition of one Gaussian potential (adapted from [116]).

The size of the Gaussians applied to the system primarily determine the accuracy of the energy profile that was created. However, the smaller the Gaussians the more that need to be applied in order to achieve a full energy profile, which in turn results in a higher computational cost. Therefore, an appropriate compromise between the two should be found for optimum simulation conditions. Without the addition of Gaussian potentials (as in traditional molecular dynamics) the simulation has to naturally overcome ΔG which leads to prolonged simulations times

The studies will generate free energy values as a function of the CVs i.e. the distance between the two probes, one in the guest and the other in the host molecule. This is achieved by forcibly moving the guest molecule towards and away from the host within a given simulation radius. By using this approach it allows for the guest and host molecule interactions to be analysed in a relatively short processing time because the molecules follow a reconstructed map of the free energy in the system[115,117]. As a result, a comprehensive study of the energy landscape of a system is generated by providing a means for escaping local energy minima, consequently providing a platform to study rare events between molecules in real-time.

The parameters and restrictions applied to a system are vital in achieving accurate data. Different systems require unique parameters based on the molecules in the system. The application of different force fields takes into account the variation in the level of constraints for molecules, as dynamics are designed to mimic nature as much as possible *in silico*.

To ensure the application of the metadynamics analysis is robust and effective, it is necessary to understand and assess, prior to running the simulation, the different parameters that can be applied from the algorithm to calculate conformational energy of the molecules, to the force fields used, as well as taking into account the effect that solvent has on a system.

1.6.2.1   Implicit and Explicit Solvation

Accurate models of molecules in solution using molecular mechanics requires a realistic model for calculating interactions that solvent can form in the system. To achieve this, calculations using both implicit and explicit solvent are necessary as they use different approaches for studying liquid state dynamics.

Implicit solvation treats the solvent system as a continuous medium as opposed to individual 'explicit' solvent molecules. Using implicit solvent allows for approximations in a system to be made that are computationally efficient, thus allowing for calculations to be carried out that would not be feasible when using explicit solvent due to the high computational cost. However, the approximations made by implicit solvent models can sometimes lead to inaccurate results[118]. For example, implicit water doesn't take into account entropic terms, such as the hydrophobic, viscosity and hydrogen bonding effects. These effects are critically important when studying liquid state interactions.

Conversely, explicit solvation uses thousands of discrete solvent molecules in a system which allows for the inclusion of entropic effects[118]. This requires a large amount of central processing unit (CPU) time compared to the equivalent implicit system. This restricts simulations using explicit-solvation to smaller system sizes and simulation times to within the tens of nanoseconds[119], unless using a supercomputer. Nevertheless, without increased parametrisation of implicit solvent systems to take into account entropic terms, molecular mechanics is still limited to the use of explicit solvation to achieve *in silico* models with higher accuracy.

1.6.2.2   Conformational Energy Searching

Molecules can adopt more than one low energy conformation which may differ only slightly in their energy values[120]. It is important to appreciate the range of low-energy conformations that are likely to be adopted by the host molecules to take into account any significant conformational changes that may arise. This is achieved by performing a conformational search.

Conformational searches can be divided into two general categories, systematic methods and Monte Carlo methods. The systematic method is used for molecules that ideally have less than seven flexible torsional angles. The number of flexible bonds is directly proportional to the number of structures generated and therefore, the larger the molecule the more structures there are to analyse and the

longer the processing time, as demonstrated in a case of predicting conformations of cyclo-hexapeptides[121]. The second method for conformational searching is the Monte Carlo method, which is an estimation procedure[122]. For larger molecules, the Monte Carlo method is a good alternative to the systematic method. In the Monte Carlo method, the position of atoms in the molecules are randomly changed by Cartesian coordinates, or by randomly changing the dihedral angle of bonds in the molecule. This generates a new conformation which is subsequently minimised[122]. The process is repeated and the resultant structures are sorted and compared according to their energies, generating a list of different conformers. The Monte Carlo method incorporates probability into the analysis, to predict whether a scenario that can happen, will actually occur in a system; such as the probability that the energy of a molecule resulting from the minimised conformation is accurate. It is the average of the generated energy values that allows for a Gaussian distribution curve to fall around the true value which in this case is the local minimum energy of a structure.

It is important for searches to locate low-energy conformations quickly but they must also return a range of conformations that are representative of all the possible conformations for a molecule. Monte Carlo methods provide a good approach that combines both efficiency and completeness.

Once identified, the minimum energy conformation can then be used to carry out metadynamics. It is possible to carry out these searches in a number of different environments e.g., water, dimethylsulphoxide (DMSO), air and vacuum. Therefore, it is essential to select the environment that approximates the conditions of the experimental work being conducted. For example, largely hydrophobic compounds are likely to show vastly different conformations in water than in DMSO or air due to hydrophobic effects. This must be taken into account when designing the method. Conformational searching takes into account implicit water in a system, this means that the interaction of water molecules with the molecules of interest is not directly represented. The addition of entropic terms that occur in metadynamics may lead to interactions that are not seen when carrying out conformational searching in implicit solvation.

Conformational searches also do not take into account thermal effects and are run at a predetermined temperature[123]. However, fluctuations in the temperature of a system can affect the conformation of a molecule. Sensors applied in real life are likely to be affected by thermal effects. Therefore, it is important to understand what changes may occur or how stable a predicted conformation is when explicit solvent and changes in temperature are added prior to carrying out metadynamics on the system, in order to contextualise the results obtained. This can be achieved using simulated annealing.

1.6.2.3   *Simulated Annealing*

Simulated annealing is a molecular dynamics technique used to investigate the stability of conformers and probe whether minima are global or local (Figure 1.23). It takes into account not only thermal effects on a system but also the effect of explicit water on the system.
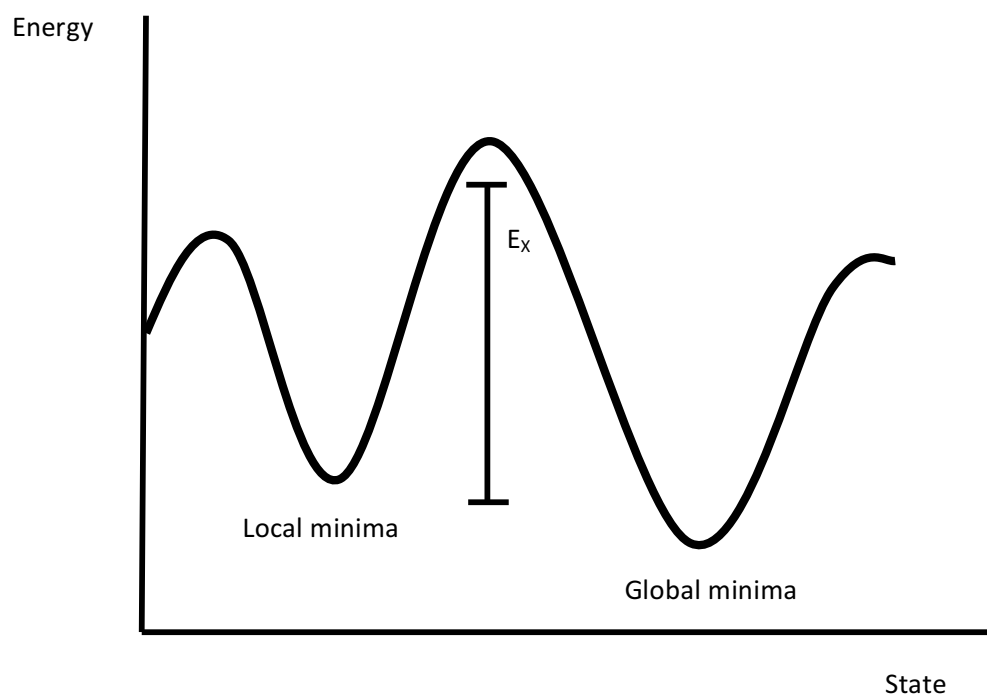
Figure 1.23 - A schematic representation of simulated annealing where E$_x$ denotes the thermal energy required to force the search from local minima to global minima.

The effect on a starting structure conformation when it is heated to a high temperature is simulated [124] i.e., what happens to the structure when the atoms have high thermal mobility.

The structure is then allowed to cool. The cooling process allows the structure to evolve to an energetically favourable final structure, which may differ from the starting one. This is a very useful process for studying the relationship between conformations and thermal energy which are invaluable in understanding the stability of predicted conformations. It is of particular importance for host molecules as interactions are distance (and sometimes direction) dependent; with a small change in conformation leading to unexpected changes in interactions with the guest molecule. The representative conformation determined using simulated annealing can be compared to the results of conformational searching to understand both thermal and solvent effects in a system. The representative conformation is then carried through to metadynamics to ensure that simulations are

started from the most stable structure. Metadynamics is a technique that is not often used to study the complexation of small molecules. Therefore, in order to validate a method, it is necessary to use proven experimental data.

1.7 Aims & Objectives

As there is a need for rapid, sensitive and selective in-field detection probes for the growing number of NPS, the primary aim of the project is to develop a selective sensory probe for the amphetamine-related new psychoactive substances. In order to achieve this, a novel approach will be adopted so as to ensure both selectivity and sensitivity. To ensure selectivity it is first imperative to understand against what the probe needs to be selective. At the commencement of this project, aminoindanes were still uncontrolled and believed to be the 'next wave' of NPS, whereas cathinones were controlled, and their popularity had remained consistently high. Therefore, it was proposed to explore a sensory probe for both aminoindanes and cathinones. Aminoindane internet products are easily purchased due to their legal status and therefore, they will be studied to understand their composition. Aminoindane internet samples will be fully analysed using HPLC and GC-MS to determine the common excipients present in internet samples, and also to quantify the concentration of active ingredient present (Chapter 2). This will help to determine the selectivity and sensitivity needs for the sensory probe.

Protein-ligand interactions will be studied based on the findings from the aminoindane analysis, and an in-depth literature review regarding cathinone street sample composition. Naturally occurring protein-ligand interactions are both selective and sensitive, and therefore by taking inspiration from nature a rationally designed host molecule based on these interactions will be developed. The examination of protein-ligand interactions for cutting agents, drugs of abuse and endogenous psychoactive substances with similar structures to both aminoindanes and cathinones will ideally allow for the development of a three-dimensional pharmacophore model (Chapter 3). A validated methodology will be developed for this analysis so that it is possible to apply such work to future sensor development to improve selectivity and aid in the design of potential host molecules. In order to design a selective sensory molecule, a representative drug from both the aminoindane and cathinones classes will be chosen upon which to design each of the pharmacophores. As discussed above, the original NPS mephedrone, is still widely abused and remains a big problem in relation to public health. The complex pharmacological profile of mephedrone goes someway to explaining why, even once controlled mephedrone has remained a popular drug of abuse. There is still a lack of effective in-field detection devices that are both selective and sensitive for mephedrone, and it is for

these reasons that mephedrone will be the primary target for the development of a sensory molecule (Chapter 3 and 4).

The binding features extracted to develop the pharmacophore model will be applied to the design of a host molecule. Knowledge of supramolecular chemistry and ideal host-guest binding will be applied to develop a host molecule which incorporates binding features, such as potential hydrogen bond donor/acceptors or aromatic functionalities for π-stacking interactions and will aid in the consensus design of potential host molecules (Chapter 4).

Based on the pharmacophore two different host scaffolds will be explored for this work, one flexible host molecule (acyclic) and one rigid host molecule (macrocycle) (Chapter 4). Upon synthesising the potential host molecules, full binding studies will be carried out using a number of spectroscopic techniques including NMR, UV/Vis and fluorescence spectroscopy. Additionally, mass spectrometry will be used, as a confirmatory technique. This will allow for binding constants to be calculated between the host and guest molecules. Binding of the host molecule will be examined against common cutting agents and drugs of abuse, identified from the aminoindane analysis and pharmacophore development to ensure selectivity. The host molecule will then be tested against a potential simulated street sample to ensure there is no cross-reactivity (Chapter 5).

Finally, the developed host molecule will be analysed *in silico* using metadynamic simulations (Chapter 6). This will help to establish if a consensus between experimentally observed binding and computationally binding can be achieved. This will be used in an attempt to accelerate and improve the process of host molecule design for NPS in the future, ultimately allowing sensor development to keep up with the rapidly growing field of NPS.

Chapter 2   Identification and Quantification of Aminoindanes in Internet Purchased NPS Products

2.1 Introduction

Understanding the complex matrix of new psychoactive products is important for considering the possible difficulties of in-field detection. Not only is it essential to recognize the array of bulking agents or cutting agents that may be present in street samples, but also the concentrations in which the active ingredient is found. This will help to determine not only the selectivity required but also the sensitivity regarding detection limits. Government analysis reports have shown that the cutting agents present do not vary substantially between the different classes, with the most common being reported as benzocaine, caffeine and lactose[125]. It is however the relative concentrations of the active ingredients that vary the most[125].

As stated in Chapter 1, at the commencement of this project in 2012 aminoindanes were believed to be the next stimulant NPS of interest. This was due to their amphetamine-like structures, which were believed to exert a similar physiological response to the popular cathinone and amphetamine classes[30]. It was decided that for this project two sensory molecules would be developed; one for the already established and controlled cathinone class, and another for the uncontrolled aminoindanes, so as to stay ahead of the rapidly adapting NPS market. In order to develop a sensory molecule, it is first important to understand first-hand the composition of products, to inform how a sensory molecule must work. Cathinones are controlled and consequently it was not possible to purchase them; however, aminoindanes are legal and hence they are still commercially available. Therefore, aminoindane internet products were purchased, and subsequently analysed. The analysis of aminoindanes still has the potential to guide the design of the cathinone sensory molecules, as well as the aminoindane sensor as reports from Laboratory of the Government Chemist (LGC) have shown that there is a large degree of overlap in the constituents found in both of these classes of compounds[19,125–127].

2.1.1 NPS Class of Interest; Aminoindanes

One group of NPS that have been re-classified into a specific drug family by the European Monitoring Centre for Drugs and Drug Addiction (EMCDDA) are the aminoindanes[128]. Aminoindanes are conformationally rigid analogues of amphetamines and were first synthesised by Nichols *et al*. for their serotonin neurotoxicity effects[129]. A number of aminoindanes have been available *via* internet

retailers since 2010, most notably 5,6-methylenedioxy-1-aminoindane (MDAI), 5-Iodo-2-aminoindane (5-IAI) and 2-aminoindane (2-AI)[32].
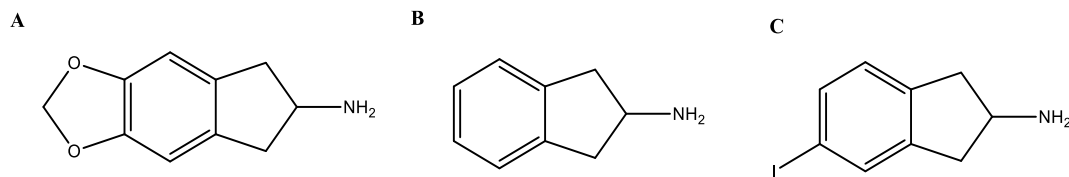
Figure 2.1 - Chemical structures for the three most common aminoindane derivatives, A. 5,6-methylenedioxy-1-aminoindane (MDAI), B. 2-aminoindane (2-AI) and C. 5-iodo-2-aminoindane (5-IAI).

Although uncontrolled in the UK up to the recent blanket ban on NPS, internet availability of these substances shifted over the last six years, where 5-IAI was suggested to be the new 'must have' NPS after the control of mephedrone in 2010[30], and in recent years the abuse of MDAI has risen significantly[130]. Until May 2015, the aminoindanes most commonly reported to the United Nations Office of Drugs and Crime (UNODC) were MDAI, 5-IAI and 2-AI[131]. As with many NPS, studies into the chemical characterisation of aminoindane products is limited as they are relatively new substances of misuse. In order to aid identification, Casale *et al*. reported the chemical characterisation of pure 5-IAI and its isomer 4-IAI, 5,6-MDAI and its isomer 4,5-MDAI using GC-MS, NMR and FT-IR[43,44]. A few studies have investigated the products of aminoindanes; however, these are usually limited to one or two products as part of a larger study[32,44,47,132]. A more comprehensive study looked at seven aminoindane products using GC-MS for identification purposes only. They identified MDAI and a range of adulterants where one product was suspected to have unknown inorganic material[40]. On-site testing methods were investigated for aminoindane products using microcrystalline tests[63], electroanalytical sensing[133] and handheld Raman spectroscopy[134] where the % w/w of the active ingredient and the adulterants present greatly influenced positive identification. Thus, there is a need to further investigate the quantities of active ingredients in these samples, to understand how this might affect the design of a sensory molecule.

At present there remains a lack of information regarding the full chemical identification and quantification of NPS products, including aminoindanes. This lack of information regarding the aminoindane class means it is hard to identify which of the aminoindane class is most prevalent in products, making it difficult to identify an individual target for a sensory molecule. In order to develop a selective sensory molecule it is important to understand what the molecule needs to be selective against, i.e. cutting agents and adulterants. It is also important to understand the concentration of active ingredient present in these products. This allows for a deeper understanding into the limits of detection that will be required for a sensory molecule. Therefore, the aim of this study is to identify

and quantify the major molecular constituents in internet purchased aminoindane products. This information can then be carried forward for the rational design of sensory molecules.

2.2 Experimental

2.2.1 Chemicals and Reagents

Analytical grade standards of 2-aminoindane hydrochloride (2-AI.HCl) and caffeine were purchased from Sigma Aldrich (Dorset, UK). The reference standards MDAI.HCl and 5-IAI.HCl were obtained from LGC standards (Teddington, UK). HPLC grade methanol, acetonitrile, water and *ortho*-phosphoric acid were purchased from Fisher Scientific (Loughborough, UK). A total of 11 products, labelled to contain an aminoindane analogue, were purchased online between February 2012 and May 2013 from seven different UK-based internet retailers. Samples prepared for chromatography analysis were placed in clear DP ID 2 mL glass vials, fitted with PTFE/silicone septa certified caps.

2.2.2 Gas Chromatography-Mass Spectrometry (GC-MS)

GC-MS experiments were performed using a Varian 450 ion trap GC and 240 MS. Analysis was done using both chemical ionisation (CI), with methane, and electron ionisation (EI) with a scan range of 40 - 1000 *m/z*. Ion trap, manifold and transfer line temperatures were set to 150, 50 and 250 $^{\circ}$C, respectively. Gas chromatographic separation was achieved using a Varian FactorFour 5 % phenyl-methyl capillary column (30 m x 0.25 mm x 0.25 μm) using helium as a carrier gas (1 mL min^{-1}) and a split ratio of 10:1. The column was heated to 50 $^{\circ}$C for 2 min following sample injection, increased to 300 $^{\circ}$C (15 $^{\circ}$C min^{-1}), held for 5 min and then cooled back to 50 $^{\circ}$C (50 $^{\circ}$C min^{-1}), with a total run time of 28.7 min. Solutions were prepared of each product using methanol (0.1 mg mL^{-1}) and filtered (0.2 μm PTFE membrane filters) prior to analysis. Mass spectra of selected peaks were compared to purchased reference standards and an in-house National Institute of Standards and Technology (NIST) and Scientific Working Group for the Analysis of Seized Drugs (SWGDRUG) library.

2.2.3 High Performance Liquid Chromatography (HPLC)

Reverse phase HPLC analysis was performed using an integrated Perkin Elmer Flexar system fitted with an in-line degasser, 100-place auto injector and a photodiode array (PDA) detector (recording 268 nm). Data analysis was carried out using Chromera-flexa software version 3.4.0.5712. Two Phenomenex C18 columns (150 x 4.6 mm) were used for the analysis, a core kinetix 5 μ XB and a non XB 5 μ column, both fitted with a guard column (AJ0-8768 C_{18}). A gradient solvent system was used where mobile phase A was composed of HPLC grade water and *ortho*-phosphoric buffer (pH 2.1), and mobile phase B was HPLC grade acetonitrile. The gradient method was 90 % mobile phase A increasing

to 50 % over 15 min with a flow rate of 1.5 mLmin^{-1} using an injection volume of 5 μL. Both mobile phases were vacuum filtered through a 0.44 mm pore nylon filter and degassed for 10 min at 25 ^{o}C using an ultrasonic bath prior to use. Stock solutions of caffeine, MDAI, 2-AI and 5-IAI (0.5 mg mL^{-1}) were prepared by adding 1.0 mg of each component weighed accurately into a 2 mL volumetric flask and made up to volume with methanol/water (50/50 v/v). The remaining calibration standards (i.e., 0.1, 0.05, 0.025, and 0.01 mg mL^{-1}) were prepared by serial dilution. The method was validated to evaluate specificity, linearity accuracy, precision, LOD, LOQ, and robustness[135]. Specificity was evaluated by ensuring acceptable resolution between each aminoindane and caffeine at ≥ 2. The correlation coefficient was used to determine the linearity (r^2 ≥ 0.999). The accuracy and precision was determined using known concentrations of each standard at high, medium and low levels (n = 6). The LOD (i.e., (3.3*standard error of the intercept)/slope) and LOQ (i.e., (10*standard error of the intercept)/slope) was calculated using the calibration curve. Three sets of standards were prepared on different days to evaluate robustness.

2.3   Results and Discussion

2.3.1   Gas Chromatography-Mass Spectrometry (GC-MS)

GC-MS is a commonly used technique for routine analysis of psychoactive substances, which has been utilised for a number of drug classes to analyse volatile components[47,136]. In this study eleven aminoindane products were purchased from seven UK distributers between February 2012 and May 2013. Primary characterisation was based on the implementation of GC-MS analyses. All mass spectral peaks with a relative abundance greater than 10 % of the base ion peak were analysed and results are shown in Table 2.1.

Table 2.1 - GC-MS results for all eleven products using chemical and electron ionisation[1].

Product name	GC-MS Retention Time (min)	Fragmentation (m/z)[a]	Confirmatory Peak CI (m/z)	NIST Library Match
P1: 2-AI	13.79 ± 0.06	42, 56, 65, 84, 91,115, 136, 144, 163, *172*	247 (M-1) 249 (M+1)	Unknown
	14.21 ± 0.07	42, 55, 67, 82, 94, 109, 122, 137, 150, 165, *194*	193 (M-1) 195 (M+1)	Caffeine
P2: 2-AI	8.903 ± 0.003	65, 77, 89, 91, 118, 130, *133*	132 (M-1) 134 (M+1)	2-AI
P3: 5-IAI	12.474 ± 0.007	42, 50, 63, 77, 91, 102, 118, 130, 149, *160*, *177*	176 (M-1) 178 (M+1)	MDAI
	14.20 ± 0.04	42, 55, 67, 82, 109, 137, 165, *194*	193 (M-1) 195 (M+1)	Caffeine
P4: 5-IAI	7.75 ± 0.06	42, 51, 65, 78, 91, 103, *133*	132 (M-1) 134 (M+1)	2-AI
P5: MDAI	12.5 ± 0.2	42, 51, 63, 77, 91, 103, 150, *160*, *177*	176 (M-1) 178 (M+1)	MDAI
P6: MDAI	8.94 ± 0.03	42, 50, 63, 91, 105, 116, *133*	132 (M-1) 134 (M+1)	2-AI
P7: MDAI	12.27 ± 0.05	42, 63, 91, 118, 130, 149, *160*, *177*	176 (M-1) 178 (M+1)	MDAI
P8: MDAI	NA	NA	NA	NA
P9: Pink Panther	12.5 ± 0.2	42, 65, 73, 91, 102, 118, 130, 149, *160*, *177*	176 (M-1) 178 (M+1)	MDAI
	8.45 ± 0.02	53, 57, 97, 124, 140, *155*	155 (M) 156 (M+1)	MPA
P10: Pink champagne	9.11 ± 0.08	42, 50, 63, 77, 91, 103, 116, *133*	132 (M-1) 134 (M+1)	2AI

	14.19 ±0.04	42, 55, 67, 82, 94, 109, 137, 165, *194*	193 (M-1) 195 (M+1)	Caffeine
P11: Blurberry	9.07 ± 0.09	42, 51, 63, 77, 91, 103, 116, *133*	132 (M-1) 134 (M+1)	2AI
	14.24 ± 0.07	42, 55, 67, 82, 94, 109, 121, 136, 165, *194*	193 (M-1) 195 (M+1)	Caffeine

[a] All numbers in bold represent the molecular ion peak [M+]: All numbers in italics represent the base ion peak.

The standards were initially run to determine the retention time of reference compounds, 2-AI eluted at 8.6 min, MDAI at 12.2 min, 5-IAI at 12.8 min and caffeine at 14.1 min. Each of the standards showed distinct fragmentation patterns using the EI ionisation, with high intensity molecular ion peaks seen for all standards. Fragmentation patterns are in good agreement with that observed by Baron *et al.*[47].

P1 contained two peaks in the GC; caffeine *m/z* 194 and an additional peak that gave a positive match for methylphenidate. Methylphenidate is a psycho stimulant drug approved for the treatment of attention deficit hyperactivity disorder (ADHD) that is commonly abused for its stimulant properties. The EI fragmentation of methylphenidate found in P1 was in good agreement with that seen for the methylphenidate standard (60 %), both showing no presence of the molecular ion peak. However, when methylphenidate standard was run the retention times of the two peaks did not correlate, 13.78 min for the sample and 11.21 min for the standard. The second highest match in the library was ethyl phenylacetate, a food flavouring, with a lower match of just 30 %. Analysis using chemical ionisation showed a molecular ion peak of *m/z* 248 which does not match with the molecular weight of methylphenidate (233 gmol^{-1}) or ethyl phenylacetate (164 gmol^{-1}). However it does relate to ethylphenidate, an analogue of methylphenidate which is also been known to be abused. However, the retention time for ethylphenidate standard, again does not match that of the unknown peak. All of these compounds have both aromatic and ester functionalities, which is common to a number of organic drug-like molecules. Therefore with the information collected no conclusion can be provided as to the identity of the unknown peak.

The aminoindanes all showed similar characteristic fragmentation patterns corresponding to the loss of NH_3. The presence of 2-AI at 133 *m/z* was detected in five products (P2, P4, P6, P10 and P11) including four products not labelled to contain 2-AI (P4, P6, P10 and P11). The fragmentation patterns and retention times for 2-AI were consistent with that seen for the standards. However, P1 did not contain any of the reputed drug, 2-AI, instead just caffeine was identified, base peak *m/z* 194. 2-AI has not previously been reported to be a common component of aminoindane products. Yet, the most

common combination found in the products (P10 and P11) analysed was a mixture of 2-AI and caffeine which was found in two of the products, while caffeine was found with MDAI in one product (P3). More worrying was the presence of an additional active ingredient, methiopropamine (MPA) molecular ion *m/z* 155; in combination with MDAI in Pink Panther (P9). The retention time of MPA was found to match the standard, with the base ion peak at *m/z* 155. MPA is a new psychoactive stimulant that is structurally related to methamphetamine that was first sold in the UK in 2010 under the name street name Blow[137]. Interestingly, Baron *et al.* also found the presence of MPA in combination with MDAI in Pink Panther samples they purchased in 2011[47]. The MPA/MDAI combination is now commonly seen on legal high websites sold under the product name M&M's[138].

Blurberry was found to contain 2-AI and caffeine, which are the reputed active ingredients. All branded products (P9-11) claimed to contain an aminoindane, although they did not state which one, as well as caffeine as the active ingredients. Pink Champagne (P10) was purchased from the same supplier as Blurberry (P11) and was found to contain the same active ingredients, 2-AI and caffeine; their physical appearance was also similar. Both Blurberry (P11) and Pink Champagne (P10) proved difficult to homogenise and dissolve in methanol as small amounts of insoluble solid material was also present even after sonication and vortexing, suggesting inorganic bulking agents. The remaining solid was filtered out before analysis. This highlights that when designing a sensor, inorganic constituents need to be taken into account along with organic. Their apparent lack of solubility in organic solvent may mean it is possible to filter out inorganic bulking agents before analysis using a sensory molecule, which could reduce the risk of interference. However, this may not be true for all inorganic bulking agents.

Two products, P3 and P4, reputed to contained 5-IAI were analysed, but neither were found to contain the molecular ion at *m/z* 259, which as seen in the standard, is characteristic of 5-IAI. However, P3 contained caffeine and MDAI while P4 contained 2-AI. Earlier studies conducted by Bond *et al*. did identify the presence of 5-IAI in samples from two different suppliers both labelled as pure 5-IAI[16]. However, in more recent studies 5-IAI was not found in a number of products labelled as 5-IAI[47].

2.3.2 High Performance Liquid Chromatography (HPLC)

To date, GC-MS has proved to be the most commonly applied analytical method to determine aminoindane product content; however, this has been limited to identification only[32,40,47]. In this study, a liquid chromatography method was developed to quantify aminoindane derivatives (i.e., 2-AI, 5-IAI and MDAI), but also to investigate any non-volatile constituents. An initial HPLC chromatographic method was developed by analysing a standard mixture stated above, using a Phenomenex Kinetex 5 μ C18 column. Four standards, 2-AI, MDAI, 5-IAI and caffeine, were analysed

to examine their chromatographic properties e.g. peak shape and tailing due to the amine functionalities. The analytes eluted at 1.67 (2-AI), 2.2 (MDAI), 6.9 (5-IAI) and 3.2 min (caffeine). However, tailing and poor resolution were observed with each compound (Figure 2.2).
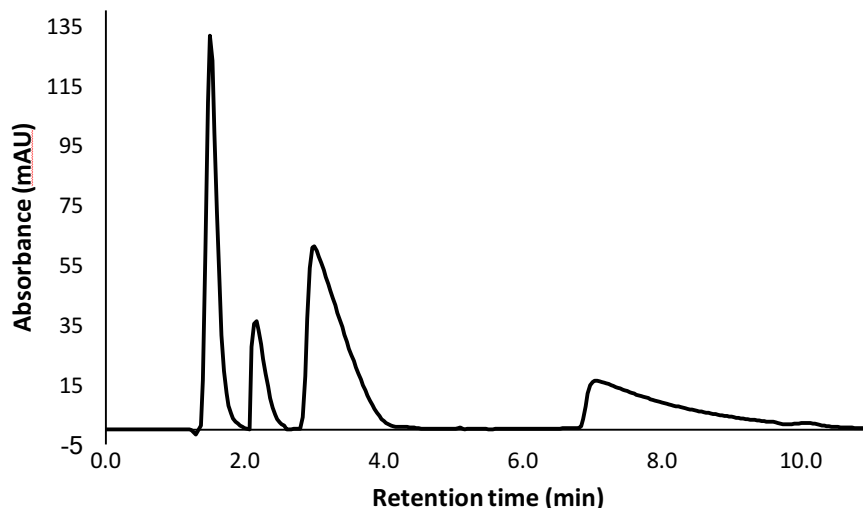
Figure 2.2 - HPLC separation of 2,AI, MDAI, caffeine and 5-IAI standards on a 5 μ C18 column 150 x 4.6 mm, AJ0-8768 C18 guard column, ACN/aqueous *ortho*phophoric acid (pH 2.1), λ= 268 nm.

This is likely due to the interaction of the branched amines of the aminoindane derivatives with the stationary phase[139]. Despite the structural similarities between 2-AI and 5-IAI, the presence of iodine in 5-IAI caused it to eluted later in the run. This is due to iodine having strong interactions with the stationary phase leading to increased peak broadening for 5-IAI. In an attempt to improved resolution, a Kinetex 5 μ C18 XB column was used to reduce tailing (Figure 2.3). Both the C18 and the XB-C18 column have the same dimensions (150 x 4.6 mm) and particle size (1.7 μm). 5-IAI showed the most pronounced improvement with the peak width at base reducing from 3.6 to 0.2 min, while 2-AI improved from 0.4 to 0.2 min. As predicted, the XB column helped to improve peak shape for basic compounds through addition of di-isobutyl side chain which end caps the underivatised silanol phase.
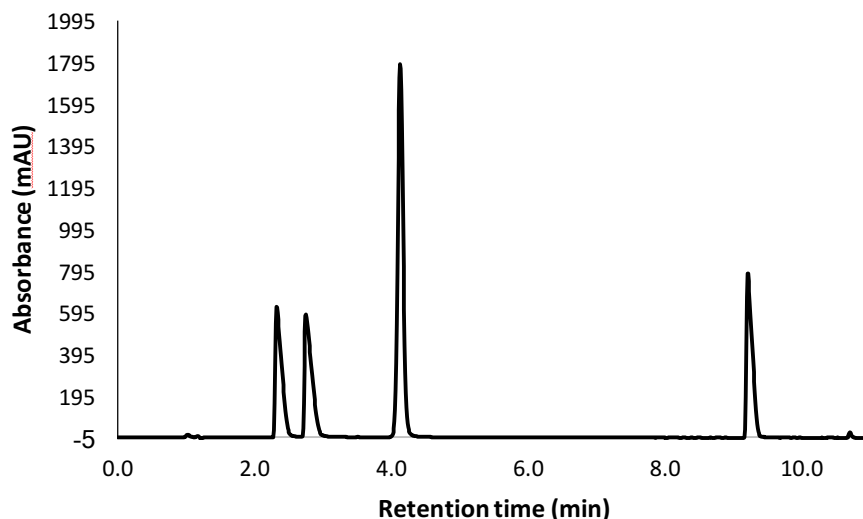
Figure 2.3 - HPLC separation of 2-AI, MDAI and 5-IAI using the XB-5 µ C18 column 150 x 4.6 mm, AJ0-8768 C18 guard column, ACN/aqueous *ortho*phophoric acid (pH 2.1), λ= 268 nm.

A large number of NPS contain at least one amino group including cathinones, tryptamines and cannabinoids. Therefore, the application of this method in terms of the separation of amines could be wide reaching. In addition to this halogens, have become a common addition to NPS structures[41]. Therefore, understanding how 5-IAI interacts with the stationary phase differently due to the presence of iodine, could be applied to future NPS studies.

Peak purity was determined for each peak in the study through use of the photo-diode array detector. The UV spectrum of each chromatogram was studied, to ensure that no additional absorbance from other substances could be observed at the same retention time. This confirmed that there is no additional analytes coeluting with the compounds of interest, which is possible in a complex mixture, which can often contain structurally related analogues not stated on packaging. If the peaks were not pure then quantification of substances would be inaccurate.

The method was evaluated according to the International Conference on Harmonisation (ICH) guidelines for validation of analytical procedures[135]. The following validation characteristics were assessed: linearity, accuracy, precision and specificity (Table 2.2). Calibration standards for a five point curve were prepared and demonstrated a linear response (r^2 = 0.999) over a range of 0.01 - 0.5 mg mL^{-1}; with good repeatability for each concentration (RSD = 0.1 - 2 %)[140]. The accuracy was determined by recovery of known concentrations of each standard at high, medium and low levels in methanol in the calibration range. Both 2-AI and caffeine showed recovery values within 13 % of the expected. For all compounds the recovery was found to be within 10 % of the expected concentration value. LOD values were calculated for caffeine, MDAI, 2-AI and 5-IAI as 3.2, 2.9, 2.5 and 3.2 µgmL^{-1}, respectively.

Limits of quantification were found to be 9.8, 7.6, 8.7 and 9.6 µgmL^{-1} for 2-AI, MDAI, 5-IAI and caffeine, respectively. Previous studies for caffeine carried out by Srdjenovic *et al*. reported an LOD of 0.7 µg ml^{-1} [141]. The LOQ's for all four compounds were relatively high compared to published data on similar drugs of abuse[132,142]. This may be due to the accuracy and repeatability around the LOD being relatively poor, which leads to a higher error associated with the intercept and slope leading to a higher LOD value. This was likely caused by limitations of the instrument used. The HPLC used for this study had two single piston pumps; this caused non-continuous delivery of solvent resulting in higher baseline noise levels which in turn affects the LOD. However, all target concentrations were above the LOQ, with adequate accuracy and recovery values. Previous studies for calculation of the LOD for calibration curves heavily weighted at low concentrations have found that using the error of the intercept as opposed to the error of the slope leads to a lower calculated value for LODs and LOQs[143,144]. On comparison of the two methods this was found to be true for each of the four standards in this study. Therefore, the method has been found to be fit for purpose.

Table 2.2 - Summary of validation data for the quantification of 2-AI, MDAI, caffeine and 5-IAI obtained using a 5 µ XB-C18 Kinetic Column (150 x 4.6 mm), AJ0-8768 C18 guard column, ACN/aqueous *ortho*phophoric acid (pH 2.1), λ= 268 nm.

	2-AI	MDAI	Caffeine	5-IAI
t_R (min)	1.04 ± 0.01	1.53 ± 0.04	3.12 ± 0.04	7.95 ± 0.05
LOD (µgmL^{-1})^a	2.5	2.9	3.2	3.2
LOQ (µgmL^{-1})^b	9.8	7.6	8.0	9.6
Precision (% RSD)				
0.025 mg mL^{-1}	1.6	2.4	1.7	3.2
0.1 mg mL^{-1}	0.88	0.97	0.36	0.57
0.5 mg mL^{-1}	0.93	0.73	1.0	0.56
Accuracy (%)				
0.025 mg mL^{-1}	99 ± 2	160 ± 2	113 ± 3	62 ± 3
0.1 mg mL^{-1}	87 ± 2	117.3 ± 0.3	107.3 ± 0.5	85 ± 1
0.5 mg mL^{-1}	99 ± 3	109.4 ± 0.7	102 ± 2	97.2 ± 0.7
Co-efficient of regression (r^2)	1.000	1.000	0.999	1.000

^{a} Limit of detection (calculated using the standard error of the intercept and the slope).
^{b} Limit of quantification (calculated using the standard deviation of the intercept and the slope).

Using the identification of constituents found in the GC-MS, HPLC was used to confirm identity and quantify the different constituents in the purchased products. HPLC analysis confirmed identification of product content found through GC-MS analyses as seen in Table 2.3. By using the reference standards, they were all confirmed to be the same constituents as identified by GC-MS. A GC-MS library search matched the unknown peak in P1 with methylphenidate; however, when the standards were examined by HPLC the retention times differed. Methylphenidate standard was found at 8.67 min while the unknown peak appeared much earlier at 3.27 min. The CI data from the GC-MS suggested that the compound could be ethylphenidate, despite the retention times not corresponding. The retention time for ethylphenidate on HPLC, using the same method was found to be 9.76 min. Unsurprisingly, due to their chemical similarity this is close to the retention time of methylphenidate. However, once the data shows no similarity to the unknown peak.

Table 2.3 - Quantification of HPLC results with confirmation of components found in GC-MS.

Product Name	HPLC Retention Time (min)	Total % w/w[a]	HPLC and GC-MS Confirmed Identity
P1: 2-AI	3.27 ± 0.01	unconfirmed	Unconfirmed
	3.20 ± 0.02	38.7 ± 0.4	Caffeine
P2: 2-AI	1.125 ± 0.007	88 ± 1	2-AI
P3: 5IAI	3.208 ± 0.002	22.9 ± 0.6	Caffeine
	1.656 ± 0.002	37 ± 2	MDAI
P4: 5-IAI	1.101 ± 0.004	67 ± 1	2-AI
P5: MDAI	1.55 ± 0.01	35.1 ± 0.5	MDAI
P6: MDAI	1.11 ± 0.02	94.4 ± 0.8	2-AI
P7: MDAI	1.550 ± 0.005	93 ± 2	MDAI
P8: MDAI	NA	NA	NA
P9: Pink Panther	1.641 ± 0.009	25.4 ± 0.5	MDAI
	1.62 ± 0.01	74 ± 1	MPA
P10: Pink Champagne	2.514 ± 0.006	13.2 ± 0.3	2-AI
	3.125 ± 0.008	17.3 ± 0.5	Caffeine
P11: Blurberry	1.117 ± 0.003	37.6 ± 0.8	2-AI
	3.131 ± 0.006	20.8 ± 0.9	Caffeine

[a] All concentrations were calculated as % w/w to 1 standard deviation.

Both the GC-MS and the HPLC data confirmed the presence of MDAI in four products (P3, P5, P7 and P9). Quantification by HPLC indicated that of these four products MDAI was found in concentrations ranging from 25.4 (P9) up to 94 % w/w (P6), which was the highest percentage of drug found in any of the products. HPLC results confirmed the presence of 2-AI and caffeine in both Pink Champagne and Blurberry (P10 and P11); however, the percentage composition was found to differ, with 13 and 38 % w/w of 2-AI found respectively. Caffeine concentrations of the samples were also not consistent with 17 % w/w in P10 and 21 % w/w in P11. Caffeine was also found in two further products at higher concentrations of 39 % w/w (P1) and 23 % w/w (P3). Caffeine is a common additive found in NPS

products due to its stimulant effect and ease of procurement. A number of previous studies have detected caffeine in NPS products[40,49]; however, the concentration of caffeine is often not reported. A study into the opioid *para*-fluorofentanyl (pFF) reported a range of 27.7 – 30.2 % w/w of caffeine in the six seized capsules[145]. This is comparable to the results found for the aminoindanes where the range of caffeine was detected at 17.3 – 38.7 % w/w. Concentrations of aminoindanes were found in the range of 13.21 – 94.4 % w/w. This is comparable to a study conducted into the content of cathinone products, which also found a large range of 11 - 85 % w/w of active ingredient, with a range of 12 - 42 % for the mephedrone containing products[146]. The identified content of Pink Champagne (P10) only accounts for 30.51 % w/w of the overall content. This is significantly lower than the other samples, and as shown in the label claim this suggests the presence of inorganic bulking agents that were not detected using either GC-MS or HPLC methods. The Pink Champagne label claims there are amino acid complexes, caffeine and cola vera as well as the active ingredients in the product. A study conducted by Comment *et al*. utilised inductively couple plasma-mass spectrometry/ atomic emission spectroscopy (ICP-MS/AES) to examine the possible inorganic constituents in ecstasy tablets[147]. They found large concentrations of calcium, magnesium and potassium all of which can be associated with bulking agents such as magnesium stearate and calcium carbonate, none of which are visible using HPLC or GC-MS. A report by the Centre for Public Health outlined all the reported cutting agents that have been found in illicit drugs as well as other contaminants such as fatal levels of lead[148]. It can be seen that it is not uncommon to find lower concentrations of active ingredients in NPS such as that seen in Pink Champagne (P10). Overall, 2-AI was found in consistently higher concentrations of up to 95 %. The increasing presence of 2-AI with aminoindane products has not been previously reported. HPLC analysis confirmed the GC-MS findings that no 5-IAI was detected in any of the products. It was previously stated that aminoindane drug labels appear to be used to cover for a mixture of substances not stated on the label[40]. Of the products analysed in this study, only 50 % contained the advertised compound.

2.4 **Conclusion**

Identification and quantification of eleven aminoindane products was carried out using GC-MS and HPLC. GC-MS was used for primary identification of products. Electron ionisation was carried out confirming the presence of four volatile organic components; caffeine, 2-AI, MDAI and MPA. An additional organic constituent was found; however, results were inconclusive as to the identity. Separation of all four peaks was achieved using an XB-C18 column giving minimal tailing, reproducible peaks and repeatability. These results were not observed using a C18 column with the same dimensions, where the amine functionalities cause peak broadening. This highlights the need for an XB-C18 column for amine based analysis, which is critical for NPS analysis. HPLC data confirms the

presence of the same constituents as seen in the GC-MS, meaning that all organics were either volatile or semi-volatile. Quantitative analysis showed concentration of aminoindanes ranged from 17 - 95 % w/w, with caffeine found in four samples ranging from 17-39 % w/w. Ten out of the eleven samples can be concluded to contain additional constituents not visible using HPLC or GC-MS. In the eleven products, total identified content varied from 30.51 % w/w (P10) to 99% w/w (P9). This highlights the importance of sensitivity for any in-field detection mechanism. The notion that NPS products are pure has been further proved in this study to be incorrect. For the products analysed, six out of the eleven matched their label claim, but no 5-IAI was detected in any of the samples. This highlights a significant problem with NPS detection, that there is little if no continuity between the purchased drugs and the label claims. The lack of 5-IAI has been noted before; this study further confirms despite 5-IAI being sold online, it is not actually present in samples. This could explain why the popularity of 5-IAI has not grown in the predicted manner. Worth mentioning is the presence of 2-AI in five samples, four of which were labelled to contain other drugs, this trend has not previously been seen and is important for understanding the prevalence of different aminoindanes. Both the GC-MS and HPLC methods stated can be used for future analysis of aminoindane products, and could be adapted for use with other amphetamine-like NPS, for fast identification and quantification of product content.

Aminoindane popularity subsided since the commencement of this work, thought to be due to their reduced potency compared to other amphetamine-like substances. Given the diminishing popularity of aminoindane derivatives during the undertaking of this project, the decision was made to no longer develop a sensory probe for the aminoindane class and instead focus the design of the sensory probe on the cathinone class. As emphasised in Chapter 1 cathinones, specifically mephedrone abuse, peaked in 2010 and has stayed prevalent ever since. Aminoindanes being legal makes them easy to obtain and hence they are readily available for analysis; this is not the case for cathinones. However, a large amount of information from the analysis of aminoindanes is still relevant when designing the sensory molecule for mephedrone. Specifically, from this work it is clear that the street samples analysed do not just contain the advertised constituents. With concentrations as low as 17 % for active ingredients, clearly the full matrix of the samples needs to be understood when designing a sensory molecule. Furthermore, the most common cutting agent identified was caffeine, so evidently the sensory molecule needs to be selective over caffeine to prevent any false positives. With 36 % of the samples not containing the active ingredient advertised, it highlights the need for selectivity over chemical analogues of the target drug. All of these findings give valuable information into the selectivity and sensitivity needs of a sensory molecule. Reports by LGC state that similar constituents have been found in cathinones as in aminoindanes[19,33,126,127,149]; therefore, the information collected

from the analysis of aminoindanes is valuable and will be taken forward to aid the rational design of a sensory molecule for cathinones.

Chapter 3   Development of a Three-Point Pharmacophore Based on Protein-Ligand Interactions

3.1 Introduction

As highlighted in Chapter 1, one of the main characteristics that current in-field NPS sensory mechanisms lack is selectivity. This is due to the growing number of structurally related NPS, as well as the range of cutting agents present in products. The importance of which was further affirmed in Chapter 2. Therefore, in this project it is proposed to use the concept of biomimetic design to tackle this problem. Protein-ligand interactions are known to be incredibly selective, and therefore an objective approach will be adopted based on these interactions for the design of a sensory molecule. When a ligand binds in a protein pocket there are points of interactions between the protein and the ligand in the cavity, it is these interactions that allow for selective recognition of the ligand. Mapping these interactions of the ligand with the receptor is known as pharmacophore modelling. Using these protein-ligand interactions to tackle selectivity in drug design using pharmacophore model is nothing new, as discussed in Chapter 1. For example, Figure 3.1 shows the outline of a pharmacophore based on interactions between a protein and serotonin. The respective distances shown are based on the spatial orientation of amino acid residues from the receptor that form a cavity which binds serotonin.
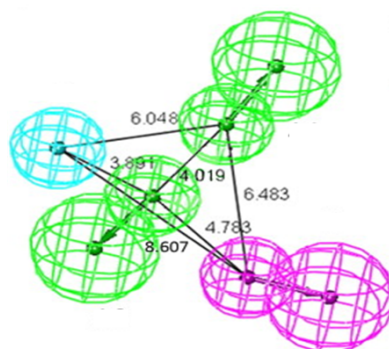
Figure 3.1 - Example of a serotonin pharmacophore. The different colours represent different pharmacophoric features; H-bonding accepting green, hydrophobic pink, and π-stacking in blue. The radius of the spheres shows the distances from a central point, over which it is feasible for the interactions to occur. Distances between the key features identified by the pharmacophore shown are reported in Angströms (Å).

The concept of pharmacophore design for the development of drug molecules (guests) is well established; however, using the technique for the design of host molecules for small molecule recognition has not been previously attempted. Using the same principles of pharmacophore design applied to the development of guest molecules, it is feasible to design host molecules for interaction with a specific guest, i.e. reverse the procedure.

This pharmacophore can then be used as the basis for designing a synthetic host molecule which maps these points and mimics the binding site. As previously discussed, proteins are large complex macromolecules. To be sure that any interactions extracted for the pharmacophore model are credible, it is important to understand the factors that can affect protein-ligand binding. There are five main factors that need to be considered when studying proteins for pharmacophore development; B factors, binding energy of ligands, solvation effects, resolution and finally position of ligands in the proteins. The importance of these factors has been discussed in detail previously (Chapter 1).

As discussed in Chapter 2, the rapid change in NPS abuse away from aminoindanes in Europe shifted the target class of interest for this project from aminoindanes to cathinones, specifically mephedrone. Given this information, the target of interest for sensor design, and therefore the pharmacophore model is mephedrone.

Therefore, the aim of this work is to develop a pharmacophore model that will aid in the rational design of a selective sensory molecule for detection of mephedrone. To achieve this, information on cutting agents from the analysis of aminoindane internet products (Chapter 2), along with literature sources that have assessed product content, will be used to develop a pharmacophoric model; upon which the design of sensory molecules will be based. This will be achieved through in-depth analysis of protein-ligand interactions for common cutting agents and chemical analogues of mephedrone. From which detailed binding information can be extrapolated to develop a pharmacophoric model.

3.2 Method

3.2.1 Identification of Experimental Structures

The identification of protein-ligand interactions started with a literature search of current drugs of abuse and common excipients that have been identified. This was done to develop an understanding of what the sensory molecule needs to be selective against. Then the binding information of these compounds can be used to rationally design a host molecule that is selective, by excluding binding properties that have been found to be favourable for cutting agents and other drugs of abuse that can be present in mephedrone products. To provide additional binding information for the development of the pharmacophore, identification of compounds that are structurally similar to mephedrone was

also carried out. Several resources were used in order to collect this information i.e. the Laboratory of the Government Chemist (LGC) drug intelligence bulletins, the Advisory Council for the Misuse of Drugs (ACMD) and the European Monitory Council for Drug and Drug Addiction (EMCDDA). In addition, serotonin and dopamine were included, as they are structurally similar to mephedrone. Paracetamol was also included due to its use as an adulterant in cathinones, but also because of its structural similarities to mephedrone. Protein interactions with paracetamol were searched for under the UK trade name as well as the US trade name, Tylenol and its chemical name acetaminophen to ensure all possible hits were collected.

The advanced search tool for Reaxys was used alongside the structure of mephedrone as the product, for search criteria "product" and "similar". The CAS Registry Number was used in order to determine structural names as well as any commonly used name that were then searched for in the Protein DataBank (PDB). All hits were collated into a spreadsheet and taken forward for quality control.

3.2.2   Quality Control

Quality control was performed to ensure that all data used in the pharmacophore modelling was robust. The flow chart shown in Figure 3.2 outlines the procedures carried out on each of the 37 proteins to ensure viability.
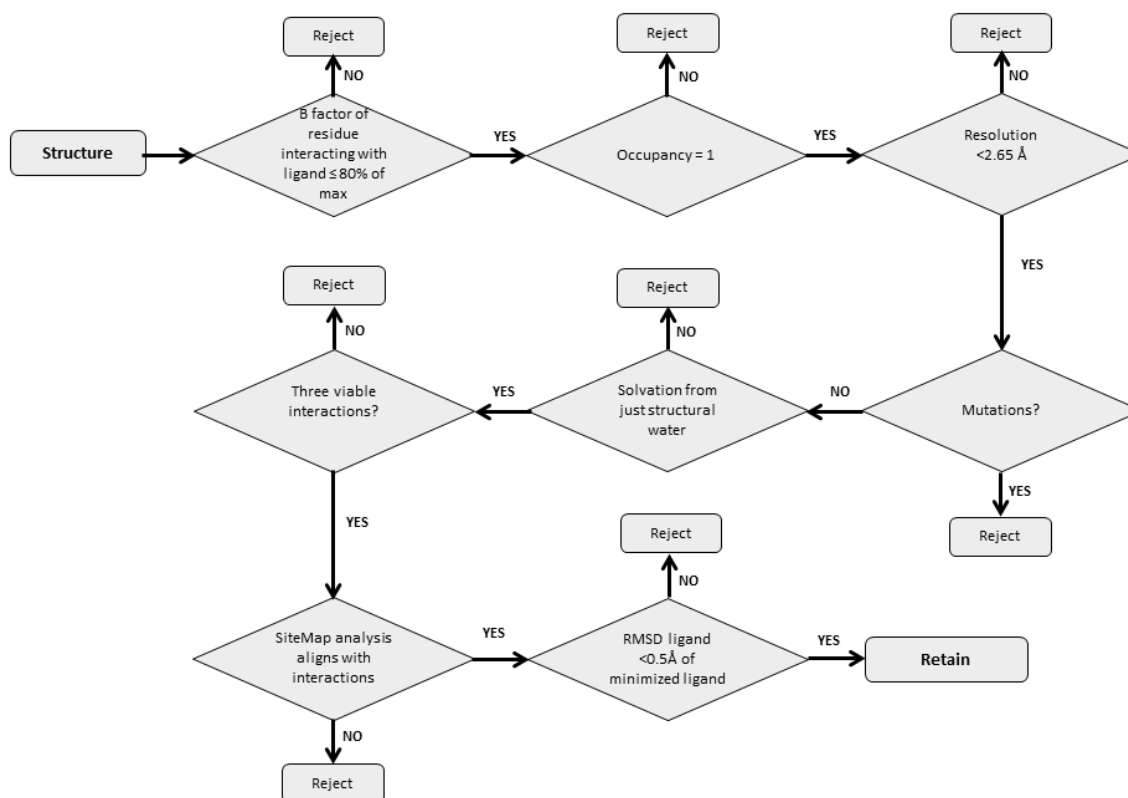
Figure 3.2 - Flow chart showing the methodology of protein quality control for X-ray crystal structures.

It was also noted which type of experimental data was being reported i.e. NMR or X-ray crystallography. For each of the proteins the PDB files were used to extract the appropriate information for ligand binding; PDB accession code, ligand ID, resolution, relative B factor, maximum B factor, occupancy and the presence of any mutations.

The interaction distances between ligand and protein, and the neighbouring residues, relative to the ligand, were determined using the Ligand Explorer 4.1.0 software on the PDB website.

For H-bonding interactions all interactions within 5 Å, a minimum acceptor angle of 90˚ and a minimum donor angle of 120˚, were included. For hydrophobic interactions a distance of 4.5 Å was used as a cut-off[150]. All neighbouring residues within 4 Å of the ligand were used to determine B factor values for the cavity, to ensure a full representation of cavity stability. All B factors of atoms in binding residues were compared against the average B factor for the PDB complex. The same parameters were applied to the analysis of all compounds included from the PDB.

Once all the criteria were considered (Figure 3.2), the primary data was studied from the published journals. This was to ensure that no information discussed in the corresponding article was different to that stated in the PDB file. The literature was also useful in helping to generate understanding as

to where in the structure the ligand is binding, i.e. ensuring that it is not occurring at an interface between two crystals which could be an artefact of crystallisation. Any proteins and binding sites that did not comply with any of the above criteria were excluded from further analysis.

3.2.3   Binding Site Analysis using *Phase*

Further analysis was performed using *Phase* in Macromodel (Schrödinger)[151]. *Phase* is software which allows for detailed analysis of protein-ligand binding from crystallographic data. All interactions for each residue in the binding site of the 37 proteins were recorded.

For all hydrophobic interactions the distances over which interactions between the protein and ligand occurred were recorded, and the type of interaction was noted. In the case of π-stacking interactions the relative orientation was noted i.e. edge/face or face/face. For hydrogen bonding the angle of interaction was also recorded.

The following parameters were used for protein preparation: assign bond order, add hydrogens, create zero order bonds to metals, create disulphide bonds and deletion of waters beyond 5 Å from hetero groups. Water molecules closer than 5 Å were included to highlight any hydrogen bonding to water that sits in the cavity and give an idea of the impact of solvation in the binding site on protein-ligand binding. Ligand diagrams were generated using residues within 5 Å of the molecule and all possible binding interactions were considered during the assessment.

Binding site analysis also allows for solvation to be observed in a binding cavity. Both structural and non-structural water molecules can interact with the ligand; however, only interactions occurring with structural water molecules were accepted. Structural water can be assumed to be an addition to the binding cavity due to their thermodynamic stability, and therefore, can be considered as an additional binding point. Highly solvated binding sites that contain non-structural water molecules have been excluded from further analysis. Structural water molecules were determined to be those that had B-factors in the same range as the residues within the binding site.

3.2.4   Binding Site Analysis using *SiteMap*

SiteMap was used (Schrödinger) to carry out binding site identification and validation[152]. The following parameters were used: 5 Å buffer, 12 site points per reported site, more restricted hydrophobic site was applied, and a standard grid using the OPLS_2005 force field. All binding sites were cropped at 4 Å from the nearest site point. Each of the interactions sites collected from *Phase* analysis were compared to the binding site analysis produced by *SiteMap*, to ensure correlation between the two before the pharmacophore was generated.

3.2.5 Ligand Minimisation using Maestro

Each of the ligands were extracted from their complexes and minimised using the minimisation tool in Maestro and default parameters. The conformation of the complexed ligand was extracted and the two ligands were overlaid using the superposition of ligands tool. The root mean square (RMS) values were calculated *in situ,* to prevent transformation. The maximum difference between atoms as well as the average RMS value for each of the ligands was calculated. All values below 0.5 Å were accepted.

3.2.6 Pharmacophore Design

For each of the protein binding sites remaining after validation, the three most favourable interactions were noted. The most favourable being H-bonding followed by π-stacking and finally hydrophobic interactions. Binding sites for the same compound that lacked consensus in terms of their pharmacophores were discarded. Similar features were aligned and the pharmacophores were overlaid. Angles and distances of typical features between pharmacophores were measured and assessed. Using the similarities between the overlaid features a consensus pharmacophore was developed. This produced a 3-point pharmacophore which was an amalgamation of each of the individual pharmacophores producing a consensus pharmacophore by averaging the geometrical components.

3.3 Results and Discussion

3.3.1 Selection Criteria

Mephedrone was chosen as the guest molecule of interest for sensor design, and therefore, the selection of guest molecules studied reflected this. The guest molecules selected fall into two categories; molecules that the sensor must be selective against, and therefore, the binding features should be excluded from the pharmacophore design, and structurally related molecules to mephedrone, whose binding properties the pharmacophore model should reflect. Selection criterion for the inclusion of protein-ligand interactions in the spreadsheet for analysis was performed through literature searches of current drugs of abuse and common excipients that have been identified in mephedrone and also supported from the aminoindane study in Chapter 2. Table 3.1 shows the compounds included in the spreadsheet and the rationale behind their selection. The LGC drug intelligence bulletins have been published quarterly since 2011 and summarizes the drug seizures in that quarter as well as highlighting common adulterants that have been identified in them[19]. They are the main source of up to date adulterant information. In addition, the Advisory Council for the Misuse of Drugs (ACMD) is a good resource for bulking agents identified in cathinone samples in the UK, in particular their report on the "Consideration of Cathinones for Controlled Status"[21]. The EMCDDA

regularly updates its websites in relation to seizures in the European Union. They published a report in 2010 related to cathinones and common adulterants, as well as a joint report with Europol into the specific abuse of mephedrone in Europe[153,154]. The LGC report published in 2012 stated that cathinones had been found to contain similar adulterants to those found in cocaine, so information has been collected from cocaine in reports dated before 2012[126].

Table 3.1 - The 15 compounds collected and considered for the protein-ligand analysis.

Compound Identified	Source	Year	Use
Benzocaine	LGC – Drug Intelligence Bulletin	2011	Anaesthetic
	LGC – Drug Intelligence Bulletin	2012	
	LGC – Drug Intelligence Bulletin	2013	
	ACMD, Consideration of Cathinones	2010	
Caffeine	LGC – Drug Intelligence Bulletin	2011	Stimulant
	LGC – Drug Intelligence Bulletin	2012	
	LGC – Drug Intelligence Bulletin	2013	
	ACMD, Consideration of Cathinones	2010	
	UNODC, Challenges of NPS	2013	
Glucose	LGC – Drug Intelligence Bulletin	2011	Bulking agent
	LGC – Drug Intelligence Bulletin	2012	
	LGC – Drug Intelligence Bulletin	2013	
Lactose	LGC – Drug Intelligence Bulletin	2011	Bulking agent
	LGC – Drug Intelligence Bulletin	2012	
	Europol-EMDCCA Joint Report	2010	
Lidocaine	Federal Registration, Department of Justice	2011	Anaesthetic
Lignocaine	LGC – Drug Intelligence Bulletin	2011	Anaesthetic
	LGC – Drug Intelligence Bulletin	2012	
	LGC – Drug Intelligence Bulletin	2013	
Paracetamol	LGC – Drug Intelligence Bulletin	2012	Analgesic
	LGC – Drug Intelligence Bulletin	2013	
	EMCDDA – Synthetic Cathinones Report	2010	
Procaine	LGC – Drug Intelligence Bulletin	2011	Anaesthetic
	LGC – Drug Intelligence Bulletin	2012	
Sucrose	LGC – Drug Intelligence Bulletin	2011	Bulking agent
	LGC – Drug Intelligence Bulletin	2012	
	LGC – Drug Intelligence Bulletin	2013	
Cocaine	EMCDDA – Synthetic Cathinones Report	2010	Stimulant, drug of abuse
	ACMD, Consideration of Cathinones	2010	
	LGC – Drug Intelligence Bulletin	2012	
Ephedrine	Europol-EMDCCA Joint Report	2010	Mephedrone Precursor, stimulant
	EMCDDA – Synthetic Cathinones Report	2010	
MDMA	Europol-EMDCCA Joint Report	2010	Stimulant, drug of abuse
Methamphetamine	U.S Department of Justice – Situation Report	2011	

	ACMD, Consideration of Cathinones	2010	Stimulant, drug of abuse
Pseudoephedrine	Europol-EMDCCA Joint Report	2010	Mephedrone Precursor, stimulant
	EMCDDA – Synthetic Cathinones Report	2010	

Ephedrine, pseudoephedrine, lignocaine and benzocaine all failed to produce hits in the Protein Database and therefore, no direct protein-ligand binding information is available for these compounds. Drugs such as MDMA and methamphetamine have not been commonly found with mephedrone in samples but have been included due to their structural similarities and are therefore predicted to have similar binding properties. They have also been included to ensure that the sensor is designed with possible drugs of abuse that could induce false positives in mind, to help increase the selectively of the sensor to mephedrone.

In order to expand the search further, information on the binding of serotonin and dopamine was included. Mephedrone works by inhibition of the dopamine and serotonin receptors and therefore, mimics the actions of serotonin and dopamine due to its structural similarities[155]. By finding valid data for the binding of these neurotransmitters, information can be extracted and used to help design an effective sensor for mephedrone. It was not possible to find binding data for dopamine and serotonin receptors, as there is a lack of crystal structures for these receptors or any closely related G-protein coupled receptors (GPCR) because of the difficulties in crystallizing membrane-bound proteins[156]. There are, however, a number of hits in the PDB of proteins that are bound to serotonin or dopamine, particularly cytochrome P450 variants. Serotonin and dopamine produced seven and four hits respectively, which were taken forward for further analysis.

Results from the initial searches of the PDB yielded 37 hits (Table 3.2). This was considered a relatively small data set to take forward into quality control studies. Therefore, to try and increase the number of structures further search tools were employed. The chemical search database, Reaxys[157] was used to try and increase the dataset. This allows for more compounds that are likely to have similar binding properties to mephedrone to be included that may not be common drugs of abuse. This produced 22 near hits for compounds, as well as 14 position/stereoisomers, as seen in Figure 3.3.
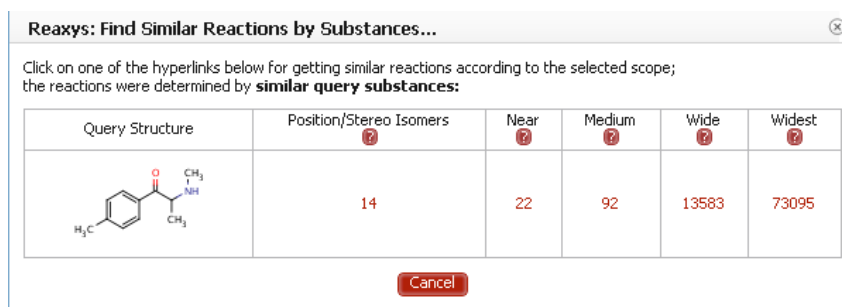
Figure 3.3 - Reaxys substance search based on structurally similar compounds to mephedrone.

Compounds with near hits are defined as including "structures containing the same ring and chain systems (possibly multiple) with the original relative positions of substituents and extended by further simple substituents such as hydrocarbons"[157]. Medium hits are defined as "structures with a wider range of rings and substituents: the degree of unsaturation, form and substitution patterns of rings is extended"[157]. Therefore, those compounds included as medium hits have not been investigated for possible binding properties. All 36 compounds classed as near hits and position/stereoisomers were investigated in terms of their structural similarities. Most of the hits in Reaxys are novel compounds that are not commonly available. None of the 36 compounds produced hits in the PDB. Therefore, no further compounds were included in the spreadsheet based on Reaxys searches. The final selection of compounds taken forward can be seen in Table 3.2. From the compounds selected, caffeine, lidocaine, paracetamol and cocaine have been included as molecules to make the sensor selective against. Methamphetamine, MDMA, serotonin and dopamine are all molecules that are structurally similar to mephedrone, and therefore, can be used to extract pharmacophoric binding features that could reflect those of mephedrone.

Table 3.2 - 37 proteins collected showing their PDB accession codes and the ligand of interest that is interacting with the protein.

PDB Accession Code	Ligand ID
3RFM	Caffeine
1C8L	Caffeine
3G6M	Caffeine
2A3B	Caffeine
1L5Q	Caffeine
1L7X	Caffeine
1GFZ	Caffeine
3DDS	Caffeine
3DDW	Caffeine
3DD1	Caffeine
3GKZ	Methamphetamine
3JQZ	Lidocaine
3TTR	Lidocaine
1Q72	Cocaine
2AJV	Cocaine
1I7Z	Cocaine
2PGZ	Cocaine
3GM0	MDMA
1TYL	Paracetamol
1TYM	Paracetamol
2DPZ	Paracetamol
2OCU	Paracetamol
3DJI	Paracetamol
3PY4	Paracetamol
4A9J	Paracetamol
4GN6	Paracetamol
3ADV	Serotonin
4DTW	Serotonin
4DUE	Serotonin
2QEH	Serotonin
3BRN	Serotonin
3NK1	Serotonin
2YMD	Serotonin
4DTZ	L-Dopamine
2QMZ	L-Dopamine

3NK2	L-Dopamine
5PAH	L-Dopamine

3.3.2   Quality Control

For each of the 37 protein-ligand complexes, detailed understanding of the protein-ligand interactions occurring was required. All protein-ligand H-bonding, π-stacking and hydrophobic interactions were identified and recorded including the residue that was interacting and the interatomic distances in Angströms (Å). All 37 proteins showed at least three interactions with the ligand, 2YMD bound to serotonin showed the greatest number, with 16 interaction points.

For each of the residues in the binding site, the B factors were recorded and the average B factor for a residue was compared against the average B factor for the protein. This is not the Wilson plot value, which is commonly used. The reason the Wilson plot value was not used is because it assumes random distribution of atoms, which is not true for all proteins, especially those with low resolution (>3 Å) or high solvation in X-ray crystallography[158], for example 3GM0. Therefore, for this work determination of relative thermodynamic stability has been achieved by using the average B factor.

The occupancy for each of the complexes was recorded; this was found to be one for all complexes. This means that for all the proteins considered the unit cells were identical throughout the crystal and no further analysis needs to be performed.

The experimental method was noted for all of the complexes, and for all 37 proteins X-ray crystallography was used as the structural elucidation method. The resolution of complexes is important when studying protein-ligand interactions using X-ray crystallography so for each complex this was recorded.

The resolution of a crystal structure denotes the quality of the data. For example 2AJV has the best resolution in this dataset at 1.5 Å. This means that it is possible to conclude that an observed interaction at a distance greater than 1.5 Å is real, within the constraints applied to forming the crystal. Any interactions below this distance cannot be verified with a great degree of certainty. Given that hydrogen bonds commonly occur between atoms at distances approximately 1.5-2.5 Å[159], any resolution higher than this does not definitively show the presence of hydrogen bonding. 3RFM has the poorest resolution at 3.6 Å and was therefore excluded; the remaining complexes have resolutions < 2.65 Å.

Mutations in a protein often occur for experimental reasons, such as to understand the effect of a particular residue on binding, or to help a protein crystallise. However, it is important to understand

if they have occurred, and where. Two of the 36 proteins studied contained mutations in the binding site; 4DTW and 4DUE. Mutations anywhere in the protein can affect the binding site as they can change the overall structure of the protein; however, mutations in the binding cavity are likely to have a more significant effect on the protein-ligand binding interactions being studied. Therefore, 4DTW and 4DUE were excluded.

To ensure that all information collected from the PDB is correct and complete the original published journal articles were investigated. This gave further insight into how the experiments were carried out as well as providing details with respect to the position of the binding sites. Seven of the proteins (3PY4, 4GN6, 2QMZ, 2OCU, 3TTR, 2DPZ and 1I7Z) did not have a corresponding journal article; these were still included for further validation, as there was no evidence to exclude them at this stage. Of the remaining 27 complexes, seven (1C8L, 1GFZ, 3JQZ, 1L5Q, 1L7X, 2PGZ and 3NK1) were excluded from further analysis as the protein-ligand interaction occurred at the interface between two crystal subunits (Figure 3.4). The most common cause for exclusion based on journal data was the protein-ligand binding occurring at the domain interface, this is a product of crystallisation due to analysis using X-ray crystallography, and not indicative of interactions that would naturally occur[160]. 5PAH was excluded due to large number of metal interactions that were stabilising the dopamine ligand in the protein. This is not a suitable representation of the type of data that needs to be extracted in order to develop the pharmacophore, or that can be incorporated into a small host molecule. In total eight proteins were excluded due to undesirable or unreliable protein-ligand binding properties; 5PAH, 1C8L, 1GFZ, 3JQZ, 1L5Q, 1L7X, 2PGZ and 3NK1.
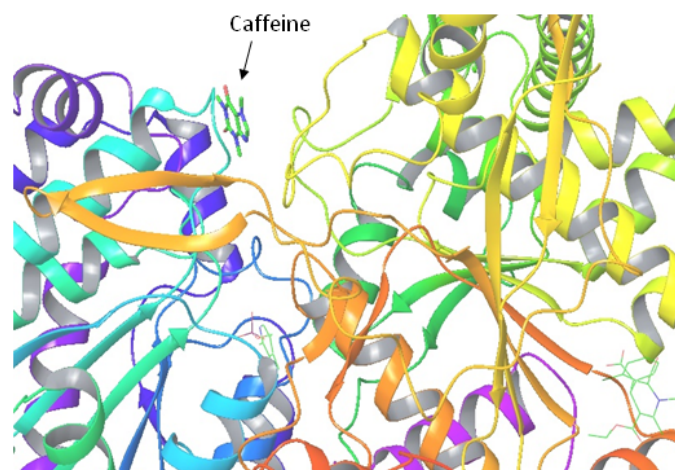
Figure 3.4 - Caffeine binding between two protein subunits in 1C8L.

The average B-factors for each residue were compared against the maximum B-factor for the protein. B-factors are an indication of thermodynamic stability; therefore, if the B-factors of the residues in

the pocket are high it's possible that the structure is not truly representative of how the protein-ligand complex is formed *in vivo* given that it is subject to a large degree of thermal mobility. For each of the 26 remaining complexes studied it was decided that all residues in the binding cavity must report B-factor values below 80 % of the maximum for that structure in order to be retained. Two complexes were excluded based on this criteria; 3DDS and 1Q72. Thus, twenty-three complexes were taken forward for binding analysis using the *Phase* software (Table 3.3). At this stage, the ligands still range from cutting agents such as caffeine to aid in selectivity, to structurally related compounds such as methamphetamine and serotonin.

Table 3.3 - All 23 proteins that were accepted after quality control and taken forward for binding analysis using *Phase*.

PDB Accession Code	Ligand ID	Resolution (Å)	Occupancy of 1.0
3G6M	Caffeine	1.65	yes
2A3B	Caffeine	1.9	yes
3DDW	Caffeine	1.9	yes
3DD1	Caffeine	2.57	yes
3GKZ	Methamphetamine	1.9	yes
2AJV	Cocaine	1.5	yes
1I7Z	Cocaine	2.3	yes
3GM0	MDMA	2.4	yes
1TYL	Paracetamol	1.9	yes
1TYM	Paracetamol	1.9	yes
2DPZ	Paracetamol	2.1	yes
2OCU	Paracetamol	2.38	yes
3DJI	Paracetamol	1.95	yes
3PY4	Paracetamol	2.42	yes
4A9J	Paracetamol	1.9	yes
4GN6	Paracetamol	2.42	yes
3ADV	Serotonin	2.27	yes
2QEH	Serotonin	2.1	yes
3BRN	Serotonin	2	yes
2YMD	Serotonin	1.96	yes
4DTZ	L-Dopamine	1.55	yes
2QMZ	L-Dopamine	2.1	yes
3NK2	L-Dopamine	2.65	yes

3.3.3   Binding Analysis using *Phase*

The *Phase* software was used to give more detailed information into the type of binding interactions between each of the ligands and the proteins they were complexed with, specifically the bond length and angles of those interactions. Each of the interactions were analysed according to the validation criteria using *Phase* to ensure they were viable. *Phase* allows for shape based screening of each of the protein-ligand interactions. This is important to understand the 3D conformation of the ligand in the protein cavity, and how this relates to the observed interactions.

To obtain the information needed to develop a pharmacophore from the proteins collected, three interaction points in the binding cavity are needed. Hydrogen bonding was considered to be the most desirable interaction, due to the strength of the interaction. For hydrogen bonding both the bond length and the angle of interaction were collected. π-stacking interactions were the next interactions considered. For these interactions the bond length and type of π-stacking interaction was noted. There are three main types of π-stacking interactions; edge/face, face/face and in special circumstances π-cation binding. For each of the π-stacking interactions the type of interaction was recorded, as this may be important when considering the final pharmacophore design. Complexes containing caffeine exclusively showed face/face π-stacking interactions, the methamphetamine and MDMA complexes contained edge/face interactions.

The final interaction considered was hydrophobic interactions. These occur between ligands and the hydrophobic areas in the protein cavity. Hydrophobic interactions are individually the weakest of the interactions; however, they are the most numerous and important for stabilising the ligand in the cavity and can affect the residues considered in the cavity for pharmacophore design.

Before analysis all proteins were prepared systematically to ensure that any problems in the protein structure were highlighted, and also to ensure all relevant hydrogen atoms were included, which allows any hydrogen bonding to be seen. After protein preparation, a number of the proteins had missing atoms, overlapping atoms, invalid atom types or alternative positions for atoms. The last one means that despite the occupancy stated as being 1 for each of the atoms from the data collected from PDB records, some of the atoms were in fact found to have an occupancy value of 0.5. This may indicate that each unit cell is not the same in the protein; however, it may also be indicative of two possible rotamers for a specific sidechain. Given the lack of information at this stage, these proteins were retained, and further validation was carried out.

Ligands usually bind by displacing water from a binding site[161]. However, highly stable water, based on thermodynamic stability (B-factors), are energetically unfavourable to displace and consequently the ligand may not bind in the cavity, or it may bind *via* the water molecules. This is not a property of

proteins that is easily mimicked in a small molecule. However, such highly stable water molecules can be considered to be structural waters, i.e. they become a feature of the binding cavity and therefore, such interactions can be considered to be as useful as those occurring through fixed residues. Such interactions that occur through thermodynamically stable water molecule were accepted.

Highly solvated cavities can also be indicative of an open binding cavity and could indicate that protein-ligand binding is less favourable. This is because open cavities are less likely to encapsulate and bind to the entire ligand, which would make it less selective as a sensor. Highly solvated protein pockets were eliminated from further analysis. There was a total of 10 protein-ligand complexes that were eliminated based on this; 3G6M, 3TTR, 2AJV, 1I72, 1TYL, 1TYM, 4A9J, 2OCU, 3DJ1 and 2QMZ.

However, high solvation was closely linked to a lack of interactions between the protein and ligands, and therefore, many exhibited both properties. In total 24 binding sites were excluded from the data set after *Phase* analysis, this means 19 proteins were excluded, as some proteins exhibited multiple binding sites with different properties. Table 3.4 shows the 9 remaining protein-ligand complexes; 2A3B binds caffeine in two different cavities both of which have been included.

Table 3.4 - Binding information for the 9 remaining protein-ligand complexes, with three primary interaction with distance, angle and type where appropriate.

Protein	Ligand	Interactions	Residue	Distance	Angle	Type
2A3B	A:CAFF 1435	π-Stacking	TRP384	3.3Å		Face/Face
		H-bonding	TRP137	2.03Å	142.4˚	
		Hydrophobic	MET43	3.68Å		
	B:CAFF 2435	π-Stacking	TRP384	2.5Å		Face/Face
		H-bonding	TRP137	2.09Å	140.5˚	
		Hydrophobic	PHE76	2.67Å		
3DDS	A:CAFF 904	π-Stacking	PHE285	4.77Å		Face/face
		π-Stacking	TYR613	2.3Å		Edge/Edge
		Hydrophobic	ALA610	3Å		
3DDW	A:CAFF903	π-Stacking	PHE285	2.6Å		Face/Face
		π-Stacking	TYR613	2.6Å		Face/Face
		Hydrophobic	ALA610	3Å		
3DD1	B:CAFF903	π-Stacking	PHE285	2.6Å		Face/Face
		π-Stacking	TYR613	2.6Å		Face/Face
		Hydrophobic	ALA610	3Å		
3GKZ	A:500 Methamphetamine	π-Stacking	TRP232	3.42Å		Edge/Face
		π-Stacking	PHE237	3.68Å		Edge/Face
		H-bonding	GLU114	1.66Å	176.5˚	Side chain
3GMO	A:B41 600 MDMA	π-Stacking	PHE237	3.66Å		Edge/Face
		H-bonding	GLU114	1.76Å	161˚	
		Hydrophobic	TYR55	3.46Å		
2DPZ	A:TYL2001 Paracetamol	π-Stacking	PHE5	2.57Å		Edge/Edge
		π-Stacking	HID48	3.54Å		Edge/Edge
		Hydrophobic	LEU 2	2.36Å		
3PY4	A:TYL598 Paracetamol	π-Stacking	HID109	3.5Å		Edge/Edge
		Positive charge	ARG255	2.65Å		
3NK2	X:LDP433	H-bonding	ASN166	2.21Å	128.6˚	
	Dopamine	Hydrophobic	TYR407	2Å		
		Hydrophobic	MET167	3Å		

3.3.4   Binding Site Analysis using *SiteMap*

In order to ensure that the chosen interactions were valid each of the final nine binding sites were subjected to *SiteMap* analysis. By validating the binding site using *SiteMap*, it ensures the ligands are positioned in favourable sites for the binding that has been identified. *SiteMap* predicts and evaluates the binding sites in a given protein, irrespective of whether the ligand is bound. This ensures that each binding point collected using *Phase* is in a favourable position, i.e. that hydrophobic interactions occur in a largely hydrophobic region of the cavity and that all hydrogen bonding interactions occur in the regions predicted. Figure 3.5 shows an example of a SiteMap produced for 3GM0 with MDMA superimposed on top to see how the ligand fits in the putative binding sites. The yellow mesh represents predicted hydrophobic regions, blue is hydrogen bond donors and red is hydrogen bond acceptors. The grey spheres represent the site points applied to the binding site for analysis.

The three residues identified as important for binding in 3GM0 are PHE 237, TYR 55 and GLU 114. PHE 237 displays a π-stacking interaction which is appropriately located in the yellow (hydrophobic) region in Figure 3.5. GLU 114 is a hydrogen bond acceptor and sits in the red region, while the hydrogen bond donor atom in MDMA is positioned in the blue region.
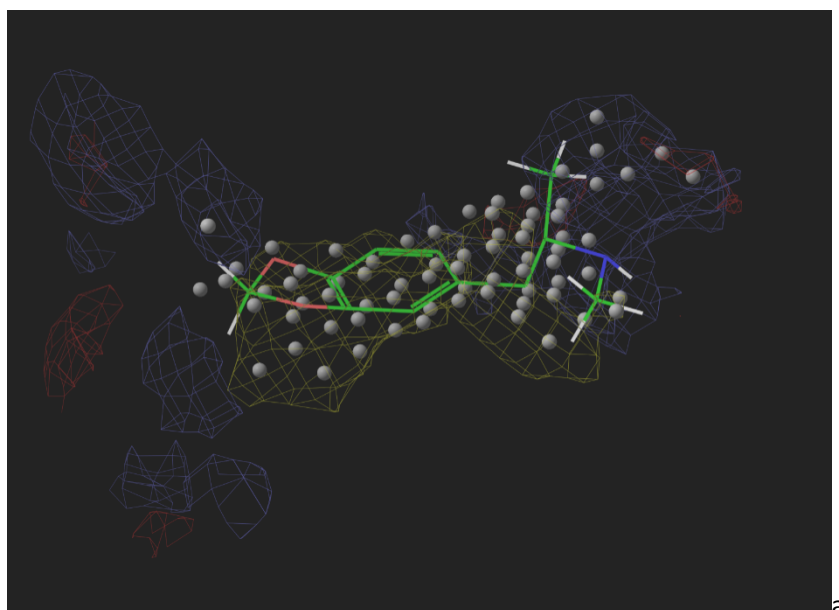
Figure 3.5 - SiteMap for 3GM0 overlaid with MDMA.

This shows that the three predicted binding interactions from *Phase* correlate with those predicted by *SiteMap*. This was found to be true for all 9 binding sites studied. The *SiteMap* for 2DPZ shows red and blue mesh regions (Figure 3.6) which would indicate positions for hydrogen bonding; however, no such interactions were found using *Phase*.
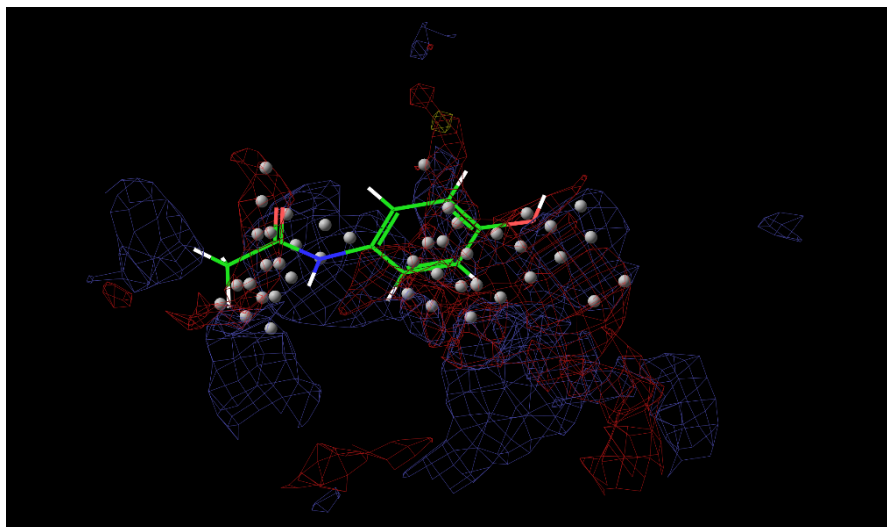
Figure 3.6 - SiteMap for 2DPZ showing large hydrogen bonding areas.

The interactions found were π-stacking and hydrophobic interactions, these residues are still positioned in the desired region. The *Phase* and *SiteMap* data shows good consensus in relation to the binding interactions observed. The final nine complexes were next subjected to ligand minimisation as a final validation step before pharmacophore development was carried out.

3.3.5   Ligand Minimisation using Maestro

Energy minimisation was carried out on each of the ligands to ensure that they were in an energetically favourable confirmation. This is because ligands can be stabilised in high energy confirmations by the presence of a large number of Van der Waals forces, which as previously mentioned is a feature of proteins that cannot be mimicked in a small molecule sensor. In order to achieve this each of the ligands was minimised to produce the minimum energy conformation, without the presence of a protein. This confirmation was then compared against that seen in each of the complexes. The two ligands were overlaid and the heavy atom root mean square (RMS) values of each were calculated. Figure 3.7 shows the minimised structure of MDMA overlaid with the conformation found complexed in 3GM0.
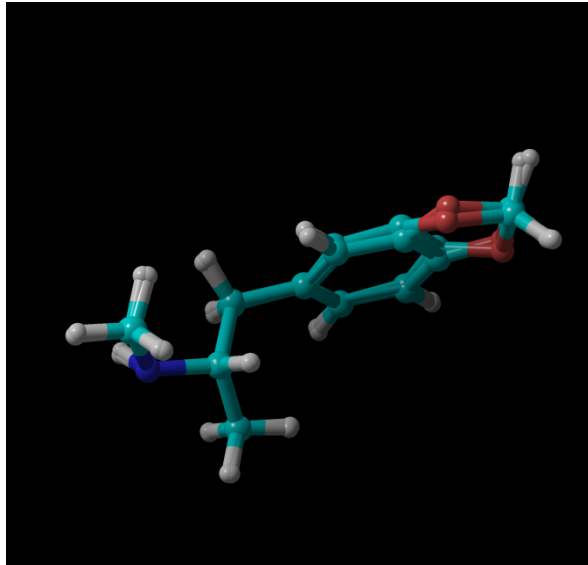
Figure 3.7 - MDMA from 3GM0 overlaid with minimised conformation of MDMA.

The total RMS for 3GM0 was calculated as 0.1237 Å, with the maximum difference between any two atoms calculated as 0.2768 Å, between the oxygen atoms of the methylene groups. This was the largest RMS value calculated and is still close to zero. The closer to zero the value the less difference between the two conformations and therefore the better the value. As can be seen in Figure 3.7 there is very little difference in the minimum energy conformation and the conformation adopted when complexed. This is true for all of the 9 ligand complexes studied, with caffeine complexed in 2A3B producing the smallest RMS at 0.0063. All 9 binding sites were taken through to be used for pharmacophore development.

Table 3.5 - Nine remaining protein-ligand complexes taken through to pharmacophore design.

PDB accession code	Ligand ID
2A3B	Caffeine
3DDS	Caffeine
3DDW	Caffeine
3DD1	Caffeine
3GKZ	Methamphetamine
3GM0	MDMA
2DPZ	Paracetamol
3PY4	Paracetamol
3NK2	L-Dopamine

3.3.6   Pharmacophore Design

Traditionally, once data collection and validation has been conducted the pharmacophore is generated using a specialised computer program[151]. However, given that these programs are based on guest molecule pharmacophores they are not suitable for host molecule design. Therefore, the pharmacophore was developed manually based on a consensus of the 3D pharmacophores for each of the remaining compounds. This was done by isolating the key binding features from each of the pharmacophores in relation to mephedrone, and averaging the geometrical components to produce a consensus pharmacophore.

Using the protein-ligand complexes listed in Table 3.5 the software package called Maestro[150] was used to build a pharmacophore for a cathinone, specifically mephedrone. The pharmacophore gives information as to which types of interactions can be utilised to facilitate binding in a cavity. This is achieved by analysing the differences in binding properties between each of the protein-ligand complexes considered and then the pharmacophore is altered to prevent non-selective binding, based on structural differences.

MDMA is structurally similar to mephedrone and can therefore provide valuable information as to possible interactions that can be utilised in a sensor for mephedrone. Figure 3.8 shows the binding of MDMA to its receptor, an anti-methamphetamine single chain antibody variable fragment. Figure 3.8A shows the specific binding properties of MDMA in the cavity with the amino acid residues. For MDMA, three interactions can be observed, one hydrogen bond and two π-stacking interactions. This information was extracted and compiled to develop a pharmacophore for MDMA (Figure 3.9). Due to their structural similarities, selectivity between mephedrone and MDMA may prove challenging. Figure 3.8B shows how the size of the binding pocket can play an important role in the selectivity of compounds, and can therefore be exploited in the sensor. Further adjustments can be made manipulating steric properties of the molecule so that the fit in the binding pocket is modified.
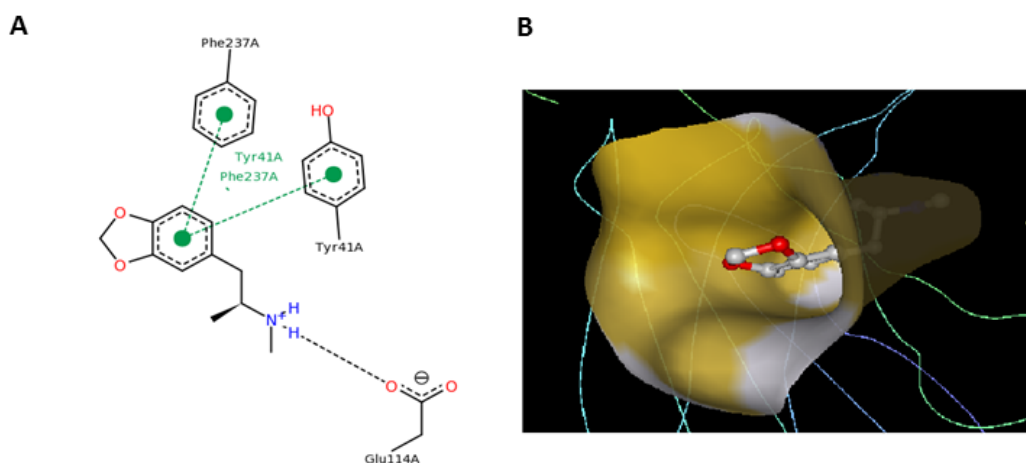
Figure 3.8 - A. Diagram of binding site of MDMA in a protein, and B. simulation of MDMA in the same protein cavity.

Once each set of data was analysed based on the above validation criteria, each of the protein-ligand interactions occurring in the 9 binding sites was converted into a three-point pharmacophore. The pharmacophoric points chosen are based on the three most favourable interactions seen for each complex, ideally hydrogen bonding and π-stacking. The angles and distances were measured for each of the binding sites; the distances are taken from the interaction point of the residues. Each of the pharmacophores were overlaid with one another and comparisons were drawn as to the similarities seen that could be utilised for mephedrone recognition. Figure 3.9 shows an example of one of these pharmacophores, developed using data on MDMA (3GM0).
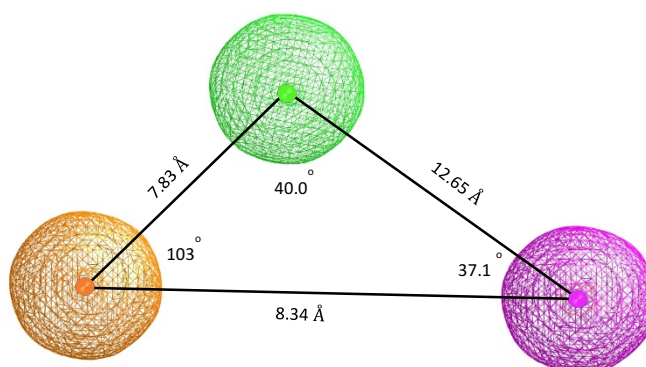
Figure 3.9 - Three-point pharmacophore based on protein 3GM0 for MDMA. The binding features are portrayed as mashed spheres, colour-coded as green, hydrogen-bond acceptor, magenta, hydrophobic and orange as aromatic rings (distances not to scale).

The pharmacophore developed based on 3GKZ binding with methamphetamine is shown in Figure 3.10 along with the combined pharmacophores from the two paracetamol-protein complexes, 2DPZ and 3PY4 and dopamine, 3NK2. Methamphetamine (Figure 3.10 A) shows similarities to the MDMA pharmacophore, (Figure 3.9) with a hydrogen bond acceptor and a π-stacking interaction. The same is also true for dopamine (Figure 3.10 C), which is structurally similar to mephedrone and also contains a hydrogen bond acceptor and π-stacking interaction. Paracetamol (Figure 3.10 B), which the sensor must be selective against shows no hydrogen bonding. This difference could be utilised to aid selectivity in the final sensor molecule. The four caffeine complexes (2A3B, 3DDS, 3DDW and 3DDI) exhibit various binding interactions depending on the protein they are in complex with, and therefore it was not possible to develop a common pharmacophore for caffeine, which is a promiscuous binder, due to its highly hydrophobic structure. It was however noted that in all caffeine-protein interactions π-stacking was the primary interaction.
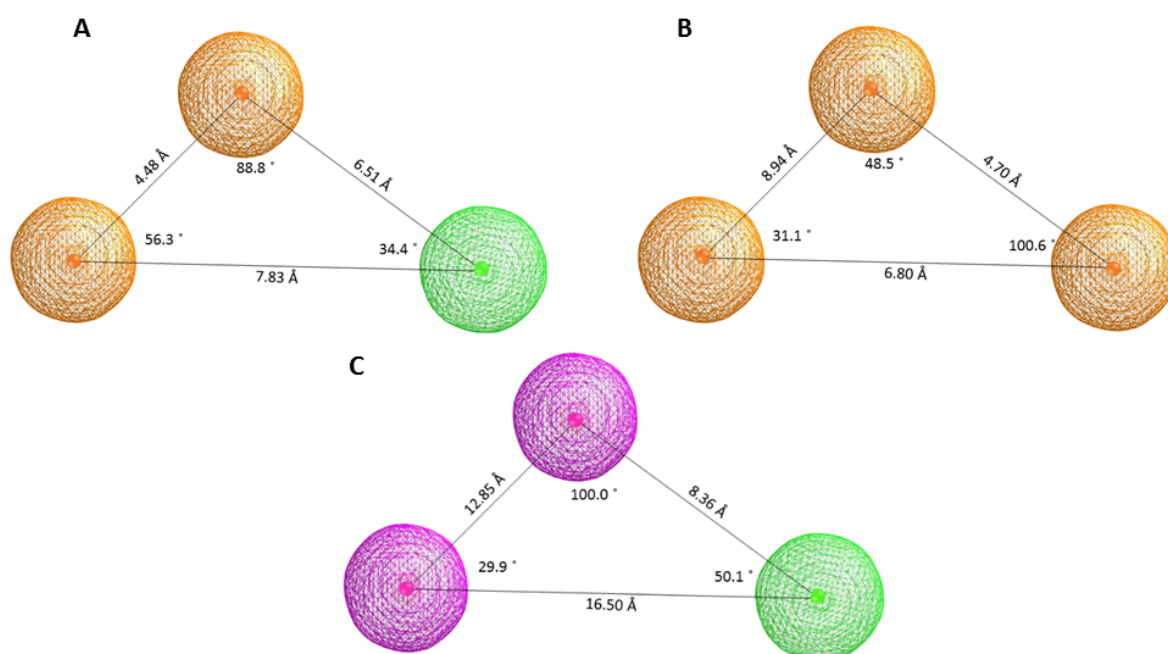
Figure 3.10 - Three-point pharmacophore based on A. methamphetamine (3GKZ), B. the combined paracetamol binding (2DPZ AND 3PY4) and C. dopamine (3NK2). The binding features are portrayed as mashed spheres, colour-coded as green, hydrogen-bond acceptor, magenta as hydrophobic and orange as π-stacking interactions (distance not to scale).

The pharmacophore as seen in Figure 3.11 is a consensus of the five remaining crystallographic experimental data sets; two paracetamol and one each for dopamine, MDMA and methamphetamine (3GKZ, 3GM0, 2DPZ, 3PY4 and 3NK2). Each of these four compounds has structural similarities to mephedrone that could be used to predict mephedrone binding, given the lack of protein-mephedrone binding data. The important interactions that can correlate to mephedrone have been

prioritised and the distances and angles have been averaged between these interactions, to produce a consensus pharmacophore based on the proteins in Table 3.5, with the exception of caffeine.
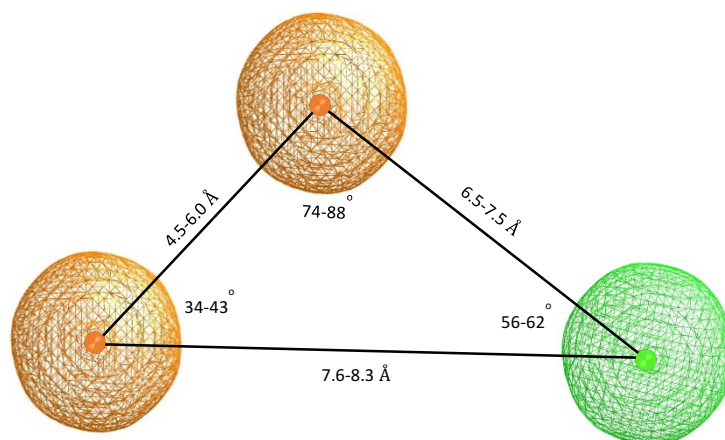
Figure 3.11 - Pharmacophore design for mephedrone binding including bond distances and angles. The binding features are portrayed as mashed spheres, colour-coded as green, hydrogen-bond acceptor and orange as aromatic rings (distances not to scale).

All four of these ligands contain structural similarities; they all contain one aromatic ring and a secondary amine (Figure 3.12). Therefore, they all demonstrated similar binding patterns. These pharmacophoric binding features are also common to the target compound, mephedrone.
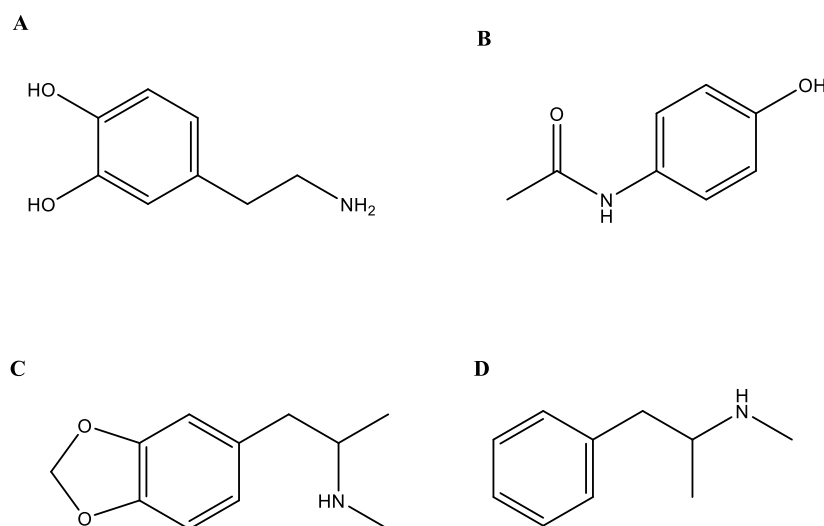
Figure 3.12 - The chemical structures for A. dopamine B. paracetamol C. MDMA and D. methamphetamine upon which the pharmacophore is based.

The four binding sites all contained one hydrogen bonding acceptor interaction and two hydrophobic or π-stacking interactions, interacting with the amine and aromatic groups. Both dopamine and

methamphetamine, two sterically similar compounds to mephedrone contain the hydrogen bond interaction in the same orientation to the hydrophobic interactions. Therefore, this geometry for the strongest predicted interaction, the hydrogen bond, is reflected in the final pharmacophore. The π-stacking interactions were favoured over hydrophobic interactions, as they are relatively stronger interactions. The spacing and conformation of these interactions will not directly match mephedrone, which needs to be considered when applying the pharmacophore design to synthetic host molecules. However, each of the interactions included in the average conformation of the pharmacophore reflect the possible binding properties or position of the functionalities in mephedrone. Another similarity to note was that all π-stacking interaction seen for the binding sites included were edge/face interactions. These similarities made it simpler to compare the five binding sites and measure the distances between similar interactions, which could be used to bind mephedrone. The angles and distances shown are given as a range based on the different individual pharmacophores that were developed. It is also incredibly difficult to develop a constrained system which synthetically mimics exact distances when designing host molecules and therefore a range makes it more feasible to design a binding cavity that approximates the pharmacophoric features. It is also more representative of the four cavities used to design the pharmacophore.

3.4 Conclusion

A three-point pharmacophore to aid in the design of a sensor molecule to selectively bind mephedrone was developed based on protein-ligand interactions of the chosen guest molecules. The initial selection criterion highlighted 14 compounds that are either commonly found in seized samples containing mephedrone, so the sensor must be selective against them or are structurally related to mephedrone and were used to make the sensor selective for mephedrone. This information was used for consideration when developing the pharmacophore which will be used to guide the synthesis of a selective host molecule. Initially, there were 37 protein-ligand complexes identified for eight of the 14 suggested compounds. The remaining six compounds produced no hits in the PDB, most notably mephedrone itself. This is believed to be due to the lack of experimental data surrounding the class of proteins that they naturally bind to i.e. transmembrane proteins. Therefore, structurally related compounds were used as the source of binding information for the pharmacophore.

The 37 protein-ligand complexes were subjected to rigorous quality control procedures, to eliminate any complexes that were not viable for use in generating pharmacophores. The interactions between each of the protein-ligand complexes along with the respective binding sites were extensively analysed using *Phase* and *Sitemap*. This allowed for any complexes to be excluded that did not contain valid and robust binding data that could be utilised in the pharmacophore, or incorporated into the

final host molecule. Thereby, excluding anything that cannot be mimicked in small molecule host binding.

After validation of each of the protein-ligand complexes was conducted, nine binding sites remained. These were taken forward to help develop a three-point consensus pharmacophore for mephedrone. Caffeine was concluded to be a promiscuous binder, and therefore no consensus pharmacophore was developed. It was determined that caffeine π-stacking interactions are largely face/face interactions, whereas the structurally related compounds such as the amphetamines were edge/face interactions. This difference could be utilised in host molecule design to gain selectivity over caffeine. The remaining five complexes were used to design the final 3-point pharmacophore. Binding features from dopamine, MDMA and methamphetamine were used to make the pharmacophore selective for mephedrone, while selectivity against cutting agents was identified from the binding information for paracetamol. Due to the variability in binding, ranges were used for both the angles and distances. The structural similarities in the four remaining ligands, dopamine, paracetamol, MDMA and methamphetamine suggests that the types of interactions occurring were similar. This aided the final pharmacophore design, and the three final binding points were found to be a hydrogen bond acceptor and two edge/face π-stacking interactions.

The hydrogen bond acceptor is expected to interact with the secondary amine in mephedrone, as is seen for MDMA and methamphetamine, while the π-stacking interactions are positioned to interact with the benzyl group in mephedrone. The one binding feature that is not accounted for in the pharmacophore is any interaction with the carbonyl functionality, due to lack of binding data. The carbonyl group in cathinones is what makes it unique to the amphetamine class, therefore, to obtain selectivity for mephedrone over amphetamines the pharmacophore would ideally include binding features that would interact with the carbonyl. This is a natural limitation when designing a sensor in this way, i.e. when no experimental protein-ligand complexation data is available for the target compound. Thus, traditional synthetic host molecule design will be employed together with the pharmacophore model which will enable an additional binding point to be added to the host molecules that does not occur in the pharmacophore model.

Importantly, the host molecules will be designed based on the understanding of how common cutting agents bind to proteins, i.e. the binding features from paracetamol and the knowledge of caffeine's affinity for face/face π-stacking. This will allow for certain features to be excluded or minimised from the host design, such as steric size of the binding cavity. This information could help to improve selectivity of potential host molecules. Host molecules for the detection of mephedrone will be designed based on the pharmacophore model, along with the additional binding information to aid in

selectivity over cutting agents. The final host molecules will be synthesised (Chapter 4) and tested (Chapter 5), to evaluate the pharmacophore based host design for the detection of mephedrone.

Chapter 4   Synthesis of Potential Host Molecules

4.1   Introduction

As discussed in Chapter 2, the main focus of the project shifted to the design and development of a sensory molecule for mephedrone, as the demand for an in-field sensory device for the aminoindanes was not deemed necessary given its reduced popularity. The pharmacophore model developed in Chapter 3 based on protein-ligand interactions (i.e., host-guest interactions), will be used to design a number of host molecules. Using host-guest chemistry the synthesis of host molecules that encompass these pharmacophoric features to selectively bind mephedrone will be attempted. As highlighted in Chapter 1, current in-field detection mechanisms lack selectivity over other drugs of abuse as well as the numerous cutting agents that can be present in NPS products. To address the problem of selectivity the host molecules will be designed based on supramolecular chemistry, which utilises non-covalent interactions such as hydrogen bonding, electrostatic and dispersion interactions, in conjunction with the pharmacophore model.

4.1.1   Sensor Selection

An empirical approach to the host molecule design was adopted in Chapter 3, which used binding patterns of small molecules with proteins to develop a pharmacophore. Based on this pharmacophore, knowledge of supramolecular host molecules was applied and two different classes of molecules were considered: macrocyclic calixarenes and acyclic anthraquinones. As discussed in Chapter 1, there are two main classifications for host molecules, flexible (acyclic) and rigid (macrocyclic) scaffolds. Both have their own unique advantages relating to interactions and enthalpy effects of binding. Calixarenes are semi-rigid, macrocyclic molecules with a pre-organised nature that lack conformational flexibility and therefore minimal re-organisation of the host molecule is seen upon addition of the guest. They have also reported high selectivity between neutral molecules[162]. Anthraquinones are more flexible and therefore allow for the host molecule to reorganise around a guest molecule upon binding. It is useful to examine both flexible and rigid host molecules in order to understand the effect that flexibility has on the binding ability and selectivity of the host molecules.

4.1.1.1   Calixarenes

Calixarenes are cyclic host molecules that are synthesised by condensation of *para*-substituted phenols with formaldehyde[103]. They form three dimensional bowl structures with hydrophobic cavities that can encapsulate smaller molecules or ions. They come in a number of ring sizes, with the number of phenolic moieties governing the size of the ring. The most commonly studied are

calix[4]arene and calix[6]arene (Figure 4.1). Calixarenes can be substituted on both the 'upper' and 'lower rims'[103,163]. The upper rim is defined as the wide rim, where the *tert*-butyl groups are situated in the 4- position, while the phenolic hydroxyl groups seen in Figure 4.1 are positioned *para* to the *tert*-butyl groups on the lower, or narrow, rim. There is a large amount of literature surrounding the substitution of the 'lower rim' as well as the 'upper rim' as the *tert*-butyl groups are easily cleaved[163,164].

Calix[4]arene   Calix[6]arene
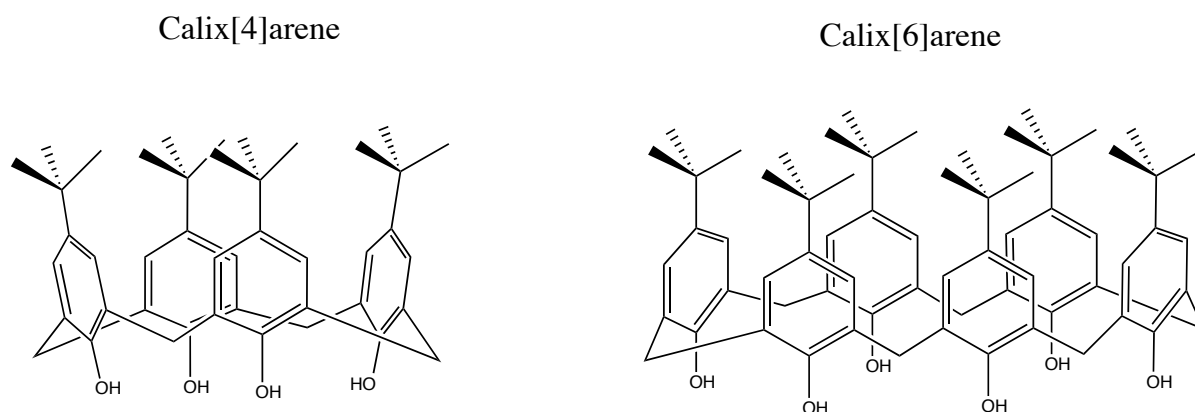
Figure 4.1 - Chemical structures of calix[4]arene and cali[6]arene. The upper and lower rim in the 1 – and 4- positions can both be substituted.

By selectively altering the upper and/or lower rim it is possible to design hosts that are capable of binding anion, neutral and cation guest species. Agraval *et al*. outlined in detail the variations of substituents that are possible on both the upper and lower rim of calixarenes[165]. Substitution on the upper rim is carried out by first de-*tert*-butylation followed by a subsequent reaction. The nonpolar aromatic groups make the compounds water insoluble, which can lead to synthetic complications. However Shinkai *et al*. found that the addition of sulfonate groups on the lower rim produces water-soluble calixarenes[166]. Some of the earliest work carried out on the alteration of calixarene structure was esterification of the lower rim hydroxyl groups. This research showed that strict control of the reaction conditions is necessary in order to produce the desired product[165]. A variety of studies have been conducted looking at the effects of different substituents, their effects on the calixarene conformation and the type of guest molecules that can be attracted, for example; etherification, bridged calixarenes and *bis*-calixarenes. The concept of dimerising calixarenes *via* substitution of the lower rim has led to the development of selective anion sensors[164]. Yilman *et al.* reviewed calixarene complexation with neutral molecules, showing that careful selection of substituents can afford high selectivity between guest molecules[162]. Both upper and lower rim substitution has been shown. Lower rim substitution is more common, thought to be due to the ease of synthesis. However, substitution of the upper rim affords access to the hydrophobic bowl of the calixarene, which can be utilised for molecule recognition. It is the ability to alter the cavity size of calixarenes, as well as the large number

of possible substitutions, that makes them very versatile with respect to host-guest complex formation. This makes it possible to be selective with respect to the size of the guest molecule[109], which is potentially useful for selective binding of mephedrone.

Calixarenes are pre-organised, semi-rigid structures that contain a high degree of rotation around the methylene bond. This leads to a number of known conformations occurring; cone, partial cone, 1,3 alternate and the 1,2 alternate (Figure 4.2)[167].
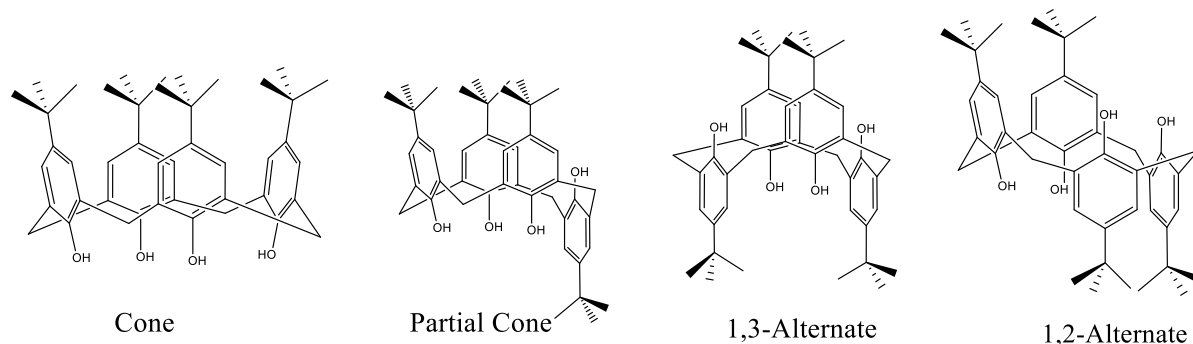
Figure 4.2 - Four possible conformations that have been reported for calixarenes.

It is possible to fix the conformation of the calixarenes into the more desirable cone conformation by selective substitution of the lower rim with bulky functional groups such as isopropyl and benzyl functionalities[164]. The larger the number of units in the calixarenes the harder it is to fix the cone structure due the bulkiness of the substituted lower rim. The effect of substitution on the conformation of the calixarene is extremely important when considering the overall binding cavity of the host molecule.

4.1.1.2   Anthraquinones

Anthraquinones are a class of naturally occurring molecules based on the 9,10-anthraquinone skeleton (Figure 4.3). They are some of the most widely used polycyclic systems in both nature and technology due to their unique physical properties[168]. The unique fluorescence properties of anthraquinones makes them ideal scaffolds for developing sensory molecules. They are naturally occurring compounds that are well studied for a number of uses including dyes, pharmaceuticals and host molecules, and a large variety of derivatives have been synthesised[169].
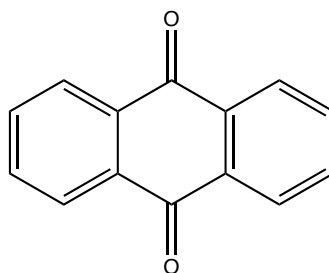
Figure 4.3 - Chemical structure for 9, 10 Anthraquinone.

Substituted anthraquinones are flexible with no pre-organised nature. They are synthesised *via* oxidation of anthracene, typically using chromium trioxide as the oxidant[170]. Anthraquinone analogues are most commonly substituted in the 4- and 5- position; however, the literature surrounding the anthraquinones show that substitution is not limited to the these positions. By altering not only the substituents but also the position of substitution around the anthraquinone scaffold the potential binding cavity can be adjusted. Dhananjeyan *et al*. examined the synthesis of a range of anthraquinone analogues, and their biological properties[169]. Mariappan *et al*. reported a number of synthesised compounds that were used as host molecules for detection of cations, and anthraquinone metal complexes were used for the detection of Cu^{2+} and Fe^{3+} ions[171]. Wu *et al*. also examined the detection of anions using anthraquinones that possess a single thiourea substitution on the ring[172]. In this study the host anthraquinone molecules showed good selectivity for fluoride ions as colourmetric sensors. Both these studies used UV/Vis spectroscopy to quantify the interactions. The fluorescent properties of anthraquinone due to their highly conjugated ring system has been greatly utilised in biological applications. Investigations into anthraquinone interactions with DNA has been well documented in literature. With anthraquinone showing strong hydrophobic interactions and hydrogen bonding which was quantified using fluorescence spectroscopy[173]. It is envisioned that these key binding properties, also identified in Chapter 3, could be easily utilised and integrated into this flexible supramolecular design for a host molecule for mephedrone.

The aim of this chapter is to synthesise a host molecule to selectively bind mephedrone using a supramolecular approach which is based on the key pharmacophoric features determined in Chapter 3. The host molecules have been designed on their ability to bind mephedrone but not the related methamphetamine and commonly used cutting agents such as caffeine and lidocaine. Two host molecule scaffolds are being explored, macrocyclic calixarenes and the more flexible anthraquinones (Figure 4.4). Calixarenes have been found to have very favourable binding constants with small molecules, using the hydrophobic bowl to selectivity bind guest molecules[162]. Their water solubility could be advantageous when looking at in-field detection as it minimises the use of organic solvents.

Anthraquinones have a conjugated ring system that is ideal for designing an optical sensor. They have also shown good selectivity in biological applications[173]. These features, along with their flexible scaffold make them an ideal choice for host molecule design.

4.2 **Experimental**

All sensor synthesis work in this thesis was carried out in Prof. Karl Wallace's Laboratory at the University of Southern Mississippi.

4.2.1 Sensor Design

The desirable pharmacophoric features have been incorporated into the design of both the calixarene and anthraquinone scaffolds, for the detection of mephedrone (Figure 4.4). The host molecules will be substituted with urea (calixarene) or thiourea (anthraquinone) moieties, attached to aromatic functionalities. Urea/thiourea groups can act as both a hydrogen bond donor and acceptor, which based on the deduction in Chapter 3 will be beneficial in the binding of host molecules. Due to a lack of binding data for the carbonyl group, this was not incorporated into the pharmacophore design. However, the carbonyl is what makes the cathinones unique compared to other amphetamine-related compounds, therefore the urea/thiourea groups can also provide an additional binding point by acting as a hydrogen bond donor to bind the carbonyl.
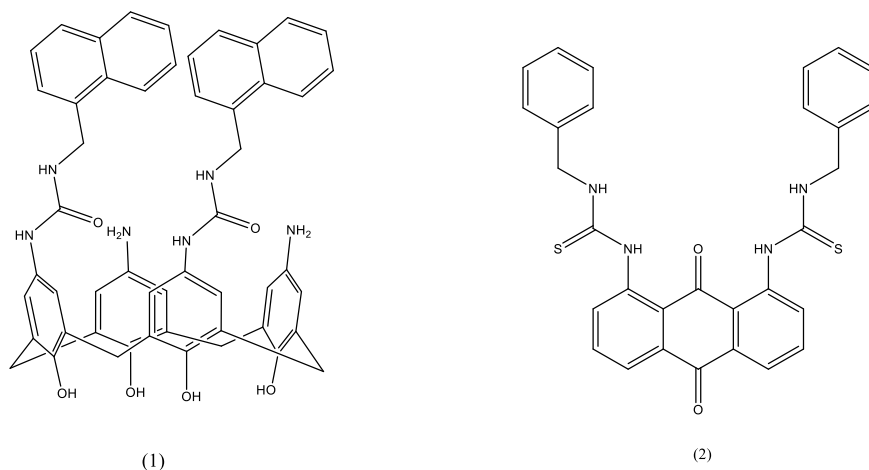
Figure 4.4 - Chemical structures for target host molecules for synthesis (1). 1,3-dithioureanaphthylcalixarene (2) 1,8-dibenzylthiourea anthraquinone.

The aromatic groups reflect the π-stacking interactions that were identified in the pharmacophore. In the calixarene molecule the hydrophobic bowl has multiple π-stacking interactions, the two π-stacking interactions in the anthraquinone are present as the two benzyl groups. The naphthyl units on the calixarene have been added to be used as potential signalling unit for use in optical spectroscopy. Both

contain two arms attached to the core structure, this is to aid in a concerted design that could allow for increased selectivity based on the steric size of guest molecules.

4.2.2 Chemicals and Reagents

All solvents used were obtained from Fisher Scientific, Pittsburgh, USA. All chemical reagents and deuterated solvents for NMR analysis were purchased from Sigma Aldrich, Montana, USA, with the exception of 4-*tert*-butylcalix[4]arene which was purchased from Sigma Aldrich, Gillingham, UK. Thin layer chromatography (TLC) silica gel with fluorescent plates 254 nm, thickness 0.2 mm, were purchased from Sigma Aldrich, Montana, USA. Silica gel for column chromatography was purchased from Silicycle (Québec City, Canada) pore size 60-200 μm.

4.2.3 Analytical Measurements

All nuclear magnetic resonance spectra (NMR) were recorded as approximately 10 % w/v solutions in deuterated chloroform (unless otherwise stated) on a Bruker 400 MHz NMR instrument, with 16 scans per spectrum. Chemical shifts are recorded in ppm, relative to the internal standard TMS and coupling constants, *J*, are recorded in Hz. The low temperature ^{1}H-NMR study was carried out on a Bruker 600 MHz in acetone-d_6, intervals of 10 degrees were applied from 25 ^{o}C down to -50 ^{o}C. The sample at each temperature point was allowed to equilibrate for 20 minutes before the spectra were recorded. Sixteen scans were carried out at each temperature point.

Fourier transfer infrared spectra (FT-IR) were measured over the range of 4000-400 cm^{-1} using a Nicolet Nexus 470 FTIR paired with a Smart Orbit ATR attachment. The characteristic functional groups are reported in wavenumbers (cm^{-1}), and are described as weak (w), medium (m), strong (s), and very strong (vs). Unless otherwise stated TLC was carried out using a mobile phase of ethyl acetate: cyclohexane (3:1 v/v). Liquid chromatography mass spectrometry (LC-MS) was carried out using a Varian Prostar 1200L quadrupole MS/MS, fitted with a Luna C18 column (3 μ; 100 mm x 4.6 mm). A flow rate of 0.25 mLmin^{-1} with acetonitrile/water (90/10 v/v).

Elemental analysis (C,H,N and S) was carried out in duplicate by Analytical and Chemical consultancy service Medac Ltd., Woking, UK.

4.2.4 NMR Titration

^{1}H-NMR titrations were carried out by preparing a 20.0 mM solution of the host molecule in acetone-d_6 (1.0 mL). Stock solutions of the drug free bases were prepared in acetone-d_6 (2.0 mL). Aliquots of 12.5 μL (12.5 μL = 0.5 molar equivalences (eq.) of drug to probe) were added and the ^{1}H-NMR spectra were recorded after each addition.

4.2.5 Calixarene Derivatives

4.2.5.1 De-tert-butylation of Calixarene[174]
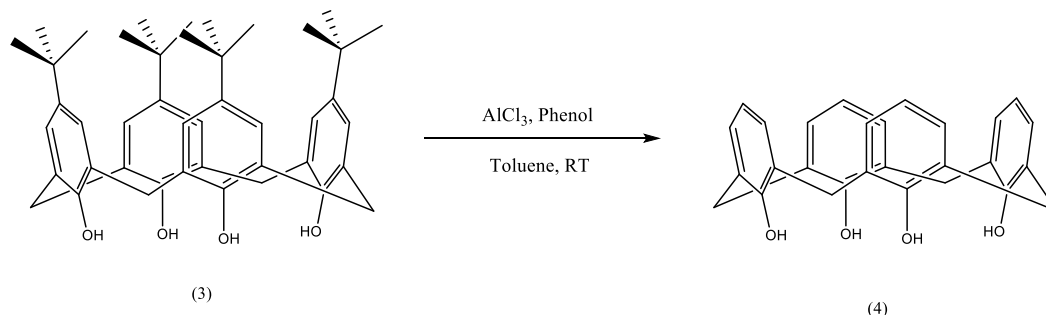
Scheme 4.1 - De-*tert*-butylation of *tert*-butylcalix[4]arene.

4-*tert*-Butylcalix[4]arene ((**3**), 2.0 g, 3.1 mmol), phenol (1.35 mL, 1.07 gmL^{-1}, 15 mmol) and anhydrous aluminium trichloride (2.0 g, 15 mmol) were dissolved in toluene (70 mL) and stirred at room temperature. The solution changed from clear to yellow after a few hours, and after stirring overnight the solution was opaque beige in colour. Hydrochloric acid (0.2 M, 5 mL) was added dropwise to the reaction mixture. The toluene phase was extracted and washed with water (3 x 25 mL), dried over MgSO$_4$, filtered and the organic layer was evaporated yielding a beige oily residue. The product was added slowly to methanol (15 mL) in ice, the product precipitated out and was filtered. The crude white solid was recrystallized from chloroform/methanol (2:3 v/v) yielding a white crystalline solid ((**4**), 990 mg, 76 %). ^{1}H-NMR (CDCl$_3$) δ, ppm: 1.82 (s, 8H, ArCH$_2$Ar), 6.71-6.73 (dd 4H, J=7.8 Ar-H), 7.01-7.02 (d, 8H, Ar-H), 10.18 (s, 4H, OH). Decomposed at 275 ^{o}C.

4.2.5.2 Nitration of Calix[4]arene[175]
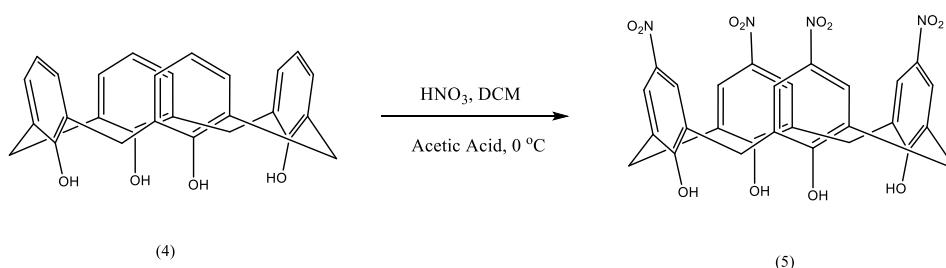
Scheme 4.2 - Nitration of calix[4]arene.

Acetic acid (5 mL) and nitric acid (2.2 mL, 70 %, 33 mmol) were slowly combined and cooled in ice. Calix[4]arene ((**4**), 250 mg, 0.6 mmol) was taken up in dichloromethane (DCM; 5 mL), and cooled in ice. The calix[4]arene solution was added dropwise to the acid mixture with stirring in ice. On

completion of addition the solution was bright orange. The mixture was stirred in ice for 5 hours, and then added to 25 mL of cold water. The residual solid precipitated out and was filtered off, washed with water followed by DCM, yielding a pale yellow solid, ((**5**), 75 mg, 13 %). ^{1}H-NMR (DMSO-d$_6$) δ, ppm: 3.40-3.16 (s, 8H, ArC$\underline{H}_2$Ar), 5.8 (s, 4H, O$\underline{H}$), 8.14 (s, 8H, Ar$\underline{H}$); IR (FT-IR) cm^{-1}: 1620 (stretch, N-O), 1300 (stretch, N-O). Decomposed at 284 ^{o}C.

4.2.5.3   Attempted Reduction of Nitrocalix[4]arene using SnCl$_2$[176,177]
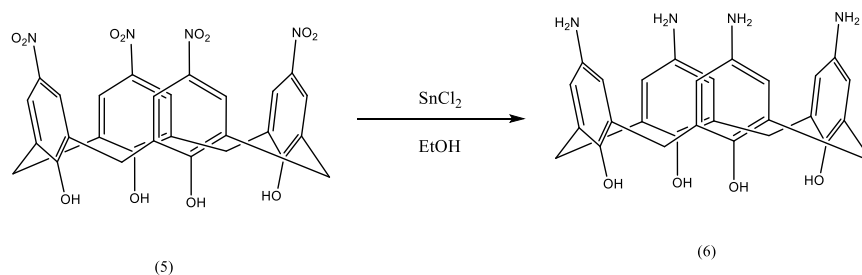
Scheme 4.3 - Reduction of nitrocalix[4]arene to aminocalix[4]arene.

Nitrocalix[4]arene ((**5**), 107 mg, 0.18 mmol) and tin(ll) chloride dihydrate (796 mg, 3.5 mmol) were mixed together in ethanol (20 mL) and refluxed for 5 hours. Once the starting material could not be detected by TLC, the reaction was cooled, and potassium hydroxide (1M) was added to adjust the solution to pH≈10. The reaction was then filtered, yielding no product. The filtrate was then evaporated to dryness, yielding a brown residue and analysed by NMR, there was no evidence that the desired product was formed. Traces of unchanged starting material are observed, with a number of unidentified peaks.

4.2.5.4   Attempted Reduction of Nitrocalix[4]arene using Pd/C[177]
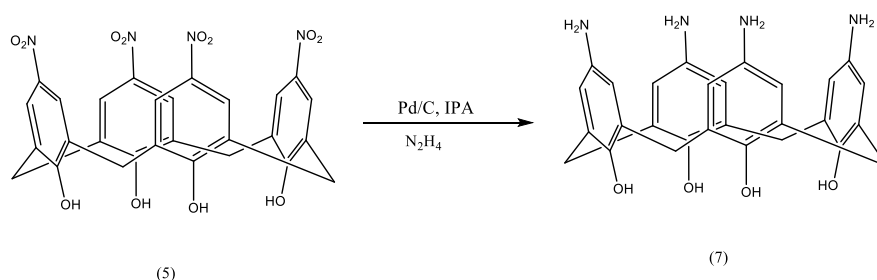
Scheme 4.4 - Reduction of nitrocalix[4]arene using Pd/C.

Nitrocalix[4]arene ((**5**), 200 mg, 0.34 mmol), hydrazine (**6**, 3.24 mL, 1.02 gmL^{-1}, 5.2 mmol) and Pd/C (0.19 mg, 1.76 mmol) were dissolved in isopropyl alcohol (IPA; 60 mL). The calixarene did not fully dissolve upon addition. The reaction was refluxed under nitrogen for 4.5 hours. The calixarene was seen to be more soluble upon heating. The reaction was then cooled and the mixture evaporated to

dryness. The resultant residue was analysed by NMR and LC-MS showing an absence of the desired product but the presence of unchanged starting material and additional uncharacterised peaks.

4.2.5.5   Di-substitution of 4-tert-butylcalix[4]arene Lower Rim[174]
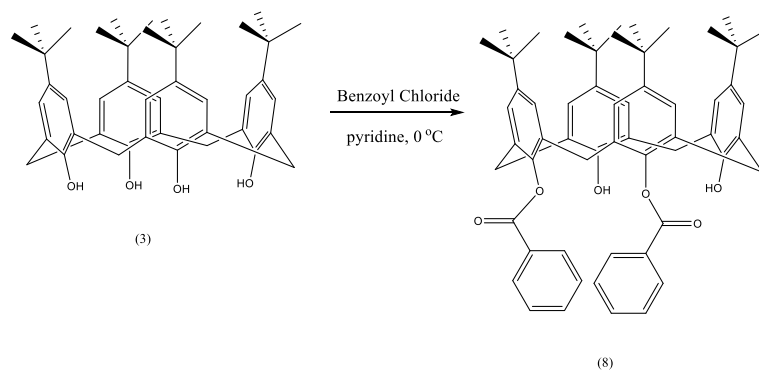
Scheme 4.5 - Di-substitution of 4-*tert*-butyl-1,3-dibenzoylcalix[4]arene.

4-*tert*-Butylcalix[4]arene ((**3**), 200 mg, 0.3 mmol) was taken up in pyridine (10 mL) and stirred in ice for an hour. Benzoyl chloride (0.29 mL, 1.21 gmL^{-1}, 2.5 mmol) was added dropwise into the reaction mixture and left to stir for 1.5 hours. The reaction mixture was poured into ice water (50 mL) and a white precipitate immediately started to form. The precipitate was filtered off, washed with water and then recrystallized from chloroform/ethanol (3:5 v/v), filtered and washed with ethanol yielding a white crystalline solid ((**8**), 50 mg, 20 %). ^{1}H-NMR (CDCl$_3$), δ ppm 1.04 (s, 18H, *t*-bu), 1.19 (s, 18H, *t*-bu), 3.53-3.57 (d, 4H, J=14.21 Hz, ArCH$_2$Ar), 4.00-4.03 (d, 4H, J=14.17 Hz, ArCH$_2$Ar), 5.18 (s, 2H, ArOH), 6.94 (s, 4H, Ar-H, (-benz)), 7.05 (s, 4H, Ar-H, (-OH)), 7.57-7.59 (t, 4H, J=7.80 Hz, *m*-Ar-H), 7.74-7.78 (t, 2H, J= 7.47 Hz, *p*-Ar-H), 8.37-8.39 (d, 4H, J=7.08 Hz, O-Ar-H). Decomposed at 263 ^{o}C.

4.2.5.6   Attempted de-tert-butylation of 4-tert-butyl 1,3 dibenzoylcalix[4]arene
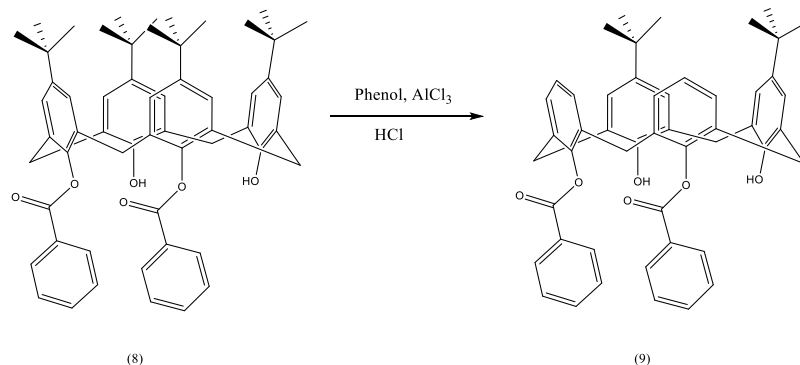
Scheme 4.6 - De-*tert*-butylation of 4-*tert*-butyl 1,3-dibenzoylcalix[4]arene.

4-t*ert*-Butylcalix[4]arene ((**8**), 53 mg, 0.06 mmol), phenol (0.027 mL, 1.07 gmL^{-1}, 0.3 mmol) and anhydrous aluminium trichloride (75 mg, 0.3 mmol) were taken up in toluene (15 mL) and stirred at room temperature. The solution went from clear to yellow after a few hours, and after stirring overnight the solution was opaque beige in colour. Hydrochloric acid (0.2 M, 5 mL) was added dropwise. The toluene phase was extracted and washed with water (3 x 15 mL), the organic layer was evaporated yielding a beige oily residue. Methanol was used in an attempt to precipitate out product, no precipitate formed. The methanol was evaporated off and the resulting residue was analysed using NMR where no presence of desired product seen.

4.2.6   Anthraquinone Derivatives

4.2.6.1   Synthesis of 1,8- diaminoanthraquinone[178]
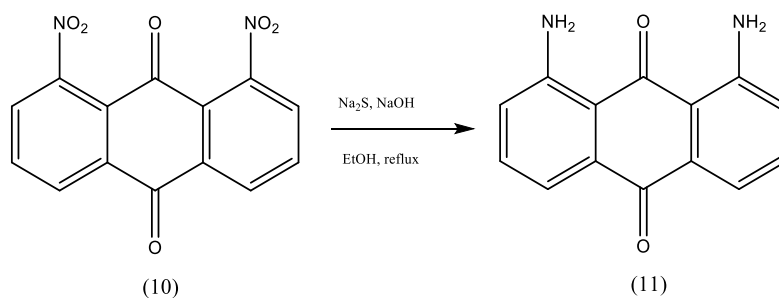
Scheme 4.7 - Synthesis of 1, 8-diaminoanthraquinone.

1,8-Dinitroanthraquinone ((**10**), 504 mg, 1.69 mmol), sodium sulphide (1.422 g, 6.76 mmol) and sodium hydroxide (275 mg, 6.76 mmol) were added to ethanol (15 mL) stirred and refluxed for 6 hours. After this time the reaction mixture was cooled in ice and an insoluble material precipitated over 1 hour. The reaction mixture was filtered under vacuum, and the solid was washed with cold water, yielding a deep purple solid ((**11**), 360 mg, 90 %). ^{1}H-NMR (400 MHz, CDCl$_3$) δ, ppm: 6.75 (s, 4H, 2N$\underline{H}_2$), 6.93-6.96 (d, 2H, *J*=12 Hz, Ar$\underline{H}$), 7.40-7.44 (dd, 2H, *J*=16 Hz, Ar$\underline{H}$), 7.60-7.63 (d, 2H, *J*=12 Hz, Ar$\underline{H}$); IR (neat) in cm^{-1}: 3377 ν_{N-H} (m), 3131 ν_{Ar-H}, 2964 $\nu_{C=C-H}$, 1701 $\nu_{C=O}$ (s). Decomposed at > 200 ^{o}C.

4.2.6.2   Attempted Synthesis of 1,8-Dibenzylthiourea anthraquinone
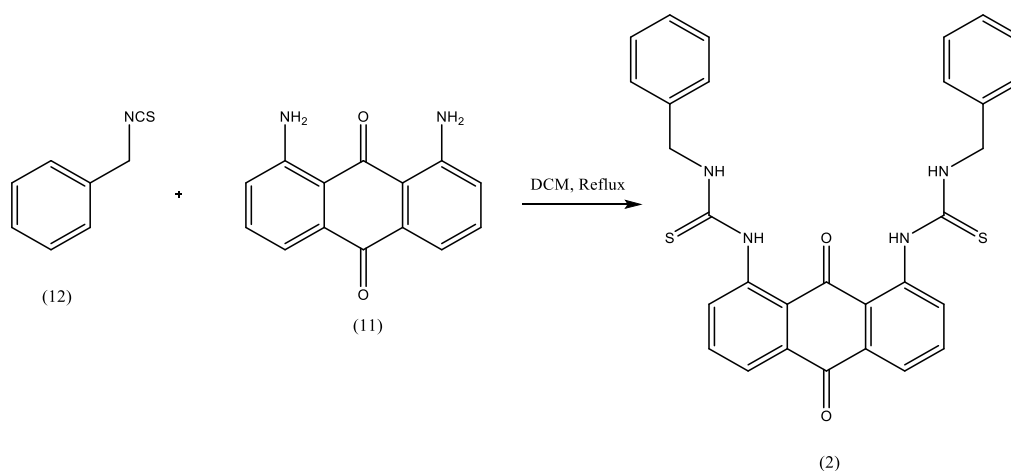
Scheme 4.8 - Synthesis of dibenzylthiourea anthraquinone.

1,8-Diaminoanthraquinone ((**11**), 81 mg, 0.4 mmol) and benzylisothiocyanate ((**12**), 111 µl, 1.13 gmL⁻¹, 0.8 mmol) were added to DCM (5.5 mL) stirred, and left to reflux. TLC analysis in ethyl acetate: cyclohexane (3:1) showed significant starting material and formation of two new spots, after 24 hours no further changes were seen using TLC. After 24 hours the reaction appeared to stop progressing and the mixture was allowed to cool. The solvent was evaporated to yield a brown oil which solidified on standing. The reaction mixture was dissolved up in ethyl acetate, and separated *via* column chromatography with silica gel, eluting with EtOAc/hexane (10/90 v/v), isolating starting material, evaporation of the two other fractions and NMR analysis showed no formation of the desired product.

4.2.6.3   Attempted Synthesis of Dibenzylthiourea anthraquinone using Triethylamine
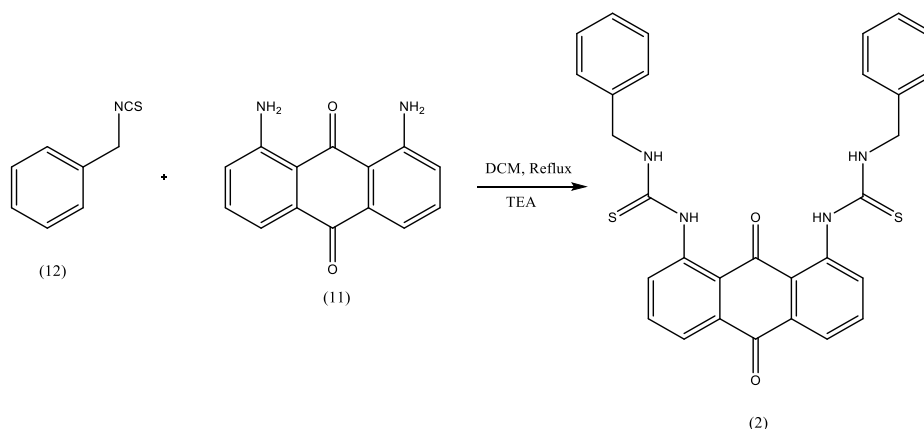
Scheme 4.9 - Synthesis of dibenzylthiourea anthraquinone using trimethylamine.

1,8-Diaminoanthraquinone ((**11**), 203 mg, 0.8 mmol), benzyl isothiocyanate ((**12**), 286 μl, 1.13 gmL^{-1}, 1.7 mmol) and triethylamine (0.26 mL, 0.73 gmL^{-1}, 1.8 mmol) were added to DCM (40 mL) and refluxed. The reaction was monitored by TLC (ethyl acetate: cyclohexane 3:1 v/v). After 24 hours the reaction appeared to stop progressing, starting material was still present together with 3 additional spots on the TLC. The reaction mixture was allowed to cool, and a precipitate formed. The reaction mixture was filtered producing a purple solid, which was found to be the starting material. The filtrate was treated with hydrochloric acid (1 M, 10 mL) to remove excess triethylamine, the organic phase was examined by TLC showing 3 spots remaining, one of which corresponded to the benzyl isothiocyanate starting material. The reaction mixture was dissolved in ethyl acetate, and separated *via* column chromatography with silica gel, eluting with EtOAc/hexane (10/90 v/v), isolating the anthraquinone and benzyl isothiocyanate starting materials and the other fraction isolated was a light brown residue which was analysed by NMR but the desired product was not detected.

4.2.6.4   Attempted Synthesis of Dibenzylthiourea anthraquinone using Triethylamine in Ethyl Acetate
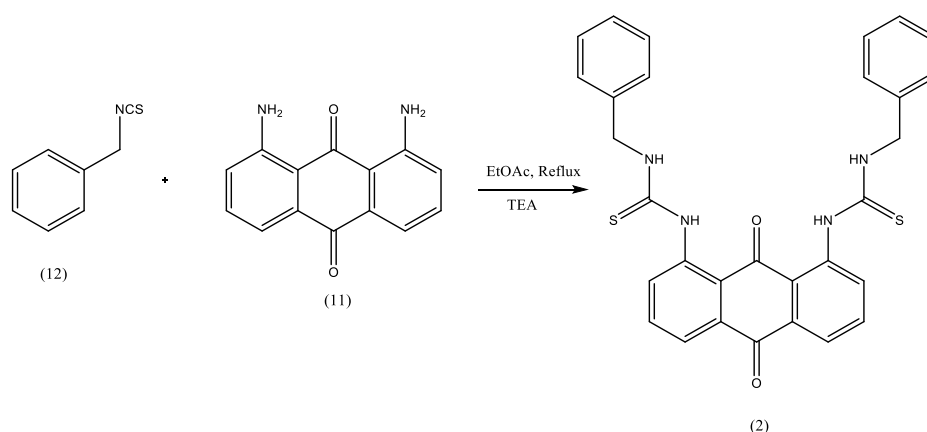
Scheme 4.10 - Synthesis of dibenzylthiourea anthraquinone using triethylamine in ethyl acetate.

1,8-Diaminoanthraquinone ((**11**), 100 mg, 0.4 mmol), benzyl isothiocyanate ((**12**), 111 μl, 1.13 gmL^{-1}, 0.9 mmol) and triethylamine (0.26 mL, 0.73 gmL^{-1}, 1.8 mmol) were added to ethyl acetate (40 mL), stirred and refluxed. The reaction was monitored *via* TLC (ethyl acetate: cyclohexane 3:1 v/v) after 24 hours the reaction appeared to stop progressing, starting material was still present along with 3 additional spots on the TLC. The reaction was filtered producing a purple solid, which was found to be anthraquinone-starting material. Filtrate was treated with hydrochloric acid (1 M) to remove excess triethylamine, TLC of the reaction mixture showed 3 spots remaining, one of which corresponded to the benzyl isothiocyanate starting material. Reaction was separated using column chromatography with silica gel eluting with EtOAc/hexane (10/90 v/v), each of the fractions were evaporated to

dryness, isolating starting material and two additional by-products, the desired product was not detected using NMR or MS.

4.2.6.5   Attempted Synthesis of Dibenzylthiourea anthraquinone in Aqueous Acetone
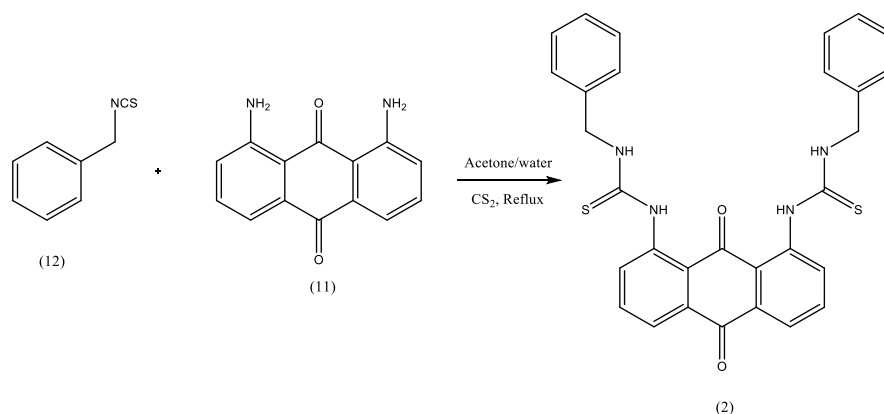
Scheme 4.11 - Synthesis of dibenzylthiourea anthraquinone in acetone and water.

1,8-Diaminoanthraquinone ((**11**), 100 mg, 0.4 mmol), benzyl isothiocyanate ((**12**), 111 μL, 1.13 gmL^{-1}, 0.9 mmol) and carbon disulphide (0.05 mL, 1.26 gmL^{-1}, 0.8 mmol) were combined in aqueous acetone (1:3, 20 mL) and refluxed. After three hours a new spot was visible on the TLC as well as the anthraquinone starting material. The reaction was monitored by TLC for 28 hours, starting material was still present, but the reaction had stopped proceeding. Reaction was removed from the heat, filtered and the filtrate was evaporated to dryness. The precipitate was analysed by NMR and was shown to be the anthraquinone starting material, the filtrate was shown to be benzyl isothiocyanate and by-products, but no detection of the desired product using NMR or MS.

4.2.6.6   Attempted Synthesis of Dibenzylthiourea Anthraquinone using P₄ Base
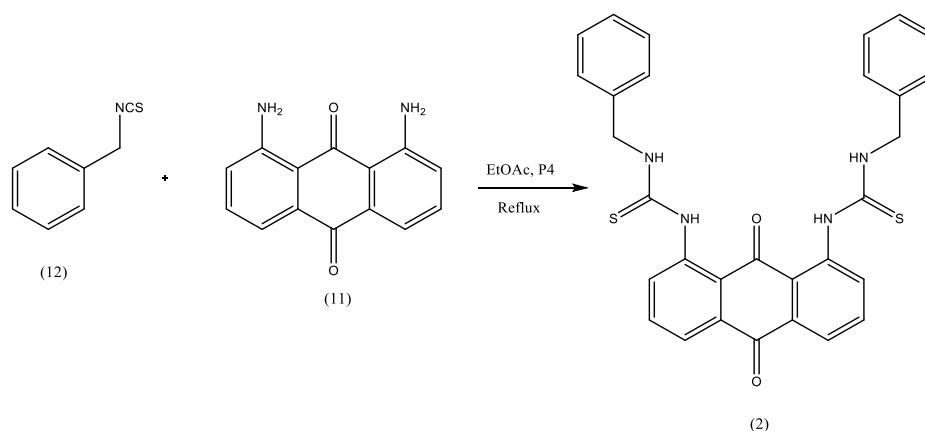
Scheme 4.12 - Synthesis of dibenzylthiourea anthraquinone using P₄ superbase.

1,8 -Diaminoanthraquinone ((**11**), 200 mg, 0.8 mmol) and phosphazene base P₄ – *tert*-butyl (1.17 g, 1.9 mmol) were stirred in ethyl acetate (35 mL) at room temperature for 10 minutes. Benzyl isothiocyanate ((**12**), 0.25 mL, 1.13 gmL^{-1}, 1.9 mmol) was taken up in ethyl acetate (2 mL) and added dropwise to the reaction mixture. The reaction was left to stir at room temperature for 64 hours, and was monitored by TLC. The reaction was filtered and the precipitate was analysed by NMR, the starting material was detected, but the desired product was not detected using NMR or MS.

4.2.7   Anthracene Derivatives

4.2.7.1   Reduction of 1,8-dinitroanthraquinone[179]
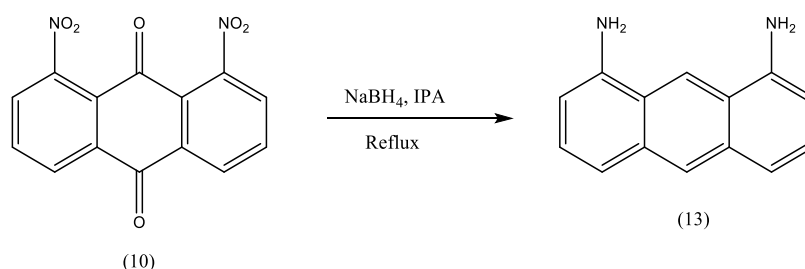
Scheme 4.13 - Reduction of 1,8-diaminoanthraquinone to 1,8-diaminoanthracene.

1,8-Dinitroanthraquinone ((**10**), 1.00 g, 4.2 mmol) was dissolved in isopropanol (IPA; 50 mL) and stirred under nitrogen for 15 minutes. Sodium borohydride (2.00 g, 53 mmol) was added and the reaction was refluxed for 36 hours. The reaction mixture was poured into iced water (100 mL) and a purple

precipitate formed, the reaction mixture was filtered and the precipitate washed with water to yield a dark purple solid ((**13**), 820 mg, 93 %). ^{1}H-NMR (400 MHz, CDCl$_3$) δ, ppm: 4.21 (s, 4H, N<u>H</u>), 6.76-6.74 (d, 2H, *J*=8 Hz Ar<u>H</u>), 7.31-7.29 (dd, 2H, *J*= 8 Hz Ar<u>H</u>), 7.49-7.47 (d, 2H, *J*= 8 Hz, Ar<u>H</u>), 8.22 (s, 1H, Ar<u>H</u>), 8.37 (s, 1H, Ar<u>H</u>); IR (neat) 3298 v_{N-H} (m), 3270 v_{Ar-H} and 1623 $v_{C=C}$ cm^{-1}; M.p. = 195-196 °C.

4.2.7.2   Attempted Synthesis of 1, 8-dibenzylthiourea anthracene using Triethylamine
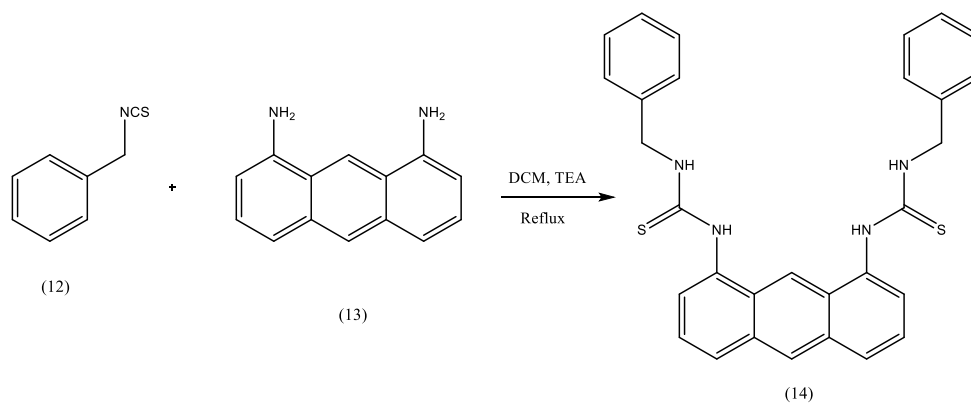
Scheme 4.14 - Synthesis of 1,8-dibenzylthiourea anthracene.

1,8-Diaminoanthracene ((**13**), 700 mg, 3.4 mmol), benzoisothiocyanate ((**12**), 0.76 mL, 1.13 gmL^{-1}, 6.7 mmol) and triethylamine (1.25 mL, 0.72 gmL^{-1}, 7.9 mmol) were added to DCM (70 mL) and refluxed for 24 hours. Monitoring by TLC showed the presence of anthracene starting material and formation of a new spot. The reaction was allowed to cool and placed in ice, a precipitate formed which was filtered off. The precipitate was washed with ethyl acetate/hexane (1:9 v/v). TLC of the precipitate showed two spots, neither of which corresponded to the starting material. The product was dissolved up in ethyl acetate and purified *via* column chromatography using silica gel and ethyl acetate: cyclohexane (3:1 v/v) eluent. Both bands were isolated and examined by NMR showing possible multiple conformers present. A variable temperature NMR study was conducted to try and freeze out the isomers for further analysis. Concluded that Compound 14 was not successfully synthesised.

4.2.7.3   Synthesis of Dibenzylthiourea anthracene in Ethanol
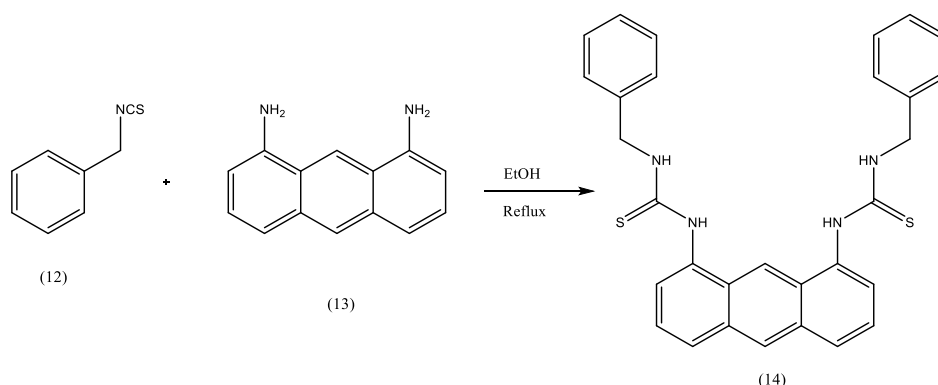
Scheme 4.15 - Synthesis of 1,8-dibenzylthiourea anthracene.

1,8-Diaminoanthracene ((**13**), 877 mg, 4.2 mmol) and benzoisothiocyanate ((**12**), 1.13 gmL^{-1}, 8.4 mL) were taken up in ethanol (100 mL) and refluxed for 2 hours. The reaction was cooled in ice, and filtered. The precipitate was washed with excess water and ethanol. The product was dried under vacuum, yielding a dark brown solid ((**14**), 1.04 g, 40 %). ^{1}H-NMR (400 MHz, acetone-d$_6$) δ, ppm: 4.78-4.79 (d, 4H, *J*= 5.5 Hz, 2C$\underline{H}_2$), 7.34-7.36 (m, 10H, Ar$\underline{H}$-benzyl), 7.55-7.56 (m, 4H, Ar$\underline{H}$-anthracene), 8.01-8.02 (d, 2H, *J*= 8.1 Hz, Ar$\underline{H}$-anthracene), 8.29 (s, 2H, 2N$\underline{H}$), 8.67 (s, 1H, Ar$\underline{H}$-anthracene), 8.78 (s, 1H, Ar$\underline{H}$-anthracene), 9.87 (s, 2H, 2N$\underline{H}$); ^{13}C-NMR (400 MHz, acetone-d$_6$) δ, ppm: 47.7 ($\underline{C}H_2$, 12/12'), 116.8 (Ar$\underline{C}$, C9), 125.5 (Ar$\underline{C}$, C2), 126.5 (Ar$\underline{C}$, C5), 126.7 (Ar$\underline{C}$, 9'), 127 (Ar$\underline{C}$, C10), 127.4 (Ar$\underline{C}$, C14/14'), 128.2 (Ar$\underline{C}$, C15/15'), 132.1 (Ar$\underline{C}$, C4'), 134.9 (Ar$\underline{C}$, C13/13'), 139 (Ar$\underline{C}$, C8), 182.4 ($\underline{C}$=S, C11/11'); IR (neat) in cm^{-1}: 3377 v_{N-H} (m), 3131 v_{Ar-H}, 2964 $v_{C=C-H}$, 1612 $v_{C=S}$ (m), 1495 $v_{C=S}$ (s), and 1250 $v_{C=S}$ (s); m.p. = 213 -214 °C. Elemental analysis (%) calculated for $C_{30}H_{26}N_4S_2$: C, 71.11; H, 5.17; N, 11.06. Re-calculated for $C_{30}H_{26}N_4S_2 \cdot H_2O$ C, 68.67; H, 4.99; N, 10.68, Found: C, 68.93, H, 4.89; N, 10.34.

4.2.8   Aniline Derivative

4.2.8.1   Synthesis of Benzylthiourea Aniline[180]
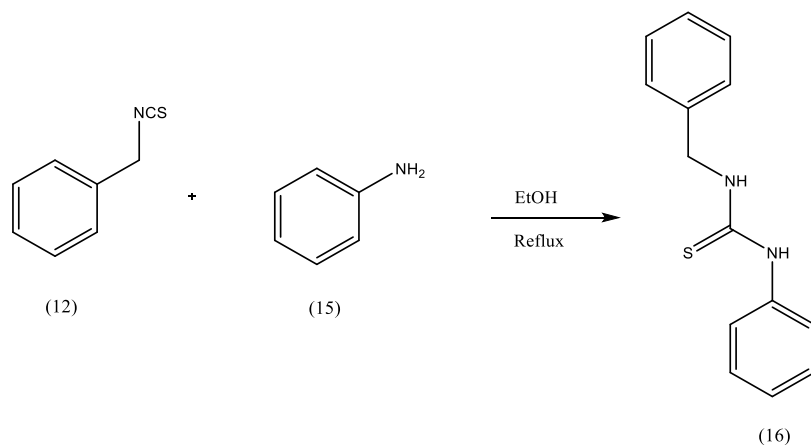
Scheme 4.16 - Synthesis of benzylthiourea aniline.

Aniline ((**15**), 400 mg, 392 μL, 4.3 mmol) and benzylisothiocyanate ((**12**), 568 μL, 1.13 gmL^{-1}, 4.3 mmol) were taken up in ethanol (30 mL) and refluxed for two hours. Upon the formation of a precipitate, the reaction was allowed to cool to room temperature and filtered. The product was dried under vacuum, yielding a cream solid ((**16**), 620 mg, 59 %). ^{1}H-NMR (400 MHz, DMSO-d$_6$) δ, ppm: 4.73-4.74 (d, 2H, *J*= 5.5 Hz, C$\underline{H}_2$), 7.10-7.12 (t, 1H, J=7.3 Hz, Ar$\underline{H}$-benzyl), 7.23-7.29 (m, 1H, Ar$\underline{H}$-aniline), 7.30-7.38 (m, 6H, Ar$\underline{H}$), 7.41-7.43 (d, 2H, *J*=7.8 Hz, ArH-aniline), 8.16 (s, 1H, N$\underline{H}$), 9.61 (s, 1H, N$\underline{H}$); ^{13}C-NMR (400 MHz, DMSO-d$_6$) δ, ppm: 47.2 ($\underline{C}$H$_2$, C8), 123.3 (Ar$\underline{C}$, C12), 124.3 (Ar$\underline{C}$, C4), 126.8 (Ar$\underline{C}$, C10/10'), 128.2 (Ar$\underline{C}$, C6), 128.6 (Ar$\underline{C}$, C5), 139 (Ar$\underline{C}$, C9), 139.1 (Ar$\underline{C}$, C1), 180.8 ($\underline{C}$=S, C7); IR (neat) in cm^{-1}: 3375 v_{N-H} (m), 3129 v_{Ar-H}, 2967 $v_{C=C-H}$, 1616 $v_{C=S}$ (m), 1495 $v_{C=S}$ (s), and 1250 $v_{C=S}$ (s); m.p. = 145-146 °C.

4.2.9   Synthesis of Mephedrone

4.2.9.1   Synthesis of 4-methyl propiophenone
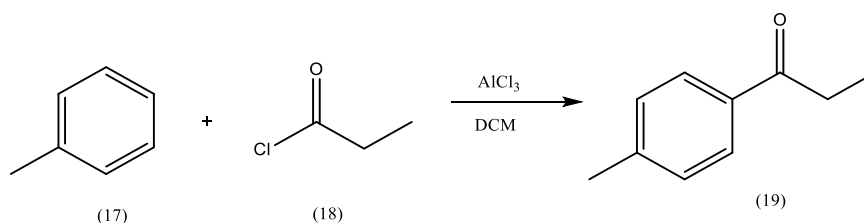
Scheme 4.17 - Synthesis of 4-methyl propiophenone.

Propionyl chloride ((**18**), 1.06 gmL^{-1}, 7.5 mL, 86 mmol) in DCM (10 mL) was added drop wise to a mixture of AlCl$_3$ (12.0 g, 86 mmol) in DCM (50 mL) with ice – cooling under a nitrogen atmosphere. The mixture was stirred for 0.5 h. Anhydrous toluene ((**17**), 0.87 gmL^{-1}, 16.2 mL, 152 mmol) was then

121

added over 0.5 h cooling in ice, the mixture was allowed to warm to room temperature and stirred for 1.5 h. The solution was added to approx. 90 mL ice water with vigorous effervescence. The organic layer was separated and the aqueous layer was re-extracted with 2 x 50 mL DCM. Combined organic extracts were washed with NaOH 5 % in H_2O (2 x 50 mL), brine (2 x 50 mL), dried over $MgSO_4$ and evaporated to give a pale yellow oil ((**19**), 11.31 g, 88 %). ^{1}H-NMR (400 MHz, $CDCl_3$) δ, ppm: 7.85-7.86 (d, 2H, J= 8.0 Hz, Ar$\underline{H}$), 7.22-7.23 (d, 2H, J= 8.0 Hz, Ar$\underline{H}$), 2.95-2.96 (q, 2H, J= 7.2 Hz, C$\underline{H}_2$CH$_3$), 2.40 (s, 3H, C$\underline{H}_3$Ar) 1.20-1.21 (t, 3H, J= 7.9 Hz, CH$_2$C$\underline{H}_3$); IR (neat) in cm^{-1}: 1682 $v_{C=O}$ (s), 1608 $v_{C=C}$ (m).

4.2.9.2   Synthesis of 4-methyl-2-bromopropiophenone
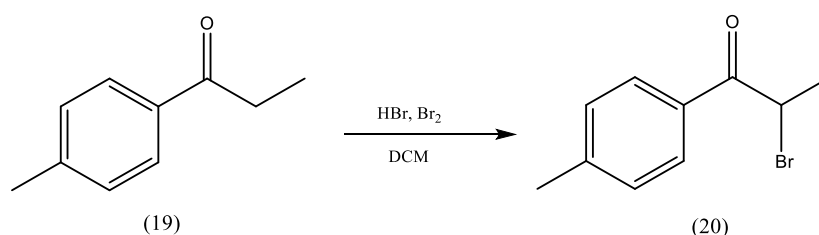
Scheme 4.18 - Synthesis of 4-methyl-2-bromopropiophenone.

To a solution of 4-methyl propiophenone ((**19**), 8.89 g, 60 mmol) in DCM (60 mL), one drop of hydrogen bromide (33 % in aqueous solution) was added followed by one drop of bromine. The mixture was stirred at room temperature until the bromine colour had dispersed. Additional bromine (3.1 mL, 3.1 gmL^{-1}) was added dropwise with stirring. The reaction mixture was stirred at room temperature for 1.5 h and then concentration *in vacuo* produced a dark brown oil which solidified on standing. The crude product was recrystallized from diethyl ether to give a white crystalline solid ((**20**), 4.5 g, 37 %). ^{1}H-NMR (400 MHz, $CDCl_3$) δ, ppm: 7.90-7.91 (d, 2H, J= 8.0 Hz, Ar$\underline{H}$), 7.27-7.28 (d, 2H, J= 8.0 Hz, Ar$\underline{H}$), 5.26-5.27 (q, 1H, J= 7.2 Hz, C$\underline{H}$Br), 2.41 (s, 3H, C$\underline{H}_3$Ar) 1.88-1.89 (d, 3H, J= 6.7 Hz, CH$_2$C$\underline{H}_3$); IR (neat) cm^{-1}: 1682 $v_{C=O}$ (s), 1608 $v_{C=C}$ (m); m.p. = 76-77 °C; lit. m.p. 76-77 °C[37].

4.2.9.3   Synthesis of 4-methyl methcathinone hydrochloride
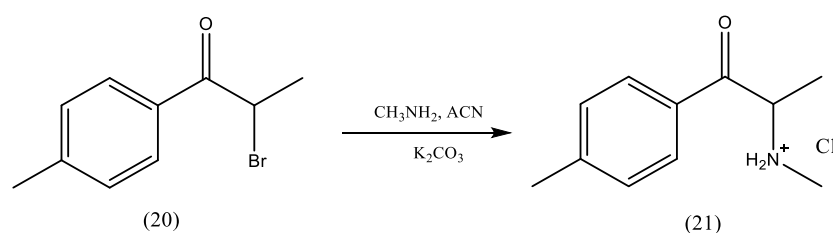
Scheme 4.19 - Synthesis of 4-methyl methcathinone hydrochloride.

To a solution of 4-methyl-2-bromopropiophenone ((**20**), 4.5 g, 19.7 mmol) in ACN (100 mL) methyl amine hydrochloride (1.33 g, 19.7 mmol) was added. Once dissolved, potassium carbonate (8.17 g, 59.1 mmol) was added. The reaction mixture was left stirring at room temperature, with a white precipitate forming throughout the reaction. The reaction was monitored *via* TLC until completion (ca. 7 h). Once the reaction had reached completion the precipitate and salts were filtered off and the filtrate was concentrated *in vacuo.* The remaining residue was redissolved in diethyl ether (50 mL), extracted with aqueous hydrochloric acid (5 %, 3 x 50 mL). The combined aqueous extracts were washed with diethyl ether (2 x 50 mL). The combined aqueous extracts were made basic (pH 9-10) using ammonium hydroxide. The crude product free base is observed to precipitate out from the aqueous solution as an oil. Diethyl ether (3 x 50 mL) was used to extract out the free base and the combined organic extracts were washed with water (2 x 50 mL) and dried over sodium sulfate, filtered and cooled in ice. Hydrochloric acid in diethyl ether (2M) was added until no more white precipitate was seen to form. The product was filtered off and recrystallized from ethanol, yielding a white crystalline solid ((**21**), 950 mg, 23 %). ^{1}H-NMR (400 MHz, CDCl$_3$) δ, ppm: 9.30 (br s, 2H, CH$_3$N$\underline{H}_2$) 7.90-7.91 (d, 2H, *J*= 8.0 Hz, Ar$\underline{H}$), 7.27-7.28 (d, 2H, *J*= 8.0 Hz, Ar$\underline{H}$), 4.19-4.22 (q, 1H, *J*= 8.1 Hz, C$\underline{H}$NH), 2.59 (s, 3H, C$\underline{H}_3$NH$_2$), 2.41 (s, 3H, C$\underline{H}_3$Ar), 1.88-1.89 (d, 3H, *J*= 6.7 Hz, CH$_2$C$\underline{H}_3$); IR (neat) in cm^{-1}: 2717 v_{N-H} (m), 1689 $v_{C=O}$ (s), 1606 $v_{C=C}$ (m); m.p. 250-252 ^{o}C; lit m.p. 251 ^{o}C[37].

4.3 Results and Discussion

4.3.1 Calixarene

As outlined above, 1,3-dithioureanaphthylcalixarene (**1**) was designed based on the pharmacophoric features proposed in Chapter 3, to selectively bind mephedrone. The hydrophobic bowl is predicted to bind to the benzyl unit of mephedrone, while the urea arms are designed to bind to both the amine and the carbonyl functionalities. The naphthyl groups have been included as potential signalling units for use with optical spectroscopy. The proposed synthetic route for compound (**1**) is shown in Scheme 4.20.
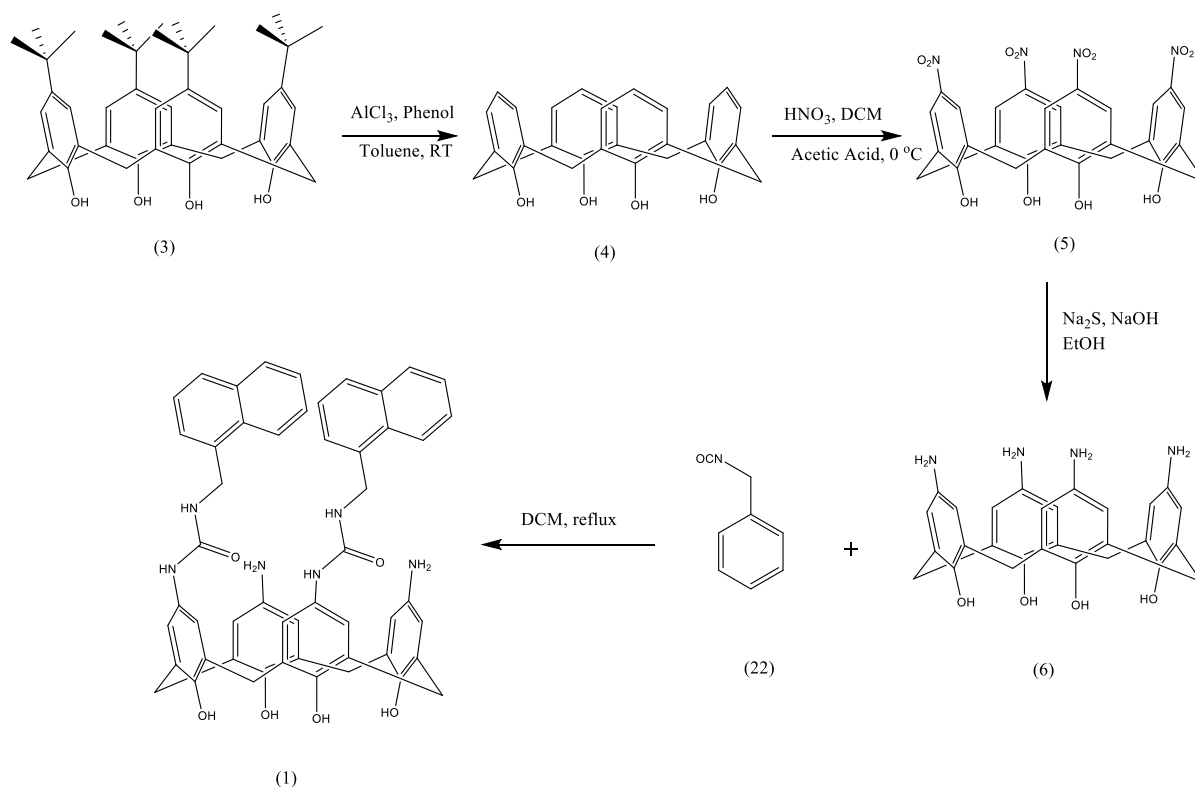
Scheme 4.20 - Proposed reaction procedure for the synthesis of 1,3-diureanaphthylcalix[4]arene.

The first step involves de-*tert*-butylation of the upper rim of the starting *tert*-butylcalix[4]arene (**3**). This is a well-established method reported in a number of literature sources[163,166,174]. The reaction was carried out in toluene *via* a retro-Friedel-Crafts de-*tert*-butylation; five equivalents of aluminium chloride were used. The reaction was left at room temperature overnight, before being worked up following a procedure set out by Elçin *et al*[174]. The most recent NMR predictions for calixarenes carried out by Magrans *et al.*[181] showed that the de-*tert*-butylated calixarene could not exclusively adopt the cone conformation. However, NMR analysis of compound (**4**) shows the Ar-CH$_2$-Ar chemical shifts at 3.57 and 3.88 ppm, which would suggest a cone conformation, as reported in the literature[182].

Compound (**4**) was then nitrated using acetic acid and nitric acid in DCM. To prevent over nitration of the upper rim, the reaction was carried out using nitric acid as the limiting reagent at low temperature. DCM was used due to the insolubility of compound (**4**) in aqueous media, however the starting material was still not completely soluble in the reaction mixture. After 2 hours the reaction was worked up as outlined in Kumar *et al.*[175]. A ^{1}H-NMR spectrum of the crude material indicated the presence of starting material as well as product; washing with DCM and ethanol produced the pure product. NMR spectra showed two chemical environments which suggests tetra substitution of the

upper calixarene rim. IR data corroborates successful nitro substitution showing IR stretches at 1620 and 1300 cm^{-1} indicative of N-O stretch of the nitro groups.

In order to introduce the urea functionalities, reduction of the nitro groups is required. Several alternative reaction conditions were examined for the reduction. There is currently no literature associated with this reaction using calixarenes and therefore known reduction conditions for different compounds were attempted. The first attempt was using tin (II) chloride, in ethanol. NMR analysis of the reaction product showed no evidence for formation of the required compound. Another well-known reductive procedure is palladium on carbon, which was carried out using isopropyl alcohol as the solvent under reflux. The starting calixarene (compound (**6**)) did not appear to completely dissolve in this solvent under reflux and the starting material was isolated upon work up of the reaction mixture. The reaction conditions used for the reduction of the nitroanthraquinones was a solution of ethanol and four equivalents of sodium sulphide. Compound (**6**) was not soluble in this reaction mixture, even under reflux conditions, and a small amount of DMSO was added to the mixture to aid solubility. This allowed the reaction to proceed, however the presence of the DMSO proved problematic and it was not possible to obtain compound (**1**) out of solution. Evaporation of the reaction mixture, led to a mixture of starting materials and the ^{1}H-NMR of the residue showed no presence of the desired product. The solubility of compound (**6**) was examined in a range of organic solvents; however, DMSO was the only solvent in which it appeared to show any degree of solubility. This is a characteristic of the calixarenes that has been noted previously[65]. Substitution of the lower rim of the calixarenes aids the solubility of these compounds both in aqueous and organic media, by disrupting the hydrogen bonding between the lower rim hydroxyl groups. In order to further study the calixarenes as host molecules, substitution on the lower rim to increase solubility was carried out.

Selective substitution of two hydroxyl groups for benzoyl groups was carried out as described by Elçin *et al*.[174]. It was found that by substituting the 1- and 3- positions with benzoyl groups, solubility of the calixarene was improved, specifically in nitric acid to allow for nitration to occur at increased yields. This also allowed for de-*tert*-butylation to occur on just two positions on the upper rim, those that are not benzoyl substituted in the *para* position.

Compound (**3**) was substituted in the 1- and 3- positions with benzoyl groups, using 2 molar equivalents of benzoyl chloride (Scheme 4.21). Splitting of the CH$_2$ protons in the NMR analysis showed symmetrical substitution, indicating that de-*tert*-butylation occurred on just the 1- and 3- positions on the upper rim. Then de-*tert*-butylation was carried out as described previously; however, the presence of the benzoyl groups prevented removal of the *tert*-butyl groups in the 1- and 3- positions. The final product remained di-*tert*-butyl substituted.
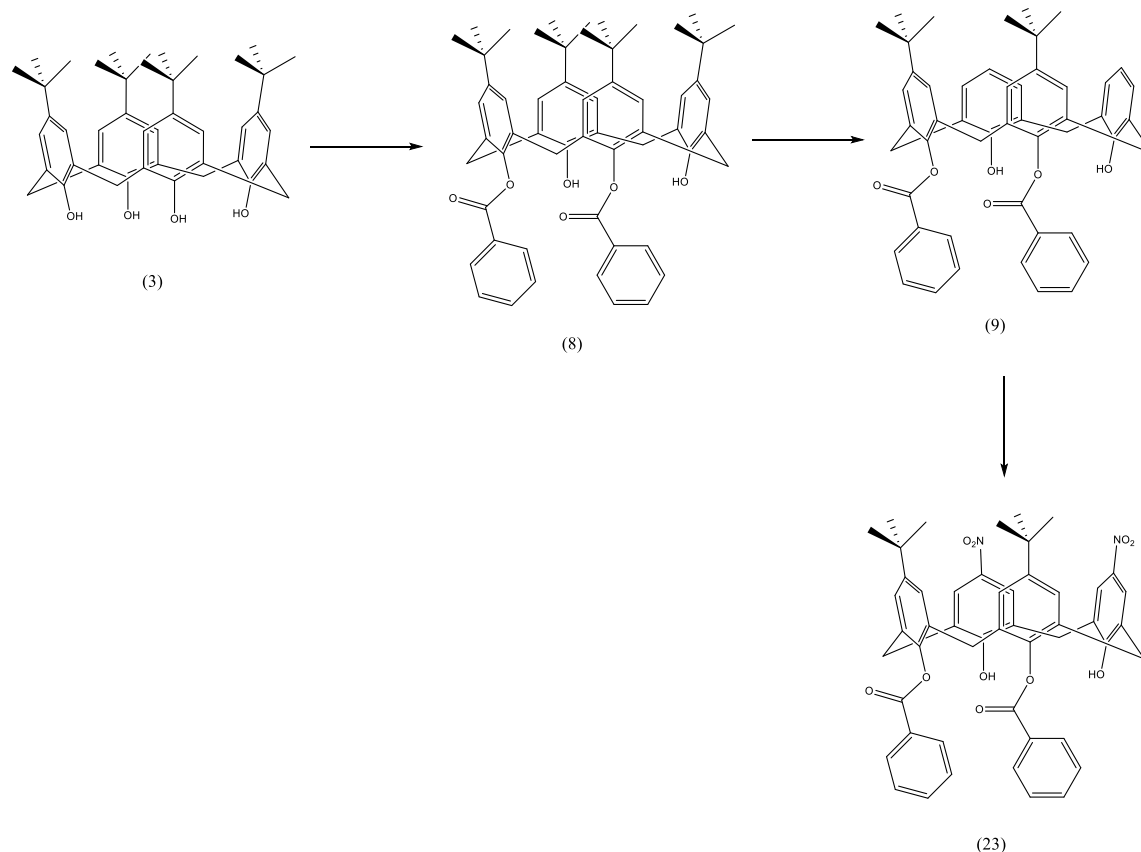
Scheme 4.21 - Proposed reaction procedure for the synthesis of dinitro-dibenzoylcalix[4]arene.

The ^{1}H-NMR spectrum corresponds to that reported in the original paper[174]. The synthesis of compound (**23**) was repeated successfully multiple times and consistently produced 20 % yields of the desired product, this is significantly lower than the 65 % reported in the literature[174]. The nitration step as carried out previously was repeated on the benzoyl calixarene derivative (**9**) however, the required product was not observed. The reaction was carried out on a 100 mg scale, due to the low yielding first step; therefore, it is possible that the scale was too small to allow for successful isolation of the desired product. This reaction will need to be repeated on a larger scale to better understand how the reaction works. Once sufficient material is obtained this will enable further experiments to be carried out on the upper rim in order to produce the desired calixarene host molecule. This could be further explored in the future as another potential host molecule for detection of mephedrone. Given the unsuccessful synthesis of the calixarene derivative, in part due to the insolubility of the calixarenes, focus was diverted to the anthraquinone derivative, which are known to have good solubility in organic solvents[183].

4.3.2   Anthraquinone

The proposed anthraquinone sensor molecule (**2**) was designed with two thiourea groups substituted in the 1,8 position of the anthraquinone, to give the ideal cavity size for mephedrone. Thioureas have

126

the ability to both donate and accept hydrogen bonds, which is ideal for the amine and carbonyl functionalities in mephedrone. The two benzyl groups are positioned to act as the π-stacking interactions present in the pharmacophore model. The anthraquinone is an ideal scaffold for an optical sensor. The flexibility of the structure may allow for the two arms to rearrange themselves around mephedrone for binding, this is one of the advantages of an acyclic supramolecular host molecule over the macrocyclic calixarenes.

The proposed reaction scheme for the synthesis of 1,8-dibenzylthiourea anthraquinone ((**2**); Scheme 4.22) was a three-step process, starting from the commercially available 1,8-dinitroanthraquinone (**10**). This should allow for reduction of the nitro groups to primary amines followed by the formation of the thiourea functionality.
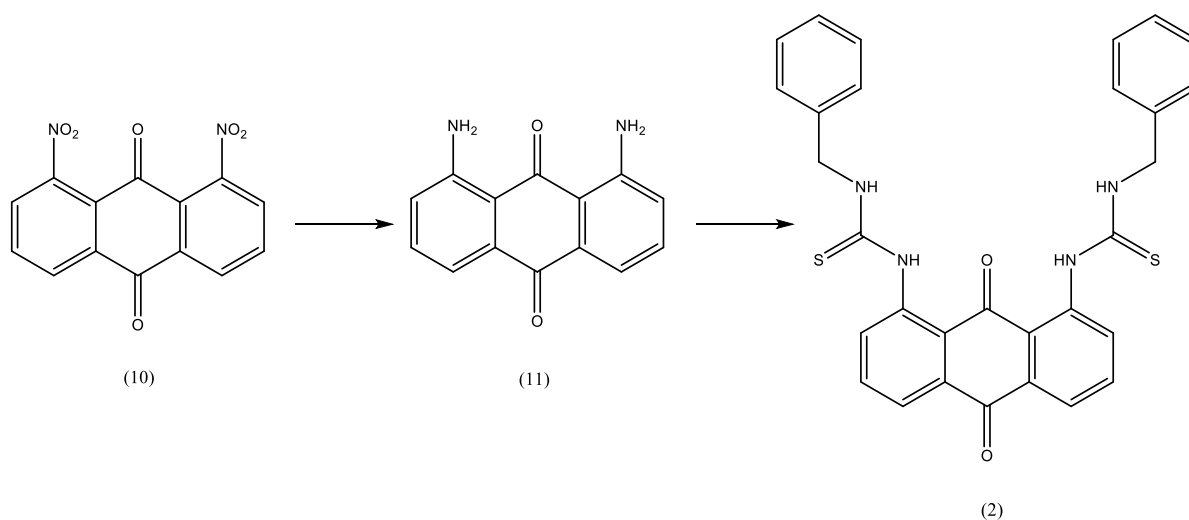
Scheme 4.22 - Proposed reaction scheme for the synthesis of 1,8-dibenzylthiourea anthraquinone.

The reduction of the 1,8-dinitroanthraquinone (**10**) was successfully repeated using sodium sulfide with yields of up to 90 %. The coupling of benzylisothiocyanate with compound (**11**) was attempted under a number of different reaction conditions to optimise the product yield, including variation of the base. Both triethylamine and sodium hydroxide were used in a variety of solvents including DCM, ethyl acetate and ethanol under reflux. Reaction times were varied from one hour to one week and the reactions were monitored by TLC. All of these reactions yielded the starting material following workup. The amino group on the anthraquinone appeared to be unreactive to all of these conditions. Previous literature concerning these reactions have been based upon anthracene moieties and not anthraquinones, meaning there was no carbonyl group positioned between the amino groups[184]. It is possible that the carbonyl group is preventing amino groups from reacting, by stabilising the structure through hydrogen bonding. As shown in Figure 4.5, it is possible for two stable six membered intramolecular rings to form due to hydrogen bonding. The stability of the intramolecular hydrogen

bonding would also explain why only starting material was isolated from the reaction mixtures. In order to investigate if this is the reason for the reaction not progressing, a phosphazene superbase was used. *Tert*-butyl-P$_4$ is a more powerful base than most amines with a pK$_{BH+}$ value of 30.1[185]. Even with such a strong base, no reaction took place and just starting material was once again isolated from the reaction mixture.
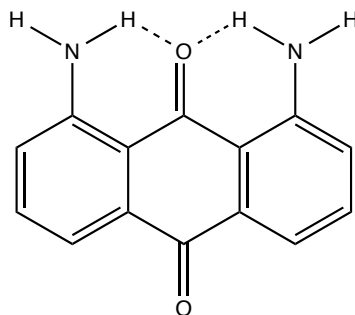
Figure 4.5 - Potential hydrogen bonding occurring between both amino functionalities and the carbonyl.

Given that the phosphazene superbase reaction was not successful, the anthraquinone sensor was redesigned. Therefore, the next step involved reduction of the dinitroanthraquinone to a diaminoanthracene moiety (Scheme 4.23), which will free up the amino functionalities to react and form the thiourea groups required for the host molecule. By removing the carbonyl functionalities the potential host molecule still encompasses the pharmacophoric features that were designed in Chapter 3, so the change in structure still contains two aromatic functionalities and hydrogen bond donors as in the perceived design.

There is considerable literature surrounding the reduction of anthraquinones. The simplest reaction reported by Wong *et al.*[179] was carried out by refluxing sodium borohydride and 1,8-dinitroanthraquinone in isopropyl alcohol for 36 hours, yielding a brown solid with yields consistently above 80 %. This is an improvement from the published yield of just 55 %.
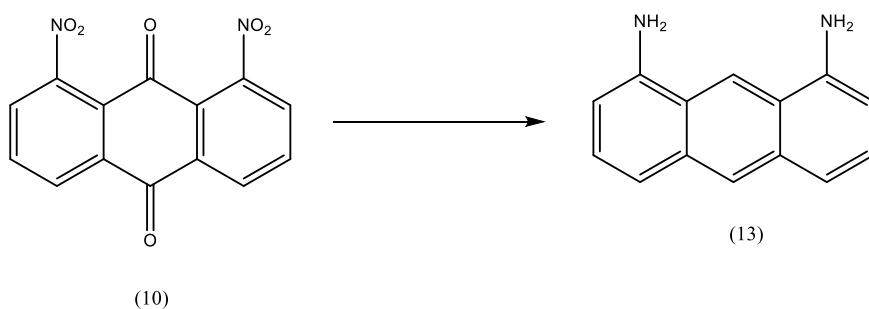
Scheme 4.23 - Reduction of anthraquinone to diaminoanthracene.

The diaminoanthracene was reacted with 2.2 equivalents of benzylisothiocyanate in DCM, to examine how the reactivity is affected by the removal of the carbonyl group. TLC examination of the reaction mixture showed 3 spots, one of which was the corresponding starting material. Column chromatography was used to separate the bands which were subsequently analysed using ^{1}H-NMR. Based on the NMR spectra the first band showed formation of the thiourea on just one amino group, producing the 'one arm' host compound. From the NMR the second band appeared to show possible formation of the desired dithiourea host molecule (**14**), with a more symmetrical splitting of the NMR peaks, and was isolated as a yellow solid. As seen in the ^{1}H-NMR (Figure 4.6) a large number of peaks were observed in the aromatic region, integrating to a total of 40 protons, which is more than the 26 protons expected for this compound.
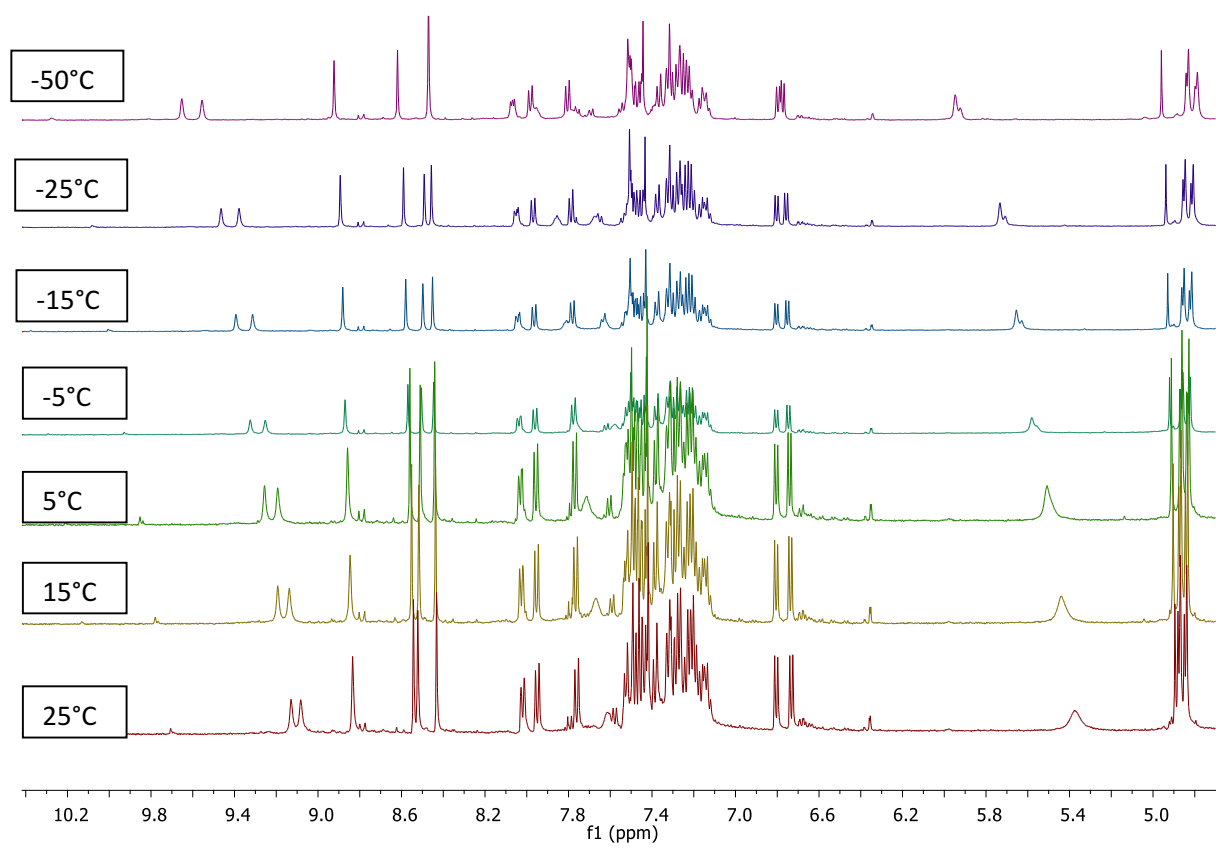
Figure 4.6 - Variable temperature ^{1}H-NMR for dithioureabenzylanthracene (14) run in acetone-d$_6$.

Four amine signals are seen in the NMR spectra which is more than the two signals that would be expected for compound (**14**) due to the symmetry. This could be due to the formation of different conformers, which has been reported previously for a number of dithiourea substituted compounds[186,187]. The conformations that have been reported are anti-anti, syn-anti and syn-syn (Figure 4.7). The syn-anti conformation produces a non-symmetrical molecule that would explain the

four different amine signals from the thiourea moiety seen in the NMR (7.61, 5.37, 9.09 and 9.12 ppm). The different conformations may also help explain why there are more signals in the aromatic region than would be expected. This may be due to the different conformers affecting the proton in position 9- of the anthracene (8.78 ppm) in different ways leading to multiple peaks being seen. To try and freeze the conformers out in an attempt to establish if it is possible to see just one in the proton NMR, a low temperature study was conducted. As seen in Figure 4.6 this did not occur as expected, a number of signals shifted, but the final spectrum, at -50 $^{\circ}$C, still does not represent the expected number of signals for one conformer.

Syn-Anti   Anti-Anti   Syn-Syn
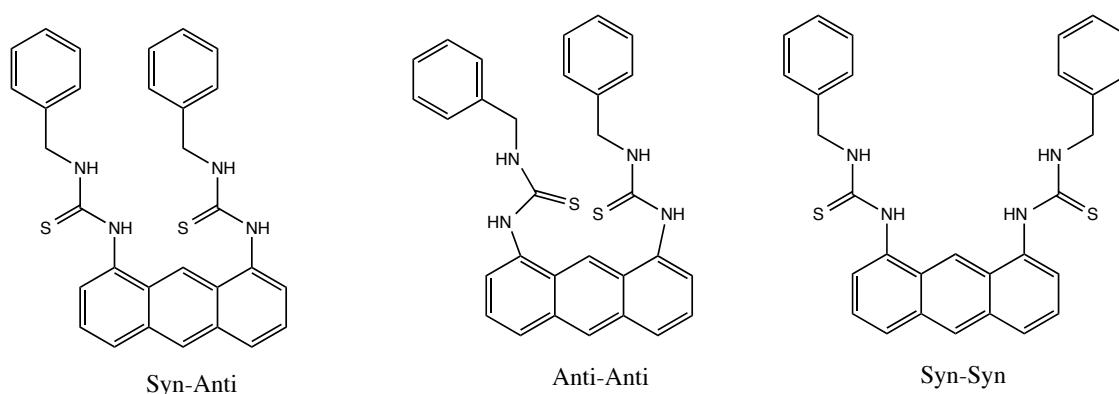
Figure 4.7 - Possible conformers for dithioureabenzylanthracene (14).

Due to the inconclusiveness of the previous reaction and the NMR studies, alternative reaction conditions for the synthesis of compounds (**14**) were examined. The literature concerning this reaction indicates that DCM is the preferred solvent. However, DCM has been known to contain traces of HCl from the production process[188] and small amounts of acid may have an effect on how the reaction progresses. For this reason ethanol was used to observe the effect. The reaction was refluxed in ethanol for two hours, in the absence of base. After two hours the reaction mixture was cooled in ice and filtered, successfully yielding compound (**14**) a dark brown solid with a yield of 80 %. ^{1}H-NMR of the product showed, as predicted, two regions for the protons in the amine and distinct aromatic peaks (Figure 4.8). Integration shows 26 protons as would be expected for compound (**14**).
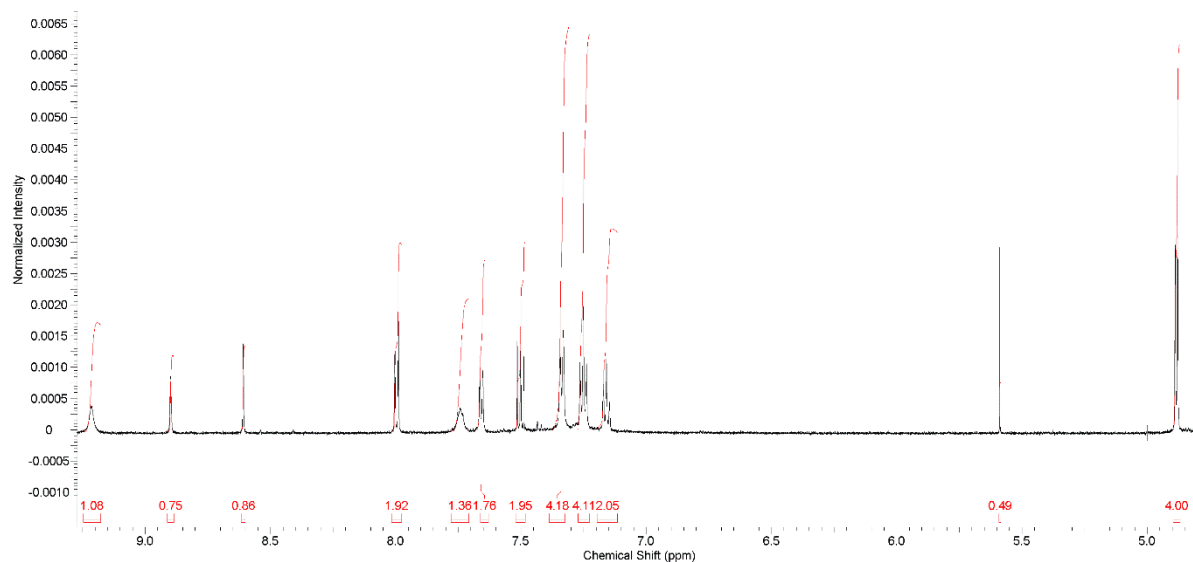
Figure 4.8 - ^{1}H-NMR for dithioureabenzylanthracene (14) run in acetone-d$_6$.

The reaction was subsequently repeated over 1 hour and 3 hours both of which produced the desired compound (**14**), however in lower yields. Therefore, it was concluded that a 2 hour reaction time was optimal with yields of up to 40 % for the full two step reaction. With compound (**14**) successfully synthesised, it was taken forward for binding studies.

Preliminary studies to examine the binding affinity of compound (**14**) were carried out alongside the continued synthesis of potential host molecules. As the synthetic work and preliminary testing were carried out in the USA, mephedrone could not be used at this point due to licencing restrictions. Therefore, the precursor to mephedrone, 4-methyl propiophenone (compound (**19**)) was initially used to examine affinity. Compound (**19**) does not contain the methylamino group in mephedrone, but does have the important aromatic and carbonyl functionalities.
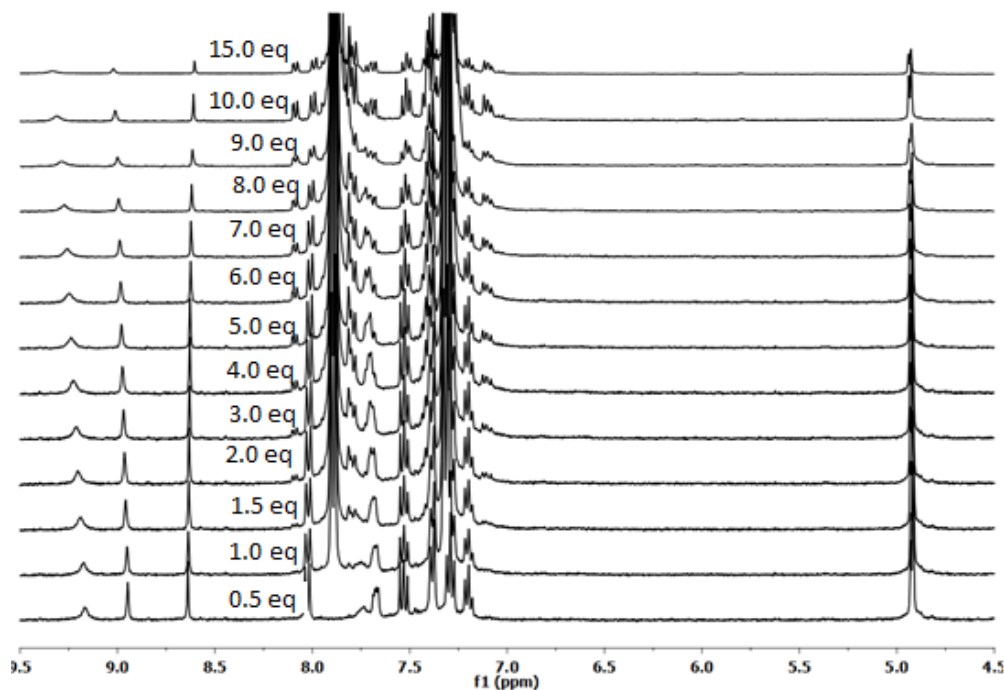
Figure 4.9 - Full ^{1}H-NMR titration of compound (14) and the mephedrone precursor 4-methyl propiophenone (compound (19)).

A full ^{1}H-NMR titration, from 0.5 to 15 eq. was carried out in acetone to determine whether compound (**19**) had an affinity with the host molecule, (**14**). In Figure 4.9 it can be seen that the signal due to the NH functionalities at 9.2 ppm in compound (**14**) are moving further downfield as compound (**16**) is added. This is indicative of hydrogen bonding occurring, which shows that there is an affinity between the host and guest. The only group present in compound (**19**) that could cause this shift is the carbonyl functionality, which could not be included in the pharmacophoric features. However, for the host molecule to be selective for mephedrone over other amphetamine related molecules an affinity for the carbonyl would be ideal, in addition to the pharmacophoric features identified in Chapter 3. The pharmacophore model predicted that there should be a π-stacking interaction with the benzyl group on mephedrone. However, no other noticeable shifts can be observed from either the host or guest. A change in chemical shift in the host molecule shows promising results for compound (**14**) having an affinity for mephedrone. Given the preliminary results based on the mephedrone precursor (**19**), compound (**14**) became the point of focus due to these promising results and therefore the synthesis of the calixarene derivatives was not continued.
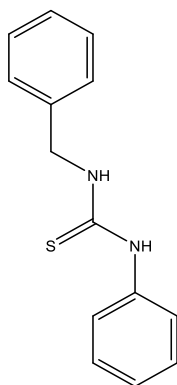
Figure 4.10 - Chemical structure for the model system, 1-benzyl-3-phenylthiourea (compound (16)).

In supramolecular chemistry it is common practice to test a simplified analogue of a host molecule, to systematically evaluate the interactions points of the host molecule which may be responsible for binding the guest. Given that compound (**14**) showed promising results, a model host sensor was synthesised which will be examined alongside compound (**14**) in Chapter 5. Compound (**16**) was prepared using ethanol and one equivalent of benzylisothiocyanate. As shown in Figure 4.10 compound (**16**) contains just one thiourea pendant arm and the anthracene moiety is replaced with an aniline group. This will help determine whether both pendant arms are necessary to establish the binding affinity with mephedrone. Based on the pharmacophore design in Chapter 3, the sterics of the binding cavity should play a large factor in selectivity. Therefore, synthesis and examination of an 'open' structure, will determine whether this is true experimentally (Chapter 5).

4.4 Conclusion

Successful de-*tert*-butylation of tetra-*tert*-butylcalix[4]arene was achieved in yields of 76 %, which is an improvement of the 68 % that was reported in the literature[174]. Di-nitro substitution of the calix[4]arene was carried out under acidic conditions and the product was characterised using both NMR and IR spectroscopy techniques. Reduction of the nitro groups was not successful due to the insolubility of the nitrocalix[4]arene in both aqueous and organic media. In order to overcome this, the lower rim of the tetra-*tert*-butylcalix[4]arene was di-substituted with benzoyl groups prior to de-*tert*-butylation. Successful de-*tert*-butylation of the di-substituted product was carried out with yields of 20 %. Nitration of the benzoylated compound was unsuccessful, possibly due to small yields in the previous steps there was insufficient material to obtain reasonable amount of product for this step. Any future attempts to use the calixarene class as host molecules for mephedrone will need to consider functionalising the lower rim, before attempting upper rim substitution, to prevent the same solubility issues. It appears to be that by keeping the hydroxyl groups on the lower rim the solubility of the molecule decreases.

The original target host molecule, 1,8-dinaphthylthiourea anthraquinone (**2**) was not successfully synthesised. This was likely due to the strength of the hydrogen bonding between the carbonyl and amine functionalities in the intermediate step of the synthetic pathway, making the compound too unreactive to undergo reactions to form the thiourea functionality. However, by reducing the anthraquinone to an anthracene moiety it allowed the reaction to proceed due to the lack of intramolecular hydrogen bonding between the carbonyl and the amine functionalities. The reduction of the anthraquinone does not alter the binding site in relation to the pharmacophore model, as the carbonyl of the anthraquinone was not considered the hydrogen bond donor. However, the anthracene moiety could now act as an additional π-stacking point, as there are two present in the pharmacophore. 1,8-Dibenzylthiourea anthracene (**14**) was successfully synthesised in yields of 40 % by refluxing compound (**13**) in ethanol in the absence of base.

Using compound (**14**), a preliminary binding study with a 4-methylpropiophenene (**19**), which is a precursor to mephedrone, was carried out using ^{1}H-NMR. There appears to be an interaction between the host and guest molecules, with the hydrogen bonding causing a downfield shift of the proton signals of the amine groups on the host molecule. Compound (**19**) varies from mephedrone by the removal of the methylamine functionality. Therefore, the only group that can cause this hydrogen bonding to occur is the carbonyl. This shows promising results to take compound (**14**) forward for full examination against mephedrone. NMR titration will give an insight into whether it is binding, as well as how it is binding as the protons involved in binding will be most affected and therefore a shift in the NMR will be observed. This will give experimental evidence into the atoms involved in binding, from which an experimental pharmacophore model can be build, which can then be compared to the pharmacophore model predictions. This will give evidence as to whether the pharmacophore design aided in the host molecule design process.

The final aim of the host is to produce an optical sensor that can be used in the field. Therefore, additional optical techniques such as UV/Vis and fluorescence spectroscopy will also be used to examine the binding affinity between the host and mephedrone. Selectivity is also very important, as discussed in detail in Chapter 3. Therefore, the binding between the host molecule and methamphetamine will also be studied, in addition to the commonly used cutting agents.

Chapter 5   Evaluation of Host Molecule Interactions with Mephedrone and Related Substances

5.1   Introduction

Compound (**13**), here after known as Probe 1 was synthesised in Chapter 4 based on the pharmacophoric model in Chapter 3. Using this host molecule, the binding affinity of the target guest molecule, mephedrone, will be evaluated later in this chapter. A number of approaches have been investigated for the in-field detection of new psychoactive substances[63,133,134]; however, there remains a need to improve the selectivity over chemical analogues and common cutting agents, while retaining sensitivity, ease of interpretation and reliability. The use of host-guest chemistry to selectively target particular analytes i.e. cations and anions is well established[102]. Less common is the use of host-guest chemistry for small molecule recognition[189,190]. With an understanding of intermolecular interactions, such as hydrogen bonding, hydrophobic interactions and π-stacking, the same techniques can be applied to small molecules[85,191]. There are a number of detection techniques used for monitoring host-guest binding. They all have their own unique advantages and disadvantages. For example NMR provides valuable information regarding the specific atoms that are involved in the interactions, but it is not very sensitive and therefore requires high sample concentrations. Optical techniques such as fluorimetry and UV/Vis spectroscopy are more sensitive than NMR and allow for much lower concentrations of analytes to be studied, but they rely on the host or guest molecule to possess either a chromophore or fluorophore in its motif that participates in binding. Fluorimetry specifically, can be carried out in a wide range of concentrations from millimolar down to nanomolar, depending on the system being studied.

Ideally for use in in-field detection Probe 1 will produce an optical change upon binding to mephedrone, e.g. a colour change. Fluorimetry or UV/Vis spectroscopy techniques can be applied to observe and quantify an optical change upon binding. This is why an anthracene unit is an ideal functional group for the host molecule, as it is known to be a good fluorophore for use in optical spectroscopy techniques[192].

Binding constants can be calculated from titration data based on a change in response versus the concentration ratios between the host and guest. At half the observed total response the dissociation constant (K_d) is equal to the concentration of the guest[193]. However, it is now more accepted to use analysis software to accurately determine binding constants from titration data[108], as more complex algorithms can be applied to fit the data.

Density functional theory (DFT) is often used for *in silico* analysis of host-guest interactions, in parallel with experimental data. DFT calculations are based on the concept that there is a relationship between total electronic energy and the overall electronic density of a system. This theory extends to the fact that ground state energy and other system properties can be uniquely defined by electron density[194]. DFT is defined by Equation 5.1 where E is energy, $\rho(r)$ denotes the density, V_{ext} states that everything occurs under constant external potential and μ is a Lagrange multiplier constant.

$$\left(\frac{\delta E[\rho(r)]}{\delta \rho(r)}\right) V_{ext} = \mu \qquad \textbf{Equation 5.1}$$

Currently DFT calculations remain the primary method for studying ground state complexation of matter *in silico*. To solve Equation 5.1 for a given system a self-consistent approach is taken. An initial estimation of density is applied to the equation to produce a set of orbitals which leads to a more accurate determination of the density, which is used for the second iteration and so on until convergence is achieved[114]. DFT calculations allow for an estimation of not only the energy of a system and its component parts, but also an indication of the binding interactions that are occurring. For example, a study of the change in conformation of the host molecule upon binding to the guest can be observed as well as the interactions between the host and guest[195,196].

An important factor in the design of Probe 1 is selectivity. The pharmacophore model of Probe 1 not only gave detailed insight into potential binding interactions, it also allowed for analysis of common cutting agents that the host molecule needs to be selective against, a necessity for reliable in-field detection. As previously discussed, certain cutting agents and excipients are more common in mephedrone street samples. For this reason, a number of chemical analogues as well as common cuttings agents will also be tested against Probe 1 (Figure 5.1).
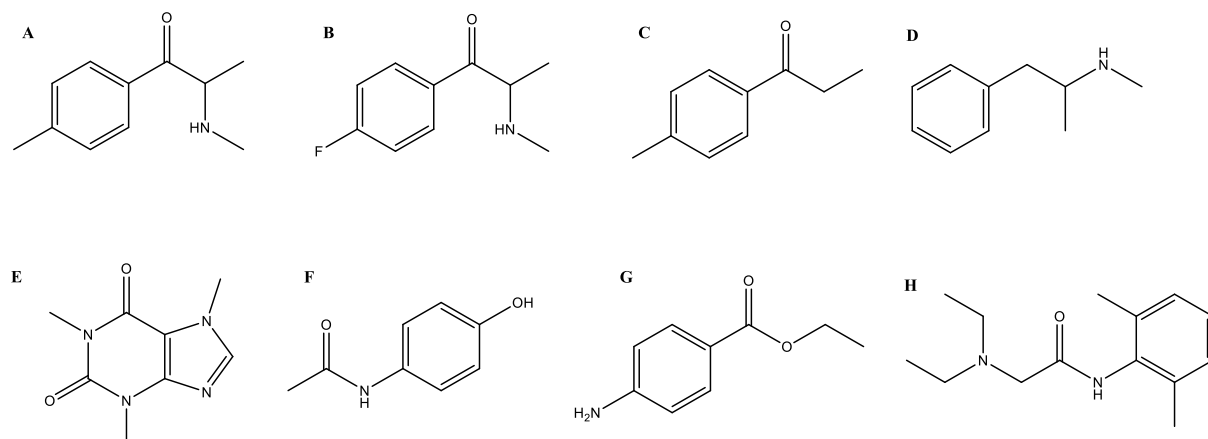
Figure 5.1 - Chemical structure of selected cathinones, chemical analogues and common cutting agents studied A. mephedrone B. flephedrone C. mephedrone precursor D. methamphetamine E. caffeine F. paracetamol G. benzocaine and H. lidocaine.

The aim of this work is to test the host molecule developed in Chapter 4 against the target guest, mephedrone, and to study selectivity against chemical analogues and common cutting agents. In order to fully study host-guest binding interactions a number of techniques were employed, nuclear magnetic resonance (NMR), UV/Vis spectroscopy, mass spectrometry (MS) and fluorimetry. NMR spectroscopy will be used to study the specific functional groups involved in possible host-guest interactions, while MS will be used as a confirmatory technique to ensure binding is occurring between Probe 1 and mephedrone, as well as to determine stoichiometry. Optical techniques such as fluorimetry and UV/Vis spectroscopy will be employed to evaluate the prospect of using Probe 1 for in-field detection applications. DFT calculations will be carried out, in an attempt to aid interpretation of host-guest interactions observed in the aforementioned techniques.

5.2 Methods

Caffeine, lidocaine, paracetamol, methamphetamine hydrochloride and benzocaine were purchased from Sigma (Dorset, UK). Tetrabutylammonium chloride was purchased from Alfa Aesar (Massachusetts, USA). Mephedrone hydrochloride was synthesised as laid out in Chapter 4 section 2.7.

5.2.1 Liberating Mephedrone Freebase

Mephedrone hydrochloride (200 mg) was dissolved in water (50 mL). The mephedrone freebase was liberated with ammonium hydroxide (pH≈10) and extracted into diethyl ether (3 x 20 mL). The organic layer was washed with water (3 x 50 mL) to ensure there was no residual anions present. The organic layer was dried over $MgSO_4$ and evaporated to dryness yielding a yellow oil.

5.2.2 NMR Spectroscopy Titration Studies

Both ^{13}C-NMR and ^{1}H-NMR titration spectra were recorded on a JEOL 600 MHz spectrometer in acetone-d$_6$, unless otherwise stated. Chemical shifts are reported in parts per million (ppm) downfield from tetramethylsilane (0 ppm) as the internal standard and coupling constants (J) are recorded in hertz (Hz). The multiplicities observed in the ^{1}H-NMR spectra are reported as (br) broad, (s) singlet, (d) doublet, (dd) doublet of doublets, (t) triplet, and (m) multiplet. All spectra are recorded at ambient temperature, unless specified otherwise. ^{1}H-NMR titrations were carried out by preparing a 20.0 mM solution of molecular Probe 1 or 2 in acetone-d$_6$ (2.0 mL). A stock solution of each free-based drug (i.e., mephedrone or flephedrone) was prepared in acetone-d$_6$ (2.0 mL). Aliquots of 2.5 µL (2.5 µL = 0.1 eq. of drug to probe) were added and a ^{1}H-NMR spectrum was recorded after each addition. Dissociation constants (K$_d$) were determined as the concentration of guest at half the observed chemical shift.

5.2.3 DFT Calculations

All DFT calculations reported were performed by Prof. Mire Zloh at the University of Hertfordshire.

A conformational search was carried out for Probe 1 alone and the Probe 1-guest complex using Hyperchem 8.10 and OPLS force field. The five lowest energy structures/complexes that were conformationally different were subjected to PM7 calculations using MOPAC2012, B3LYP 6-311++G(2d,2p) performed in orca. The lowest energy complexes for each NPS with Probe 1 was optimized at the DFT level, and that was followed by generating and optimizing alternative complexes for comparison, i.e. to ensure that the minimum conformation of both drugs was in fact achieved. The mephedrone and flephedrone were studied in their respective binding positions, i.e. mephedrone was positioned to bind to Probe 1 outside of the binding pocket and flephedrone was position in the binding pocket and DFT calculations were re-run.

5.2.4 UV/Vis Spectroscopy Studies

UV/Vis absorption spectra were recorded on a Cary 100 spectrometer. A solution of Probe 1, 2.5 mM was prepared in HPLC grade acetone. A 0.01 M mephedrone freebase solution was prepared and aliquots of 25 µL (25 µL = 0.25 eq. of mephedrone freebase to Probe 1) were added to a cuvette with 2 mL of Probe 1; spectrum were collected after each addition. All spectra were run at 25 ˚C with a scan range of 330 - 700 nm. The scan rate was set to 600 nm min^{-1}, with a signal averaging time of 0.1 s.

5.2.5 Fluorescence Spectroscopy Studies

Fluorescence emission studies were carried out on a Perkin Elmer LS-55. A solution of Probe 1, 5.0 µM was prepared in HPLC grade acetone. An additional solution containing 5.0 µM Probe 1 and 2.5 mM of guest (mephedrone or flephedrone freebase) was prepared, to prevent dilution effects upon addition to the solution of Probe 1. Aliquots of 50 µL (50 µL = 0.5 eq. of guest to Probe 1) were added to the cuvette containing 2 mL of Probe 1, spectra were collected after each addition from 0.5 to 50 eq. All spectra were run at 25 ˚C. For all mephedrone experiments the excitation wavelength (λ_{ex}) was 410 nm with a scan range of 425 − 700 nm was applied. For flephedrone λ_{ex} = 392 nm, with a scan range of 405 − 700 nm was used. The slit width for both excitation and emission was set to 7.5 nm with a scan speed of 500 nm min^{-1}. For all experiments the cuvette remained inside instrument holder throughout the experiment, and additions were made directly into the cuvette, waiting two minutes between additions and spectrum collection.

For benzocaine, lidocaine, paracetamol and caffeine solutions of 2.5 mM were prepared in acetone and aliquots of 50 µL (50 µL = 0.5 eq. of guest to Probe 1) were added from 0.5 to 50 eq. directly into the cuvette containing a 5.0 µM solution of Probe 1 (2 mL). An excitation wavelength of 410 nm was used and the same instrument parameters as above.

Using the same instrument parameters, studies using neat, i.e. undiluted mephedrone and flephedrone were conducted, whereby a 5.0 µM solution Probe 1 in acetone was prepared and the guest was added in 5 µL aliquots (5 µL = 150 eq. of guest to Probe 1). Spectra was collected from 150 to 1950 eq. of guest to Probe 1. The same parameters were used to study neat benzocaine, lidocaine, paracetamol and caffeine where 1 mg portions of each of the cutting agents was added.

Further studies were conducted using a range of concentrations of guest in acetone. For the dilutions studies in acetone, five solutions of mephedrone freebase in acetone were prepared with the following concentrations: 2.98, 1.96, 1.49, 0.99, 0.74, and 0.60 M. Spectra was collected up to 450 eq. of guest to Probe 1.

5.2.6 Mass Spectrometry

Mass spectrometry studies were was performed using a Varian Prostar 1200L quadrupole MS/MS *via* direct injection using an ESI source. For analysis of the Probe 1 and mephedrone, 10 eq. of mephedrone freebase were added to a 0.5 mg mL^{-1} solution of Probe 1 in acetone. Formic acid (1 % v/v) was added to each sample as an ionizing agent before injection. An additional experiment was performed where 20 µl of deuterated water was added to the mephedrone and Probe 1 mixture and the ESI-MS was acquired in both the positive and negative ion mode. The final

optimised methods was established as, needle voltage 5000 V, capillary voltage 40 V, detector voltage 1500 V, drying gas temperature was 275 ˚C, and the nebulizer pressure was 40 psi, with the drying gas at 15 psi for all experiments. For MS/MS experiments the same above instrumental parameters were applied, in addition the collision energies were set as -5, -14 and -22 V and the capillary voltages were set as as 10, 95 and 10 V, using argon as the collision gas.

5.2.7 Simulated Street Sample Protocol

Mephedrone hydrochloride (100 mg), benzocaine (100 mg) and caffeine (100 mg) were combined and dissolved in water (50 mL). The mixture was filtered to remove the undissolved particulates, from the insoluble cutting agents. The mephedrone freebase was liberated with ammonium hydroxide (pH≈10) and extracted into diethyl ether (3 x 20 mL). The organic layer was washed with water (3 x 50 mL) to ensure there was no residual anions present. The organic layer was dried over $MgSO_4$ and evaporated to dryness yielding a yellow oil with small amounts of white solid from the remaining cutting agents. The remaining residue was tested against Probe 1 using ^{1}H-NMR using the same method applied to the previous titrations experiments.

5.3 Results and Discussion

5.3.1 NMR Spectroscopy Testing

The initial technique used to evaluate the interaction between the host and guest molecules was ^{1}H-NMR. This technique allows for determination of whether binding occurs, as well as the atoms that are involved in the binding. From this information is it possible to deduce the orientation that binding is occurring, specifically the types of intermolecular interactions working. From this information it is also possible to calculate association constants.

Choice of solvent is important when carrying out binding studies as certain solvents are known to be competitive binding solvents, meaning that the energy needed to displace the solvent in the binding cavity is higher for certain solvents. For example, some solvents (e.g. water) hydrogen bond to the host and guest molecules. Probe 1 showed poor solubility in most organic and aqueous solvent. The only solvents it dissolved in were acetone and dimethyl sulfoxide (DMSO). DMSO is known to be a very competitive binding solvent due to it being a strong hydrogen bond acceptor, and has been shown to be an inappropriate solvent for host-guest binding studies[197]. Therefore acetone-d_6 was the solvent used for all NMR titrations.

5.3.1.1   Chloride Testing

As previously discussed in Chapter 1, mephedrone is most commonly found in the form of a hydrochloride salt. Anions, such as chloride, are known to be strong hydrogen bond acceptors[103]. Thioureas have been incorporated into the host design due to their hydrogen bonding abilities and therefore, it needs to be determined whether any interference from the chloride binding could impair the ability to evaluate mephedrone specific binding. Tetrabutylammononium chloride (TBACl) was used as a stable source of chloride anions to determine the affinity between Probe 1 and chloride ions.
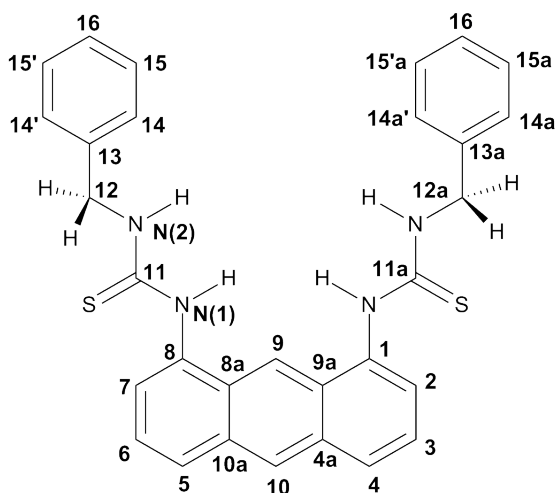
Figure 5.2 - Structure of 1,8-dibenzylthiourea anthracene (Probe 1), with NMR assignments.

The ^{1}H-NMR titration of Probe 1 against TBACl is shown in Figure 5.3. When looking at binding between small molecules in NMR, fast exchange interactions are occurring. This means that the chemical shift of a given peak is the weighted average of the free and bound states, observable in an equilibrium system[110]. This therefore is taken into account when calculating any association constants from chemical shifts.

Downfield shifts of six proton environments, N(1), N(2), 9, 10, 12 and 14 can be seen. The peaks associated with the NH groups (environments N(1) and N(2)) have the most noticeable shifts, with a total change of 1.6 ppm each. This downfield shift suggests that the NH groups are hydrogen bonding to the chloride anion. Hydrogen bonding causes the protons involved to become deshielded due to the hydrogen bonding lengthening the O-H bond, this reduces the valence electron density around the proton. Consequently, the more hydrogen bonding that occurs in the system, and the stronger the interaction, the more the proton peak will shift when the guest is added. The system was found to reach equilibrium at two equivalents of Probe 1 to chloride.

The total chemical shift for NH(1), (starting at 9.51 ppm) was 1.56 ppm, giving an association constant (K_a) for Probe 1 and chloride as 500 M^{-1}. For small molecule binding this is relatively weak with literature showing binding between anions and small molecules ten times higher than that reported here[172,198].
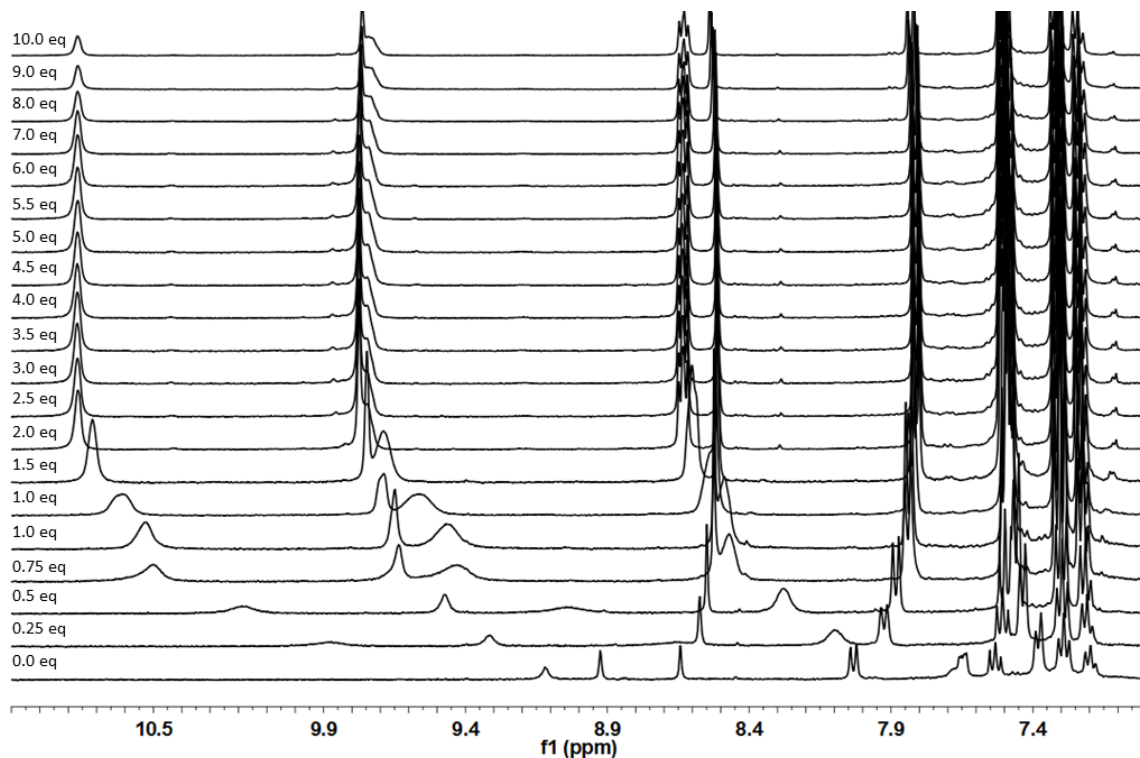
Figure 5.3 - ^{1}H-NMR titration of tetrabutylammonium chloride against Probe 1 in acetone-d_6 from 0 to 10 eq.

Protons 9 and 10 on the anthracene unit shift upon addition of chloride ions from 8.9 to 9.8 ppm and 8.6 to 8.4 ppm respectively. The shift downfield for proton 9 and the shift upfield for proton 10 are representative of the protons undertaking π-anion interactions. As previously discussed in Chapter 1, there is a large amount of literature surrounding π-anion interactions[199,200]. These interactions are often utilised for anion-host binding and have been found to have energetically favourable binding interaction of 20–50 kJ mol^{-1} [199]. The difference in the change in chemical shifts seen for protons 9 and 10 is most likely due to the anion not binding directly above the centroid of the aromatic ring. This causes a change in the electron density around protons 9 and 10 and as a result the change in their chemical shift varies accordingly.

Figure 5.3 shows that Probe 1 has a good affinity for chloride ions, which needs to be taken into account when looking at mephedrone hydrochloride, as well as other constituents in products that may be present as hydrochloride salts. Chloride binding to Probe 1 could potentially induce false positives if it is found to bind in the same way as mephedrone. Given Probe 1's high affinity for chloride

ions, it may be possible to simultaneously bind chloride and mephedrone in one probe, but first Probe 1 will need to be evaluated for mephedrone binding.

5.3.1.2   Mephedrone Testing

In order to assess mephedrone binding independently of chloride ions, all mephedrone NMR experiments were conducted using the mephedrone freebase. A discussed on Chapter 1, the freebase form of a number of cathinone analogues have been found to be unstable; however, the length of stability has not previously been quantified. Therefore, a full ^{1}H-NMR stability study of mephedrone freebase in acetone-d_6 was carried out before any binding studies were performed. Figure 5.4 shows the stacked NMR plot from T = 0 to T = 18 hours, where slight degradation started to occur due to reduction of the amine group causing new peaks to appear in the alkyl region of the spectra (highlighted by the red circle). Given that significant degradation is only seen from 18 hours, it was concluded that mephedrone freebase is stable enough to conduct binding studies assuming that it is completed in this time frame. Consequently, for all binding studies the mephedrone freebase was liberated immediately prior to any experimental work, and was used no more than 12 hours after it was extracted.
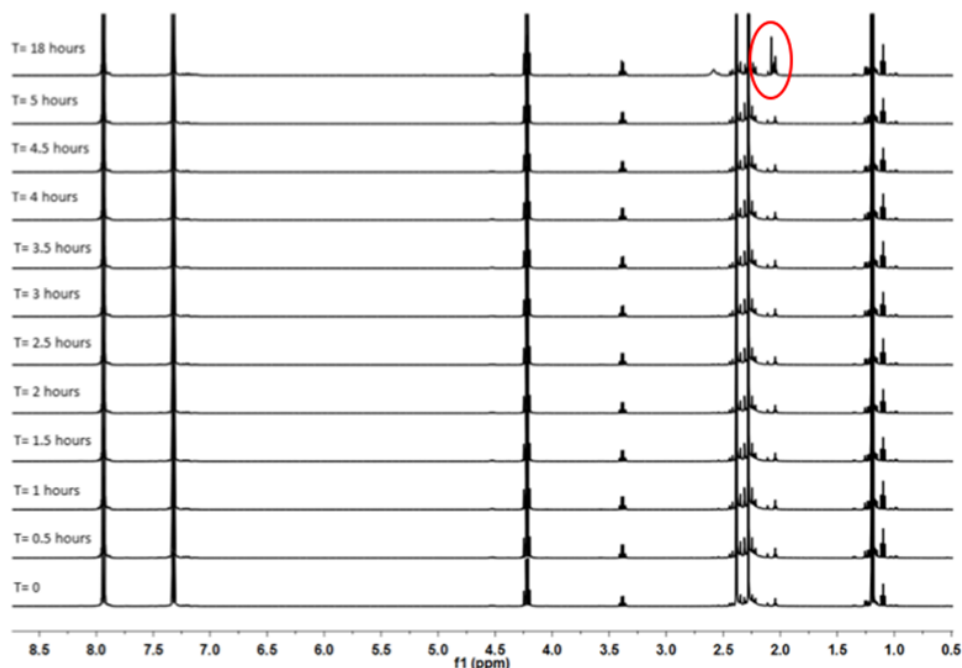
Figure 5.4 - [1]**H-NMR stability study of mephedrone freebase from T=0 to 18 hours carried out in acetone-d_6.**

For the binding studies between mephedrone and Probe 1, the concentration of Probe 1 was kept the same as the anion experiments at 20 mM in acetone-d_6 for continuity. Thirteen data points were collected from zero eq. of mephedrone to Probe 1 up to 10 eq. The same 6 proton environments

observed for chloride, shift upon the addition of mephedrone (Figure 5.5). These are two anthracene protons (9 and 10), four NH protons in two chemical environments ((N)1 and (N)2), the methylene group (12) and slight shifts in the benzyl aromatic protons (14, 14a).
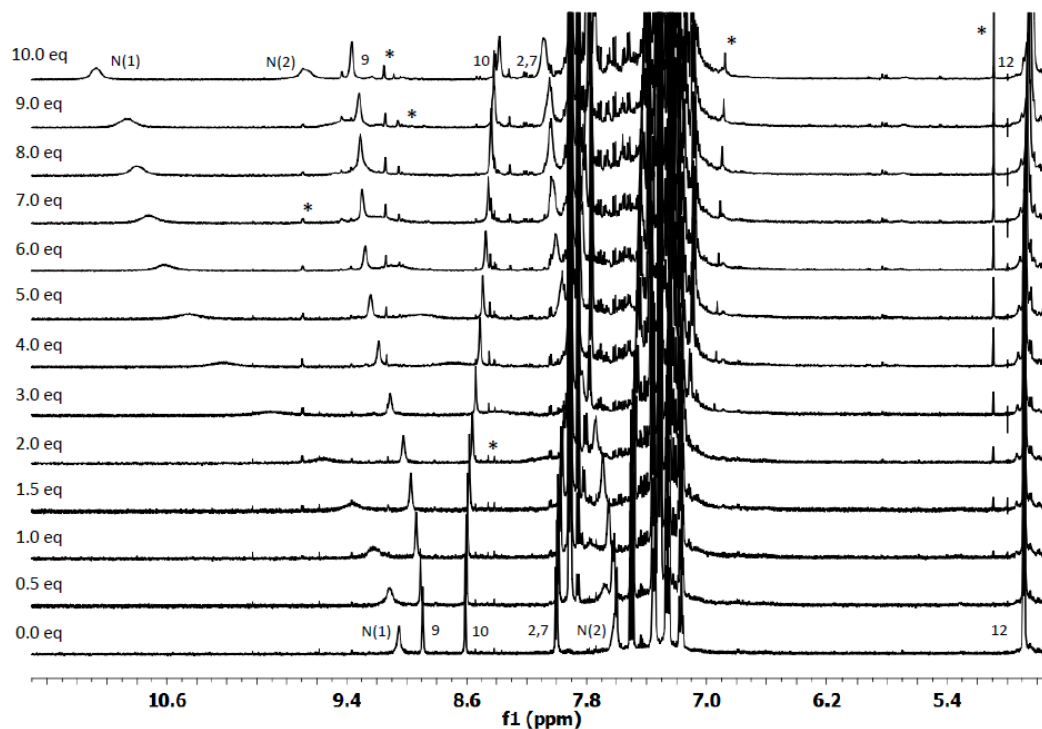
Figure 5.5 - ¹H-NMR titration of Probe 1 with mephedrone in acetone (20 mM). Due to the instability of the free-based mephedrone new ¹H-NMR signals as the result of degradation appeared as the titrations commenced and are marked with asterisks (*).

Both NH groups from Probe 1 shift downfield upon addition of mephedrone. This is due to them hydrogen bonding with mephedrone, one with the carbonyl and another with the amine functionality. Both the NH groups of Probe 1 move a total of 2.1 ppm each upon the addition of ten eq. of mephedrone to Probe 1. This indicates that they both have the same binding constant as the dissociation constant is proportional to the concentration of mephedrone at half the observed shift. This would suggest that they both bind to mephedrone concurrently, i.e. in a 1:1 ratio between host and guest. Figure 5.6 shows the Scatchard plot for NH(1) based on the NMR titration of mephedrone and Probe 1. From the Scatchard plot the association constant (K_a) was estimated at 104 M^{-1}. Despite mephedrone showing the greater total shift, chloride has a stronger affinity at K_a = 500 M^{-1}, as the concentration needed to induce the same response was lower for chloride then mephedrone. Given the symmetrical nature of Probe 1 it cannot be concluded whether it is the NH's directly attached to the anthracene that are binding, the NH's with the methylene linker, or both. It is also hard to conclude

whether they are acting as hydrogen bond donors or acceptors, as NH groups have the ability to act as both.

As both NH environments are effected during binding, it can be concluded that both arms of Probe 1 are interacting with mephedrone. For that reason one arm must be acting as a hydrogen bond donor to the carbonyl and one arm hydrogen bonding to the amine in mephedrone. Given that the amine functionality in mephedrone freebase cannot be observed in the spectrum, it cannot be deduced as to whether it is acting as a hydrogen bond donor or acceptor.
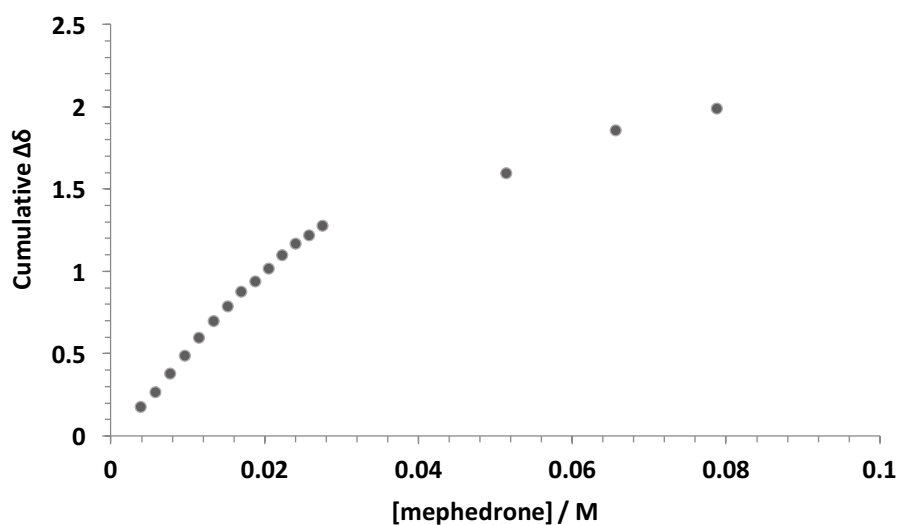
Figure 5.6 - Scatchard plot for the binding of NH(1) in Probe 1 upon the addition of mephedrone up to 10 eq. (10 eq. = 0.08 M).

A less noticeable difference, but still imperative to understanding how the host-guest interaction may be occurring, is the shift seen for protons in positions 9 and 10 (highlighted in Figure 5.5) on the anthracene moiety. Proton 9 shifts downfield while proton 10 shifts upfield. These changes are likely both induced by π-stacking interactions. As discussed in Chapter 1, π-stacking can occur in a number of ways between aromatic residues, it can be edge/face or face/face. The effect that π-stacking has on aromatic protons using NMR can help determine which type of π-stacking is occurring[85]. Proton 9 shifting downfield means that it is becoming more deshielded, this is indicative of face/face π-stacking, due to the increased effect of the magnetic field on the aromatic protons. The opposite is true for proton 10 which shifts upfield. This may be due to unsymmetrical interactions between the mephedrone and the two protons either side of the central anthracene unit. This would mean that the deshielding effects of the binding between Probe 1 and mephedrone are different. Which proton is π-stacking with Probe 1 cannot be conclusively determined from the data collected thus far.

Mephedrone has its own organic framework, and therefore the chemical shifts from mephedrone can be analysed to further determine how it is binding to Probe 1. For mephedrone there are noteworthy chemical shift changes seen for the methyl (4.20 to 4.25 ppm) and the two methyl groups (0.02 ppm shift upfield). The methine and two methyl groups on mephedrone are in close proximity to the β-carbonyl and amine functionalities, which undergo hydrogen bonding. This causes a decrease in the electron density around the methine and two methyl groups, which results in downfield chemical shifts.

From the pharmacophore model (Chapter 3), the carbonyl group was not considered to be part of the binding motif, due to lack of experimental binding data. However, carbonyls are good hydrogen bond acceptors and therefore, it is important to study how it acts experimentally upon binding. Using ^{1}H-NMR it is not possible to see the effect of the carbonyl group as it does not contain a proton, therefore a carbon NMR titration was attempted. Unfortunately, even with increasing the number of scans the carbonyl peak in ^{13}C-NMR was of low intensity and it was not possible to get any definitive results as to whether a change in chemical shift can be observed upon binding.

To study how the choice of solvent affects binding affinity, the same titration experiment was conducted in DMSO. This was also carried out to gain more experimental data to help with correlation for metadynamics studies (Chapter 6). *In silico* analysis is currently limited to being carried out in methanol, water, octanol or DMSO. Out of these solvents Probe 1 is only soluble in DMSO. Therefore, experimental data in DMSO could aid in the emulation of experimental results *in silico*. No interaction between Probe 1 and mephedrone in DMSO was observed up to 10 eq. of mephedrone (Figure 5.7).
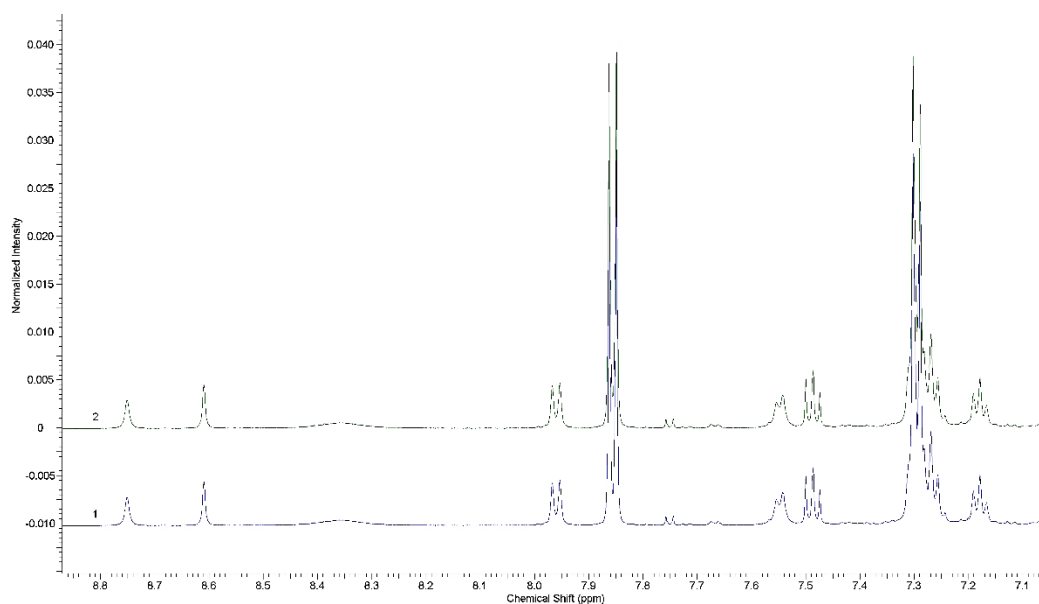
Figure 5.7 - ^{1}H-NMR spectrum showing Probe 1 with mephedrone at 0.25 eq. (1) and 10 eq. (2) in DMSO.

DMSO is known to be a competitive binding solvent due to its high affinity for hydrogen bonding. This hydrogen bonding increases the solvation energy barrier that host-guest interactions need to overcome, therefore usually decreasing the association constant. Consequently, no interaction for mephedrone and Probe 1 is seen when DMSO is used as the experimental solvent. This confirms that acetone was the ideal choice of solvent, based on the small range of solubility. It also gives more experimental data that can be taken forward for metadynamics analysis, which will be examined in Chapter 6.

5.3.1.3   Flephedrone Testing

To further understand how mephedrone is binding and the selectivity of Probe 1, another cathinone analogue was studied. Flephedrone was chosen as a comparison cathinone as it differs from mephedrone by only the 4-fluoro motif (Figure 5.1), and could provide valuable information into how a small structural change could affect binding and consequently selectivity.

To prevent any interaction with chloride anions, flephedrone was also used as a freebase for all binding studies. The same conditions used for mephedrone titrations were applied to flephedrone and Probe 1, to ensure consistency. The ^{1}H-NMR titration of flephedrone with Probe 1 (Figure 5.8) shows that the same proton environments shift as seen for mephedrone, (NH(1), NH(2), 9, 10, 12 and 14) however the shifts are less pronounced. Upon the addition of 10 eq. of flephedrone a total shift of 1.10 ppm for NH(1) was observed, compared to 1.99 ppm for mephedrone. This shows that flephedrone does bind to Probe 1, however the addition of the fluorine group decreases the K_a to 9.8 M^{-1} which is a 10 fold decrease compared to mephedrone.
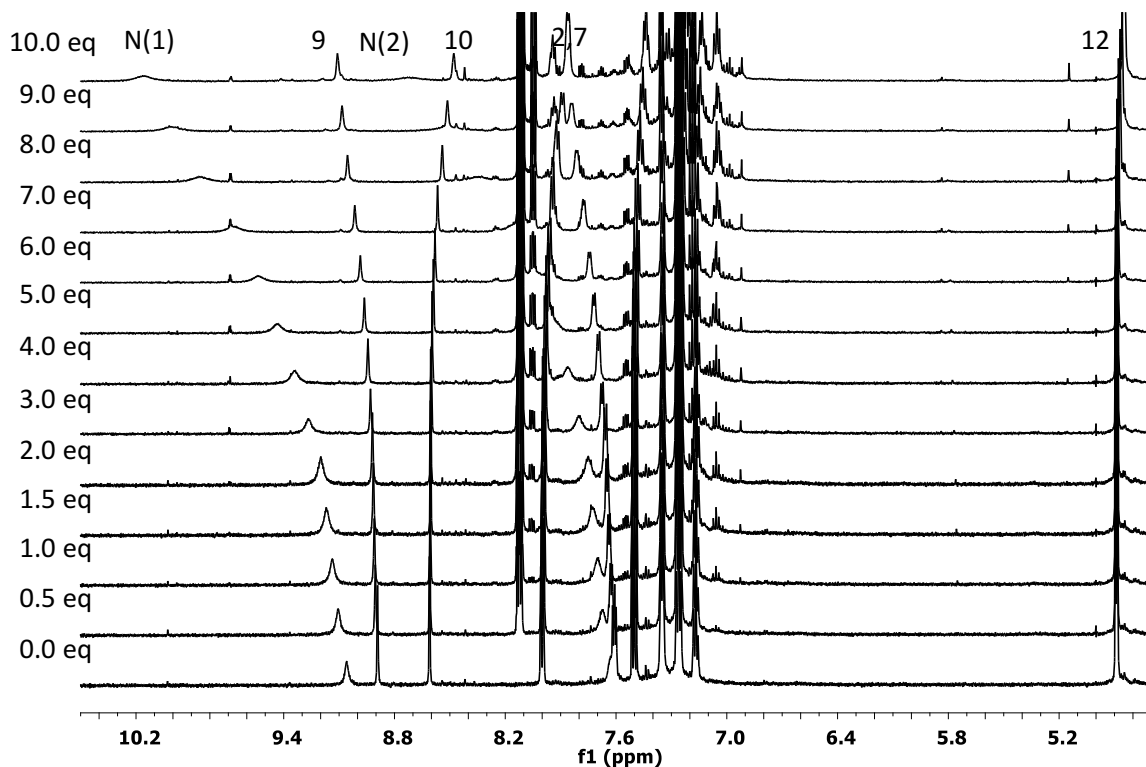
Figure 5.8 - ^{1}H-NMR titration of Probe 1 with flephedrone in acetone-d_6 (20 mM).

This correlation between the proton environments effected suggests that the same interactions are occurring between Probe 1 and flephedrone that are seen for mephedrone. This is not unexpected as flephedrone contains the carbonyl, amine and aromatic functionalities which were the binding points in mephedrone, in the same motif. However, the addition of the electronegative fluorine atom on the aromatic ring clearly has an effect on the amine and carbonyl functionalities, which decreases the binding affinity to Probe 1. Given that hydrogen bonds are electrostatic interactions, small changes in electronegativity can have strong effects on the strength of hydrogen bonding. The fluorine drawing electron density away from the aromatic ring could decrease the electron density around the oxygen of the carbonyl group. This could explain the decrease in the strength of hydrogen bonding seen in the NMR titration. However, the change in binding could also be due to the fluorine on the ring preventing flephedrone binding in the same orientation as mephedrone. This cannot be concluded just from NMR experiments, and will be further investigated in later sections.

5.3.1.4   Methamphetamine

Methamphetamine and mephedrone have been found to be co-administered by users, with one case even proving fatal[201]. Therefore, it is important to be able to distinguish between the two in an in-field test. Methamphetamine and mephedrone have very similar structures (Figure 5.9). Current in-field detection mechanisms in the literature fail to adequately distinguish between the two[61] due to

similaries in their chemical structure. It is possible that methamphetamine can cause false positives when testing for mephedrone. Therefore, selectivity over methamphetamine is necessary for an in-field detection probe for mephedrone.
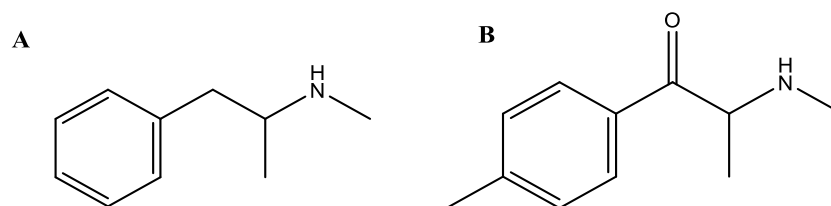
Figure 5.9 - Chemical structure of A. methamphetamine and B. mephedrone.

Methamphetamine differs from mephedrone by a carbonyl and tolyl moiety, and therefore still contains two of the three binding points identified in mephedrone. It has already been determined from studying 4-methyl propiophenone in Chapter 4, that binding can still be observed on removal of the amine functionality, however with a significantly reduced association constant. By studying methamphetamine binding with Probe 1 further understanding on how the removal of the carbonyl functionality effects binding can be established.

As with the cathinone analogues methamphetamine was studied in its free base form. There is no literature studies for the stability of methamphetamine free base in acetone, so a full stability study was carried out over 48 hours. Unlike the cathinone analogues no degradation was seen up to 24 hours, however slight impurities start to appear after 48 hours. For continuity methamphetamine free base was liberated prior to all experiments and used the same day.

No significant binding is seen from 0.25 eq. to 8 eq. (Figure 5.10), after which slight shifts in the NH(1) and NH(2) peaks were observed. For mephedrone the binding starts to plateau at 4 eq., this shows that Probe 1 exerts good selectivity over methamphetamine.
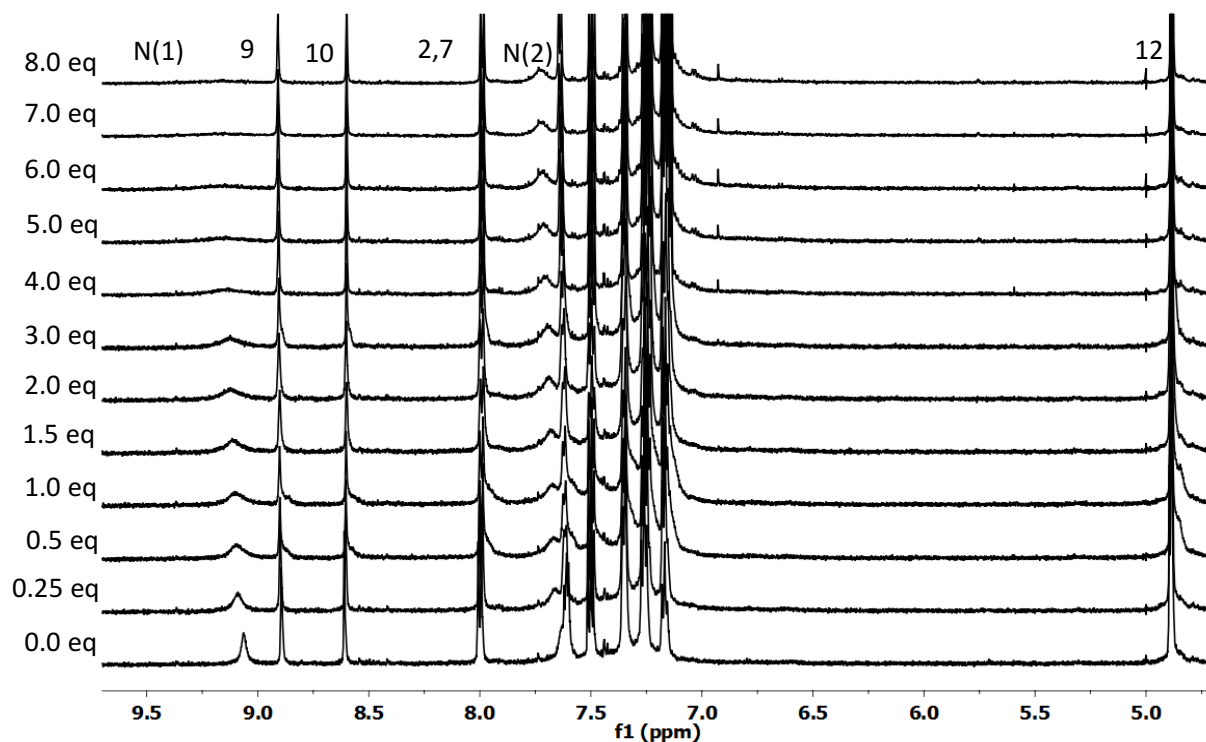
Figure 5.10 - ^{1}H-NMR titration for Probe 1 and methamphetamine freebase in acetone-d$_6$ (20 mM).

Current literature reporting sensory mechanisms for mephedrone have shown no selectivity over methamphetamine, due to its structural similarity[61,133]. This appears to be due to the probe being designed to interact with just the amine functionality. This functionality is not unique to the cathinone class, or even the amphetamines. Most stimulant drugs of abuse contain an amine functionality, as they act through inhibition of monoamine transporters[202].

Studying how Probe 1 binds when the amine functionality (4-methyl propiophenone) and the carbonyl (methamphetamine) are systematically removed gives a good understanding into how mephedrone binds. The removal of the amine functionality has a 10 fold decrease in chemical shift of NH(1) by 4 eq. of 4-methyl propiophenone to Probe 1. While removal of the carbonyl group shows no binding at 4 eq. Demonstrating that both groups are needed to achieve the binding observed with mephedrone.

This indicates that Probe 1 is unique as a NPS sensory mechanism as it uses a concerted design that takes into account not only multiple binding groups, but also the geometrical conformation of these groups. Using this design, based on the pharmacophoric model, results indicate that Probe 1 has good selectivity over methamphetamine.

5.3.1.5   Aniline Model Sensor (Probe 2)

As mentioned is Chapter 4, when studying supramolecular complexes that contain multiple binding sites it is common practice to use a model system that contains just one of the binding sites. This is to

see whether the entire motif of the molecule is necessary to observe the binding affinity. For this reason, Probe 2 was synthesised in Chapter 4, (Figure 5.11) which contains just one thiourea pendant arm and no anthracene unit.
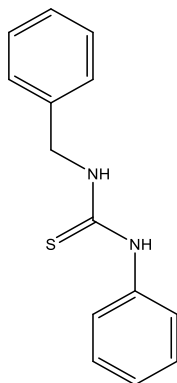
Figure 5.11 - Chemical structure of model system, 1-benzyl-3-phenylthiourea (Probe 2).

As a comparison ^{1}H-NMR titration experiments were carried out with Probe 2 against both mephedrone and flephedrone. Probe 2 binds to mephedrone (Figure 5.12) but very weakly, 10 eq. of mephedrone only induces a total chemical shift of 0.2 ppm, compared to 2.1 ppm for mephedrone. Flephedrone however exerts only a small change in chemical shift during the titration experiment, with NH(1) moving a total of 0.2 ppm over 10 eq. This is a fivefold decrease in binding compared to Probe 1 and flephedrone.
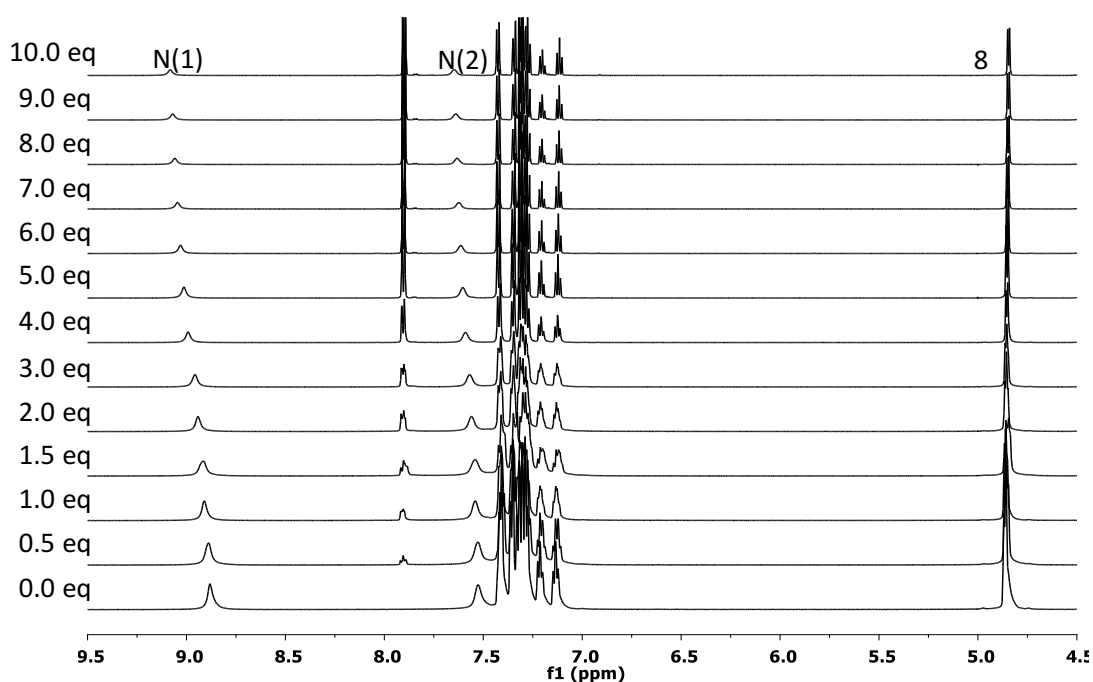
Figure 5.12 - ^{1}H-NMR titration of model compound (Probe 2) upon the addition of mephedrone freebase in acetone-d$_6$.

This diminished binding affinity for both the cathinone analogues with Probe 2, compared to Probe 1, highlights the need for the both thiourea arms to gain the association constant observed with Probe 1. This allows for cooperative binding in a concerted fashion that is seen for Probe 1. The cooperative binding between Probe 1 and mephedrone allows for increased selectivity, as each binding point in mephedrone that interacts with Probe 1 increases the binding affinity[203]. Therefore the decrease in the association constant can be seen to be triggered by the removal of any binding point. This shows that the pharmacophore modelling using a three point binding interaction was necessary, as it is the presence of three interaction points between Probe 1 and mephedrone that provides the greatest association constant. This shows that pharmacophore design provides a good basis for small-molecule host design.

Further information into how mephedrone and flephedrone bind to Probe 1 could be achieved through density functional theory (DFT) calculations, which uses empirical *in silico* computational visualisations of binding interactions based on parametrized data sets. These calculations can aid in the rationalisation of binding occurring between the host and guest molecules.

5.3.2   DFT Calculations

5.3.2.1   *Mephedrone*

In order to aid in the rationalisation of the binding interactions seen using ^{1}H-NMR between mephedrone and Probe 1, density functional theory (DFT) calculations were performed. DFT
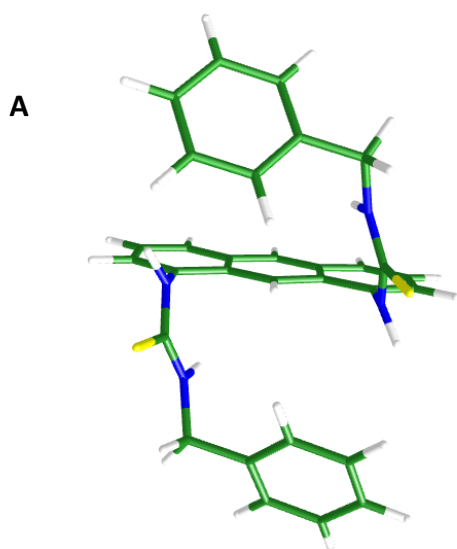
calculations allow for an *in silico* empirical prediction of interactions between two molecules. Minimum energy conformations of Probe 1 and mephedrone were generated.

B
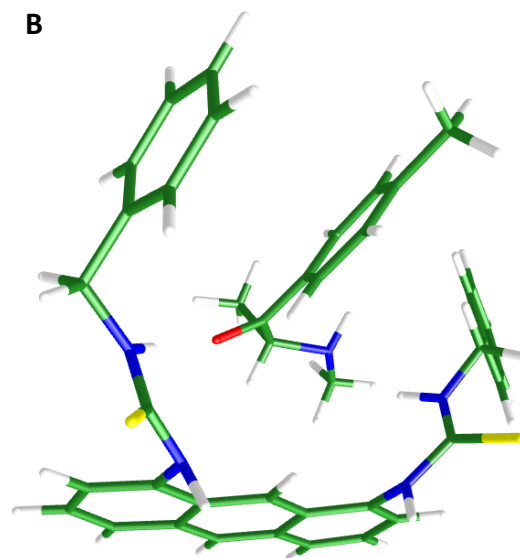
Figure 5.13 - An image of A. minimum conformation of Probe 1 uncomplexed and B. minimum conformation of Probe 1 complexed to mephedrone, based on optimised DFT calculations.

Two low energy conformations were obtained for Probe 1 in the gas phase, which were both taken forward for analysis of the bound complexes using DFT calculations. Interaction energies were then calculated between Probe 1 and mephedrone based on the minimum energy conformation of the complex.

The interaction energy between Probe 1 and mephedrone was calculated using energies of the most stable respective conformations according Equation 5.2.

$$\Delta E = E_{complex} - \left(E_{free\ host} + E_{free\ guest}\right) \quad \textbf{Equation 5.2}$$

Where $E_{complex}$, $E_{free\ host}$ and $E_{free\ guest}$ represent respectively the total energy of the complex, the optimized free Probe 1, and the optimized free guest energy. Probe 1 with mephedrone bound in the binding pocket has a favourable interaction energy of -12.05 kJ mol^{-1} (Figure 5.13 B).

There is a very noticeable change in conformation between the unbound and bound Probe 1, with a maximum RMSD of 36.29 Å between the two conformations (Figure 5.13). This shows that the host molecule reorganises to encompass mephedrone into the binding site. The deformation energy of Probe 1 to allow this interaction to occur was calculated as 1824 kJ mol^{-1}. This is a very large deformation energy, which suggests that the binding of mephedrone is very energetically favourable

in order overcome such a large energy barrier. This would suggest that the mephedrone-host complex is very strong. The optimised bound conformation (Figure 5.14) shows mephedrone bound in the cleft of Probe 1 *via* an array of hydrogen bonding interactions and a π-stacking interaction. These results are consistent with the chemical shifts observed in the NMR experiments.
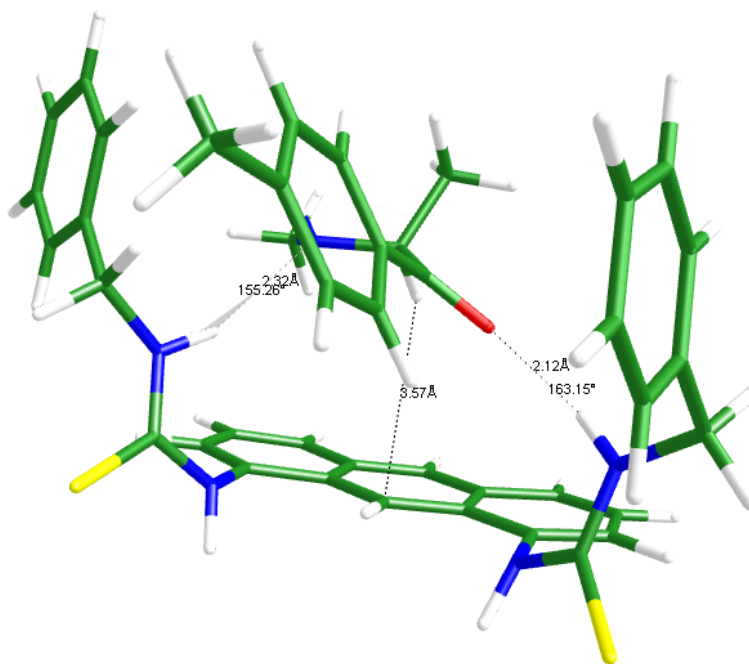
Figure 5.14 - An image showing the minimum energy conformation of Probe 1 bound to mephedrone, showing the hydrogen bonding and π-stacking interactions occurring between Probe 1 and mephedrone.

There are three interactions between Probe 1 and mephedrone at the minimum conformation (Figure 5.14). Both arms of the probe interact with mephedrone, but interestingly it is just NH(2), attached to the methylene linkers, that directly interacts with mephedrone. There appears to be no interaction with NH(1) attached to the anthracene unit. As previously discussed, this could not be concluded from the NMR data alone, due to the symmetry of the host molecule. Both the NH groups are acting as hydrogen bond donors, one to the carbonyl and another to the nitrogen of the amine in mephedrone. Both hydrogen bonding interactions occur in favourable orientations, 2.32 Å, 155.26° and 2.12 Å and 163.15°, which lie within the ideal dimensions for hydrogen bonding[159]. Given that in the NMR titrations both NH groups shift in the same proportions upon binding, it would make sense that they are binding concurrently, i.e. binding occurring in a consensus fashion. The DFT calculations are in good agreement with the NMR; that the benzyl group on the mephedrone doesn't interact, and that it is the methine of the chiral carbon in mephedrone that has a π-interaction with proton 9 on the anthracene. This arrangement of interactions was not predicted from the pharmacophore design,

however there are still two binding points that correlate to the pharmacophore. Based on the DFT predictions in parallel with the NMR results an experimental binding pharmacophore was developed (Figure 5.15).
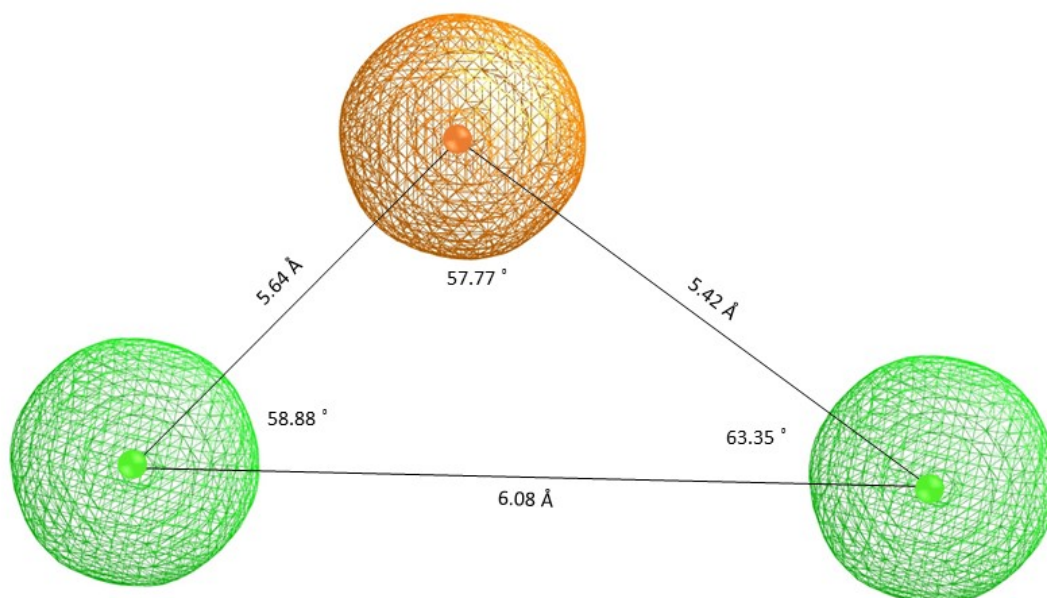
Figure 5.15 - An image showing the binding pharmacophore of Probe 1 based on DFT calculations, where green represents hydrogen bond donors and the orange sphere is a π-stacking interaction.

It is not unexpected that the distances and angles from the experimental pharmacophore show variation from the predicated pharmacophore, as the two pharmacophore models are based on very different binding data, and the pharmacophore model does not consider the carbonyl functionality. What can be seen is that there is a hydrogen bond donor and a π-stacking interaction as predicted, and more significantly both pharmacophores show a three-point binding interaction (Figure 3.11). The proposed 1:1 stoichiometry based on the experimental results of the host-guest interaction is supported by the DFT calculations.

5.3.2.2   Flephedrone

As with mephedrone, the minimum energy conformation of flephedrone was generated and studied with Probe 1 to generate a minimum energy conformation of the complex. Despite the chemical similarities of the two cathinone analogues, the DFT calculations of flephedrone bound to Probe 1 shows a distinctly different binding orientation. The favourable energy conformation seen in Figure 5.16 has an interaction energy of -32.97 kJ mol^{-1}.
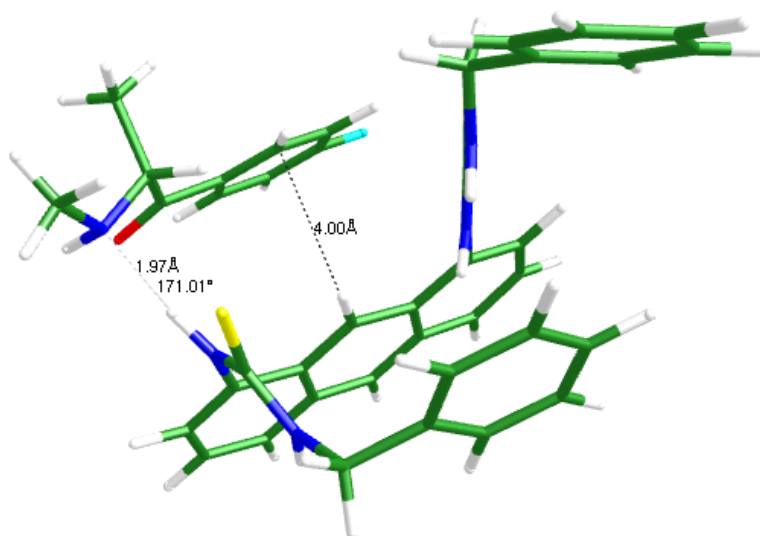
Figure 5.16 - An image showing the lowest energy conformation for complexation of flephedrone with Probe 1, with hydrogen bonding and π-stacking interactions indicated.

The deformation energy for Probe 1 to form this complex is -10.17 kJ mol^{-1}. The conformation of Probe 1 does not change as much as when mephedrone is bound, with a maximum RMSD of 9.88 Å between the bound and unbound conformations of Probe 1. This explains why the deformation energy is much higher when bound to mephedrone. However, what can be seen is that the binding orientation of flephedrone is different to that seen for mephedrone, with just two interactions present; one hydrogen bond between NH(1) and the carbonyl of mephedrone and a π-stacking interaction between proton 9 and the benzyl of mephedrone. This shows that the introduction of the electronegative fluorine has a large effect on the binding orientation, as well as the strength of binding, as seen in the NMR titration experiment.

5.3.3   Mass Spectrometry Testing

5.3.3.1   *Mephedrone*

To further investigate the interactions observed using NMR, verification of binding as well as stoichiometry, mass spectrometry binding studies were carried out. Mass spectrometry was performed through direct infusion using electrospray ionisation (ESI). As previously shown, solvent interactions with host and guest molecules can have considerable effects on binding. By using mass spectrometry, it is more likely that binding will be seen in the absence of solvent as measurement are made in the gas state.

Probe 1 was dissolved up in acetone and the instrument parameters were optimised to achieve the highest percentage abundance. Ten equivalences of mephedrone freebase was added to Probe 1 in acetone, and data was acquired. Figure 5.17 shows the mass spectrum of Probe 1 after the addition of mephedrone where four distinct peaks are observed, mephedrone freebase at *m/z* 178.4, with the most common fragment at *m/z* 160.4, Probe 1 at *m/z* 507.5 and the Probe 1-mephedrone complex at *m/z* 684.7. The MS was run in positive mode and therefore all masses stated are M+1. The spectrum was run with a scan range of *m/z* 100 - 1000 to see if any peaks from a different binding stoichiometry could be observed. No peaks were observed past *m/z* 684.7, which confirms what was predicted in both the DFT and the NMR experiments that the complex forms in a 1:1 ratio. It also provides further evidence that the chemical shift changes upon binding observed in the NMR is due to the mephedrone binding and not residual chloride ions. Given that the same chemical environments in NMR are effected in both binding interactions, the NMR could not definitively say that there wasn't any chlorine remaining in the sample that was causing the effect. To further confirm that the mass adduct peak at *m/z* 684.7 corresponds to the formation of a complex between the mephedrone and Probe 1, MS/MS was conducted on this mass peak. This showed that the complex peak at *m/z* 684.7 is further fragmented into the constituent peaks of *m/z* 178.4 and 507.5.
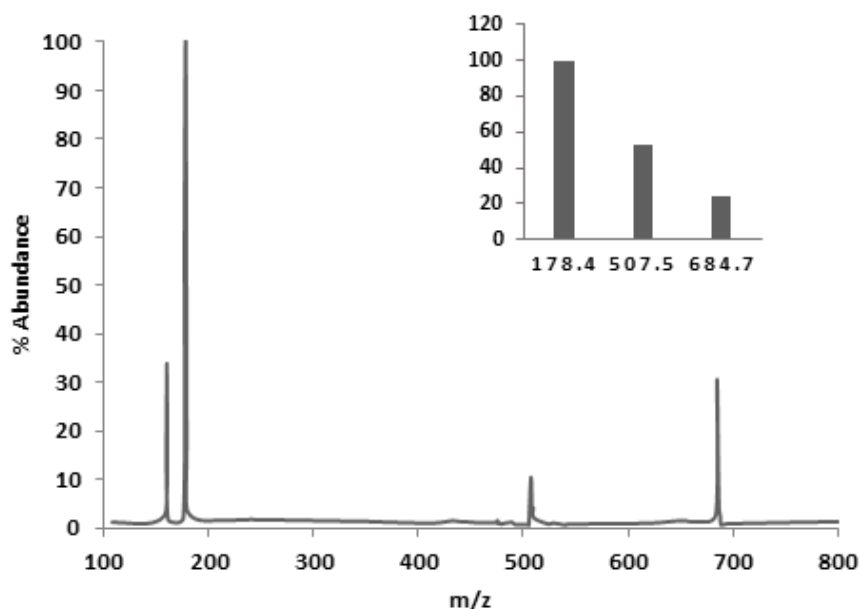
Figure 5.17 - ESI-MS of Probe 1 *m/z* 509, mephedrone freebase *m/z* 179 and complexed Probe 1-mephedrone *m/z* 685. Insert: MS/MS data for Probe 1 and mephedrone.

To further confirm that the Probe 1-mephedrone adduct mass signal was not an artefact, deuterated water was added to the sample. This lead to the relative increase of the adduct peak from *m/z* 684.7

to a range of *m/z* 688.8 to 690.7, due to deuterium displacement of labile protons on Probe 1. From the mass spectrometry data, it can be confidently concluded that mephedrone and Probe 1 form a supramolecular complex as suggested by the NMR data and DFT calculations in a 1:1 stoichiometry.

Ten eq. of mephedrone hydrochloride was added to Probe 1 in acetone to see whether it is possible to observe any competition between chloride and mephedrone. Interestingly, mephedrone appears to preferentially bind to Probe 1 with the adduct peak at *m/z* 684.7 still observed. There was no peak corresponding to the mass of Probe 1 and chloride in positive or negative modes. This is an interesting finding as the NMR data showed that chloride has a stronger association constant than mephedrone. This difference could be due to the varied conditions in which the two experiments are conducted.

5.3.3.2   Flephedrone

To further study the interactions seen using NMR, Probe 1 and flephedrone freebase were studied using ESI-MS. The same conditions used for mephedrone were applied to flephedrone to allow for a direct comparison. As shown in Figure 5.18, there are five distinct peaks in the spectrum, flephedrone freebase at *m/z* 182.4, with the two most abundant fragments at *m/z* 164 and 150[204], Probe 1 at *m/z* 507.5 and Probe 1-flephedrone complex at *m/z* 688.7. Once again it confirms what was predicted from the NMR data, that the complex forms in a 1:1 ratio because no peaks were observed further up the spectrum that would indicate a different binding stoichiometry was occurring.
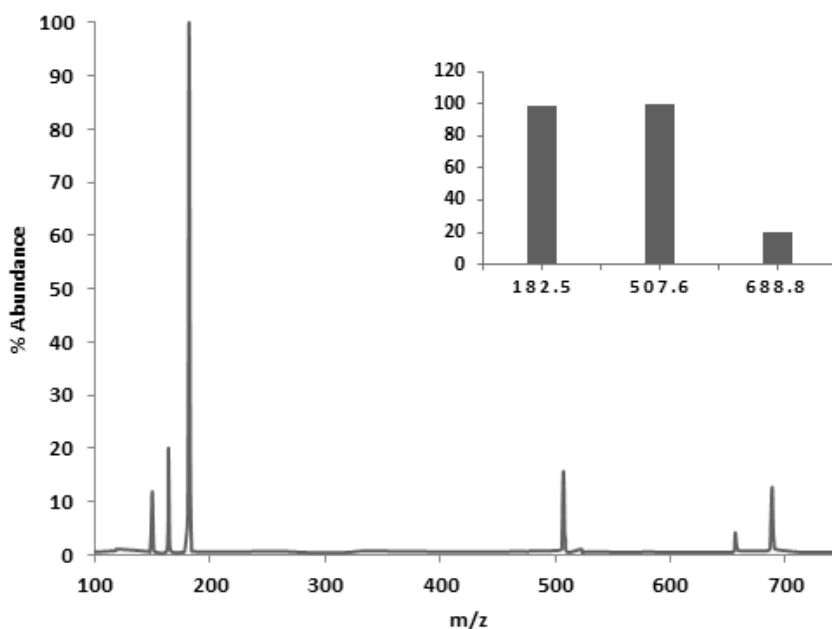
Figure 5.18 - ESI-MS of Probe 1 *m/z* 509, flephedrone freebase *m/z* 182 and complexed Probe 1-mephedrone *m/z* 689. Insert: MS/MS data for Probe 1 and flephedrone.

Interestingly during infusion the ratio of bound to unbound Probe 1 favoured the unbound formation. This is contrary to what is seen for mephedrone where the equilibrium appears to shift in favour of the complex, suggesting that the association constant for mephedrone and Probe 1 is greater. This reflects the findings from the NMR binding study, with mephedrone showing a stronger association constant, i.e. greater change in chemical shift. Once again MS/MS was performed on the spectrum seen in Figure 5.18 which confirmed that the complex peak was further broken down into its constituent parts: flephedrone *m/z* 182.4 and Probe 1 *m/z* 507.5. This confirms that the peak at *m/z* 684.7 is due to the complex and not an artefact.

5.3.4   UV/Vis Spectroscopy Testing

The NMR results in combination with the DFT calculations suggest that flephedrone interacts with the anthracene moiety on Probe 1 in a different way to mephedrone. Additionally flephedrone interacts with NH(1) which is not seen for mephedrone. This suggests that the two cathinone analogues could potentially have different optical responses upon binding. Therefore, both flephedrone and mephedrone were evaluated using UV/Vis and fluorimetry in an attempt to characterise their binding using optical spectroscopy. This could provide valuable information to develop Probe 1 into an optical in-field sensor, and also provide more information into the binding mechanism.

5.3.4.1   *Mephedrone*

As previously discussed the primary aim of this work is to produce an in-field detection probe for mephedrone. One of the simplest ways to achieve this is through an optical change upon binding i.e. a colour change upon addition of the drug to a solution of the host molecule. From the NMR and MS work it can be concluded that Probe 1 and mephedrone form a supramolecular complex. To test whether binding can be observed using optical techniques, UV/Vis analysis was conducted.

Individual UV/Vis spectra of Probe 1 and mephedrone were run to determine the absorption spectrum of both molecules (Figure 5.19). Mephedrone has its own unique absorption spectrum, and therefore it is imperative that this is taken into account when studying the binding interactions with Probe 1.
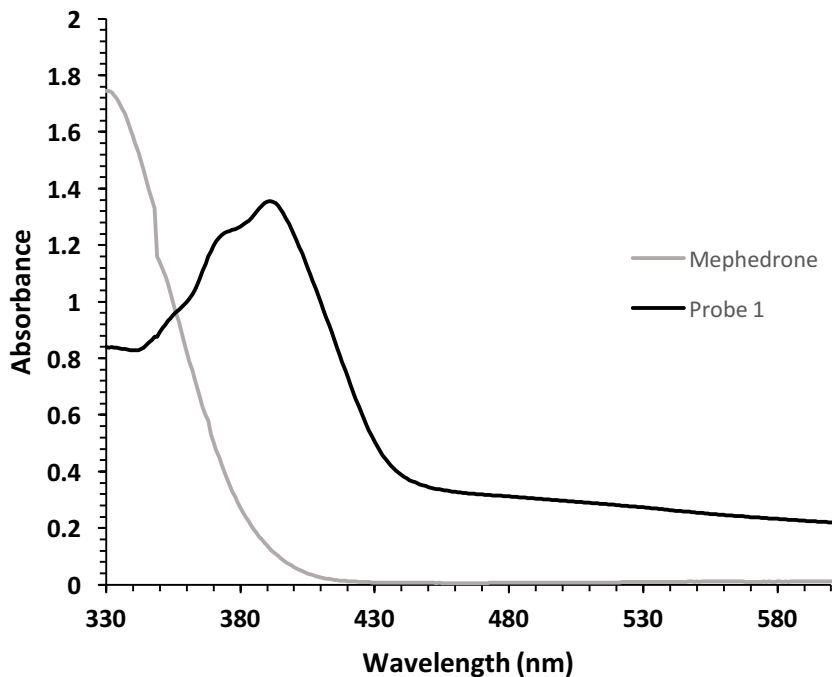
Figure 5.19 - Absorption spectrum of mephedrone (grey) and Probe 1 (black) from 330 - 600 nm.

The spectrum was run with a scan range of 330 - 600 nm. This is due to the UV/Vis cut off of acetone being reported at 330 nm[205] i.e., below this wavelength the spectrum seen is dominated by acetone. A maximum absorbance wavelength (λ_{max}) for Probe 1 is seen at 392 nm while mephedrone is at 332 nm (Figure 5.19). The absorption spectrum of mephedrone has been previously reported in ethanol with λ_{max} = 264 nm, which is below the scan range in this experiment[206]. The absorbance spectrum of Probe 1 is indicative of an anthracene moiety, where a pattern of three peaks can be observed at 356, 372 and 392 nm[207]. The three peaks are not as distinct as they would be for an unsubstituted anthracene. It has previously been shown that the absorbance spectrum of anthracene is greatly affected by the choice and position of substituents on the ring[207]. There is an overlap between spectra of mephedrone and Probe 1 from 330-410 nm, which was taken into account when studying the change in absorbance caused by the addition of mephedrone to Probe 1. A full UV/Vis titration was carried out in acetone, with Probe 1 kept at a constant concentration of 2.5 mM. Mephedrone freebase was dissolved up in acetone, as with the NMR experiments the molar ratio of mephedrone was studied from 0.25 eq. up to 10 eq.
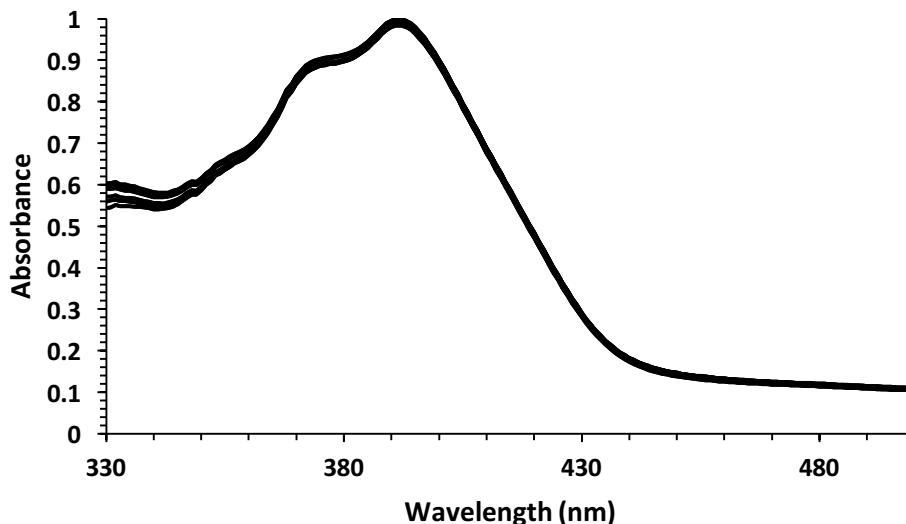
Figure 5.20 - UV/Vis absorption spectra for the titration study, between Probe 1 and mephedrone from 0.25 eq. to 10 molar eq. of mephedrone.

As seen in Figure 5.20 there is virtually no change in the absorbance spectrum of Probe 1 upon the addition of mephedrone. In order to see a change in the absorbance spectrum of Probe 1 due to mephedrone, there needs to be an interaction between the absorbing chromophore in Probe 1, which given the spectrum of Probe 1 would be an interaction with anthracene moiety and mephedrone. The DFT calculations and NMR experiments indicate that there is only a small interaction occurring between the anthracene and mephedrone upon binding. Therefore, it is not unforeseen that no change in absorbance is observed upon the addition of mephedrone to Probe 1.

5.3.4.2   Flephedrone

The absorption spectra of flephedrone and Probe 1 were recorded separately (Figure 5.21). As seen with mephedrone, the absorbance spectrum of the host and guest overlap from 330-399 nm, and therefore any increase in absorbance due to the addition of flephedrone needs to be accounted for.
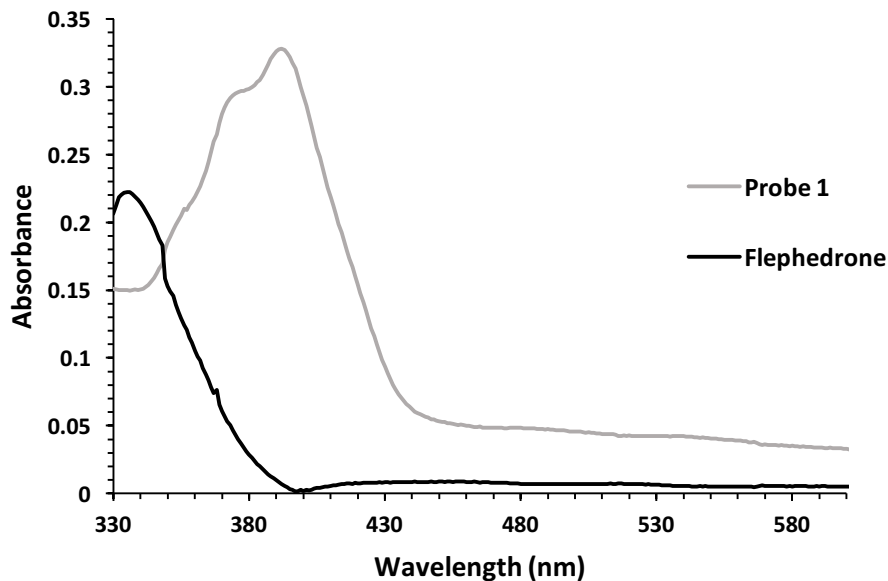
Figure 5.21 - UV/Vis absorbance spectrum of Probe 1 (grey) and flephedrone (black) from 330 – 600 nm in acetone.

A full UV/Vis titration was carried out from 0.25 - 10 eq. in acetone (Figure 5.22). Probe 1 was kept at a constant concentration of 2.5 mM and aliquots of flephedrone freebase in acetone were added directly to the cuvette.
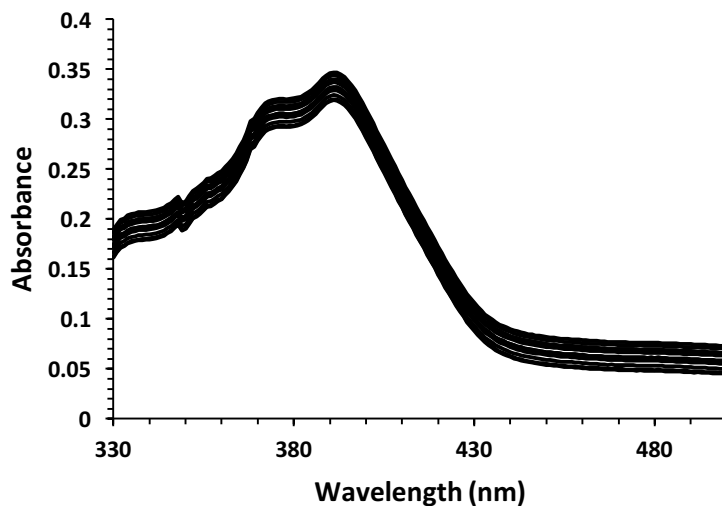
Figure 5.22 - UV/Vis absorption spectra for the titration study, between Probe 1 and flephedrone from 0.25 eq. to 10 molar eq. of mephedrone in acetone.

Despite the DFT calculations predicting more of an influence on the anthracene unit upon addition of flephedrone, no significant change in absorbance was seen upon addition of flephedrone. It is possible that complexation cannot be observed in UV/Vis in the ground state, therefore fluorescence titration

studies will be carried out for both flephedrone and mephedrone to understand if an optical change can be observed in the excited state.

5.3.5 Fluorescence Spectroscopy Testing

5.3.5.1 Mephedrone

The fluorescence spectra of mephedrone and Probe 1 were collected separately to determine the emission profile of both molecules, mephedrone was found to not fluoresce (Figure 5.22) at an excitation wavelength of 392 nm. This means that only the emission of Probe 1 can be studied to understand binding interactions. Commonly the absorbance λ_{max} of Probe 1 would be used as the excitation wavelength for studying fluorescence, to ensure the best sensitivity. As seen in Figure 5.19 the absorption spectrum of Probe 1 and mephedrone overlap at λ_{max} = 410 nm. It is possible that mephedrone could absorb the emitted light at 410 nm, which could affect the results observed. With this is mind the excitation wavelength used for all fluorescence titrations with mephedrone and Probe 1 was 392 nm to prevent mephedrone absorbing the excited light and therefore interfering with the emission spectrum of Probe 1. The maximum emission wavelength for Probe 1 was found to be 489 nm (Figure 5.23).
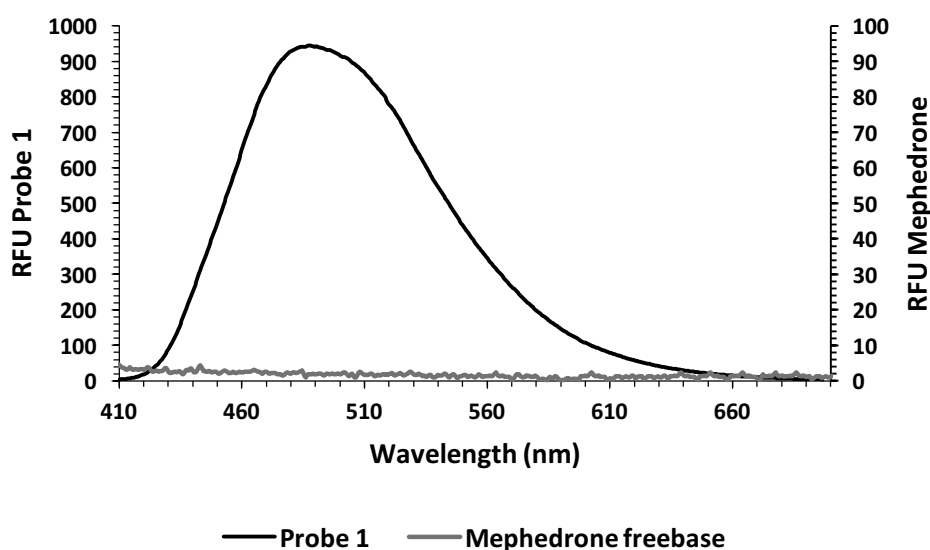
Figure 5.23 - Emission profiles for Probe 1 and mephedrone freebase, λ_{ex} = of 392 nm and a scan range of 410 - 700 nm.

For consistency with NMR and UV/Vis experiments, acetone was used for all fluorescence experiments, with mephedrone made up in a 0.01 M solution in acetone. A full titration was carried out from 0.25 to 50 molar eq. An extended titration was carried out, as no change was observed up to 10 eq.

As shown in Figure 5.24 the emission spectrum does not change during the titration. Once again based on the previous data, that suggested there is only a slight interaction between the anthracene and mephedrone, it is not unexpected that once again no interaction that causes an optical signal is occurring in the same molar ratios as seen for NMR analysis.
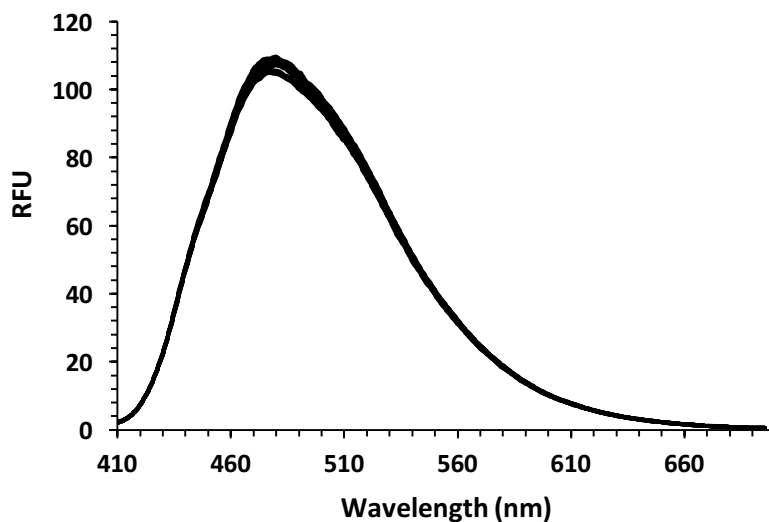
Figure 5.24 - Fluorescence titration with Probe 1 and mephedrone in acetone showing no change in intensity, λ_{ex} = 392 nm and a scan range of 410 - 700 nm.

For all experiments conducted thus far mephedrone freebase was made up to concentration in acetone, and aliquots of this solution were added to Probe 1 for the titration experiments. For fluorescence the concentration of this solution is much lower than that used for NMR to reflect the sensitivity of the instrument. To understand if the difference in results seen for NMR and fluorimetry is an effect of concentration, neat mephedrone freebase (i.e. not dissolved in acetone prior to use) as well as higher concentrations of mephedrone freebase in acetone were studied. This means that higher equivalents of mephedrone could be added to the system without dilution effects occurring due to addition of microliters of acetone to the cuvette.

Mephedrone freebase is an oil and therefore, in order to determine the concentration of mephedrone added, the density of the oil was calculated as 0.53 ± 0.01 g mL^{-1}.

As seen in Figure 5.25, addition of neat mephedrone freebase leads to an optical response with the intensity starting at the bottom red line and increasing to the second red line upon the first addition of mephedrone (150 eq.), and then increasing again after the second addition to the top red line (300 eq.).
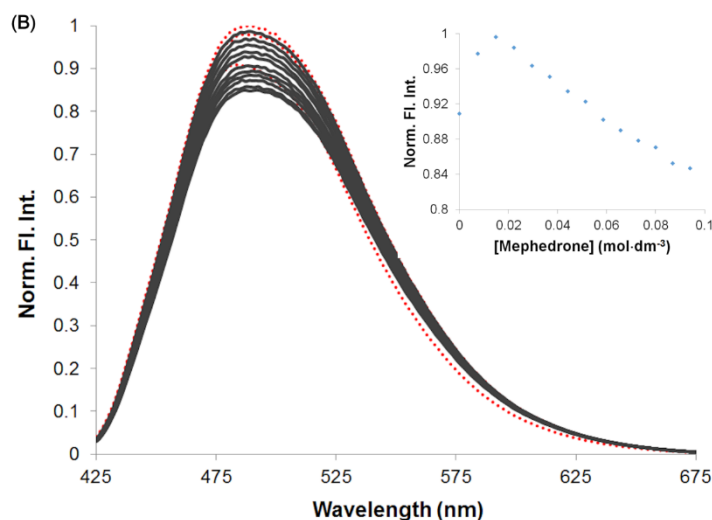
Figure 5.25 - Fluorescence titration for Probe 1 and neat mephedrone freebase, λ_{ex} = 392 nm. 5 µL aliquots of mephedrone freebase were added per data point. The red line at the bottom indicates Probe 1 before addition of mephedrone, the second red line indicates the first addition of mephedrone, and the top red line indicates the second addition of mephedrone. The remaining black lines indicate the sequential decrease of intensity due to further addition of mephedrone freebase.

However, from 450 eq. and above the emission is quenched and the intensity decreases sequentially by a total intensity of 552 after 1950 eq. The mechanism by which this occurs is not fully understood; however, the experiment was repeated in triplicate and resulted in a similar profile for each replicate. There appears to be competing binding mechanisms occurring in the excited state, which are concentration dependent. As previously discussed (Chapter 1), for the fluorescence intensity to increase there must be one of two things occurring, charge transfer or FRET, i.e. there must be intermolecular energy transfer occurring between the host and guest[192]. If the lone pairs of the thioureas are donating to the anthracene ring in Probe 1 then it is possible that upon binding to the lone pairs of NH(1) this may allow for a charge transfer mechanism to arise. However, the DFT calculations suggest that binding is occurring with NH(2), which would not allow charge transfer to occur upon binding. For the fluorescence intensity to decrease above 450 eq. of mephedrone there must be a subsequent quenching mechanism occurring[192]. It is possible that higher concentrations of mephedrone causes a shift in the equilibrium of binding due to saturation of the host, leading to a change in the principal binding mechanism. There is no current literature present on these two mechanisms occurring in the same system, especially at such high molar ratios.

Another interesting observation from the fluorescence titration of neat mephedrone freebase is the 10 nm red shift of the emission spectrum seen after the first addition of mephedrone. This shift only occurs after the first addition, and is not seen in the initial titration experiments where mephedrone is diluted in acetone before addition.

To study if this unique fluorescence response is concentration dependent and not time dependent (i.e. fluorescence goes up on the first addition of mephedrone irrespective of the concentration added), 450 eq. of mephedrone freebase was added directly to the solution of Probe 1. The intensity immediately decreased upon addition, showing that the increase and subsequent decrease seen in Figure 5.25 is due to the concentration added. This again supports the theory that at higher concentrations the binding equilibrium shifts towards a competing quenching mechanism over the charge transfer reaction that must be occurring originally to cause the initial increase in intensity.

Currently, there is NMR binding information from 0.25 to 10 eq. of mephedrone freebase to Probe 1 and fluorescence binding information from 150 to 1950 eq. The binding information provided from these two techniques currently does not correlate. In order to bridge the gap between these two techniques and understand if the change seen is due to different concentrations used for the two techniques, serial dilutions of mephedrone freebase in acetone were prepared and multiple titration experiments were conducted. Interestingly, for all the dilution experiments, irrespective of concentration, the fluorescence intensity quenched after each addition (Figure 5.26). This is contrary to what is observed for neat mephedrone, where the first two additions lead to an increase in intensity. Another observation is that there is no red shift with the addition of mephedrone when it is first diluted in acetone. This suggests that the addition of acetone to mephedrone before addition affects the mechanism of binding to Probe 1 during fluorescence. This dilution effect is not seen for NMR.
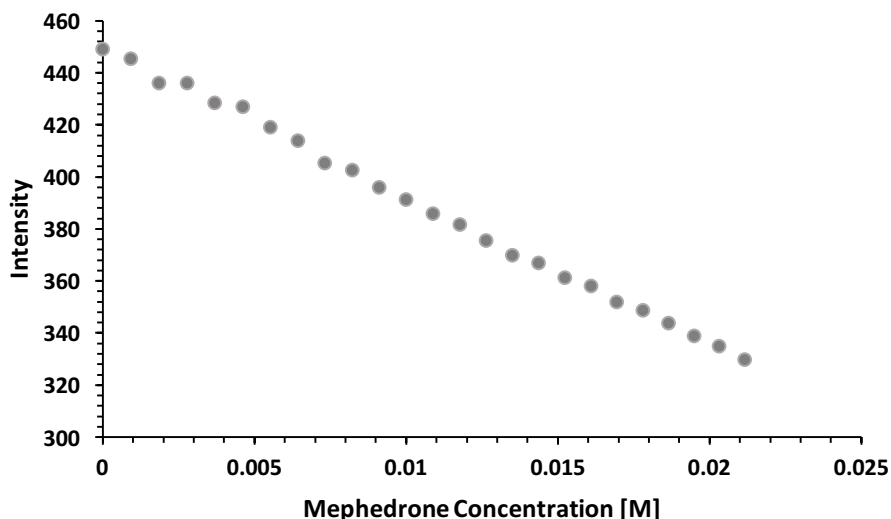
Figure 5.26 - Fluorescence binding isotherm for Probe 1 and mephedrone from a stock solution of 0.74 M, 15 - 1950 eq., λ_{ex} = 392 nm.

After completing a series of experiments using fluorescence to study the binding between mephedrone and Probe 1 in a wide range of molar equivalents (15 to 1950 eq.). It is clear that binding at high concentrations induces an optical response upon binding between Probe 1 and mephedrone. However, the mechanism by which this works is not yet fully characterised as there appears to be multiple mechanisms by which this occurs depending on the concentration of mephedrone added, and whether it is in solution before addition. What is promising is that there is a reproducible optical response of Probe 1 upon binding to mephedrone, and therefore Probe 1 has potential to be used as an optical in-field detection mechanism, but further characterisation is needed first. One possible route to explore would be characterisation using single photon fluorimetry.

5.3.5.2   Flephedrone

From the absorbance spectrum of flephedrone and Probe 1 an excitation wavelength of 410 nm was chosen. This is to correlate with the maximum absorbance of Probe 1 observed in the UV/Vis experiments, which also showed no absorption of flephedrone, which could interfere with the emission spectrum of Probe 1. A full titration was carried out from 0.25 to 50 eq. of flephedrone in acetone, adding directly to the cuvette. Again no change in the emission spectrum was seen when flephedrone was added in acetone at low concentrations (Figure 5.27).
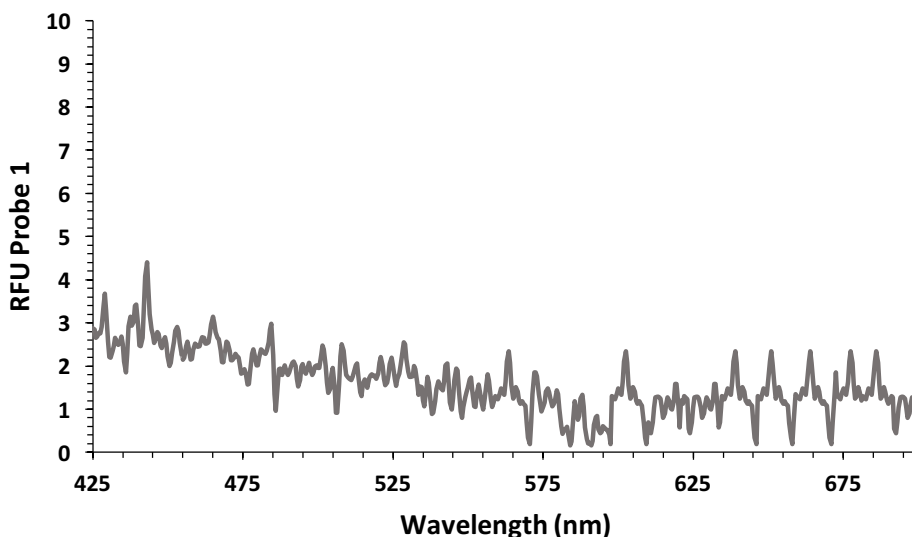
Figure 5.27 - Emission profile for flephedrone freebase, λ_{ex} = 410 nm and a scan range of 425 - 700 nm.

Given the phenomenon seen for mephedrone, where the addition of undiluted (neat) mephedrone lead to an optical response, the same was attempted for flephedrone. Upon the addition of neat flephedrone freebase there is a clear optical response (Figure 5.28). The bottom red line indicates the emission spectrum of Probe 1 in the absence of flephedrone, the top red line indicates the first addition of flephedrone (150 eq.) which shows a fluorescence intensity increase of 493. After the first addition the intensity starts to decrease. The insert shows graphically how this change in fluorescence correlates to the concentration of flephedrone in the system. As predicted from the DFT calculations flephedrone induces a greater optical response then mephedrone upon addition to Probe 1. This is predicted to be due to the increased interaction with the anthracene moiety, specifically proton 9. However, as with mephedrone a response is only induced upon high concentration of the guest, i.e. 150 eq., which is contrary to the results seen for both MS and NMR. As with mephedrone, the mechanism causing this unique binding isotherm is not fully understood. This change in the mechanism of binding between NMR and fluorimetry may be caused by a shift in the equilibrium at increased concentrations of guest saturating Probe 1 and therefore binding in a different way. Unlike with mephedrone there is no red shift seen for the emission spectrum upon addition of neat flephedrone. This further confirms that flephedrone and mephedrone are binding in different orientations.
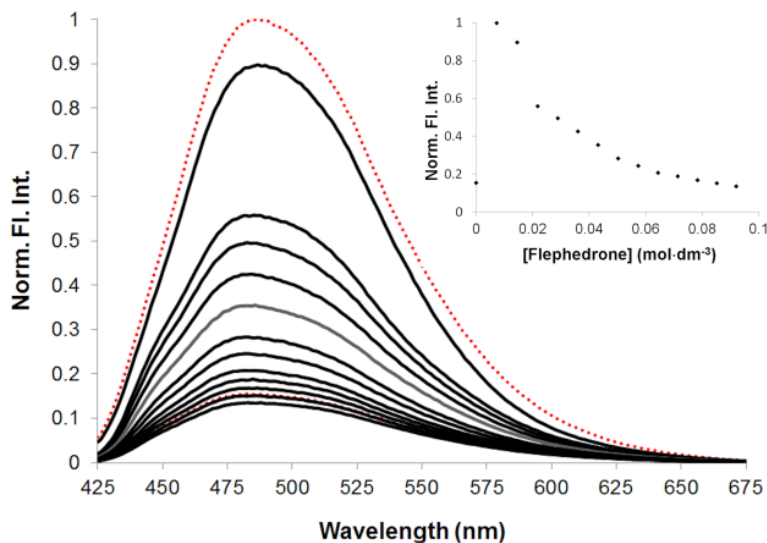
Figure 5.28 - Fluorescence titration of Probe 1 and flephedrone freebase added in 5 µL aliquots of neat mephedrone freebase. The bottom red line is Probe 1 before addition of mephedrone, and the top red line is after the first addition of mephedrone. The black lines are the subsequent additions. Insert: Plot of concentration of NPS and the quenching of fluorescence intensity at 485 nm (acetone, 5.0 µM, λ_{ex} = 410 nm).

For quantitative laboratory purposes such high molar equivalents of drug are not ideal. However, for use as an in-field detection mechanism the addition of undiluted drug to induce and optical response could be deemed more practical as no solvent would be required.

Once the binding between Probe 1 and mephedrone was characterised the next stage was to test selectivity against common cutting agents, which have also been found to induce false positives when testing drugs of abuse[61,134].

5.3.6 Selectivity Testing

Mephedrone is not found pure in street samples, consequently it is important to assess the selectivity of Probe 1 against the most common cutting agents that could be present in the street samples alongside mephedrone. The analysis of aminoindane products in Chapter 2 highlighted that NPS products may contain other active ingredients. From the development of the pharmacophore it was seen that many cutting agents have very similar chemical structures, and therefore could have very similar binding motifs to mephedrone. The pharmacophore model was developed to not only design a binding motif for mephedrone, but also to understand how to ensure selectivity against common cutting agents. Selectivity of Probe 1 over methamphetamine has already been shown. Further studies need to be conducted to investigate the selectivity of Probe 1 over common cutting agents.

From the binding analysis of mephedrone and flephedrone with Probe 1 so far, the ^{1}H-NMR data provides the most valuable binding information. It has allowed for understanding into which atoms

are involved in binding, predicted stoichiometry as well as providing information with low molar equivalents (0-10 eq.) compared to the optical studies. Consequently, selectivity studies will be carried out using ^{1}H-NMR to allow for direct comparison with the mephedrone results.

5.3.6.1   NMR Spectroscopy

In order to test selectivity of Probe 1 for mephedrone, four of the most common cutting agents were chosen, benzocaine, caffeine, paracetamol and lidocaine (Figure 5.29)[16,49,208]. ^{1}H-NMR testing was carried out between each guest molecule separately and Probe 1. Again for consistency all analysis was carried out in acetone-d$_6$.
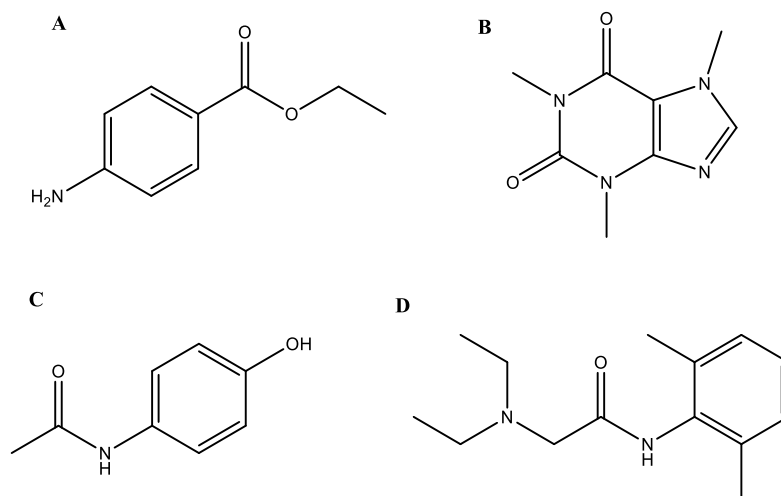
Figure 5.29 - Chemical structures of four common cutting agents, A. benzocaine B. caffeine C. paracetamol and D. lidocaine.

A spectrum of Probe 1 was acquired followed by the addition of 10 eq. of the guest molecules separately. The NMR analysis of benzocaine with Probe 1 is shown in Figure 5.30. No change in the chemical shifts of either the host or guest can be seen. The analysis of the remaining three cutting agents; caffeine, lidocaine and paracetamol show the same results. To ensure this is also true at higher molar ratios each system was run with 50 eq. of guest. There was still no change seen in any of the chemical shifts for all four cutting agents. This shows with confidence that Probe 1 is selective over four of the most common cutting agents known to be found in mephedrone street samples.
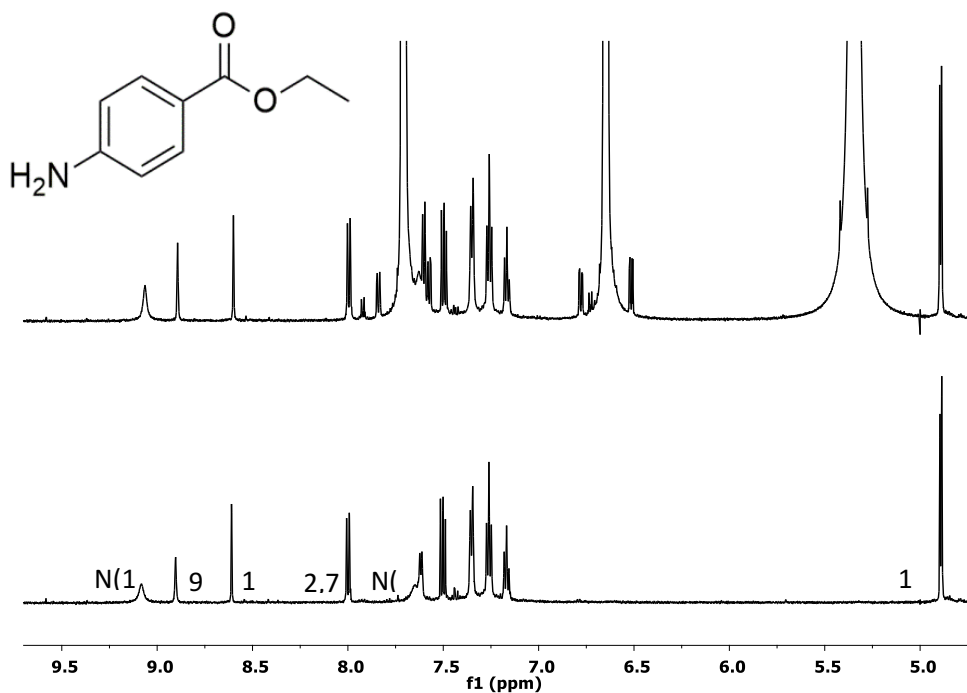
Figure 5.30 - ^{1}H-NMR spectra of Probe 1 (bottom) plus after the addition of ten eq. of benzocaine (top) in acetone-d$_6$.

All of the cutting agents contain at least one functional group in common with mephedrone. However, the size, conformation and orientations are distinctly different. This again highlights the advantage of utilising a concerted design. This is very promising given that previous literature states the problem with cutting agents leading to false positives and negatives[63,133].

If these results are taken into account in relation to both the mephedrone testing and DFT calculations it is not surprising that no interaction is seen. The DFT calculations show a very large deformation energy for Probe 1 upon binding to mephedrone. To overcome this energy barrier the interaction must be very energetically favourable, which as shown above is due to the three-point binding interaction occurring. By removing one of these functional groups it reduces the binding affinity (mephedrone precursor) or prevents binding at all (methamphetamine). By completely changing the orientation of these functional groups, as well as reducing the number of binding points (cutting agents), it prevents any interaction from occurring with Probe 1, thereby creating a selective sensor for mephedrone.

5.3.6.2   Fluorescence Spectroscopy

NMR results showed no interaction between Probe 1 and caffeine, lidocaine, benzocaine or paracetamol. However fluorimetry is far more sensitive than NMR, and an optical sensor is the final aim of the project. Therefore, each of the cutting agents was tested against Probe 1 to see whether a fluorescence response could be observed with Probe 1. Each of the cutting agents was run as a 2.5

mM solution in acetone individually, with λ_{ex} = 392 nm. No fluorescent response was observed for any of the cutting agents.

All cutting agents were tested using the same conditions as mephedrone and spectra was collected from 0.5 to 50 eq. Figure 5.31 shows the titration curve for caffeine, no response can be seen up to 50 eq. The same is observed for the lidocaine, benzocaine and paracetamol.
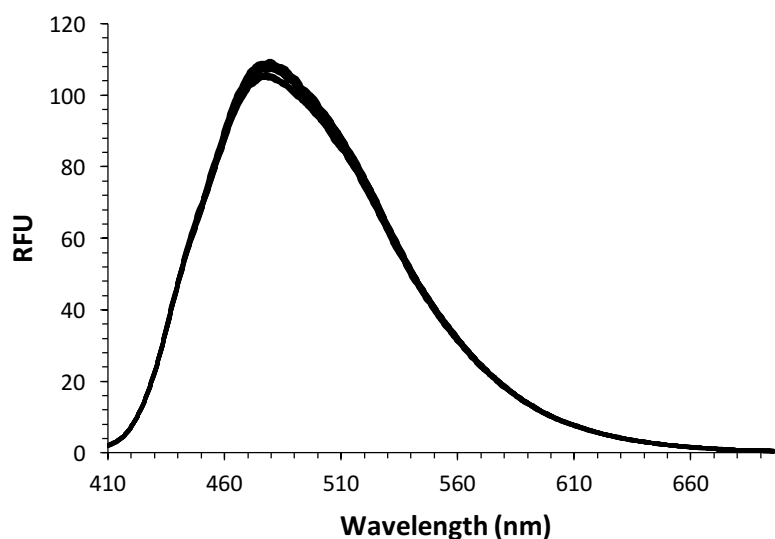
Figure 5.31 - Fluorescence titration of Probe 1 (5.0 μM) and caffeine added in 50 μL aliquots of a 2.5 mM solution in acetone from 0.5 - 50 eq., λ_{ex} = 392 nm.

However, when mephedrone is diluted in acetone prior to addition no response is observed either. Therefore each of the cutting agents was also added in neat to Probe 1 in the cuvette in 1 mg portions up to 500 eq. Above this molar concentration, the solution was saturated. For each of the cutting agents again no response was observed. This demonstrates that Probe 1 shows selectivity over both dilute and neat cutting agents using both NMR and fluorimetry.

5.3.6.3   Street Samples

As shown from the analysis of aminoindane street samples in Chapter 2, varying concentrations of active ingredients can be combined with any number of cutting agents. To ensure that mephedrone can be detected in such mixtures, the two most common cutting agents present in NPS[63,136]: benzocaine and caffeine were studied in combination with mephedrone. It has already been shown that caffeine and benzocaine do not bind to the Probe 1, therefore any interaction that occurs in a mixture should be due to mephedrone. Benzocaine, caffeine and mephedrone hydrochloride were combined in equal proportions. The entire mixture was taken up in water, and the solution was filtered to remove the undissolved caffeine and benzocaine, which are less soluble in water than mephedrone

hydrochloride. The remaining procedure was carried out and upon evaporation a mixture of the mephedrone oil and white solid remained. A portion of this mixture was dissolved up in acetone-d_6 for NMR analysis. A full ^{1}H-NMR titration was carried out as seen in Figure 5.32, showing the expanded aromatic region. The shift of the NH groups and 9, 10 positions of anthracene can still clearly be seen, which indicates that binding is occurring. The total shift is noticeably less than that seen for mephedrone when studied on its own. This is because the sample analysed against Probe 1 is not entirely mephedrone and therefore the molar equivalents relate to the entirety of the street sample contents.
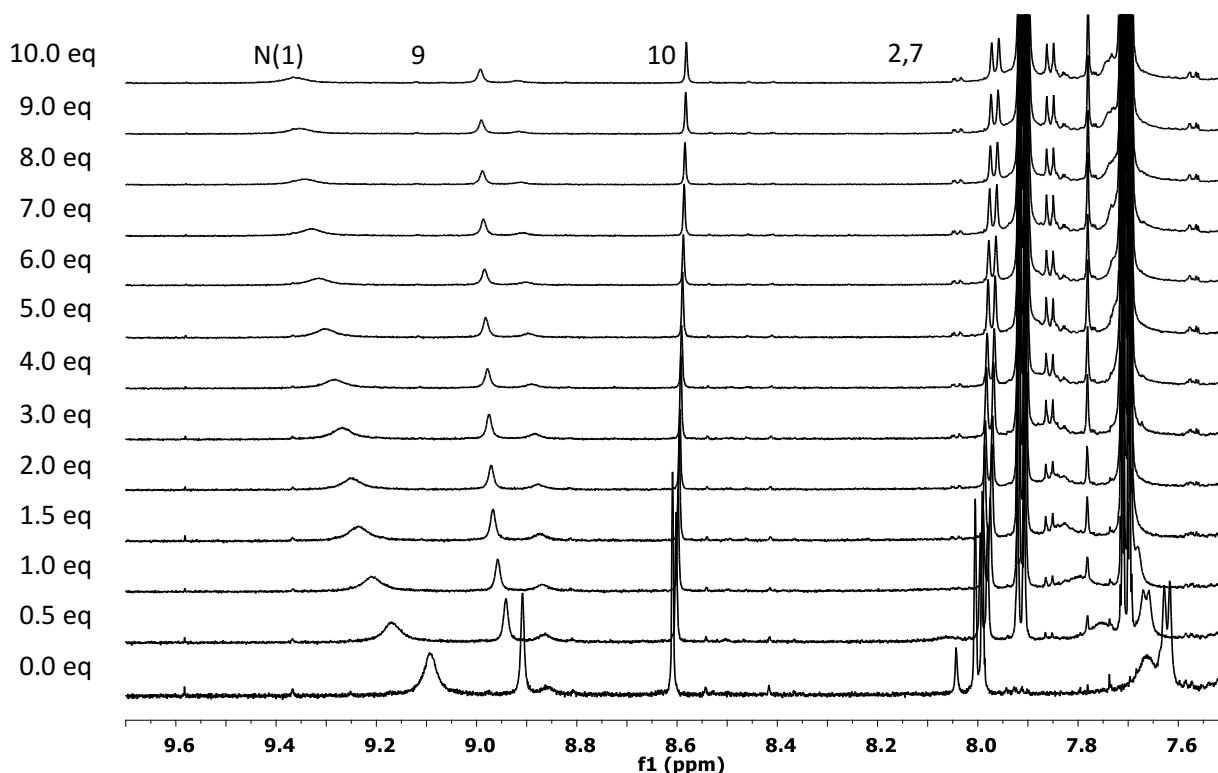
Figure 5.32 - Expansion of ^{1}H-NMR titration of Probe 1 (19.7 mM acetone-d_6) against the simulated street sample containing benzocaine, caffeine and mephedrone.

When comparing 10 eq. of just mephedrone to 10 eq. of the street sample, the relative concentration of mephedrone compared to Probe 1 can be easily determined by using approximately one and a half times more mephedrone than Probe 1. This induces a total chemical shift for NH(1) of 0.18 ppm. Whereas the integral ratios of Probe 1 to mephedrone in the pure samples is 1:10. This induces a total chemical shift for NH(1) of 2 ppm. This is ten times higher than the shift seen for the street sample, which may in the first instance appear to be due to the cutting agents interfering with binding. However, when the relative integrals for Probe 1 and mephedrone are taken into account it can be seen to be reflective of concentration effects. Therefore, showing that the presence of cutting agents in the sample does not affect the chemical shifts of Probe 1, and therefore does not affect the

association constant of mephedrone binding to Probe 1, as the relative concentrations show the same chemical shift.

5.4 Conclusion

Probe 1 was tested against a selection of guest molecules; mephedrone, flephedrone, methamphetamine, 4-methyl propiophenone, lidocaine, caffeine, paracetamol and benzocaine as well as chloride anions. Chloride anions showed the strongest binding affinity with a K_a of 500 M^{-1}, followed by mephedrone at 104 M^{-1}. This affinity for chloride anions means mephedrone could not be tested in the hydrochloride salt form, which is how it is primarily found in street samples. To overcome this, the freebase of mephedrone was used for all experiments, so as to study the binding interactions in the absence of any interaction from chloride. Full ^{1}H-NMR titrations were carried for mephedrone with Probe 1, which showed that there were chemical shifts seen for both NH groups in Probe 1, as well as protons 9 and 10 on the anthracene. Small changes are also seen for alkyl protons in mephedrone; however, due to the amine proton in mephedrone exchanging, no definitive hydrogen bonding interaction could be observed from mephedrone. The three binding points the sensor molecule was designed to include according to the pharmacophore model were a hydrogen bonding group and two π-stacking interactions. The shifts in the NMR indicate that there are two hydrogen bonds and one π-stacking interaction between Host 1 and mephedrone. Although it doesn't show a complete correlation to the predicted pharmacophore model, it does show a three-point binding motif in a concerted fashion, with binding shown to both the amine and aromatic functionalities, which does correspond to the pharmacophore model.

The choice of solvent proved critical for the binding studies, with no response seen when DMSO was used as the experimental solvent. Mass spectrometry confirmed that the interaction occurring during NMR is caused by a 1:1 complex of Probe 1 and mephedrone. It also proved that the complex must be fairly stable to stay together through the ESI-MS conditions. Further confirmation of Probe 1 and mephedrone complexation in a 1:1 ratio was determined through deuterium and MS/MS studies. Another cathinone analogue, flephedrone was analysed to understand selectivity. The addition of the fluoro group on the aromatic ring reduces the binding affinity by tenfold (K_a = 10 M^{-1}). This can be concluded to be due to concerted sensor design. Further evidence for the consensus binding of Probe 1 and mephedrone is seen when studying Probe 2. The removal of the second thiourea arm in Probe 2 shows a 10 fold decrease in K_a for mephedrone. This is additionally rationalised using the DFT calculations which shows mephedrone binding to both arms of Probe 1. This highlights the importance of a three-point binding motif that was highlighted in the pharmacophore model in Chapter 3. Also flephedrone and mephedrone are shown to bind in different orientations perhaps due to the change

in electronegativity by the addition of the fluorine functionality. This demonstrates how a small change in chemical structure can affect the binding affinity.

Fluorescence and UV/Vis spectroscopy were used to study an optical change that may be observed upon binding. Both mephedrone and flephedrone showed no interactions using UV/Vis spectroscopy even at high molar ratios (300 eq.). A number of experiments were conducted using fluorescence spectroscopy. Mephedrone was dissolved in acetone and up to 50 molar equivalents of mephedrone was added to Probe 1, no change in the emission spectrum was observed. The same was also found for flephedrone. However, when mephedrone is added as a neat oil (i.e. not dissolved up in acetone prior to addition) at high molar equivalents there is a very noticeable change in the emission spectrum. For mephedrone, from 150 eq. to 300 eq. the intensity increases and a small red shift in the spectrum is observed, after which the emission is quenched. The exact mechanism of action taking place is not understood. For flephedrone there is also an interaction observed at high concentrations of flephedrone neat oil and the change in intensity is even more pronounced then for mephedrone. The first addition of 150 eq. causes an increase in intensity and all further additions lead to quenching. The DFT calculations show a change in orientation between flephedrone and mephedrone binding with Probe 1. Indicating a decrease in the hydrogen bonding interactions for flephedrone and Probe 1, which is evident from the NMR experiments. However, the DFT calculations do show a stronger interaction of flephedrone with the anthracene moiety, which could explain why flephedrone shows a stronger binding response using fluorescence.

Again the fluorescence mechanisms involved in this are not fully understood at present, there is little, if any, literature about the molecular sensing of cathinone to consult. However, it does show promising results for using Probe 1 in-field as an optical response can be observed. High molar ratios must be taken into account though, as this reduces the sensitivity of the sensory molecule. As highlighted in Chapter 1, an optical change upon binding is the ideal mechanism for simple in-field detection, and therefore this should be further explored to see how it can be fully characterised and optimised for in-field use.

In summary, Probe 1 displayed greater affinity with mephedrone versus methamphetamine and other related analogues *via* ^{1}H-NMR. This suggest a greater preference for a β-ketoamine arrangement. This is supported by the systematic analysis of mephedrone, methamphetamine, mephedrone precursor and flephedrone.

Chapter 2 emphasised the need for selectivity in the presence of a number of different cutting agents. The results show that addition of common cutting agents did not affect the interaction between mephedrone and Probe 1 which is promising for use with street samples. The development of an in-

field detection mechanism is a continuing endeavour; however, significant knowledge about the structural components necessary to selectivity bind mephedrone has been gained based on pharmacophore design (Chapter 3) and use of supramolecular chemistry.

Chapter 6   *In-Silico* Analysis of Potential Host-Guest Interactions

6.1 Introduction

The ability to accurately predict binding affinities for host-guest interactions is a much sought after goal. Reliable *in silico* data can not only provide valuable information on whether interactions occur between the host and guest and the types of interactions, but also help to minimise time consuming laboratory synthesis of potential sensor (host) molecules which may ultimately prove unsuccessful, by guiding the decision making process for synthesis.

6.1.1 Metadynamic simulations of host molecules

The concept of metadynamic simulations for large molecules has been studied for a number of years to evaluate the free energy of complex formation between proteins and ligands. Using the principles applied to proteins as discussed in the Introduction (Chapter 1), it is feasible that *in silico* binding data between small molecules could be used to predict binding affinities, which in turn could guide the synthetic development of small host molecules. As discussed in Chapter 1, the choice of simulation conditions and collective variables (CV) will be vital in establishing a quality system to ensure that the free energy values calculated are as representative of experimental values as possible. The choice of CVs is imperative to the reliability of the metadynamic simulations. Ideally the CVs chosen should clearly distinguish between different conformational variations during the simulations i.e., initial, final and intermediate conformations. They should also represent all kinetically slow events, such as structural phase transitions, that may be relevant to reconstructing a free energy profile of the system[209]. Given that the focus of interest of these studies is the binding between host and guest molecules, the variable most important to understanding the process of interest is the distance between the host and guest molecules.

An example of the output data collected on completed metadynamics simulations is presented in Figure 6.1. This data allows the minimum energy complex to be identified as well allowing full analysis of all conformations in the system and their corresponding free energy potential.
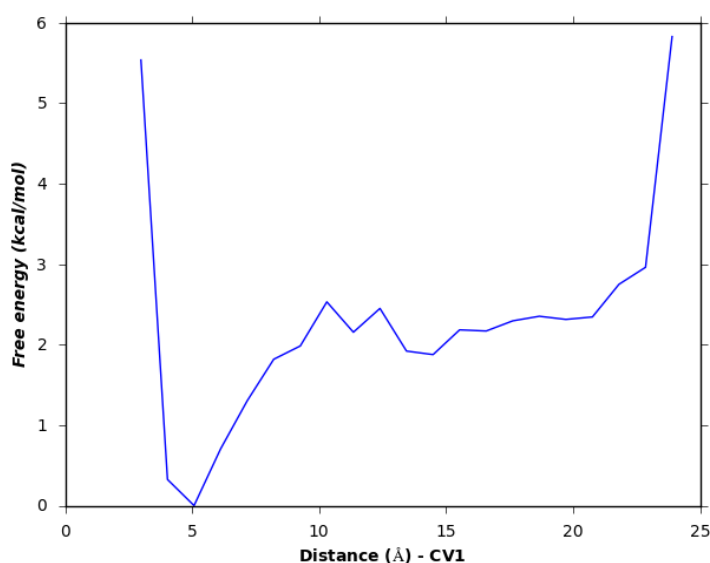
Figure 6.1 - Example of metadynamics data output which shows the free energy as a function of distance, based on the collective variables chosen, in this case distance between specified atoms in the host and guest molecules. The minimum energy is seen at a distance of 5.2 Å.

Using metadynamics to predict binding between small molecules in this way is a novel concept with little literature surrounding its use[210]. It has the ability to vastly change the area of host molecule development by allowing for the prediction of host-guest binding, which could dramatically reduce the time of sensor development.

Dibenzylthiourea anthracene (Host 1)

Dinaphthylthioruea anthraquinone (Host 2)

Dinaphthylurea tetrahydroxycalix(4)arene (Host 3)
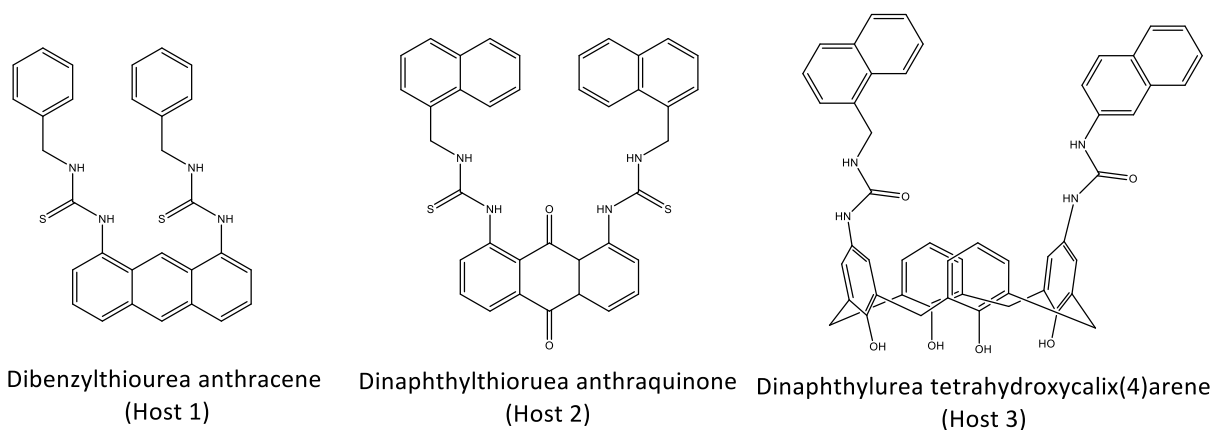
Figure 6.2 - Chemical structures of the three host molecules analysed using metadynamic simulations.

The aim of this work was to develop an approach that shows a consensus between the experimental results reported in Chapter 5 for the host-guest complexes and *in silico* binding data, which could then be used for future sensor development. Simulations were run for sensor Host 1 (Figure 6.2), which was the final host molecule prepared in Chapter 4 and tested in Chapter 5. The same approach was

applied to two additional sensor designs (Figure 6.2), dinaphthylthiourea anthraquinone (Host 2, Figure 6.2) and dinaphthylurea tetrahydroxylcalix(4)arene (Host 3, Figure 6.2). The synthesis of which was examined in Chapter 4, so as to indicate whether future synthetic development of these sensor molecules could be worthwhile based on *in silico* binding data.

6.2 Experimental

6.2.1 Ligand Preparation

All molecules were drawn in ChemDraw and converted into 3D Mol2 files for use in Maestro. Ligands were prepared before any simulations were performed to ensure all 3D structures were correct. Using LigPrep version 3.6 in Maestro, OPLS_2005 force field[211] was applied, with a pH of 7 ± 1 in chloride buffer. Hydrogens atoms were added to all molecules, and the final prepared ligands were used for all further analysis.

6.2.2 Conformational Search

All compounds were saved in Mol2 format and imported into Maestro (Schrodinger). Conformational searching calculations were performed using MacroModel with an OPLS_2005 force field[211] and implicit water solvent system, Generalized Born/Surface Area (GB/SA)[212]. Due to the lack of crystallographic data for the host molecules being investigated no constraints were applied to the system. The Polak-Ribiere conjugate gradient (PRCG) minimisation method was applied to all compounds, with the Monte Carlo Multiple Minimum (MCMM) torsional sampling method for conformational searching using 1000 steps and a 21 kJ mol^{-1} window for conformers. Minimum conformation energy values and number of conformers were recorded. Once lowest energy conformers were obtained, the interaction of the host molecules with mephedrone, amphetamine and caffeine were investigated. The guest molecules were randomly placed near the host molecule outside of the putative binding site, predicted based on experimental interactions, to guard against biasing results. The same parameters applied for single molecule conformational searching were used to obtain the minimum energy conformation for the host-guest complexes with 2000 steps used instead of 1000 to account for the increased system size.

6.2.3 Simulated Annealing

The starting structures used in simulated annealing studies were the minimum energy conformers established by the conformational search carried out in MacroModel. Simulated annealing was carried out using Desmond[213]. A system for studying each of the host molecules was built using periodic boundary conditions and a 10 Å cubic buffer box applied around each host molecule. This allows for a

20 Å distance between any two host molecules which guards against the formation of artefact interactions between two molecules in different units. Six steps were applied during the simulated annealing cycle, heating from 0 K to 1000 K at a linear gradient and held at 1000 K for 500 ps, cooling to 400 K over a period of 1 ns, followed by a simulation time of 3.13 ns (Table 6.1). Energy and coordinates of the system were recorded at 1 and 5 ps, respectively. Studies were repeated for all host molecules. The temperature was regulated with the Nose-Hoover chain thermostat[214] with a relaxation time of 1.0 ps. Non-bonded interactions had a 10 Å cutoff and for long-range Coulomb interactions the smooth-particle-mesh Ewald method[215] was applied. The RESPA integrator[214] was used to carry out integration of bonded, non-bonded-near and tat with steps of 2.0, 2.0 and 6.0 fs. Simulated annealing was carried out in water, methanol and dimethyl sulfoxide (DMSO) for Hosts 1 and 3 and water for Host 2. All conformations from the simulation trajectory were extracted into separate files and clustered based on their RMSD to determine the most common cluster, and therefore the most common conformation from the simulation. The clustering script in Maestro was used in order to achieve this.

Table 6.1 - Simulated annealing conditions used for studying host molecules.

Time (ps)	Temperature (K)
30	10
100	100
200	300
300	400
500	1000
1000	1000
1000	400

An additional test was carried out for dibenzylthiourea anthracene (Host 1) to ensure that the conformational space is explored in 3.13 ns over 6 steps. An extended simulated annealing study was carried out that consisted of heating and cooling over 5 rounds as shown in Table 6.2. This was carried out over 17.13 ns. The same parameters for the system were applied as above.

Table 6.2 - Extended simulated annealing experiment carried out for dibenzylthiourea anthracene.

Time (ps)	Temperature (K)
30	10
100	100
200	300
300	400
500	1000
1000	1000
1000	400
1000	400
500	1000
1000	1000
1000	400
1000	400
500	1000
1000	1000
1000	400
1000	400
500	1000
1000	1000
1000	400
1000	400
500	1000
1000	1000
1000	400

6.2.4 Metadynamics

The three host molecule starting structures used for the metadynamics study were the representative energy conformations from the conformational search and simulated annealing studies. Desmond was used for all metadynamics studies[213]. The settings for system building were identical to those used in the simulated annealing study, except the periodic boundary box was increased to 30 Å to allow for additional movement of the molecules.

Two atoms, one from the guest and one from the host molecule, were chosen as probes for the CV based on the minimised structures. Atoms with poor flexibility were selected to avoid excess

movement that can occur on flexible groups, such as alkyl chains, as well as to prevent the molecule from moving outside of the box during the simulation. The distance between the molecules is calculated between these two probes to allow for a distance against free energy plot to be generated.

A number of different parameters were studied so as to ensure that the final approach was as high quality as possible. Simulations times of 2, 5, 10 and 50 ns were examined, with buffer sizes of both 20 and 30 Å, as well as varying the number of CVs. For mephedrone and methamphetamine that naturally occur as salts the neutral, charged and addition of a chloride ion were examined. Given that experimentally the chloride ion is shown to bind very strongly to the sensor, the effect of the chloride *in silico* was also explored.

The final method chosen was a simulation time of 5 ns, with a 30 Å buffer box in water, methanol and DMSO, recording between 1 to 5 intervals. To define how the molecules moved in the simulation the default values of 0.05 Å for distance, 0.03 radi (1.8°) for angles and 0.05 radi (3.0°) for dihedral angles were used. Just one CV was examined which consisted of one probe on each of the host and guest molecules, this was determined based on the least flexible atoms from the conformational searching. This approach was found to give the best compromise between computational cost and quality results. Desmond trajectory viewing and analysis tool was used to visualise the results.

In order to try and correlate the *in silico* data with the experimental data further studies were carried out into how the host-guest complexes interacted in organic solvents. Both DMSO and methanol were used with the same parameters discussed above, to allow for a direct comparison of the free energy profile, and complexation conformations in different solvent systems.

6.3   Results and Discussion

6.3.1   Conformational Searching

Conformational analysis of the three host molecules; dibenzylthiourea anthracene (Host 1), dinaphthylthiourea anthraquinone (Host 2) and dinaphthylurea tetrahydroxylcalix(4)arene (Host 3) was carried out and the results for each are presented below.

In order to try and predict conformations of both the host and guest molecules in water that are represented implicitly, conformational searching of each guest molecule was carried out as well as conformational searching of host-guest complexes in the same system. This is a preliminary method for understanding the enthalpy contribution for complexation of the bound and unbound host molecules. Mephedrone, caffeine and methamphetamine were used as guest molecules to understand the selectivity of the host molecules *in silico*, this will also be a direct comparison for

dibenzylthiourea anthracene (Host 1) with the experimental results discussed in Chapter 5. Caffeine was chosen as a representative cutting agent as it is prevalent in internet products (Chapter 2), while methamphetamine was chosen due to its structural similarities to mephedrone, which previous in-field detection mechanisms have failed to show selectivity against. As previously mentioned, selectivity is a crucial aspect of sensor development, and the use of metadynamics could potentially be incorporated into future strategies to predict selectivity of potential host molecules, before synthesis is carried out.

6.3.1.1   Dibenzylthiourea Anthracene (Host 1)

Conformational searching of dibenzylthiourea anthracene (Host 1) produced 203 conformations within the 21 kJ mol^{-1} energy window. The lowest energy conformer shown in Figure 6.3 represents the most stable conformation found with an energy value of 16.38 kJ mol^{-1}; this was found 6 times out of the 1000 steps performed. The difference between the lowest energy conformer found and the highest energy conformer in the selected energy window is shown in Figure 6.3. The change in energy (ΔE= 20.45 kJ mol^{-1}) results in a noticeable difference in conformation of Host 1 (Figure 6.3). This highlights the need for full analysis of the conformational space to ensure that metadynamic studies are based on a minimised energy structure to give the best representation for the free energy data being produced.

Lowest Energy Conformer   Highest Energy Conformer
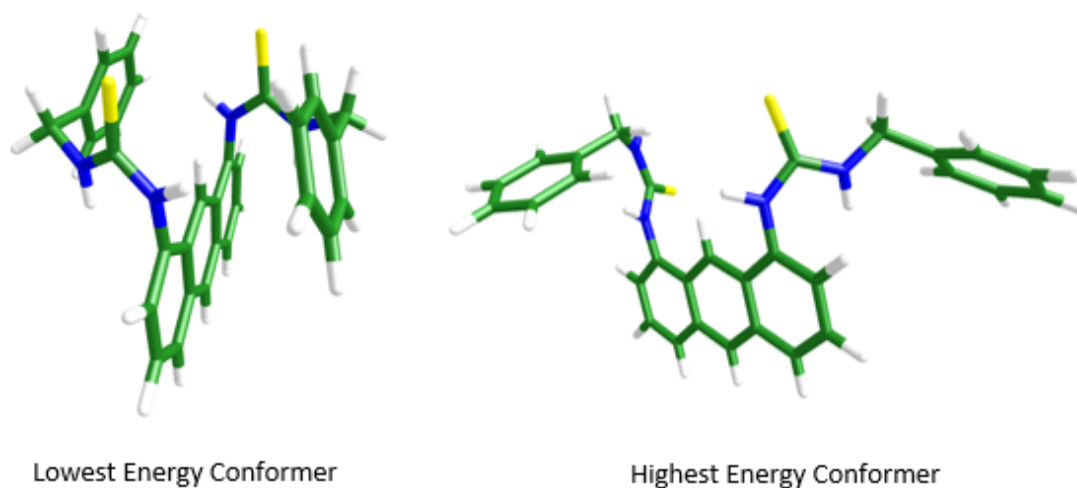
Figure 6.3 - An image showing the lowest energy conformer for Host 1 (16.38 kJ mol^{-1}) and highest energy conformer (36.83 kJ mol^{-1}) generated through conformational searching in Maestro within the selected window of 21 kJ mol^{-1}.

Host 1 was then examined with mephedrone in the putative binding site to establish the effect the addition of the guest molecule would have on the minimum conformation of Host 1 in implicit water. Conformational searching using 2000 steps produced 299 conformers, the minimum structure had an energy of 4.18 kJ mol^{-1}. The same study using caffeine as the guest molecule resulted in 269 unique

structures with a lowest energy conformation of -291.65 kJ mol^{-1}. Host 1 with methamphetamine produced the least number of conformers with 194 over 2000 steps with the lowest energy conformer at 27.30 kJ mol^{-1}. It is worth noting that the energy values calculated during conformational searching are relative, not absolute, and therefore cannot be compared between systems. This is because the number and type of atoms has a large impact on the energy values obtained during molecular mechanics calculations. It is however possible to see the change in energy of the system when mephedrone is added so it gives an impression of whether it is energetically favourable for host-guest complexation to take place. This can be established using Equation 6.1, which takes into account the energy value of the minimum structure of the host (E_H) and guest molecules (E_G) separately as a comparison of the complex (E_C).

$$\Delta E = E_C - (E_H + E_G) \qquad \textbf{Equation 6.1}$$

The change in energy (ΔE) of Host 1 with each of the three guest molecules; mephedrone, methamphetamine and caffeine as well as the bound and unbound energy values are presented in Table 6.3.

Table 6.3 - Energy of bound Host 1 with mephedrone, caffeine and methamphetamine in water. E_H, E_G, E_C are the energy of the host, guest and complex respectively. ΔE is the calculated change in energy upon formation of the complex (kJ mol^{-1}).

Complex	E_H (kJ mol^{-1})	E_G (kJ mol^{-1})	E_C (kJ mol^{-1})	ΔE (kJ mol^{-1})
Host 1 and Mephedrone	4.26	-162.21	-7.86	150.09
Host 1 and Caffeine	-291.65	-21.98	-599.68	-286.05
Host 1 and Methamphetamine	-27.30	-154.47	-70.98	110.79

The largest negative ΔE shows the most favourable binding as it represents the greatest change in energy caused by the binding of a guest molecule. The data presented in Table 6.3 indicates that caffeine has the most favourable binding with Host 1. This is not what was observed experimentally (Chapter 5) as no interaction was seen to occur between caffeine and Host 1. This is where simulated annealing and metadynamics is advantageous, the effect of explicit water to more accurately mimic the electrostatics observed in experimental conditions. It is worth noting that entropic factors are not considered on examination of conformational energy values.

6.3.1.2   Dinapthylthiourea Anthraquinone (Host 2)

Conformational searching of dinaphthylthiourea anthraquinone (Host 2) produced 110 unique conformations. The lowest energy conformation had an energy of 96.16 kJ mol^{-1} and is shown in

Figure 6.4. It appears that the anthraquinone and two naphthyl moieties are π-stacking in order to stabilise the structure to produce the lowest energy conformation. As with Host 1 the highest energy conformation produced in the 21 kJ mol^{-1} energy window is noticeably different from the lowest energy conformation.

Lowest Energy Conformation   Highest Energy Conformation
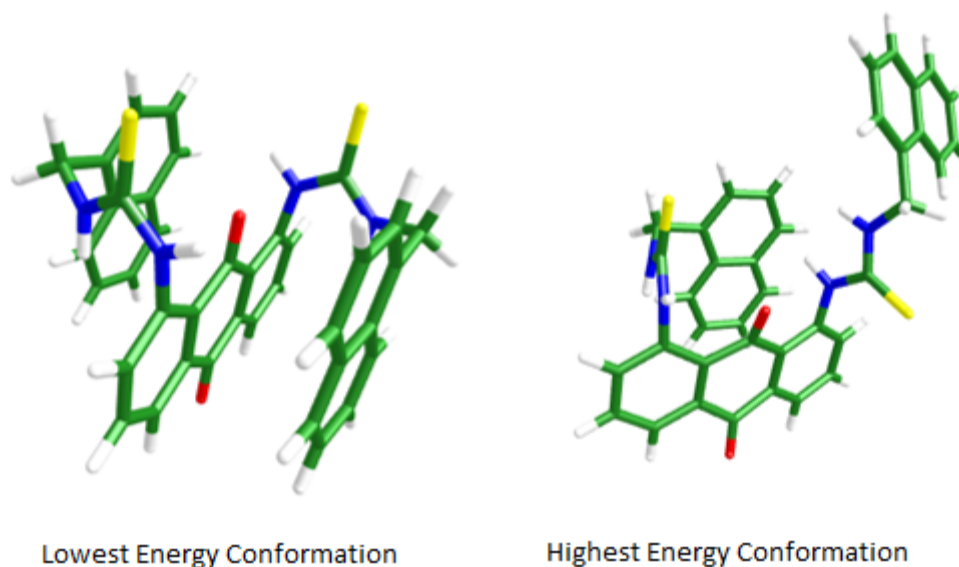
Figure 6.4 - An image showing the lowest energy conformer for Host 2 (96.16 kJ mol^{-1}) and highest energy conformer (117.16 kJ mol^{-1}) generated through conformational searching in Maestro within the selected window of 21 kJ mol^{-1}.

The change of conformation of Host 2 was then explored with the addition of mephedrone, methamphetamine and caffeine. Host 2 and mephedrone produced 49 conformers with the lowest energy of -157.01 kJ mol^{-1}, caffeine and Host 2 produced 31 conformers with a lowest energy of -17.05 kJ mol^{-1} and methamphetamine with Host 2 produced 180 conformers with a minimum energy of -118.65 kJ mol^{-1}. The data presented in Table 6.4 shows the ΔE values calculated in the same way as for Host 1. Once again caffeine appears to have the most favourable interaction with Host 2; however, there is only a small difference between caffeine and mephedrone. Methamphetamine shows the least favourable interaction with Host 2. Host 1 and Host 2 have similar conformations; however, they appear to show a marked difference in selectivity at this stage. This is an interesting outcome that will be explored in more detail during the metadynamic simulations, where the interaction energies in systems with explicit solvent can be compared.

Table 6.4 - Energy of bound Host 2 with mephedrone, caffeine and methamphetamine in water. E$_H$, E$_G$, E$_C$ are the energy of the host, guest and complex respectively. ΔE (kJ mol^{-1}) is the calculated change in energy upon formation of the complex.

Complex Name	E_H (kJ mol^{-1})	E_G (kJ mol^{-1})	E_C (kJ mol^{-1})	ΔE (kJ mol^{-1})
Host 2 and Mephedrone	-157.01	-162.21	-410.19	-90.97
Host 2 and Caffeine	-17.05	-21.98	-130.26	-91.23
Host 2 and Methamphetamine	-118.64	-154.47	-333.45	-60.34

6.3.1.3 Dinaphthylurea Tetrahydroxylcalix(4)arene (Host 3)

Conformational searching of dinaphthylurea tetrahydroxylcalix(4)arene (Host 3) produced 32 unique conformations, in the 21 kJ mol^{-1} energy window. The lowest energy conformation seen in Figure 6.5 has an energy value of -306.80 kJ mol^{-1} and is the most stable conformation found. It can also been seen that the highest energy conformation for Host 3 does not show considerable differences in conformation compared to the lowest energy conformation despite the 19.93 kJ mol^{-1} difference in energy. The presence of the hydroxyl groups on the lower rim are known to form strong hydrogen bonds which stabilised the cone conformation of the ring. Therefore, a large amount of energy is required to disrupt this structure. This is an ideal conformation as it allows for the hydrophobic cavity to form which can be a good binding site for small molecules.

Lowest Energy Conformation   Highest Energy Conformation
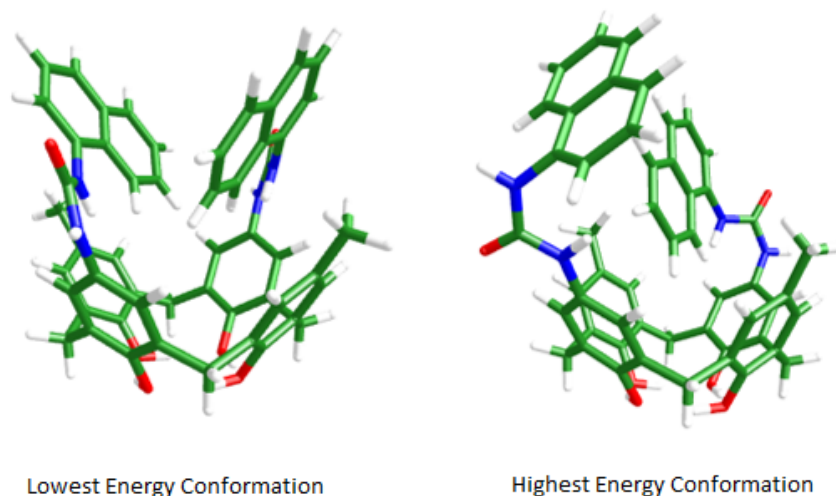
Figure 6.5 - An image showing the lowest energy conformer for Host 3 (-306.80 kJ mol^{-1}) and highest energy conformer (-286.87 kJ mol^{-1}) generated through conformational searching in Maestro within the selected window of 21 kJ mol^{-1}.

Host 3 was studied with mephedrone, methamphetamine and caffeine. Host 3 and mephedrone produced 272 unique conformers with a lowest energy values of -230.75 kJ mol^{-1}, methamphetamine and Host 3 produced 167 conformers with the lowest energy conformer at -374.61 kJ mol^{-1} and caffeine with Host 3 produced 192 conformers with a lowest energy value of -658.49 kJ mol^{-1}. The results of these investigations are shown in Table 6.5. Host 3 appears to have a preferential interaction with caffeine over methamphetamine and mephedrone. In fact, mephedrone appears to be the least

favourable guest molecule with Host 3, as it has the largest positive change in energy compared to the other guest molecules.

Table 6.5 - Energy of bound Host 3 with mephedrone, caffeine and methamphetamine in water. E_H, E_G, E_C are the energy of host, guest, and complex respectively. ΔE is the calculated change in energy upon formation of the complex (kJ mol^{-1}).

Complex	E_H (kJ mol^{-1})	E_G (kJ mol^{-1})	E_C (kJ mol^{-1})	ΔE (kJ mol^{-1})
Host 3 and Mephedrone	-230.75	-162.21	-631.21	238.26
Host 3 and Caffeine	-658.49	-21.98	-1032.16	-351.69
Host 3 and Methamphetamine	-374.61	-154.47	-442.42	86.66

Based on the conformational searching, Host 1 and 2 appear to be the most flexible with the greatest change in conformation seen in the 21 kJ mol^{-1} energy window. While Host 3 shows the least conformational change in the energy window applied. This is expected due to the rigidity of the calixarene backbone, little change in conformation is anticipated as the system is more rigid. Host 1 and 2 are designed to be flexible so as to adjust their conformation upon addition of the guest, and therefore more changes in conformation would be expected over a small energy range. All three of the host molecules examined appear to preferentially bind caffeine over methamphetamine and mephedrone.

6.3.2 Simulated Annealing

In order to further explore the conformational space of each of the host molecules and avoid bias of starting conformation from implicit analysis, a more realistic representation of the conformation of each of the host molecules in explicit solvent was achieved using conformational searching, the next step was to carry out simulated annealing on each of the hosts. The starting conformation used was the lowest energy conformation obtained using the conformational searching carried out. Simulated annealing will provide more evidence that the conformations achieved are the global minima as opposed to the local minima that may have been found using conformational searching. It will also take into account explicit solvation which can have a large effect on conformations of molecules. Once the simulated annealing was carried out, all the conformations from the cooling steps were extracted and a clustering script in Maestro was used to determine the conformation appearing with highest frequency based on the most common cluster.

6.3.2.1   Dibenzylthiourea Anthracene (Host 1)

Host 1 was subjected to two different methods of simulated annealing. The first was the 3.13 ns run with one stage of heating and cooling. From this simulation the resulting conformers were extracted

from the trajectory and subjected to conformer clustering based on their root mean square deviation (RMSD). From the 5 clusters produced cluster 2 contained 133 conformers which was the most commonly populated group. The average conformation found in this cluster is shown in Figure 6.6. Without accurate free energy values to accompany the conformations it cannot be determined for certain that the global minimum conformation has been achieved; however, it is a reasonable assumption that the most prevalent cluster would be the most representative conformation and therefore the local energy minimum[216]. The minimum energy conformation seen for this method is similar to that produced using conformational searching, and good agreement is seen between the implicit and explicit systems.

Figure 6.6 - An image showing the representative conformation of Host 1 in the most common cluster from 3.13 ns simulated annealing in water based on clustering all conformations from the Maestro simulation.

In order to determine whether the 3.13 ns simulation time is sufficient to achieve an accurate prediction of the minimum conformation an extended simulated annealing method of 17.13 ns was used. The representative conformation achieved using the extended simulation time differs markedly from that using the 3.13 ns simulations (conformations presented in Figure 6.6 and 6.7). Due to the increased simulation time used for the second method, the conformation seen in Figure 6.7 is a more realistic representation of the minimum energy conformation. As such this conformation will be taken forward for the metadynamic studies. The disadvantage of the extended method is that it has higher computational cost compared to the 3.13 ns method, increasing the total run time to a week using 16 CPUs, as opposed to 14 hours. This has to be weighed up against the sampling of the conformational space. For less flexible structures that show little variation in conformation space using conformational searching techniques, they do not necessarily warrant the additional computational cost for simulated annealing.

Figure 6.7 - An image showing the representative conformation of Host 1 in the most common cluster from 17.13 ns extended simulated annealing experiment in water based on the clustering carried out on all conformations from the Maestro simulation.

When comparing the representative conformation from the extended simulated annealing study to the conformation searching a noticeable difference is seen based on the calculated maximum RMSD of 7.0 Å. This suggests that explicit water has a large impact on the conformation of Host 1. Given the effect of explicit water on the conformation space and knowing that experimentally Host 1 is insoluble in water, two additional solvents, DMSO and methanol, were investigated in which to carry out simulated annealing. Ideally acetone would be used to most accurately mimic the experimental conditions used in Chapter 5; however, there are currently no acetone solvent box available. For Host 1 in methanol the most common cluster contained 230 conformations. Figure 6.8 shows the representative conformation of Host 1 after a 3.13 ns simulation. It can be seen that it is to some extent similar to the minimum conformation found for Host 1 using the same method in water.
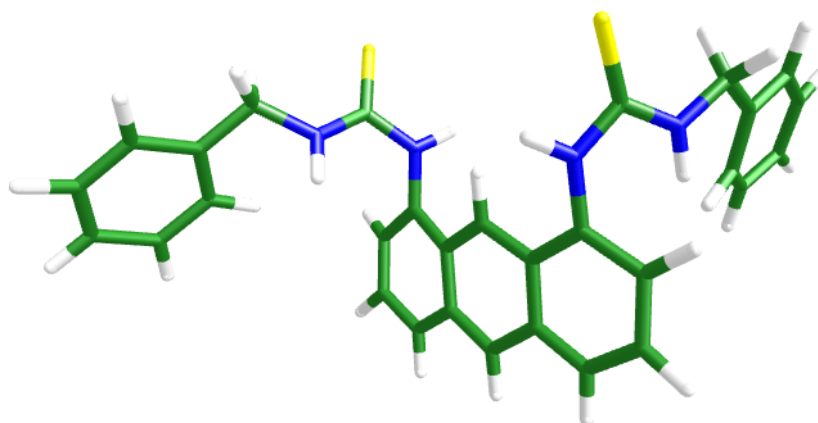
Figure 6.8 - An image showing the representative conformation of Host 1 in the most common cluster from 17.13 ns extended simulated annealing experiment in methanol based on the clustering carried out on all conformations from the Maestro simulation.

Experimentally, Host 1 is only sparingly soluble in methanol; however, is it more soluble in DMSO. It can be seen in Figure 6.9 that the representative conformation achieved for Host 1 in DMSO is distinctly different from that found for water (RMSD = 6.47 Å) and methanol (RMSD = 5.68 Å). This suggests that the type of solvent has an influence on the conformation of Host 1, and that the experimental solubility of the Host is important when carrying out the *in silico* simulations. It is for this reason that metadynamics will be carried out in water, methanol and DMSO to examine the effect explicit solvent has on the binding properties of the hosts.
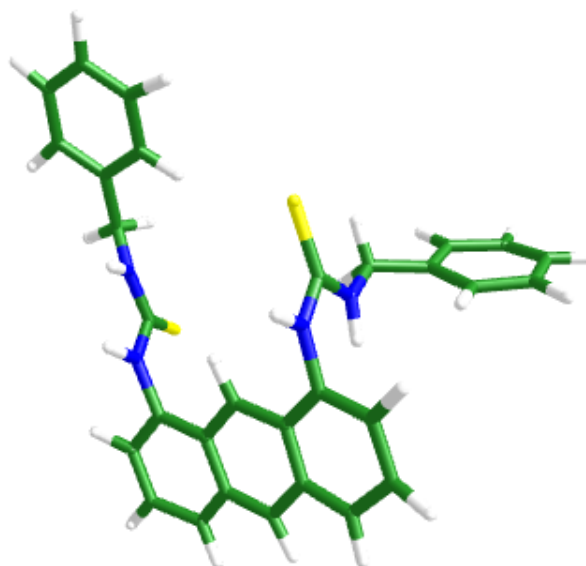
Figure 6.9 - An image showing the representative conformation of Host 1 in the most common cluster from 17.13 ns extended simulated annealing experiment in DMSO based on the clustering carried out on all conformations from the Maestro simulation.

Small molecules have not been extensively studied *in silico* and it cannot be assumed that they are water soluble. Ideally the conformational space in explicit solvent would be further explored with more solvents that Host 1 is known to be soluble in; however, we are limited by the solvent parameters available in the software program.

6.3.2.2   *Dinaphthylthiourea Anthraquinone (Host 2)*

Host 2 was subjected to a 3.13 ns simulated annealing study by heating a system up to 1000 K before cooling. A representative conformation of the most common cluster extracted from the simulation is shown in Figure 6.10. Similarities can be seen with the representative conformation produced using

implicit water in conformational searching. This suggests that both methods are complementary for Host 2. Once again it appears as though the naphthyl moieties are π-stacking with the anthraquinone ring system in order to stabilise the conformation. Given the hydrophobic nature of anthraquinones and aromatic functionalities it is anticipated that in simulated annealing due to the presence of explicit water, Host 2 forms a closed conformation to reduce its interaction with water. This would suggest, as with Host 1, that the use of organic solvents may be more suitable for exploring the conformational space that this molecule can explore.
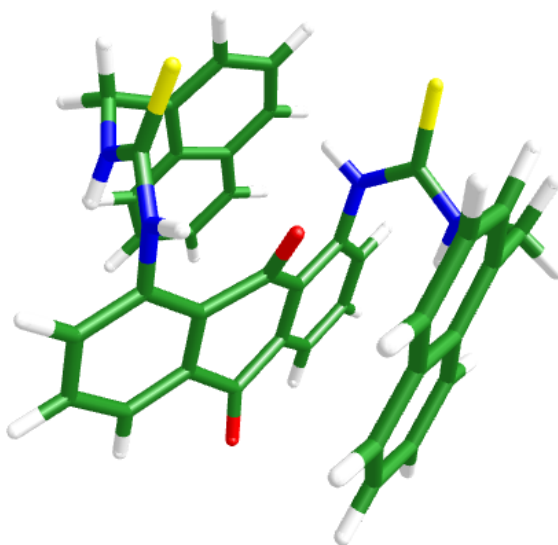
Figure 6.10 - An image showing the representative conformation of Host 2 in the most common cluster from 3.13 ns simulated annealing experiment in water based on the clustering carried out on all conformations from the Maestro simulation.

In order to examine the effect of different solvent systems, as with Host 1, simulated annealing was carried out in DMSO and methanol over 3.13 ns. A representative conformation from the most common cluster of Host 2 in methanol is shown in Figure 6.11. It exhibits distinct differences from the most stable conformation seen in water (RMSD = 6.01 Å). It also shows differences in conformation to that seen for Host 1 in methanol (RMSD = 5.95 Å). The conformation is more open and the naphthyl groups are no longer positioned so as to allow π-stacking to occur with the anthraquinone moiety.
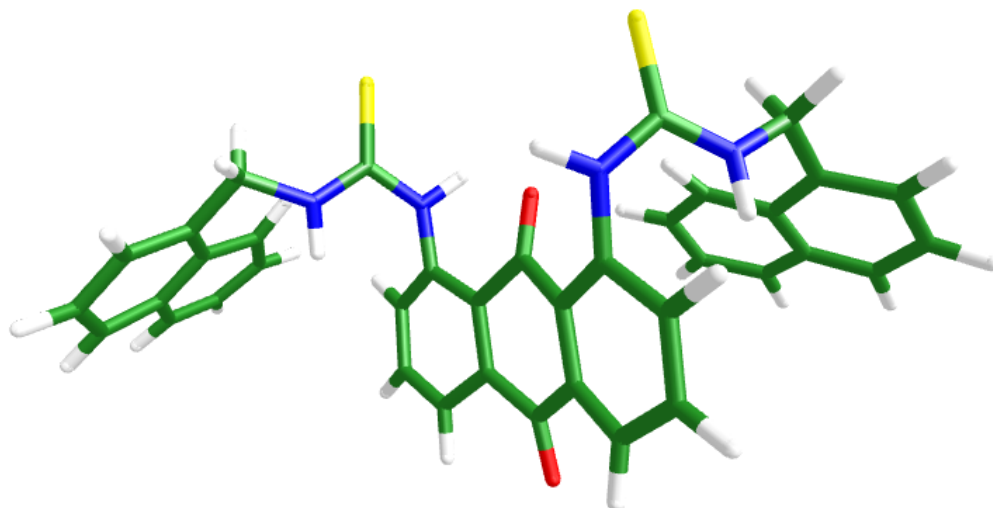
Figure 6.11 - An image showing the representative conformation of Host 2 in the most common cluster from 3.13 ns simulated annealing experiment in methanol based on the clustering carried out on all conformations from the Maestro simulation.

Host 2 was run in DMSO as well, and as seen in Figure 6.12, the most representative conformation based on the most populated cluster once again shows distinct differences from both methanol and water, with the two arms of the host positioning themselves on the same side of the central anthraquinone moiety. As with Host 1 the changes in conformation in different solvent systems highlights the importance of selecting the correct environment. This is especially important when looking at a system with explicit solvent as the solvent directly interacts with the host molecules.
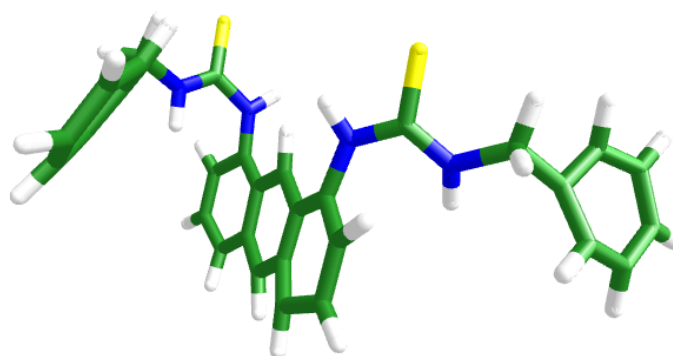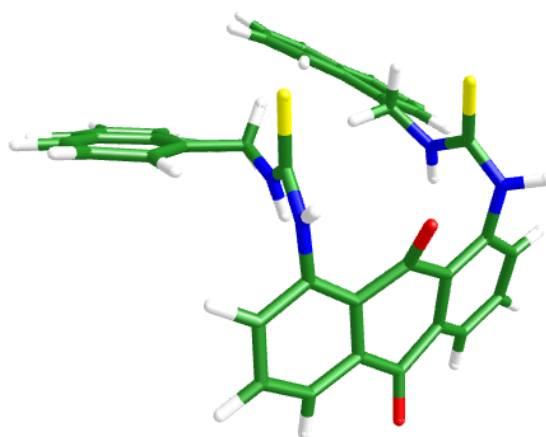
Figure 6.12 - An image showing the representative conformation of Host 2 in the most common cluster from 3.13 ns simulated annealing experiment in DMSO based on the clustering carried out on all conformations from the Maestro simulation.

6.3.2.3 *Dinaphthylurea Tetrahydroxylcalix(4)arene (Host 3)*

Calixarenes are known to be water soluble which is a valuable feature for a sensor[65]. This is one of the reasons for exploring calixarenes as potential host molecules for the detection of mephedrone. This lends itself to *in silico* work which is largely developed for water soluble substances. Of the 400 extracted conformations from the simulated annealing one of the five clusters contained 386 conformations, this cluster is accepted to be the most representative conformational shape in the system. A representative conformation of the most common cluster is shown in Figure 6.13. The conformation seen in simulated annealing is different from the one produced using conformational searching.

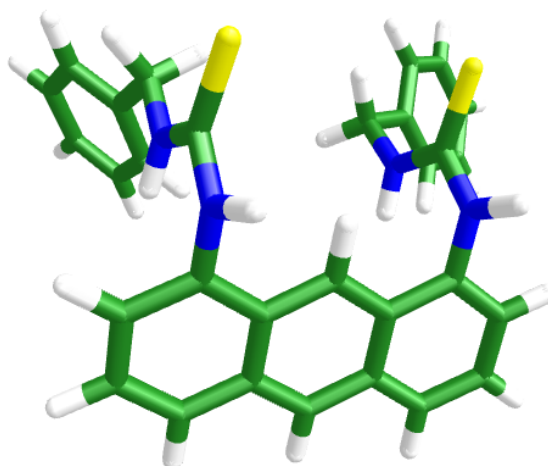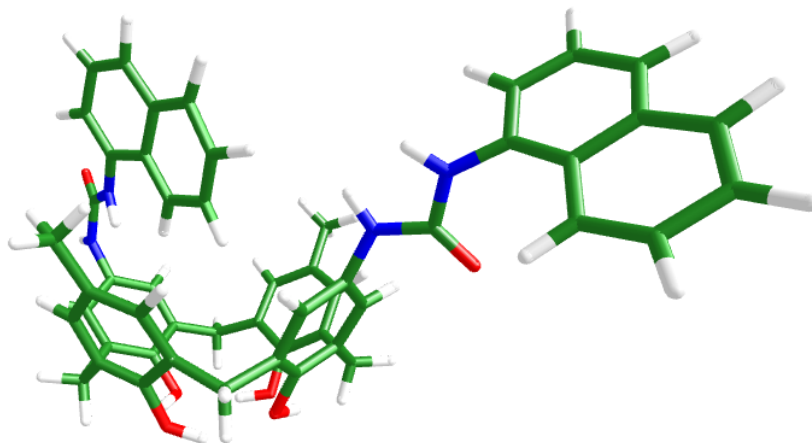**Figure 6.13 - An image showing the representative conformation of Host 3 in the most common cluster from 3.13 ns simulated annealing experiment in water based on the clustering carried out on all conformations from the Maestro simulation.**

The representative conformation seen from simulated annealing shows the hydrophobic cavity more open than that seen for conformational searching. This is more favourable to allow a guest molecule inside the calixarene cavity for binding. The commonality between the conformations from the two different methods is that the calixarene ring has retained the cone conformation. It is favourable as calixarenes are known to adopt a number of conformations, such as the 1, 4 alternate (as discussed in Chapter 4) which is less amenable to host-guest binding of mephedrone.

As calixarenes are known to be water soluble, and are less soluble in organic solvents; therefore, further studies using organic solvents will not be carried out.

As simulated annealing takes into account the effect of explicit solvent on the conformation of the host molecules the metadynamic studies will be carried out using the minimum conformations extracted from the simulated annealing studies.

6.3.3 Metadynamics

The experimental data in Chapter 5 has shown conclusively that Host 1 binds to mephedrone freebase and has shown a high degree of selectivity by not binding to caffeine or methamphetamine, with up to 10 equivalents tested in acetone. The use of metadynamics is intended to emulate experimental results *in silico*. If a suitable model is established, it will then be applied to Hosts 2 and 3 in an attempt to predict experimental binding *in silico*. This approach will hopefully give an indication of whether it is worthwhile synthesising the host molecules which can be carried forward for binding studies.

6.3.3.1 Dibenzylthiourea Anthracene (Host 1)

In order to ensure a quality final approach based on emulating the experimental results collected on Host 1, a number of variables were changed and examined: simulation time, mephedrone charge state, solvent, system size and position of CVs. Charged, uncharged and the inclusion of chloride counter ion were studied to see what effect this would have on binding. In street samples mephedrone would be found as the more stable hydrochloride salt as opposed to the freebase studied in Chapter 5. Experimentally when acetone is used mephedrone freebase is unionised, as mephedrone has a predicted pKa of between 8.4-9.5[45] and acetone has a pKa of 20[217]. In all solvents examined mephedrone is unionised. The results for Host 1 with mephedrone in a number of different experimental conditions is presented in Table 6.6. It is worth noting that both the *R* and *S* enantiomers were tested and both showed the same results.

Table 6.6 - Results of metadynamics method development of Host 1 with mephedrone in water.

Simulation Time (ns)	Charge/ions	Buffer Size (Å)	CV[1]	Minimum Free Energy (kJ mol^{-1})	CV Distance (Å)	Complexation[2]
5	Cl counter ion	30	1	-43.26	26.45	no
5	charged	30	1	-37.87	23.83	no
5	Cl counter ion	20	1 (Cl)	-39.29	22.49	no
5	Cl counter ion	30	1 (Cl)	-40.80	27.85	no
5	charged	20	1	-61.09	17.50	no
2	neutral	30	1	-63.93	6.06	no
5	Cl counter ion	20	1	-65.77	4.35	yes
10	Cl counter ion	20	1	-114.52	15.60	no

[1](Cl) denotes a chloride counter ion is present.

[2]Complexation showing host-guest binding relative to that seen for experimental work at the minimum free energy of the system.

Noticeably only one out of the 8 simulations show mephedrone and Host 1 forming a complex at the minimum free energy of the simulation. It can be observed in Figure 6.14 that the only possible interaction between Host 1 and mephedrone that is occurring at this conformation is the non-specific edge/face π-stacking between the benzyl of the mephedrone and the anthracene in Host 1. It does give the second lowest free energy of all the mephedrone and Host 1 simulations, which shows that it must be favourable but no interaction is seen at the minimum energy of the simulation. This conformation, however, is not what is seen from the experimental work, as Host 1 is not water soluble and therefore, experimental binding data cannot be obtained in water.
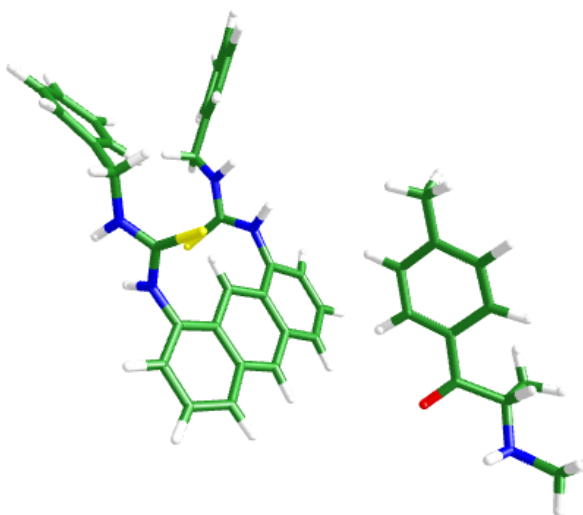
Figure 6.14 - An imagine showing the minimum free energy complex for Host 1 and mephedrone, 20 Å system, 5 ns simulation with chloride counter ion in water (chloride is not observed near the host or guest at minimum energy) from the metadynamics analysis in Maestro.

Under the same experimental conditions, but with an increased simulation time of 10 ns no interaction is seen between Host 1 and mephedrone at the minimum energy for the system. The computational cost of a 10 ns simulation is very high, even with a buffer size of 20 Å. The computational time increases linearly with simulation time; therefore, a 5 ns simulation is a good compromise between computational cost and accuracy of simulations to ensure the full free energy landscape is explored.

The computational running time increases exponentially with an increase in the system size due to the increased number of atoms in the system. Therefore, it is important to consider the system size carefully. If the system is too small it will force the host and guest together, not allowing the evaluation of the free energy of the system when the molecules are apart to be fully explored, which may lead

to false results. If the system is too large then the computational cost will be too high, and therefore not practical. By increasing the system size, it increases the buffer in the system and therefore the simulation needs to account for this increase. The trajectories for the 20 Å buffer system simulations appear to not show the host and guest apart for a lot of the simulation, even at the furthest distance they are still in 12 Å of each other. Ideally to fully explore the free energy landscape there should be more free movement, as would occur in an experimental solvent system. For this reason, a system size of 30 Å buffer has been selected. The trajectories for the 30 Å buffer system simulations show more free movement in the system of both the host and the guest throughout the simulation.

Host 1 was run with mephedrone in a 30 Å buffer system, over 5 ns and the full energy landscape was explored to determine whether a complex was formed at any point during the simulation. At the minimum energy of -37.87 kJ mol^{-1} no complexation was observed; however, a favourable interaction was seen at -35.73 kJ mol^{-1} which is within 6 % of the absolute minimum energy, meaning it is feasible that this conformation could be adopted in solution. The conformation at this energy shown in Figure 6.15, with the hydrogen bond between the carbonyl of the mephedrone and the NH of the thiourea from Host 1; both the angle and distance of which are favourable. There are also two sites of possible π-stacking of the mephedrone benzyl group to the Host. None of the other simulations between Host 1 and mephedrone in a water system showed any favourable complexations in the simulations.
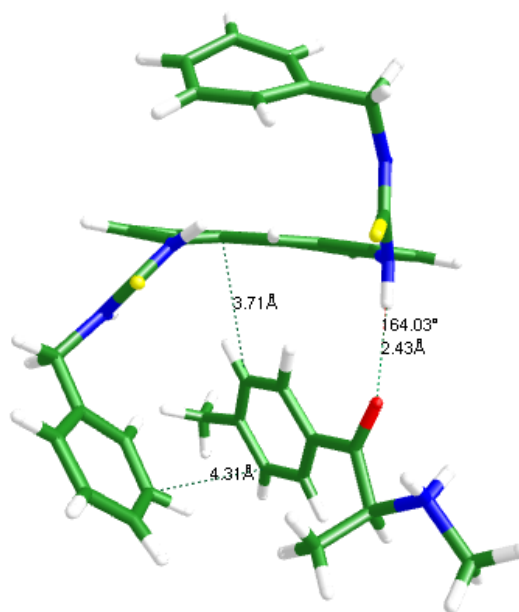
Figure 6.15 - An image showing Host 1 and mephedrone in water in one of conformation seen from the simulation in Maestro (CV= 4.14 Å, E= -35.73 kJ mol^{-1}).

Experimentally chloride has a high binding affinity for Host 1. In order to examine this *in silico* and see whether the same effect can be seen, the chloride anion in the system was selected as a probe for the CV and the interaction been the host and chloride was explored using metadynamics. For a system size of both 20 and 30 Å no complexation at a favourable free energy was observed, this is in contrast to the experimental results. However, there are a number of low energy minima found in the simulation, one of which shows that the chloride does hydrogen bond with Host 1 within the 30 Å buffer system, with an energy of -33.64 kJ mol^{-1} (Figure 6.16).
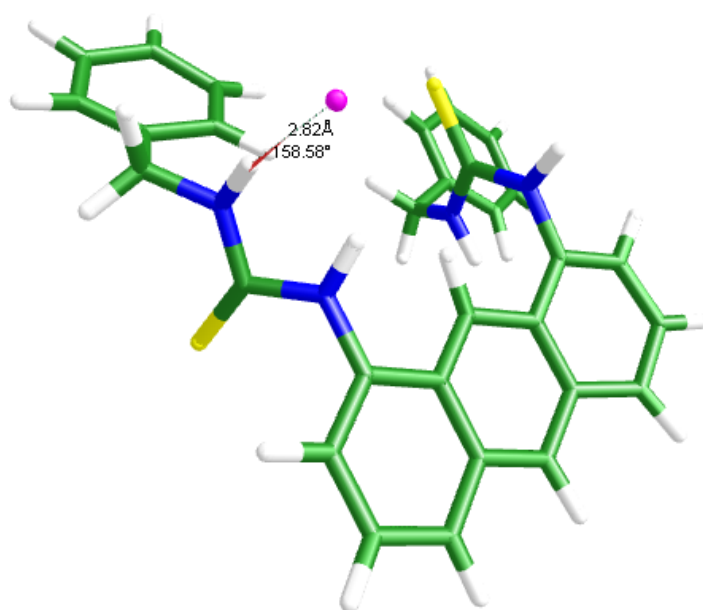
Figure 6.16 - An image showing hydrogen bonding between the chloride counter ion (represented as pink sphere) and Host 1 (CV= 4.48 Å, E= -33.64 kJ mol^{-1}) in the metadynamics simulation in Maestro.

It appears from the metadynamics studies in water that Host 1 prefers to adopt the conformation seen in the conformation searching study, with the benzyl groups π-stacking with the anthracene moiety. This may be due to solvent effects, as Host 1 is known to be insoluble in water, and this conformation appears to allow for the minimum contact with water.

As seen in the simulated annealing studies the choice of solvent has a large effect on the conformations of the molecules, which in turn can affect host-guest binding. For this reason, metadynamic simulations were carried out using DMSO and methanol in a 30 Å system over 5 ns which was established in the metadynamic studies using water.

Different solvents interact with molecules in different ways, for example water and DMSO are known to be competitive binding solvents due to their strong hydrogen bonding properties. This means that in order for mephedrone to bind to the host molecule it would have to displace the solvent that is

binding, which involves overcoming an additional energy barrier. This could be energetically unfavourable if the host-guest binding is not favourable enough.

Host 1 in DMSO showed no favourable interactions between mephedrone and Host 1 throughout the simulations. The lowest energy conformation of -56.23 kJ mol^{-1} occurred at a CV distance of 24.53 Å. Interestingly, DMSO can be seen to hydrogen bond to both Host 1 and mephedrone throughout the simulation.

Polar aprotic solvents such as DMSO have been shown to be good hydrogen bond acceptors[218], this can block potential hydrogen bond donors such as the NH groups in the thiourea moieties on Host 1. It is shown in Figure 6.17 that three sites of hydrogen bonding occur between Host 1 and the DMSO.
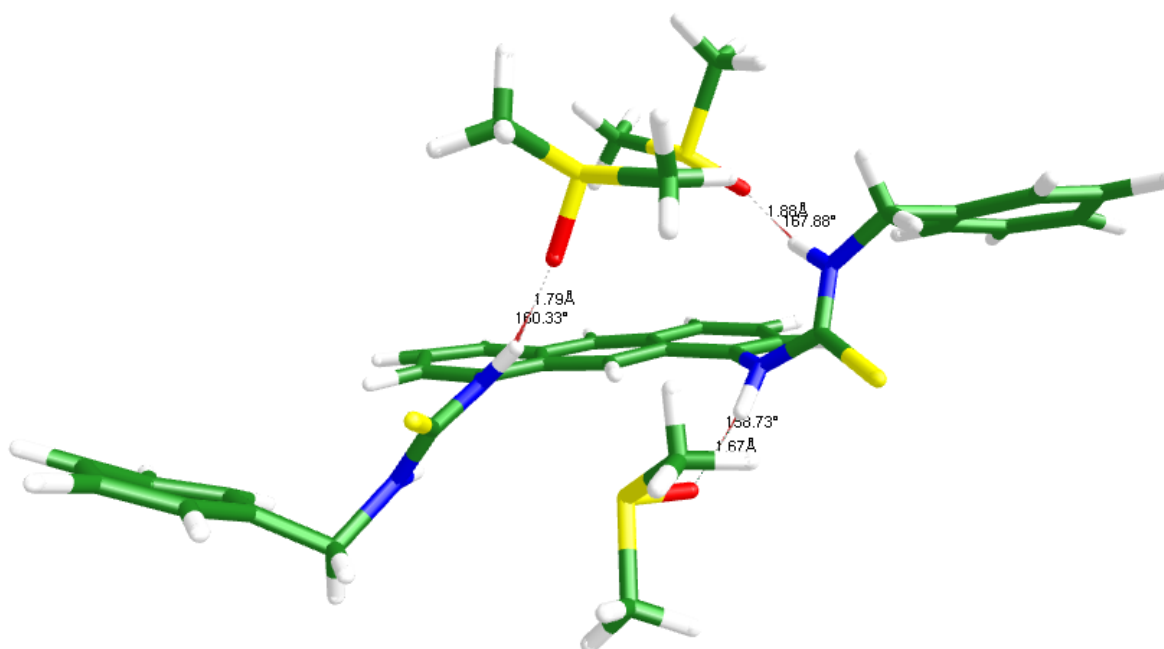
Figure 6.17 - An image showing Host 1 hydrogen bonding with DMSO during the metadynamics simulations in Maestro. Three binding points can be seen between the host and the surrounding solvent.

These are sites that have experimentally been shown to interact with mephedrone, in acetone. The introduction of a competitive binding solvent appears to show that it is more energetically favourable for Host 1 to bind to the solvent as opposed to mephedrone; therefore, preventing complexation being seen *in silico*.
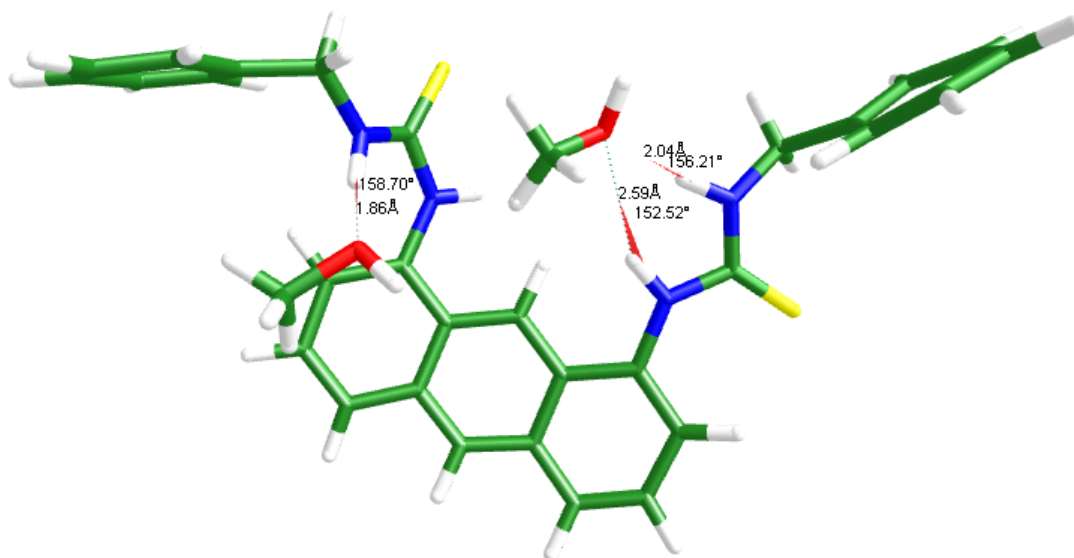
Figure 6.18 - An image showing Host 1 hydrogen bonding with methanol during the metadynamics system in Maestro. Three binding points can be seen between the host and the surrounding solvent.

The same effect is also seen for methanol solvent systems. Methanol is a polar protic solvent that has the ability to act as both hydrogen bond acceptor and donor. It can be seen in Figure 6.18 that in methanol without the presence of mephedrone, Host 1 also hydrogen bonds to the solvent. Interestingly methanol is only seen to act as a hydrogen bond acceptor in this system. Despite this effect Host 1 and mephedrone are seen to interact at the lowest system energy (-39.04 kJ mol^{-1}) at a distance of 5.65 Å (Figure 6.19).
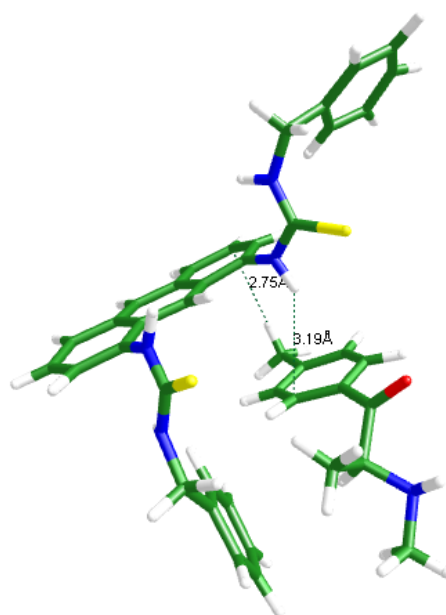
Figure 6.19 - An imagine showing Host 1 and mephedrone in methanol in the lowest energy conformation for the simulation in Maestro (CV= 5.65 Å, E= -39.04 kJ mol^{-1}).

Despite an interaction occurring *in silico* the interactions seen are not in agreement with those seen experimentally, with no hydrogen bonding seen. As seen in Figure 6.19 this NH group in Host 1 does not appear to be hydrogen bonding with methanol, which leaves it open to bind to the mephedrone molecule. This would mean that a lower energy barrier is overcome to displace the solvent from this position and allow for binding to occur.

Interestingly, we see methanol hydrogen bonding with mephedrone whilst bound to Host 1 at the minimum energy conformation of the system (Figure 6.20). The amine functionality in mephedrone in the experimental results is an important binding feature for the host-guest interaction. However, in the presence of a competitive binding solvent this site is blocked by the presence of methanol. This may suggest that the solvent interaction is more favourable then the host-guest interaction at the position; therefore, preventing the same binding seen experimentally, to occur *in silico*.
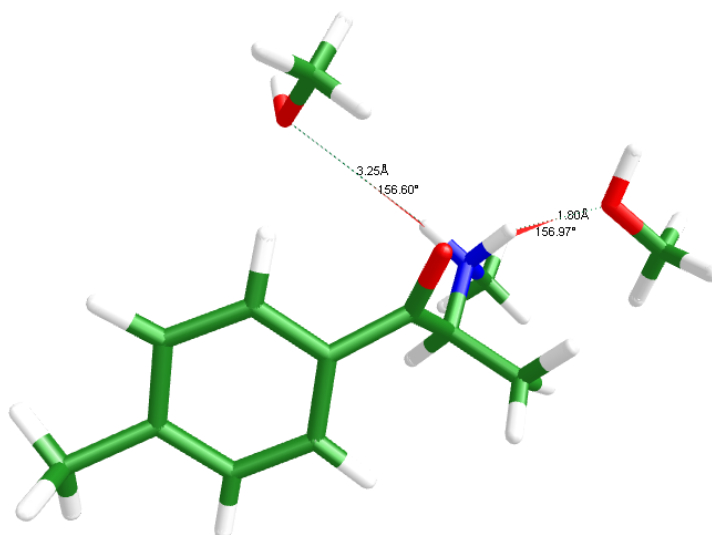
Figure 6.20 - An image showing mephedrone hydrogen bonding with methanol taken from the minimum energy conformation during a metadynamics simulation in Maestro, where mephedrone is bound to Host 1.

It is not possible to quantify the effect solvent has on the binding between the host and guest using metadynamics techniques. However, it does demonstrate that it is an effect that needs to be taken into consideration when choosing a solvent system for small molecule binding, something which has not previously been discussed in this context. This further highlights the need for parameterisation for solvent boxes for solvents such as acetone, which is known to be a non-competitive binder, so as to simulate the experimental conditions.

6.3.3.2   Anthracene selectivity testing

In order to examine selectivity of cutting agents and structurally similar compounds *in silico*, caffeine and methamphetamine were also tested against Host 1 (Table 6.7). This was carried out

experimentally in Chapter 5, and neither were seen to bind to Host 1. *In silico* there was also no binding affinity observed between caffeine and the host at the minimum energy but complexation is seen at an energy of -48.20 kJ mol^{-1} which is only 1.00 kJ mol^{-1} away from the minimum energy, and more favourable then the interaction seen for methamphetamine. At this energy we see π-stacking between the caffeine and the anthracene moiety. Caffeine's ability to π-stack is well known, as seen in Chapter 5, where most of the interactions seen with proteins are non-specific π-stacking interactions. Methamphetamine binds to Host 1 at the minimum free energy for the system (-43.26 kJ mol^{-1}), which is in contrast to what is seen experimentally.

Table 6.7 - Metadynamics results for Host 1 with caffeine and methamphetamine in water.

Ligand	Simulation Time (ns)	Charge/ ions	System Size (Å)	CV	Minimum Free Energy (kJ mol^{-1})	CV Distance (Å)	Complexation[1]
Caffeine	5	No ions	30	1	-49.12	5.84	no
Methamphetamine	5	Charged	30	1	-43.26	5.42	yes

[1] Complexation at minimum free energy

The complexation of methamphetamine with Host 1 (Figure 6.21) shows non-specific binding with face/face π-stacking between the two molecules, but no hydrogen bonding. It does show a lower free energy value, which is more favourable than that seen for mephedrone and Host 1. This suggests that methamphetamine would have a higher binding constant with Host 1 than mephedrone, which is in contrast to the experimental data, where binding is not observed between Host 1 and methamphetamine with up to 10 equivalent additions of the guest.
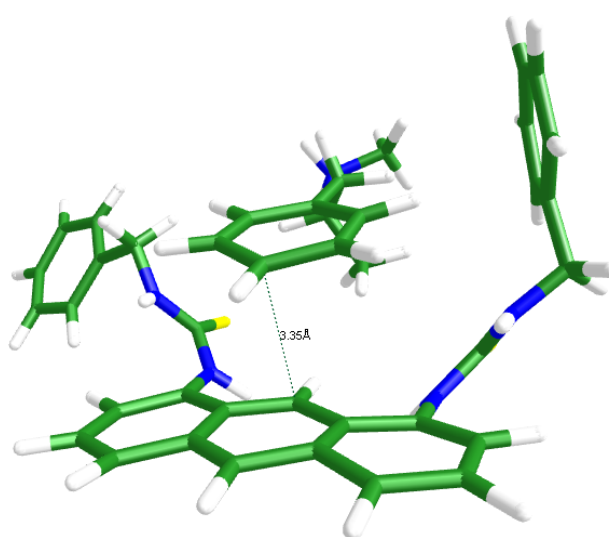
Figure 6.21 - An image showing Host 1 complexed with methamphetamine in water (CV= 5.42 Å, E= -43.26 kJ mol^{-1}) during a metadynamics simulation in Maestro.

As already seen in Chapter 5, choice of solvent has a significant effect on the conformation of a complex, for this reason the metadynamic studies for methamphetamine and caffeine were repeated using DMSO and methanol. In both DMSO and methanol, methamphetamine was not found to form a complex with Host 1 at the minimum energy conformation. However, in methanol with an energy of -33.43 kJ mol^{-1} there is non-specific binding with the methamphetamine π-stacking with the anthracene moiety. Nevertheless experimentally no π-stacking interaction was observed. Methamphetamine and Host 1 in DMSO show consensus to the experimental results, as there is no favourable complexation seen throughout the simulation. This is likely due to both the host and methamphetamine hydrogen bonding to DMSO; therefore, preventing complexation occurring.

Table 6.8 - Metadynamics results for Host 1 with caffeine and methamphetamine in methanol and DMSO.

Ligand	Solvent	Charge/ions	Minimum Free Energy (kJ mol^{-1})	CV Distance (Å)	Complexation[1]
Caffeine	Methanol	No charge	-39.24	8.21	Yes
Caffeine	DMSO	No charge	-45.98	19.87	No
Methamphetamine	Methanol	Charged	-37.17	25.17	No
Methamphetamine	DMSO	Charged	-53.64	21.93	No

[1] Complexation at minimum free energy

Caffeine and Host 1 in methanol showed complexation at the minimum energy. The caffeine molecule positions itself to π-stack with the benzyl units on Host 1. This is not seen experimentally where no interaction is seen with the benzyl groups using NMR analysis (Chapter 5). However, the minimum energy of this system is not as favourable as that seen for using DMSO where Host 1 and caffeine favour being uncomplexed. The caffeine and Host 1 in DMSO shows positive correlation with the experimental results as at no point in the simulation is complexation seen. The lowest energy of the system occurs when caffeine is 19.87 Å away from Host 1.

Table 6.9 - Mephedrone, caffeine and methamphetamine metadynamics results with Host 1. In final method of 5 ns simulation, 30 Å system in varying solvents.

Ligand	Solvent	Complexation at minimum energy	Minimum energy (kJ mol^{-1})	Correlates to experimental?
Mephedrone	Water	No	-63.93	No
Mephedrone	DMSO	No	-56.23	No
Mephedrone	Methanol	Yes	-39.04	No - non-specific binding
Caffeine	Water	No	-49.12	Yes
Caffeine	DMSO	No	-45.98	Yes
Caffeine	Methanol	Yes	-39.25	No
Methamphetamine	Water	Yes	-43.26	No
Methamphetamine	DMSO	No	-53.64	Yes
Methamphetamine	Methanol	No	-37.15	Yes

The data in Table 6.9 shows the final results for the metadynamics simulations for Host 1 with mephedrone, caffeine and methamphetamine. The results shown are for the final approach which was a 5 ns simulation time in a 30 Å system with the three solvents that were examined, water, methanol and DMSO. The association to the experimental data is in relation to not only whether the host and guest bind in the system, at the minimum free energy, but also whether the interaction (in the case of mephedrone, which binds experimentally) is the same as that observed experimentally. Hence, it is expected that hydrogen bonding should be observed between Host 1 and mephedrone rather than just π-stacking interactions, which is not the case.

6.3.3.3 Anthraquinones and Calixarenes

The metadynamic results obtained with Host 1 were used in an attempt to produce a quality model; however, no significant correlation between the experimental and *in silico* results was achieved. Results so far show no substantial evidence to warrant applying the developed method to Host 2 and 3, as any data obtained will not be reliable and it is unlikely that the *in silico* data would positively compare to experimental results. For this reason metadynamic simulations for Host 2 and 3 have not been reported. Once further development has been carried out on establishing parameters for a working solvent model that is in agreement with experimental results, it would then be worthwhile revisiting the above approach with an acetone solvent system. The aim of this chapter was to attempt to mimic the experimental results obtained in Chapter 5 in an *in silico* system, to improve future host molecule design. However, metadynamic simulations are limited by the parameters available in the

software, such as available parametrized solvent systems; therefore, further development was not continued at this stage.

6.4 Conclusion

A novel approach for the use of *in silico* analysis to study host-guest binding of small molecules was explored in order to improve the process of sensor development. The binding data collected from Chapter 5 was used as an experimental comparison. The strength of binding observed experimentally is relatively weak compared to systems that are usually studied *in silico*. This makes it harder to replicate such binding, and this can be considered to be one of the major limitations of applying metadynamics analysis to this work.

Simulated annealing and conformational searching give different minimum conformations for Host 1 and 3. Conformational searching gives absolute energy values which are ideal for direct comparison of conformers but it is carried out with implicit solvent. While simulated annealing is carried out in explicit solvent which is more applicable to metadynamics applications. A consensus between the minimum conformations for Host 2 was found using the two techniques. This would suggest that the minimum energy of Host 1 is not largely affected by thermodynamic effects as increased enthalpy has less effect on conformation compared to Host 1 and 3. Both energy and explicit solvent need to be taken into account when determining the minimum conformation for starting structures for metadynamic studies. Simulated annealing highlighted the difference in conformations using the three chosen solvents; water, methanol and DMSO. For each of the three host molecules different representative conformations were found in each of the solvent systems. Therefore, it was important to study the effect different solvent systems have when used in the metadynamic studies, to try and develop a quality model. The importance of solvent choice in binding studies was seen experimentally in Chapter 5, with no complexation seen for Host 1 and mephedrone in DMSO. This was reiterated with methanol and DMSO hydrogen bonding to the host and guest molecules *in silico*, i.e. acting as competitive binding solvent and thus, preventing complexation. This was further seen in metadynamics where Host 1 shows no consensus with the experimental data for mephedrone binding in any of the solvent systems; water, DMSO and methanol.

In water, caffeine and Host 1 do not show any interactions. This agrees with what is observed experimentally. However, methamphetamine, does show binding at the minimum energy with Host 1. Therefore, in water we do not see a full consensus with the experimental results for mephedrone, caffeine and methamphetamine. This could not be tested experimentally, as Host 1 is not soluble in water. To ensure a complete comparison between the *in silico* binding and experimental work the same parameters would have to be applied to both, i.e. the same solvent system used for both studies.

As previously discussed, due to the lack of parametrization for an acetone solvent box *in silico*, and the lack of solubility in methanol experimentally, there was no solvent system available that could be applied to both techniques. It would be interesting to study complexation in acetone if a solvent box were to be developed. DMSO does appears to be the most favourable solvent for the metadynamic simulations, as mephedrone, caffeine and methamphetamine do not show complexation at the minimum energy which is what is seen experimentally. Ideally comparison between experimental and *in silico* data would be carried out when complexation has occurred, to study the conformation of the complex as opposed to just showing a correlation in the lack of complexation.

Therefore, it can be concluded that out of the three solvents applied; methanol, DMSO and water, none of them show complete consensus with complexation seen in the experimental results (Chapter 5). Consequently, given the lack of a quality model based on the Host 1 experimental results it seemed futile to apply the model to Hosts 2 and 3, until a suitable force field and parameters are built that can allow for simulations to be explored in acetone. Until the solvent used experimentally can be replicated *in silico* as a implemented solvent box it is not possible to determine whether metadynamics is an appropriate technique for small molecule binding analysis. An important finding that became evident from this work is the importance of solvent choice, as metadynamics showed what is already known experimentally, that DMSO is a competitive binding solvent and can hinder binding *in silico* in the same way observed experimentally.

Chapter 7 General Discussion and Future Work

7.1 General Discussion

The primary aim of this project was to design, synthesise and test host molecules for the detection of amphetamine-related new psychoactive substances (NPS). The two classes of NPS chosen were the cathinones, because of their continuing prevalence in society even after they were controlled in 2010, and the uncontrolled aminoindanes which were predicted at the commencement of this project to be the new popular amphetamine-like NPS. With 226 amphetamine-like substances currently available in Europe, current methods available for the detection of NPS lack selectivity for use with an ever expanding number of NPS. The lack of selectivity from current detection mechanism is largely caused by their mechanism of detection relying on just one functional group in a molecule for a positive result. Therefore, in an attempt to improve selectivity a novel approach was applied to the design of the host molecules that incorporates the entire structure of the molecule using host/guest design. Selectivity is one of the leading problems facing NPS analysis, as there are so many amphetamine-like NPS available that are structurally similar, as well as the numerous cutting agents used in formulations, whose presence can lead to false positives.

The first stage of designing a host molecule was to gain first-hand knowledge of the constituents in internet samples of the NPS selected, cathinones and aminoindanes. Cathinones have been controlled since the start of this study, and subsequently it was not possible to purchase them for analysis purposes. On the other hand, aminoindane internet products were uncontrolled and thus purchased and analysed. The analysis of the aminoindane products led to a number of valuable findings for development of a sensory molecule. The most important being a deeper understanding of the complexity of NPS products. The concentration range of active ingredients was found to vary from between 17 and 95 %. The most common cutting agent was found to be caffeine, which was taken into consideration in relation to the selectivity of a host molecule. Only between 31 and 99 % of the composition of the internet products were identified. The inability to determine the remaining proportion of the samples using HPLC and GC-MS indicates that there is a high proportion of inorganic material. These inorganic cutting agents can not only mask the active ingredients, making detection of the active ingredient more challenging, but they also dilute the active ingredient leading to a need for more sensitive detection mechanisms. The selectivity of host-guest systems means that the sensor probe should have no affinity for the additional constituents in the products, and will detect the target guest in the complex matrix.

It is imperative that the device is selective over not only the large variety of cutting agents, but also against other common drugs of abuse, as it cannot be assumed that the only active ingredient is the one specified on the label. Equally it highlights the complexity of developing a simple ligand based sensory molecule for mephedrone, given the structural similarities of amphetamine-like derivatives, as well as the numerous cutting agents that may be present, such as caffeine and lidocaine. In Chapter 2 is was found that active ingredients not listed on the packaging are commonly present in samples. There are also reports of structurally related cutting agents like benzocaine and paracetamol that have been found in mephedrone samples, which have also been known to cause false positives in current detection mechanisms.

At the commencement of this project aminoindanes were believed to become the next big wave in NPS, following the control of the cathinone class. For this reason, the project started out being aimed at producing two sensory molecules for amphetamine-like NPS; one for the controlled cathinones and another for uncontrolled aminoindanes. However, as discussed previously the popularity of aminoindanes did not rise to the levels predicted in 2011. This in part is thought to be due to their reduced potency compared to other amphetamine-like compounds. For this reason, it was decided to focus exclusively on the cathinone class, whose popularity has not dramatically changed over the course of this project. Since the introduction of cathinones onto the drug market, mephedrone has consistently remained the most prevalent, and yet there still remains a lack of selective in-field sensory mechanisms. It is for this reason that mephedrone was chosen as the primary target for the design of a sensory molecule.

In order to develop a selective sensory molecule for mephedrone, biomimetic design was applied. Biomimetic design works on the principle that the most selective interactions that occur are in nature. It is an approach that aims at isolating the features that makes systems in nature selective and imitating them synthetically. In this project it was applied to mimicking the selectivity of protein-ligand interactions in a small host molecule. To achieve this, the second stage of this project was to use protein-ligand binding to achieve a greater understanding of how structurally similar compounds interact with proteins, and therefore try and mimic this selectivity in a small molecule. This technique is commonly used for drug design, but has not yet been reversed and used for the design of host molecules. Mephedrone was chosen as the target guest molecule upon which a host molecule would be designed.

Protein-ligand interactions are incredibly selective, and are known to have very high sensitivity. However, these advantages can often be associated with their size and the quantity of intermolecular interactions between the protein and target molecule. It is not possible to mimic the strength of the

van der Waals interactions seen in proteins with a small molecule host. Therefore, it was important to deduce the essential intermolecular interactions that occur between the protein and ligand that can be mimicked on a small scale, i.e. hydrogen bonding and π-stacking. A complete data set of the interactions between proteins, cutting agents of interest (highlighted from the aminoindane analysis as well as a comprehensive literature search).

One limitation of the pharmacophore development was the lack of experimental protein binding information for mephedrone, or any cathinone derivative in the Protein DataBank. Currently there is no experimental data for any cathinone binding to proteins. This is likely due to the types of proteins they interact with, transmembrane proteins. There is very little structural information on these proteins as they are hydrophobic, and therefore it is not easy to crystallise them out in their natural state. However, there was still information relating to the cutting agents identified, endogenous psychoactive substances and amphetamine derivatives. A database was developed based on these compounds, considering a number of criteria for validation; B factors, occupancy, resolution, mutations, solvation and the quality of the interactions extracted. Validation of the extracted data ensured that all binding information included in the final pharmacophore design was robust and could be mimicked in a small molecule (Figure 3.2).

A flow chart was developed for treatment of the data, to ensure the integrity of the results extracted (Figure 3.2). This methodology of protein-ligand interactions to develop a small molecule probe could potentially be utilised for any target molecule, assuming protein-binding information is readily available. This is the first time such methodology has been developed, and could have useful applications for future host molecule development. Given the lack of binding information for the target drug, mephedrone, the final pharmacophore design was based on amphetamine-like structures, as well as cutting agents that the host molecule needs to be selective against. Individual pharmacophores for dopamine, MDMA, methamphetamine and paracetamol were developed. From these, a consensus pharmacophore was developed based on the interactions most likely to mimic mephedrone binding. These were found to be a hydrogen bond acceptor and two π-stacking interactions (Figure 3.11).

From the analysis of the aminoindanes and reviewed literature it has already been deduced that selectivity over caffeine is very important (Chapter 2). The binding information from the PDB for caffeine with a number of proteins, shows that it could be considered to be a promiscuous binder. Caffeine is a hydrophilic molecule, with strong π-stacking capabilities due its polarised π system. These electrostatic effects lead to caffeine π-stacking with numerous proteins, with no correlation to the types of amino acids and the spacial orientation of the interactions. It was found however that caffeine

primarily π-stacks in an edge/face orientation, whereas amphetamine-like structures were found to bind in a face/face orientation. It is the promiscuous nature of caffeine that presents a problem when just considering the geometrical orientation of the three pharmacophoric features. This is significant for the future design of any amphetamine-like sensors, as caffeine has been found to be a common cutting agent in a number of amphetamine-like products. Caffeine is larger than mephedrone and structurally different; therefore, another characteristic that was considered for host molecule design was the steric size of the binding cavity. By studying how amphetamine derivatives and cutting agents bind to proteins, it was possible to gain an understanding of how the host molecule should not bind, and what types of orientations were likely to prevent binding to molecules other than mephedrone.

It was concluded that designing a supramolecular flexible probe molecule that re-organises itself around mephedrone, would be the ideal solution. It is this implementation of supramolecular chemistry in a concerted design that includes all the pharmacophore features identified that would appear to be the key to the selectivity of the host molecule.

From the pharmacophore model, the synthesis of two proposed host molecules were studied, macrocyclic calixarenes and acyclic anthraquinones. Both designs incorporated functional groups capable of hydrogen bonding and π-stacking. Synthesis of the anthraquinone analogue proved unsuccessful, due to the strength of the intramolecular hydrogen bonding preventing the synthesis progressing. Therefore, the anthraquinone was reduced down to the anthracene to make the final probe molecule, 1,8-dibenzylthiourea anthracene (Figure 7.1) in 80 % yields. Probe 1 encompasses all the features noted from the pharmacophore; benzene and anthracene for the two π-stacking features and thiourea groups as hydrogen bond donors/acceptors.
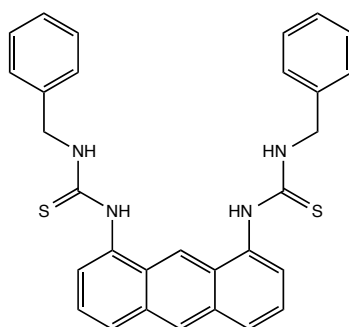
Figure 7.1 - Chemical structure for Probe 1, 1,8-dibenzylthiourea anthracene.

A limitation to the pharmacophore work, was the lack of binding data for mephedrone, this means that the carbonyl in the cathinone analogue was not considered in the model. Given that the carbonyl group is what makes cathinones distinctive compared to other amphetamine-like compounds, this still needed to be considered in the probe molecule design, to improve selectivity. To include the

carbonyl in the host molecule binding motif, a hydrogen bond donor was included in the design. To prevent altering the geometrical design of the pharmacophore, upon which the host molecule was designed, the thiourea groups incorporated were selected so they could act as both donors and acceptors. The sulphur not only improves the hydrogen bond donor capabilities of the amines for binding to the carbonyl, due to its electronegativity, but can also acts as a hydrogen bond acceptor itself for the amino group[219].

As previously discussed, mephedrone is usually found as a hydrochloride salt. The freebase is known to be an unstable oil and is not preferential as a street drug. Consequently, it was essential to test chloride ions with the probe molecule before anything else, to ensure selectivity. Chloride ions were found to have a strong affinity with Probe 1, showing a 1:1 binding stoichiometry. In order to fully test mephedrone binding independently of chloride ions, binding studies were conducted without the presence of chloride, i.e. the freebase form of the drug was used. Stability studies showed that mephedrone freebase is stable for up to 18 hours. Having to extract the freebase of mephedrone before analysis works in a laboratory based environment; however, it is not ideal for in-field applications.

From the ^{1}H-NMR it was found that mephedrone binds to Probe 1 with equilibrium achieved at 4 molar equivalents of mephedrone to Probe 1. When adding mephedrone, the two NH peaks from the thiourea groups were significantly shifted down-field. These shifts were concluded to be due to binding of both the carbonyl and the amine functionalities in mephedrone to Probe 1. Interestingly, the amine in mephedrone acts as a hydrogen bond acceptor, not a donor as predicted in the pharmacophore model.

The pharmacophore identified two π-stacking interactions between the host and mephedrone. One of these is seen between the C(9)H and the C(10)H on the anthracene, and the tolyl methyl moiety in mephedrone. A strong π-stacking interaction with anthracene would be predicted to induce a strong optical response in both UV/Vis and fluorescence spectroscopy. However, this is not seen, with high concentrations of mephedrone needed to induce a noticeable response. It could therefore be deduced that this is not a particularly strong interaction. The relatively weak binding constant of 104 M^{-1} calculated for Probe 1-mephedrone complexation may be a reflection of this[198].

The two methyl groups in mephedrone do show a change in chemical shift upon binding; however, there is no corresponding shift change for the benzyl groups in the host molecule. The benzyl groups were positioned based on the pharmacophore design to interact with mephedrone. Instead the shift in the methyl group was concluded to be due to the methine and two methyl groups being in close proximity to the β-carbonyl and amine functionalities, which undergo hydrogen bonding with Probe

1, as opposed to π-stacking. Therefore, only one π-stacking interaction is seen between Probe 1 and mephedrone, contrary to the two predicted in the pharmacophore model.

Systematic analysis of flephedrone, methamphetamine and mephedrone precursor using NMR provided more rational as to how mephedrone and Probe 1 were binding, through analysis of the chemical shifts. The hydrogen bonding of the amine and carbonyl functionalities of mephedrone were concluded to be the two main binding interactions with Probe 1. By removing the amine functionality (mephedrone precursor) binding still occurred through the carbonyl; however, the association constant was tenfold lower. Removal of the carbonyl functionality (methamphetamine) saw no binding interaction up to 8 molar equivalents. This indicates that hydrogen bonding between the carbonyl and the amine of the thiourea is the primary interaction. The carbonyl was predicted to be the key to the selectivity of the host molecule over other amphetamine-like compounds. This was found to be true, with Probe 1 exerting selectivity over methamphetamine, despite it containing the other binding points found in mephedrone; the amine and aromatic groups. Based on systematic analysis the selectivity of Probe 1 is concluded to be for the β-keto arrangement, unique to the cathinone class. This selectivity of a potential in-field detection mechanism for mephedrone over methamphetamine is what makes Probe 1 unique to other mechanisms currently in literature. The concerted design of Probe 1, as designed based on protein-ligand interactions would appear to be key to this selectivity. This becomes even more apparent when studying the interactions between Probe 1 and flephedrone. As discussed in Chapter 5, flephedrone differs to mephedrone by the addition of a fluorine in place of a methyl functionality on the *para* position of the aromatic ring. This change in electronegativity on the aromatic ring had very noticeable effects on the binding to Probe 1. ^{1}H-NMR binding studies showed that flephedrone had a reduced affinity to Probe 1 in comparison to mephedrone, although the same atoms were involved in binding. This would suggest that complexation occurs in the same way as mephedrone. In order to rationalise the binding of Probe 1 further, molecular modelling calculations were performed.

The minimum energy conformations were generated for both mephedrone and Probe 1. The maximum RMSD for the change in conformation between the bound and unbound Probe 1 was calculated as 36.29 Å, which shows that Probe 1 is reorganising itself upon the addition of mephedrone. The optimised structure shows mephedrone bound in the cleft of Probe 1 *via* an array of hydrogen bonding interactions and a π-π interaction (Figure 5.8). The proposed geometry based on the NMR studies of the Probe 1–mephedrone interaction is supported by the DFT calculations.

Molecular modelling calculations conducted on Probe 1 and flephedrone suggested that flephedrone does not bind in the same orientation as mephedrone, but does interacts with the same atoms in

Probe 1, as seen in from NMR (Figure 5.18). An interaction energy of -32.97 kJ mol^{-1} was calculated, which is more favourable then that seen for mephedrone. However, this is not reflected in the NMR binding studies which showed preferential binding for mephedrone. It appears that the electronegativity of fluorine reduces the hydrogen bonding capabilities of the carbonyl and amine in flephedrone, thereby, reducing the affinity to Probe 1. The effect fluorine has on the electrostatics of the aromatic ring, to which it is directly attached, appears to increase its affinity to the electron rich anthracene, thus causing the change in conformation compared to mephedrone. This draws attention to the consensus design of Probe 1, where binding is effected by even a small change in the chemical structure of the guest molecule. This consensus approach for host molecule design has never before been shown for detection of NPS. It was predicted that this increased binding with the anthracene unit could increase the optical response of flephedrone upon binding. As with mephedrone, no binding is seen in UV/Vis even at high concentrations. At low concentrations there is also no noticeable fluorescence response, again the same seen for mephedrone. However, at high concentrations flephedone does show an increased optical change upon binding compared to mephedrone. This difference, despite it only occurring at high concentrations, is an important binding effect that needs to be taken into consideration if further development into using Probe 1 as an optical sensor is to be carried out.

Binding studies carried out using ESI-MS suggest a stronger interaction than calculated using NMR. ESI-MS indicates that the strength of the interaction is very favourable, as it remains complexed through harsh ionisation conditions. This could be due to the large deformation energy predicted through DFT calculations, suggesting that once the complex is formed it is more favourable to stay complexed then to overcome the energy to rearrange. The MS analysis also indicates that the complexation is reversible, as changing the instrument conditions alters the ratio of bound and unbound observed in the spectrum. This is also supported by MS/MS experiments, whereby the Probe 1-mephedrone complex fragments into the free-drug and Probe 1 upon dissociation to form two distinct signals at *m/z* 179 and 507 respectively. Interestingly, when mephedrone hydrochloride is studied using ESI-MS, mephedrone still binds to Probe 1, in the same proportions as seen for the freebase. It was not possible to distinguish between the binding of mephedrone and chloride by NMR, as the same atoms are effected when both guest molecules bind. However, the MS studies suggest that despite chloride having a stronger binding constant with Probe 1 according to NMR, mephedrone appears to still bind preferentially, at least in the conditions used in ESI-MS. This is a phenomenon that could be further explored to understand whether there is a way of utilising this in-field, to prevent the free base of mephedrone needing to be extracted before analysis.

The importance of selectivity for any potential host molecule has been discussed in detail. Mephedrone products are not pure, they can be cut with a number of other substances. Selectivity over these cutting agents appears to be the primary limitation of current in-field mechanisms[133]. From literature searches and the aminoindane product analysis, a number of cutting agents and psychoactive substances were identified, to which the probe molecule must ideally be selective against. The most crucial were identified as: caffeine, benzocaine, lidocaine, paracetamol and methamphetamine. For this reason, Probe 1 was tested against all of these compounds using ^{1}H-NMR binding studies. It was concluded from this work that Probe 1 displays selectivity over all of these compounds up to the 10 molar equivalents tested. Probe 1 was also tested against a simulated street samples containing equal proportions of mephedrone hydrochloride, benzocaine and caffeine; the two most common cutting agents identified from literature. It was found that mephedrone could still be detected when studied in a simulated street sample. This is very promising, as previous sensory approaches for mephedrone have lacked selectivity against one or more of these cutting agents. The selectivity over methamphetamine is particularly encouraging, as the chemical structure only differs from mephedrone by the removal of the carbonyl and tolyl functionalities. This, to the best of the author's knowledge, has never been achieved for a small molecule detection mechanism before. Interestingly, when Probe 1 is bound to mephedrone the sigmoidal behaviour seen in the binding isotherm (Figure 7.2) suggests that cooperativity is occurring. With the three non-covalent interactions occur in a cooperative manner. The DFT calculations also suggests that the rearrangement of Probe 1 to incorporate mephedrone requires all three binding points to overcome the predicted deformation energy of 1824 kJ mol^{-1}. This cooperativity can be attributed to the consensus design of Probe 1 and appears to be the reason behind the selectivity of the host molecule. Neutral molecule detection can be difficult with flexible probes as there is often a high degree of flexibility whereby a multitude of non-covalent interactions are required to work in a concerted fashion to overcome any entropic considerations; however, this appears to be the key to the selectivity of Probe 1.
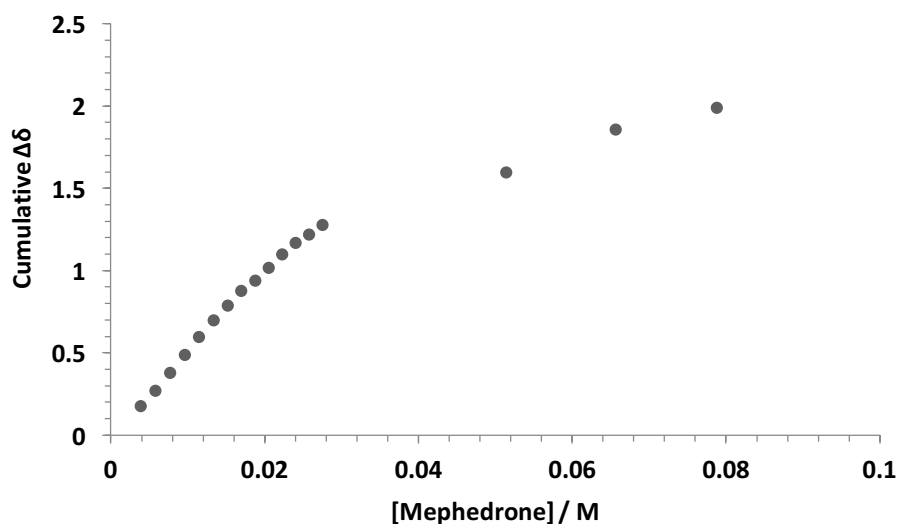
Figure 7.2 - NMR binding isotherm for mephedrone with Probe 1.

This substantiates the importance of understanding protein-ligand interactions, meaning selectivity of proteins is achieved through an array of interactions specifically designed to occur concurrently with the target molecule. Without all of these binding features, in a predetermined geometrical arrangement, re-organisation of the probe molecule does not occur, and therefore no complexation is seen.

Currently the design and development of effective host molecules is very time consuming. One of the aims of this project, was to develop new methodology from which this process could be improved. Pharmacophore design based on protein-ligand interactions has shown promise as one way in which this could be achieved. Another possible method that was considered in this work was the use of molecular dynamics analysis, specifically metadynamics. This is a novel approach that has never been applied to small molecule binding before. The idea behind this was to develop a new approach that could predict small molecule binding affinity *in silico.* If successful this could greatly improve the development of host molecules, and decrease the amount of time and money spent on laboratory based development.

To try and develop a protocol that could achieve this, a number of factors were studied such as conformational space, consideration of explicit and implicit solvation and parametrisation of the system. Given that this approach has never been applied to small molecule systems, the analysis was validated with the experimental work carried out in Chapter 5. The aim was to then apply this approach to the host molecules that were not successfully synthesised in Chapter 4 and gain information into whether they could be predicted to bind to mephedrone selectively.

Probe 1 was studied with three of the same guest molecules that were studied experimentally: mephedrone, caffeine and methamphetamine. Mephedrone was studied as both the hydrochloride salt and the freebase. After varying a number of parameters in the system including; buffer size, simulation time, starting conformation, collective variable and solvent, no correlation was found with the experimental results. The analysis of mephedrone and Probe 1 in DMSO did show a correlation with the experimental with no complexation seen. However, no complexation was seen in water or methanol either so it is hard to deduce whether these results are a limitation of the system, or indicative of experimental results, as no experimental results could be collected in methanol or water. Ideally acetone would be used as the solvent for simulation; however, *in silico* modelling is limited by the resources available from the software package used and there is currently no solvent box developed for the use of acetone *in silico*. Unsuccessful correlation between the experimental and *in silico* binding data was concluded to be due to three reasons. The first, and probably the most significant being the weak binding constant found for this system experimentally. *In silico* binding studies are usually applied to large molecules with much high association constants, making It easier to observe the binding occurring. The second limitation was the inability to study the host molecules in acetone (the solvent used experimentally). The NMR binding study performed in DMSO shows the importance of solvent choice, with no complexation observed. The other reason could be due to the choice of force field applied to the system. At the time of this work, there was no force field available that fully incorporated the electronic properties and torsional space of small molecules. The force field used was OPLS_2005, which at the time of the project was the most appropriate choice. However, its average coverage for prediction of torsional space per bond is 25 %. This is not as much of a problem when looking at macromolecules such as proteins, as the error is averaged out over a much larger number of atoms; however, for small molecules this error is exaggerated and could be the cause of the poor emulation of experimental results. OPLS_2005 also assumes that charges on atoms are fixed, which is not often true when studying intermolecular interactions. Therefore, it is possible given that intermolecular interactions are driven by the electronic considerations between the host and guest molecule, that poor emulation of small molecules could prevent accurate prediction of binding information from being collected.

7.2 **Future work**

7.2.1 **Host Molecule Improvements**

Currently Probe 1 is a good working model for a potential in-field detection mechanism, as it shows a clear selectivity for the β-keto arrangement of the cathinone class. However, there are still a number of limitations that need to be considered. Currently the mechanism by which a change in fluorescence

occurs upon binding is not fully characterised, as there appears to be multiple competing mechanisms. This could be further explored with the possibility of using single photon fluorescence. Upon deeper understanding of the concentration effects associated with the binding mechanism of Probe 1 and mephedrone, the possibly of using 1,8 dibenzylthiourea anthracene as a fluorescent in-field probe could be explored further. NMR and fluorescence spectroscopy techniques both show good selectivity for Probe 1 to mephedrone, over methamphetamine, caffeine, paracetamol, benzocaine and lidocaine. Differences are seen in respect to sensitivity, with NMR and MS analysis showing a response upon binding at low concentrations while a fluorescence response upon binding can only be observed at high concentrations. Understanding the lack of an optical response at low concentrations is imperative to understanding the sensitivity of Probe 1 for use in-field. Another limitation is the affinity of chloride ions to Probe 1. Ideally a simple in-field detection device should require little to no sample preparation. However, it could be possible to explore the use of a microfluidic device that incorporates a liquid separation, to extract the freebase followed by optical detection using Probe 1. Such a device could still allow for the end user to have little technical knowledge, while retaining the selectivity and sensitivity required. Ideally to be used in-field the sensory molecule would be soluble in an aqueous media to prevent the use of organic solvents such as acetone which is currently used. Therefore, further development should be applied to improving the solubility of Probe 1.

One conclusion that is clear from this work is that the complexity of in-field NPS detection has grown with the ever-increasing number of substances being abused. It is for this reason that is seems unlikely that a simple test such as the Marquis test for methamphetamine, or Scott's test for cocaine will be applicable to NPS detection, due to their lack of specificity. Therefore, the notion of using a more sophisticated technique such as a microfluidic device for future in-field detection, is not as excessive as it may have been deemed a few years ago.

The pharmacophore design showed promise as one way that the design of host molecules could be improved. The one key limitation in this project was the lack of experimental binding data for cathinones. This was due to their affinity for transmembrane proteins, which have proven to be difficult to isolate and therefore there is a lack of structural X-ray crystallography data. However, there was recently a study that isolated the human cannabinoid receptor (CB1) bound to endogenous compounds[220]. This shows that in future there may be a larger selection of experimental data upon which to base the pharmacophore model. This could help to improve the development of pharmacophore models upon which the host molecules could be designed.

7.2.2   Metadynamics

Ideally the host molecules need to be tested *in silico* in the same conditions used experimentally to be sure of complete consensus between systems. Therefore, Probe 1 needs to be tested in an acetone solvent system, this will give more evidence as to whether it is the force field or the solvent choice that is preventing binding from being observed. Currently, the use of an acetone solvent box for simulations has not been parametrised and therefore it is not possible to carry out these simulations in acetone with a good level of accuracy.

It would also be interesting to carry out the same metadynamics experiments from Chapter 6 using the new OPLS3 software that has recently been launched, which has been specifically designed for small drug-like molecules in mind. It has been shown to have improved accuracy across all aspects of small molecule analysis[221]. OPLS3 reportedly has a 30 % improvement over earlier OPLS versions for prediction of ligand binding. Specifically, it accounts for polarizable charges on atoms which is particularly significant when dealing with intermolecular interactions. This could provide useful information as to whether the lack of viable results was due to the force field limitations.

Ideally the development of metadynamics analysis would be based on host-guest interactions that show a high binding constant. Using such experimental data, along with the above improvements, metadynamics analysis could show promise for the analysis of small molecule binding. Only once an approach is developed that shows good consensus with proven experimental results, will it be reasonable to then apply this to novel host molecules to explore small molecule binding in an attempt to guide the synthetic process.

References

(1)   Sullivan, R. J.; Hagen, E. H. Psychotropic Substance-Seeking: Evolutionary Pathology or Adaptation? *Addiction* **2002**, *97* (4), 389–400.

(2)   WHO. Management of Substance Abuse http://www.who.int/substance_abuse/terminology/psychoactive_substances/en/index.html (accessed Jul 26, 2016).

(3)   Leslie Iversen. *Drugs- a Very Short Introduction*, 1st ed.; Oxford University Press: Gosport, 2001.

(4)   Vetulani, J. Review Drug Addiction. Part 1. Psychoactive Substances of the Old World. *Pol. J. Pharmacol.* **2001**, *53*, 201–214.

(5)   Shulgin, A; Shulgin, A. *PiHKAL*; Transform Press: Berkeley, 1992.

(6)   Shulgin, A. T. The Vaults of Erowid https://www.erowid.org/psychoactives/guides/handbook_lsd25.shtml (accessed Jul 6, 2016).

(7)   Schmidt, M. M.; Sharma, A.; Schifano, F.; Feinmann, C. "Legal Highs" on the Met-Evaluation of UK-Based Websites, Products and Product Information. *Forensic Sci. Int.* **2011**, *206* (1–3), 92–97.

(8)   Mohamed, W. M. Y.; Ben Hamida, S.; Cassel, J.-C.; de Vasconcelos, A. P.; Jones, B. C. MDMA: Interactions With Other Psychoactive Drugs. *Pharmacol. Biochem. Behav.* **2011**, *99* (4), 759–774.

(9)   Kobie Whetstone. An Analysis of MDMA-Induced Neurotoxicity http://mdma.net/kobie/index.html (accessed Jul 7, 2016).

(10)   EMCDDA. *EU Drug Markets Report. In-Depth Analysis*; Publications, E. J., Ed.; Luxembourg: Publications Office of the European Union, 2016.

(11)   Vardakou, I.; Pistos, C.; Spiliopoulou, C. Drugs for Youth Via Internet and The Example of Mephedrone. *Toxicol. Lett.* **2011**, *201* (3), 191–195.

(12)   Iversen, L. *Consideration of Novel Psychoactive Substances ('Legal Highs')*; 2011.

(13)   Home Office. *Psychoactive Substances Act 2016*; 2016.

(14)   Amsterdam, J. Van; Nutt, D. Generic Legislation of New Psychoactive Drugs. *J. Psychopharmacol.* **2013**, *0* (January), 1–8.

(15) Power, M. MixMag http://www.mixmag.net/feature/ecstasy-in-2015/ (accessed Jun 6, 2016).

(16) Ayres, T. C.; Bond, J. W. A Chemical Analysis Examining the Pharmacology of Novel Psychoactive Substances Freely Available Over the Internet and Their Impact on Public (Ill)health. Legal Highs or Illegal Highs? *BMJ Open* **2012**, *2* (4), 1–8.

(17) Measham, F. Social Issues in the Use of Novel Psychoactive Substances. In *Novel Psychoactive Substances: Classification, Pharmacology and Toxicology*; Dargon, P., Wood, D., Eds.; Elsevier, 2013; pp 105–127.

(18) UNODC. *World Drug Report*; 2015.

(19) Anderson, M. *Drugs Intelligence Bulletin*; 2011.

(20) Iversen, L.; White, M.; Treble, R. Designer Psychostimulants: Pharmacology and Differences. *Neuropharmacology* **2014**, *87*, 59–65.

(21) Iversen, L. *Consideration of Cathinones*; 2010.

(22) McGraw, M.; McGraw, L. Bath Salts: Not as Harmless as They Sound. *J. Emerg. Nurs.* **2012**, *38* (6), 582–588.

(23) EMCDDA. *New Psychoactive Substances in Europe*; 2015.

(24) Corkery, J.; Claridge, H.; Loi, B.; Goodair, C.; Schifano, F.; Deaths, S. A. *Drug-Related Deaths in the UK : 2012 Annual Report 2013 National Programme on Substance Abuse Deaths Annual Report 2013 on Deaths Between*; 2013.

(25) Fearn, V. *Deaths Involving Legal Highs in England and Wales between 2004 and 2013*; 2016.

(26) Dybdal-Hargreaves, N. F.; Holder, N. D.; Ottoson, P. E.; Sweeney, M. D.; Williams, T. Mephedrone: Public Health Risk, Mechanisms of Action, and Behavioral Effects. *Eur. J. Pharmacol.* **2013**, *714* (1–3), 32–40.

(27) Iversen, L.; White, M.; Treble, R. Designer Psychostimulants: Pharmacology and Differences. *Neuropharmacology* **2014**, *87*, 1–7.

(28) Baumann, M. H.; Ayestas, M. a; Partilla, J. S.; Sink, J. R.; Shulgin, A. T.; Daley, P. F.; Brandt, S. D.; Rothman, R. B.; Ruoho, A. E.; Cozzi, N. V. The Designer Methcathinone Analogs, Mephedrone and Methylone, Are Substrates for Monoamine Transporters in Brain Tissue. *Neuropsychopharmacology* **2012**, *37* (5), 1192–1203.

(29) Home Office. A Change to the Misuse of Drugs Act 1971 : Control of Mephedrone and other

Cathinone Derivatives http://www.homeoffice.gov.uk/about-us/corporate-publications-strategy/home-office-circulars/circulars-2010/010-2010/ (accessed Jul 20, 2016).

(30)   Sainsbury, P. D.; Kicman, A. T.; Archer, R. P.; King, L. A.; Braithwaite, R. A. Aminoindanes-the Next Wave of "Legal Highs"? *Drug Test. Anal.* **2011**, *3* (7–8), 479–482.

(31)   Nichols, D. E.; Brewster, W. K.; Johnson, M. P.; Oberlender, R.; Riggs, R. M. Nonneurotoxic Tetralin and Indan Analogues of 3,4-(Methylenedioxy)amphetamine (MDA). *J. Med. Chem.* **1990**, *33* (2), 703–710.

(32)   Assi, S.; Fergus, S.; Stair, J. L.; Corazza, O.; Schifano, F. Emergence and Identification of New Designer Drug Products from the Internet. *Eur. Pharm. Rev.* **2011**, *16* (4), 68–72.

(33)   Ames, D. *Drugs Intelligence Bulletin - Q2*; 2013.

(34)   Ames, D. *Drugs Intelligence Bulletin - Q1*; 2012.

(35)   Ames, D. *Drugs Intelligence Bulletin - Q3*; 2012.

(36)   Johnson, M. P.; Conarty, F.; Nichols, E. [3H] Monoamine Releasing and Uptake Inhibition Properties of 3,4-Methylenedioxymethamphetamine and P-Chloroamphetamine Analogues. *Eur. J. Pharmacol.* **1991**, *200*, 9–16.

(37)   Santali, E. Y.; Cadogan, A.-K.; Daeid, N. N.; Savage, K. A.; Sutcliffe, O. B. Synthesis, Full Chemical Characterisation and Development of Validated Methods for the Quantification of (±)-4'-Methylmethcathinone (Mephedrone): A New "Legal High". *J. Pharm. Biomed. Anal.* **2011**, *56* (2), 246–255.

(38)   Shortall, E. S.; Green, R. A.; Fone, K. C. F.; King, M. V. Caffeine Alters the Behavioural and Body Temperature Responses to Mephedrone Without Causing Long-Term Neurotoxicity in Rats. *J. Psychopharmacol.* **2016**, *30* (7), 698–706.

(39)   Josef M. Peters. Factors Affecting Caffine Toxicity: A Review of the Literature. *J. Clin. Pharmacol.* **1967**, *7* (3), 131–141.

(40)   Baron, M. Analysis of Legal Highs - Do They Contain What It Says on the Tin? *Drug Test. Anal.* **2011**, *3* (9), 576–581.

(41)   UNODC. *The Challenge of New Psychoactive Substances*; 2013.

(42)   Smith, J. P.; Sutcliffe, O. B.; Banks, C. E. An Overview of Recent Developments in the Analytical Detection of New Psychoactive Substances (NPSs). *Analyst* **2015**, *140* (15), 4932–4948.

(43)   Casale, J. F.; Hays, P. A. Characterization of the "Methylenedioxy-2-Aminoindans." *Microgram J.* **2011**, *8* (2), 1–10.

(44)   Casale, J. F.; Hays, P. A. The Characterization of 4- and 5-Iodo-2-Aminoindan. *Microgram J.* **2012**, *9* (1), 18–26.

(45)   Gibbons, S.; Zloh, M. An Analysis of the "Legal High" Mephedrone. *Bioorg. Med. Chem. Lett.* **2010**, *20* (14), 4135–4139.

(46)   Archer, R. P. Fluoromethcathinone, a New Substance of Abuse. *Forensic Sci. Int.* **2009**, *185* (1–3), 10–20.

(47)   Elie, M. P.; Elie, L. E.; Baron, M. G. Keeping Pace with NPS Releases: Fast GC-MS Screening of Legal High Products. *Drug Test. Anal.* **2013**, *5* (5), 281–290.

(48)   Leffler, A. M.; Smith, P. B.; de Armas, A.; Dorman, F. L. The Analytical Investigation of Synthetic Street Drugs Containing Cathinone Analogs. *Forensic Sci. Int.* **2014**, *234*, 50–56.

(49)   Brandt, S. D.; Sumnall, H. R.; Measham, F.; Cole, J. Analyses of Second-Generation "Legal Highs" in the UK: Initial Findings. *Drug Test. Anal.* **2010**, *2* (8), 377–382.

(50)   Palfrey, S.; Labib, M. A Simple HPLC Method for the Separation of Amphetamine Isomers in Urine and Its Application in Differentiating Between "Street" Amphetamine and Prescribed D-Amphetamine. *Ann.Clin.Biochem.* **1996**, *33*, 344–346.

(51)   Pavlova, V.; Jovanović, S. P. Simultaneous Determination of Amphetamine, Methamphetamine, and Caffeine in Seized Tablets by High-Performance Liquid Chromatography. *Acta Chromatogr.* **2007**, *0* (18), 157–167.

(52)   Ammann, D.; McLaren, J. M.; Gerostamoulos, D.; Beyer, J. Detection and Quantification of New Designer Drugs in Human Blood: Part 2 - Designer Cathinones. *J. Anal. Toxicol.* **2012**, *36* (6), 381–389.

(53)   Ammann, J.; McLaren, J. M.; Gerostamoulos, D.; Beyer, J. Detection and Quantification of New Designer Drugs in Human Blood: Part 1 - Synthetic Cannabinoids. *J. Anal. Toxicol.* **2012**, *36* (6), 372–380.

(54)   Toole, K. E.; Fu, S.; Shimmon, R. G.; Kraymen, N.; Taflaga, S. Color Tests for the Preliminary Identification of Methcathinone and Analogues of Methcathinone. *Microgram J.* **2007**, *9* (1), 27–32.

(55)   Philp, M.; Shimmon, R.; Stojanovska, N.; Tahtouh, M.; Fu, S. Development and Validation of a

Presumptive Colour Spot Test Method for the Detection of Piperazine Analogues in Seized Illicit Materials. *Anal. Methods* **2013**, *5* (20), 5353–5838.

(56)   Wood, D. M.; Dargan, P. I. Mephedrone (4-Methylmethcathinone): What Is New in Our Understanding of Its Use and Toxicity. *Prog. Neuropsychopharmacol. Biol. Psychiatry* **2012**, *39* (2), 227–233.

(57)   Toole, K. E.; Fu, S.; Shimmon, R. G.; Kraymen, N.; Taflaga, S. Color Tests for the Preliminary Identification of Methcathinone and Analogues of Methcathinone. **2007**, *9* (1), 27–32.

(58)   Hilton, J. P.; Nguyen, T. H.; Pei, R.; Stojanovic, M.; Lin, Q. A Microfluidic Affinity Sensor for the Detection of Cocaine. *Sensors Actuators A Phys.* **2011**, *166* (2), 241–246.

(59)   Masseroni, D.; Biavardi, E.; Genovese, D.; Rampazzo, E.; Prodi, L.; Dalcanale, E. A Fluorescent Probe for Ecstasy. *Chem. Commun.* **2015**, *51* (1), 12799–12802.

(60)   Cumba, L. R.; Kolliopoulos, A. V.; Smith, J. P.; Thompson, P. D.; Evans, P. R.; Sutcliffe, O. B.; do Carmo, D. R.; Banks, C. E. Forensic Electrochemistry: Indirect Electrochemical Sensing of the Components of the New Psychoactive Substance "Synthacaine." *Analyst* **2015**, *140*, 5536–5545.

(61)   Smith, J. P.; Metters, J. P.; Khreit, O. I. G.; Sutcliffe, O. B.; Banks, C. E. Forensic Electrochemistry Applied to the Sensing of New Psychoactive Substances: Electroanalytical Sensing of Synthetic Cathinones and Analytical Validation in the Quantification of Seized Street Samples. *Anal. Chem.* **2014**, *86*, 9985–9992.

(62)   Krishnaiah, V.; Rami Reddy, Y. V.; Hanuman Reddy, V.; Thirupalu Reddy, V.; MadhuSudana Rao, G. Electrochemical Reduction Behaviour of Mephedrone Drug at a Dropping Mercury Electrode and Its Pharmaceutical Determination in Spiked Human Urine Samples. *Int. J. Sci. Res.* **2012**, *1* (4), 2277–8179.

(63)   Elie, L.; Baron, M.; Croxton, R.; Elie, M. Microcrystalline Identification of Selected Designer Drugs. *Forensic Sci. Int.* **2012**, *214* (1–3), 182–188.

(64)   Ellefsen, K. N.; Anizan, S.; Castaneto, M. S.; Desrosiers, N. A.; Martin, T. M.; Klette, L.; Huestis, M. A. Validation of the Only Commercially Available Immunoassay for Synthetic Cathinones in Urine : Randox Drugs of Abuse V Biochip Array Technology. *Drug Test. Anal.* **2014**, *6*, 728–738.

(65)   Shinkai, S. Molecular Recognition of Calixarene-Based Host Molecules. *J. Incl. Phenom. Mol. Recognit. Chem.* **1989**, *7* (2), 193–201.

(66)   Xu, M.; Wu, S.; Zeng, F.; Yu, C. Cyclodextrin Supramolecular Complex as a Water-Soluble
         Ratiometric Sensor for Ferric Ion Sensing. *Langmuir* **2010**, *26* (6), 4529–4534.

(67)   Tsukube, H. Biomimetic Membrane Transport via Designed Macrocyclic Host Molecules. *J.
         Coord. Chem.* **1987**, *16*, 101–129.

(68)   Bell, T. W.; Hext, N. M. Supramolecular Optical Chemosensors for Organic Analytes. *Chem. Soc.
         Rev.* **2004**, *33* (9), 589–598.

(69)   Yuan, X.; Forman, B. M. Detection of Designer Steroids. *J. Nucl. Recept. Signal. Atlas* **2005**, *3*
         (2), 1–5.

(70)   Boncheva, M.; Whitesides, G. M. Biomimetic Approaches to the Design of Functional Self-
         Assembling Systems. In *Dekker Encyclopedia of Nanoscience and Nanotechnology*; 2004; Vol.
         28, p 727.

(71)   Berman, H. M.; Westbrook, J.; Feng, Z.; Gilliland, G.; Bhat, T. N.; Weissig, H.; Shindyalov, I. N.;
         Bourne, P. E. The Protein Data Bank. *Nucleic Acids Res.* **2000**, *28* (1), 235–242.

(72)   Gao, Q.; Yang, L.; Zhu, Y. Pharmacophore Based Drug Design Approach as a Practical Process in
         Drug Discovery. *Curr. Comput. Aided. Drug Des.* **2010**, *6*, 37–49.

(73)   Wermuth, C. G.; Ganellin, C. R.; Lindberg, P.; Mitscher, L. A. Glossary of Terms Used in Medicinal
         Chemistry (IUPAC Recommendations 1998). *Pure Appl. Chem.* **2009**, *70* (5), 1365–3075.

(74)   Patrick, G. L. *An Introduction to Medicinal Chemistry*, Fourth Edi.; Oxford University Press:
         Oxford, 2009.

(75)   Gao, Q.; Yang, L.; Zhu, Y.; Simcere, J.; Xuan, N.; Avenue, W.; District, X. W. Pharmacophore
         Based Drug Design Approach as a Practical Process in Drug Discovery. *Curr. Comput. Aided.
         Drug Des.* **2010**, *6*, 37–49.

(76)   McGregor, M. J.; Muskal, S. M. Pharmacophore Fingerprinting. 1. Application to QSAR and
         Focused Library Design. *J. Chem. Inf. Comput. Sci.* **1999**, *39* (3), 569–574.

(77)   Wang, W.; Corporation, B.; Way, D. Instability, Stabilization, and Formulation of Liquid Protein
         Pharmaceuticals. *Int. J. Pharm.* **1999**, *185*, 129–188.

(78)   Campbell, N. A.; Reece, J. B. *Biology*, Internatio.; Wilbur, B., Ed.; Pearson, 2005.

(79)   Silva, N. H. C. S.; Vilela, C.; Marrucho, I. M.; Freire, C. S. R.; Neto, C. P.; Silvestre, A. J. D. Protein-
         Based Materials: From Sources to Innovative Sustainable Materials for Biomedical

Applications. *J. Mater. Chem. B* **2014**, *2*, 3715–3740.

(80) Liang, J.; Edelsbrunner, H.; Woodward, C. Anatomy of Protein Pockets and Cavities: Measurement of Binding Site Geometry and Implications for Ligand Design. *Protein Sci.* **1998**, *7*, 1884–1897.

(81) Dunn, F. M. Protein-Ligand Interactions: General Description. *Citeable Rev. Life Sci.* **2010**.

(82) Nilapwar, S. Characterization and Exploitation of Protein Ligand Interactions for Structure Based Drug Design, University College London, 2009.

(83) Sheu, S.-Y.; Yang, D.-Y.; Selzle, H. L.; Schlag, E. W. Energetics of Hydrogen Bonds in Peptides. *Proc. Natl. Acad. Sci. U. S. A.* **2003**, *100* (22), 12683–12687.

(84) Hunter, C. A.; Sanders, J. K. M. The Nature of Pi-Pi Interactions. *J. Am. Chem. Soc.* **1990**, *112* (2), 5525–5534.

(85) Martinez, C. R.; Iverson, B. L. Rethinking the Term "Pi-Stacking." *Chem. Sci.* **2012**, *3*, 2191–2201.

(86) Anslyn, E. V.; Dougherty, D. A. *Modern Physical Organic Chemistry*, first edit.; University Science Books: Sausalito, CA, 2006.

(87) Chasman, D. I. *Protein Structure Determination, Analysis, and Applications for Drug Discovery*, First Edit.; Marcel Dekker, Inc.: New York, 2003.

(88) RSCB. Protein DataBank http://www.rcsb.org/pdb/static.do?p=general_information/about_pdb/nature_of_3d_struct ural_data.html (accessed Jul 14, 2016).

(89) Ravi, V. K.; Goel, M.; Kotamarthi, H. C.; Ainavarapu, S. R. K.; Swaminathan, R. Preventing Disulfide Bond Formation Weakens Non-Covalent Forces Among Lysozyme Aggregates. *PLoS One* **2014**, *9* (2), 1–11.

(90) Derewenda, Z. S. The Use of Recombinant Methods and Molecular Engineering in Protein Crystallization. *Methods* **2004**, *34*, 354–363.

(91) Listwan, P.; Terwilliger, T. C.; Waldo, G. S. Automated, High-Throughput Platform for Protein Solubility Screening Using a Split-GFP System. *J. Struct. Funct. Genomics* **2009**, *10*, 47–55.

(92) Ooi, L. *Principles of X-Ray Crystallography*, First Edit.; Oxford University Press: Oxford, 2010.

(93) Rhodes, G. *A Glossary of Terms from Crystallography, NMR, and Homology Modeling*, Third Edit.; Academic Press, 2006.

(94) Fraser, J. S.; van den Bedem, H.; Samelson, a. J.; Lang, P. T.; Holton, J. M.; Echols, N.; Alber, T. Accessing Protein Conformational Ensembles Using Room-Temperature X-Ray Crystallography. *Proc. Natl. Acad. Sci.* **2011**, *108* (39), 16247–16252.

(95) Kuzmanic, A.; Pannu, N. S.; Zagrovic, B. X-Ray Refinement Significantly Underestimates the Level of Microscopic Heterogeneity in Biomolecular Crystals. *Nat. Commun.* **2014**, *5* (3220), 1–10.

(96) Clore, G. M.; Gronenborn, A. M. Determining the Structures of Large Proteins and Protein Complexes by NMR. *Trends Biotechnol.* **1998**, *16* (97), 22–34.

(97) Sibille, N.; Favier, A.; Azuaga, A. I.; Ganshaw, G.; Bott, R.; Bonvin, A. M. J. J.; Boelens, R.; van Nuland, N. A. J. Comparative NMR Study on the Impact of Point Mutations on Protein Stability of Pseudomonas Mendocina Lipase. *Protein Sci.* **2006**, *15* (8), 1915–1927.

(98) Spronk, C. A. E. M.; Nabuurs, S. B.; Krieger, E.; Vriend, G.; Vuister, G. W. Validation of Protein Structures Derived by NMR Spectroscopy. *Prog. Nucl. Magn. Reson. Spectrosc.* **2004**, *45* (3–4), 315–337.

(99) RSCB. Protein DataBank http://www.rcsb.org/pdb/statistics/histogram.do?mdcat=mvStructure&mditem=structureMolecularWeight&name=Molecular Weight (Structure)# (accessed Jul 17, 2016).

(100) Creighton, T. E. *Proteins: Structures and Molecular Properties*; W.H. Freeman, 1992.

(101) Lehn, J. M. Cryptates: The Chemistry of Macropolycyclic Inclusion Complexes. *Acc. Chem. Res.* **1978**, *11* (2), 49–57.

(102) Lehn, J. M. Supramolecular Chemistry—Scope and Perspectives Molecules, Supermolecules, and Molecular Devices (Nobel Lecture). *Angew Chem Int Ed Engl.* **1988**, *27* (1), 89–112.

(103) Steed, J. W.; Turner, D. R.; Wallace, K. J. *Core Concepts in Supramolecular Chemistry and Nanochemistry*, 1st ed.; Wiley, 2007.

(104) Schalley, C. A.; Kaufmann, L. *Analytical Methods in Supramolecular Chemistry*, 2nd Editio.; Schalley, C. A., Ed.; Wiley-VCH, 2012.

(105) Kubo, Y.; Maeda, S.; Tokita, S.; Kubo, M. Colorimetric Chiral Recognition by a Molecular Sensor. *Nat. Commun.* **1996**, 522–524.

(106) Cram, D. J. Preorganization—From Solvents to Spherands. *Angew Chem Int Ed Engl.* **1986**, *25* (12), 1039–1057.

(107) Van Dijk, E. H.; Myles, D. J. T.; Van der Veen, M. H.; Hummelen, J. C. Synthesis and Properties of an Anthraquinone-Based Redox Switch for Molecular Electronics. *Org. Lett.* **2006**, *8* (11), 2333–2336.

(108) Thordarson, P. Determining Association Constants from Titration Experiments in Supramolecular Chemistry. *Chem. Soc. Rev.* **2011**, *40*, 1305–1323.

(109) Guo, D.-S.; Uzunova, V. D.; Su, X.; Liu, Y.; Nau, W. M. Operational Calixarene-Based Fluorescent Sensing Systems for Choline and Acetylcholine and Their Application to Enzymatic Reactions. *Chem. Sci.* **2011**, *2* (9), 1722–1734.

(110) Fielding, L. NMR Methods for the Determination of Protein-Ligand Dissociation Constants. *Prog. Nucl. Magn. Reson. Spectrosc.* **2007**, *51* (4), 219–242.

(111) Williams, D. H.; Fleming, I. *Spectroscopic Methods in Organic Chemistry*, 5th ed.; McGraw-Hill Book Company, 1995.

(112) Raman Parkesh, Emma B. Veale, T. G. Stratergies, Fluoresence Detection Principles and. In *Chemosensors principles, stratergies and applications*; Binghe Wang, E. V. A., Ed.; Wiley, 2011; pp 229–252.

(113) Allen, M. P. Introduction to Molecular Dynamics Simulation. *Comput. Soft Matter From Synth. Polym. to Proteins* **2004**, *23* (2), 1–28.

(114) Leach, A. R. *Molecular Modelling Principles and Applications*, Second Edi.; Pearson Education Ltd, 2001.

(115) Barducci, A.; Bonomi, M.; Parrinello, M. Metadynamics. *Wiley Interdiscip. Rev. Comput. Mol. Sci.* **2011**, *1* (5), 826–843.

(116) Cheng, B. Quora https://www.quora.com/How-does-Metadynamics-calculate-the-potential-mean-force-PMF-or-the-free-energy-profile-of-a-reaction-coordinate (accessed Oct 12, 2015).

(117) Laio, A.; Gervasio, F. L. Metadynamics: A Method to Simulate Rare Events and Reconstruct the Free Energy in Biophysics, Chemistry and Material Science. *Reports Prog. Phys.* **2008**, *71* (12), 126601.

(118) Huang, A.; Stultz, C. M. Conformational Sampling With Implicit Solvent Models: Application to the PHF6 Peptide in Tau Protein. *Biophys. J.* **2007**, *92* (1), 34–45.

(119) Hoda, N.; Larson, R. G. Explicit- and Implicit-Solvent Molecular Dynamics Simulations of Complex Formation Between Polycations and Polyanions. *Macromolecules* **2009**, *42* (22),

8851–8863.

(120) Jorgensen, W. L.; Maxwell, D. S.; Tirado-rives, J. Development and Testing of the OPLS All-Atom Force Field on Conformational Energetics and Properties of Organic Liquids. *J. Am. Chem. Soc.* **1996**, *7863* (15), 11225–11236.

(121) Petrella, R. J. A Versatile Method for Systematic Conformational Searches: Application to CheY. *J. Comput. Chem.* **2012**, *32* (11), 2369–2385.

(122) Harrison, R. L.; Carlo, M. Introduction to Monte Carlo Simulation. *AIP Conf. Proceeding* **2010**, *1204*, 17–21.

(123) Standard, J. M. *Introduction to Conformation Searching*; 2013.

(124) Url, S.; Archive, T. J.; Archive, T. Optimisation by Simulated Annealing. **2007**, *220* (4598), 671–680.

(125) Daily, S. *National Drugs Intelligence Bulletin - Q1*; 2014.

(126) Ames, D. *Drugs Intelligence Bulletin - Q4*; 2012.

(127) Ames, D. *Drugs Intelligence Bulletin*; 2012.

(128) Gallegos, A. *New Psychoactive Substances and the EU Early Warning System : Chemistry Matters*; EMCDDA: Rome, 2014.

(129) Nichols, D. E.; Johnson, M. P.; Oberlender, R. 5-Iodo-2-Aminoindan, a Nonneurotoxic Analogue of P-Iodoamphetamine. *Pharmacol. Biochem. Behav.* **1991**, *38* (1), 135–139.

(130) Gallagher, C. T.; Assi, S.; Stair, J. L.; Fergus, S.; Corazza, O.; Corkery, J. M. 5,6-Methylenedioxy-2-Aminoindane : From Laboratory Curiosity to "Legal High." *Hum. Psychopharmacol.* **2012**, *27*, 106–112.

(131) UNODC. UNODC Laboratory and Scientific Section Portals https://www.unodc.org/LSS/SubstanceGroup/Details/8fd64573-c567-4734-a258-76d1d95dca25 (accessed Jul 14, 2015).

(132) Strano-Rossi, S.; Anzillotti, L.; Castrignanò, E.; Romolo, F. S.; Chiarotti, M. Ultra High Performance Liquid Chromatography-Electrospray Ionization-Tandem Mass Spectrometry Screening Method for Direct Analysis of Designer Drugs, "spice" and Stimulants in Oral Fluid. *J. Chromatogr. A* **2012**, *1258*, 37–42.

(133) Smith, J. P.; Metters, J. P.; Irving, C.; Sutcliffe, O. B.; Banks, C. E. Forensic Electrochemistry: The

Electroanalytical Sensing of Synthetic Cathinone-Derivates and Their Accompanying Adulterants In "legal high" Products. *Analyst* **2014**, *139*, 389–400.

(134) Assi, S.; Guirguis, A.; Halsey, S.; Fergus, S.; Stair, J. L. Analytical Methods Analysis of "Legal High" Substances and Common Adulterants Using Handheld Spectroscopic. *Anal. Methods* **2014**, *7*, 736–746.

(135) Harmonisaton, I. C. *Validation of Analytical Procedures: Text and Methodology*; 2005; Vol. 1994.

(136) Nic Daeid, N.; Savage, K. A.; Ramsay, D.; Holland, C.; Sutcliffe, O. B. Development of Gas Chromatography-Mass Spectrometry (GC-MS) and Other Rapid Screening Methods for the Analysis of 16 "Legal High" Cathinone Derivatives. *Sci. Justice* **2014**, *54* (1), 22–31.

(137) Angelov, D.; O'Brien, J.; Kavanagh, P. The Synthesis of 1-(2-Thienyl)-2-(Methylamino) Propane (Methiopropamine) and Its 3-Thienyl Isomer for Use as Reference Standards. *Drug Test. Anal.* **2011**, *5* (3), 145–149.

(138) RCNET-Chemicals. Research Chemicals https://rcnet-chemicals.com/mdai-mpa-combo-pellets.html (accessed Feb 26, 2015).

(139) Long, W. J.; Henderson, J. W. *Chromatography of Nitrogen-Containing Compounds Without Triethylamine Application*; 2007.

(140) CDER. *Reviewer Guidance ' Validation of Chromatographic Methods*; 1994.

(141) Srdjenovic, B.; Djordjevic-Milic, V.; Grujic, N.; Injac, R.; Lepojevic, Z. Simultaneous HPLC Determination of Caffeine, Theobromine, and Theophylline in Food, Drinks, and Herbal Products. *J. Chromatogr. Sci.* **2008**, *46* (February), 144–149.

(142) Bell, C.; George, C.; Kicman, A. T.; Traynor, A. Development of a Rapid LC-MS/MS Method for Direct Urinalysis of Designer Drugs. *Drug Test. Anal.* **2011**, *3* (7–8), 496–504.

(143) Dolan, J. System Suitability. *LCGC North Am.* **2004**, *22* (5), 430–435.

(144) Dolan, J. Calibration Curves, Part V: Curve Weighting. *LCGC North Am.* **2009**, *27* (7), 534–540.

(145) De Boer, D.; Goemans, W. P. J.; Ghezavat, V. R.; Van Ooijen, R. D.; Maes, R. A. A. Seizure of Illicitly Produced Para-Fluorofentanyl: Quantitative Analysis of the Content of Capsules and Tablets. *J. Pharm. Biomed. Anal.* **2003**, *31*, 557–562.

(146) Leffler, A. M.; Smith, P. B.; de Armas, A.; Dorman, F. L. The Analytical Investigation of Synthetic

Street Drugs Containing Cathinone Analogs. *Forensic Sci. Int.* **2014**, *234*, 50–56.

(147)   Comment, S.; Lock, E.; Zingg, C.; Jakob, A. The Analysis of Ecstacy Tablets by ICP/MS and ICP/AES. *Probl. Forensic Sci.* **2001**, *46*, 132–145.

(148)   Cole, C.; Jones, L.; Mcveigh, J.; Kicman, A.; Syed, Q.; Bellis, M. A. *CUT; A Guide to Adulterants, Bulking Agents and Other Contaminants Found in Illicit Drugs*; 2010.

(149)   Ames, D. *Drugs Intelligence Bulletin -Q1*; 2013.

(150)   Schrödinger Release 2014-3. Maestro. New York 2014.

(151)   Dixon, S. L.; Smondyrev, A. M.; Rao, S. N. PHASE: A Novel Approach to Pharmacophore Modeling and 3D Database Searching. *Chem. Biol. Drug Des.* **2006**, *67* (5), 370–372.

(152)   Halgren, T. New Method for Fast and Accurate Binding-Site Identification and Analysis. *Chem. Biol. Drug Des.* **2007**, *69* (2), 146–148.

(153)   EMCDDA. *European Drug Report Trends and Developments*; 2014.

(154)   EMCDDA. *Europol – EMCDDA Joint Report on a New Psychoactive Substance : 4-Methylmethcathinone In Accordance with Article 5 of Council Decision 2005 / 387 / JHA on the Information Exchange , Risk Assessment and Control of New Psychoactive Substances Contents*; 2010.

(155)   Iversen, L.; Gibbons, S.; Treble, R.; Setola, V.; Huang, X.-P.; Roth, B. L. Neurochemical Profiles of Some Novel Psychoactive Substances. *Eur. J. Pharmacol.* **2013**, *700* (1–3), 147–151.

(156)   Carpenter, E. P.; Beis, K.; Cameron, A. D.; Iwata, S. Overcoming the Challenges of Membrane Protein Crystallography. *Curr. Opin. Struct. Biol.* **2008**, *18* (5), 581–586.

(157)   Elsvier. Reaxys https://www.reaxys.com/reaxys/secured/search.do (accessed Feb 12, 2015).

(158)   Drenth, J. *Principles of Protein X-Ray Crystallography*, Third Edit.; Springer, 1993.

(159)   Jeffrey, G. A. *An Introduction to Hydrogen Bonding*, 1st ed.; Oxford University Press: New York, 1997.

(160)   Jones, S.; Marin, A.; Thornton, J. M. Protein Domain Interfaces: Characterization and Comparison with Oligomeric Protein Interfaces. *Protein Eng.* **2000**, *13* (2), 77–82.

(161)   Qvist, J.; Davidovic, M.; Hamelberg, D.; Halle, B. A Dry Ligand-Binding Cavity in a Solvated Protein. *Proc. Natl. Acad. Sci. U. S. A.* **2008**, *105* (17), 6296–6301.

(162) Yilmaz, M.; Erdemir, S. Calixarene-Based Receptors for Molecular Recognition. *Turkish J. Chem.* **2013**, *37* (4), 558–585.

(163) Sliwa, W.; Deska, M. Functionalization Reactions of Calixarenes. *ARKIVOC* **2011**, *1*, 496–551.

(164) Jose, P.; Menon, S. Lower-Rim Substituted Calixarenes and Their Applications. *Bioinorg. Chem. Appl.* **2007**, *2007* (Figure 1), 65815.

(165) Agrawal, Y. K.; Pancholi, J. P.; Vyas, J. M. Design and Synthesis of Calixarene. *J. Sci. Ind. Res. (India).* **2009**, *68* (September), 745–768.

(166) Shinkai, S.; Mori, S.; Tsubaki, T. New Water-Soluable Host Molecules Derived from Calix[6]arene. *Tetrahedron Lett.* **1984**, *25* (46), 5315–5318.

(167) Gutsche, C. D.; Dhawan, B.; Kwang, H. Properties of the Calixarenes from P-Tert-Butylphenol. *J. Am. Chem. Soc.* **1981**, *1* (9), 3782–3792.

(168) Dudko, E. V; Kalosha, I. I.; Tolkachev, V. A. Mechanism for Quenching of the Luminescene of 9,10-Anthraquinone Vapor by Oxygen. *J. Appl. Spectrosc.* **2008**, *75* (1), 80–85.

(169) Dhananjeyan, M. R.; Milev, Y. P.; Kron, M. A.; Nair, M. G. Synthesis and Activity of Substituted Anthraquinones Against a Human Filarial Parasite, Brugia Malayi. *J. Med. Chem.* **2005**, *48* (8), 2822–2830.

(170) Ahluwalia, V. K.; Aggarwal, R. *Comprehensive Practical Organic Chemistry: Preparations and Quantitative Analysis*; University Press: Dehli, 2000.

(171) Mariappan, K.; Basa, P. N.; Balasubramanian, V.; Fuoss, S.; Sykes, A. G. Synthesis, Reactivity, Catenation and X-Ray Crystallography of Ag+ and Cu+ Complexes of Anthraquinone-Based Selenoethers: A Luminescent Chemodosimeter for Cu2+ and Fe3+. *Polyhedron* **2013**, *55*, 144–154.

(172) Wu, F.; Hu, M.; Wu, Y.; Tan, X.; Zhao, Y.; Ji, Z. Fluoride-Selective Colorimetric Sensor Based on Thiourea Binding Site and Anthraquinone Reporter. *Spectrochmica Acta* **2006**, *65*, 633–637.

(173) Yang, L.; Fu, Z.; Niu, X.; Zhang, G.; Cui, F.; Zhou, C. Probing the Interaction of Anthraquinone with DNA by Spectroscopy, Molecular Modelling and Cancer Cell Imagine Technique. *Chem. Biol. Interact.* **2015**, *233*, 62–70.

(174) Elçin, S.; Deligöz, H. Di-Substituted Azocalix[4]arenes Containing Chromogenic Groups: Synthesis, Characterization, Extraction, and Thermal Behavior. *Tetrahedron* **2013**, *69* (33), 6832–6838.

(175) Kumar, S.; Kurur, N. D.; Chawla, H. M.; Varadarajan, R. A Convenient One Pot One Step Synthesis of Para-Nitro Calixarene via Ipsonitration. *Synth. Commun.* **2001**, *31* (5), 775–779.

(176) Van Wageningen, A. M. A.; Snip, E.; Verboom, W.; Reinhoudt, D. N.; Boerrigter, H. Synthesis and Application of Iso(thio)cyanate-Functionlized Calix[4]arenes. *Liebigs Ann.* **1997**, *11*, 2235–2245.

(177) Sun, X.; Zheng, H.; Li, Z.; Vysotsky, M. O. Improved Procedure for the Synthesis of Calix [4] Arenes with Four Amino Groups on the Wide Rim. *Int. Res. J. Pure Appl. Chem.* **2014**, *4* (3), 352–361.

(178) Lee, C.-C.; Huang, K.-F.; Chang, D.-M.; Hsu, J.-J.; Huang, F.-C.; Shih, K.-N.; Chen, C.-L.; Chen, T.-C.; Chen, R.-H.; Lin, J.-J.; Huang, H.-S. Design, Synthesis and Evaluation of Telomerase Inhibitory, hTERT Repressing, and Anti-Proliferation Activities of Symmetrical 1,8-Disubstituted Amidoanthraquinones. *Eur. J. Med. Chem.* **2012**, *50*, 102–112.

(179) Cheung, K.-C.; Wong, W.-L.; So, M.-H.; Zhou, Z.-Y.; Yan, S.-C.; Wong, K.-Y. A Dinuclear Ruthenium Catalyst with Confined Cavity: Selectivity in the Addition of Aliphatic Carboxylic Acids in Phenylacetate. *Chem. Commun.* **2013**, *49*, 710–712.

(180) Vishnyakova, T. P.; Golubeva, I. A.; Glebova, E. V. Substituted Ureas. Methods of Synthesis and Applications. *Russ. Chem. Rev.* **1985**, *54* (3), 249–261.

(181) Magrans, J. O.; Mendoza, J. De. Are 1,3-Di- O -benzoylcalix[4]arenes an Exception to the 13 C-NMR Rule for Conformational Determination? *J. Org. Chem.* **1997**, *3263* (7), 4518–4520.

(182) Casnati, A.; De Mendoza, J.; Reinhoudt, D. N.; Ungaro, R. *Determination of Calixarene Conformations by Means of NMR Techniques*; Springer Netherlands, 1999.

(183) Cepeda, E. a.; Diaz, M. Solubility of Anthracene and Anthraquinone in Acetonitrile, Methyl Ethyl Ketone, Isopropol Alcohol and Their Mixtures. *Fluid Phase Equilib.* **1996**, *121* (1–2), 267–272.

(184) Kim, S. K.; Singh, N. J.; Kim, S. J.; Swamy, K. M. K.; Kim, S. H.; Lee, K.-H.; Kim, K. S.; Yoon, J. Anthracene Derivatives Bearing Two Urea Groups as Fluorescent Receptors for Anions. *Tetrahedron* **2005**, *61* (19), 4545–4550.

(185) Schwesinger, R. Phosphazene Base P4-T-Bu. *Encycl. Reagents Org. Synth.* **2010**, 8–10.

(186) Makuc, D.; Hiscock, J. R.; Light, M. E.; Gale, P. A.; Plavec, J. NMR Studies of Anion-Induced Conformational Changes in Diindolylureas and Diindolylthioureas. *Beilstein J. Org. Chem.* **2011**, *7*, 1205–1214.

(187)   Bryantsev, V. S.; Hay, B. P. Conformational Preferences and Internal Rotation in Alkyl- and Phenyl-Substituted Thiourea Derivatives. *J. Phys. Chem. A* **2006**, *110* (14), 4678–4688.

(188)   Zhang, W. *Dichloromethane*; 1998; Vol. 4.

(189)   He, J.-L.; Wu, Z.-S.; Zhou, H.; Wang, H.-Q.; Jiang, J.-H.; Shen, G.-L.; Yu, R.-Q. Fluorescence Aptameric Sensor for Strand Displacement Amplification Detection of Cocaine. *Anal. Chem.* **2010**, *82* (4), 1358–1364.

(190)   Moreno, D.; Díaz de Greñu, B.; García, B.; Ibeas, S.; Torroba, T. A Turn-on Fluorogenic Probe for Detection of MDMA from Ecstasy Tablets. *Chem. Commun. (Camb).* **2012**, *48* (24), 2994–2996.

(191)   Li, H.; Yang, Y.-W. W. Gold Nanoparticles Functionalized with Supramolecular Macrocycles. *Chinese Chem. Lett.* **2013**, *24* (7), 545–552.

(192)   Lakowicz, J. R. *Principles of Fluorescence Spectroscopy Principles of Fluorescence Spectroscopy*; 2006.

(193)   Connors, K. A. *Binding Constants The Measurement of Molecular Complex Stability*, First Edit.; Wiley-ISP, 1989.

(194)   Hohenberg, P.; Kohn, W. Inhomogeneous Electron Gas. *Phys. Rev. B* **1964**, *136* (3B), 864–871.

(195)   Nora, M.; Fatiha, M.; Leila, N.; Sakina, H.; DjamelEddine, K. Density Functional Study of Inclusion Complex of Albendazole/Cucurbit [7]uril: Structure, Electronic Properties, NBO, GIAO and TD-DFT Analysis. *J. Mol. Liq.* **2015**, *211*, 40–47.

(196)   Galindo-Murillo, R.; Olmedo-Romero, A.; Cruz-Flores, E.; Petrar, P. M.; Kunsagi-Mate, S.; Barroso-Flores, J. Calix[n]arene-Based Drug Carriers: A DFT Study of Their Electronic Interactions with a Chemotherapeutic Agent Used Against Leukemia. *Comput. Theor. Chem.* **2014**, *1035*, 84–91.

(197)   Kularatne, S. A.; Burns, D. H. Buried Solvent Determines Both Anion Binding Selectivity and Binding Stoichiometry with Hydrogen Bonding Receptors. *J. Org. Chem.* **2005**, *70* (7), 2803–2807.

(198)   Cho, E. N. R.; Li, Y.; Kim, H.; Hyun, M. H. A Colorimetric Chiral Sensor Based on Chiral Crown Ether for the Recognition of the Two Enantiomers of Primary Amino Alcohols and Amines. *Chirality* **2011**, *353* (July 2010), 349–353.

(199)   Schottel, B. L.; Chifotides, H. T.; Dunbar, K. R. Anion-π Interactions. *Chem. Soc. Rev.* **2008**, *37* (1), 68–83.

(200) Robertazzi, A.; Krull, F.; Knapp, E.-W.; Gamez, P. Recent Advances in Anion–π Interactions. *CrystEngComm* **2011**, *13* (10), 3293.

(201) Vaiano, F.; Busardò, F. P.; Palumbo, D.; Kyriakou, C.; Fioravanti, A.; Catalani, V.; Mari, F.; Bertol, E. A Novel Screening Method for 64 New Psychoactive Substances and 5 Amphetamines in Blood by LC–MS/MS and Application to Real Cases. *J. Pharm. Biomed. Anal.* **2016**, *129*, 441–449.

(202) Iversen, L.; Gibbons, S.; Treble, R.; Setola, V.; Huang, X. P.; Roth, B. L. Neurochemical Profiles of Some Novel Psychoactive Substances. *Eur. J. Pharmacol.* **2013**, *700* (1–3), 147–151.

(203) Hunter, C. A.; Anderson, H. L. What Is Cooperativity? *Angew. Chemie - Int. Ed.* **2009**, *48*, 7488–7499.

(204) Zuba, D. Identification of Cathinones and Other Active Components of "Legal Highs" by Mass Spectrometric Methods. *TrAC Trends Anal. Chem.* **2012**, *32*, 15–30.

(205) Reichardt, C.; Welton, T. *Solvent and Solvent Effects in Organic Chemistry*, Fourth Edi.; Wiley-VCH, 2011.

(206) Khreit, O. I. G.; Irving, C.; Schmidt, E.; Parkinson, J. A.; Nic Daeid, N.; Sutcliffe, O. B. Synthesis, Full Chemical Characterisation and Development of Validated Methods for the Quantification of the Components Found in the Evolved "legal high" NRG-2. *J. Pharm. Biomed. Anal.* **2012**, *61*, 122–135.

(207) Norman-Jones, R. The Ultraviolet Absorption Spectra of Anthracene Derivatives. *Chem. Rev.* **1947**, *41* (2), 353–371.

(208) UNODC. *Global Synthetic Drugs Assessment*; 2014.

(209) Laio, A.; Gervasio, F. L. Metadynamics: A Method to Simulate Rare Events and Reconstruct the Free Energy in Biophysics, Chemistry and Material Science. *Reports Prog. Phys.* **2008**, *71* (12), 126601–126623.

(210) Hsiao, Y. W.; Söderhjelm, P. Prediction of SAMPL4 Host-Guest Binding Affinities Using Funnel Metadynamics. *J. Comput. Aided. Mol. Des.* **2014**, *28* (4), 443–454.

(211) Shivakumar, D.; Williams, J.; Wu, Y.; Damm, W.; Shelley, J.; Sherman, W. Prediction of Absolute Solvation Free Energies Using Molecular Dynamics Free Energy Perturbation and the OPLS Force Field. *J. Chem. Theory Comput.* **2010**, *6* (5), 1509–1519.

(212) Still, W. C.; Tempczyk, A.; Hawley, R. C.; Hendrickson, T. Semianalytical Treatment of Solvation

for Molecular Mechanics and Dynamics. *J. Am. Chem. Soc.* **1990**, *112* (16), 6127–6129.

(213)   Bowers, K. J.; Chow, E.; Xu, H.; Dror, R. O.; Eastwood, M. P.; Gregersen, B. A.; Klepeis, J. L.; Kolossvary, I.; Moraes, M. A.; Sacerdoti, F. D.; Salmon, J. K.; Shan, Y.; Shaw, D. E. Scalable Algorithms for Molecular Dynamics Simulations on Commodity Clusters. In *Proceedings of the ACM/IEEE Conference on Supercomputing (SC06), Tampa, Florida, November*; 2006; pp 11–17.

(214)   Tuckerman, M.; Berne, B. J.; Martyna, G. J. Reversible Multiple Time Scale Molecular Dynamics. *J. Chem. Phys.* **1992**, *97* (3), 1990–2001.

(215)   Essmann, U.; Perera, L.; Berkowitz, M. L.; Darden, T.; Lee, H.; Pedersen, L. G. A Smooth Particle Mesh Ewald Method. *J Chem Phys* **1995**, *103* (1995), 8577–8593.

(216)   Cook, B.; Kavraki, L. E.; Motwani, R. Efficient Clustering of Molecular Conformations. In *Second CGC Workshop on Computational Geometry*; 1997; pp 3–6.

(217)   Pearson, R. G.; Dillon, R. L. Rates of Ionization of Pseudo Acids. 1 IV. Relation between Rates and Equilibria. *J. Am. Chem. Soc.* **1953**, *75* (7), 2439–2443.

(218)   Zhang, D.-W.; Wong, H.; Ting-Li, Z. *Hydrogen Bonded Supramolecular Structures*, 1st ed.; Li, Z., Wu, L.-Z., Eds.; Springer: Berlin, 2015.

(219)   Li, D. T.; Swearingen, J. K.; Kaminsky, W.; Kelman, D. R.; West, D. X. Study of the Sulfur Atom as Hydrogen Bond Acceptor in N(2)-Pyridylmethyl-N-Arylthioureas. *J. Chem. Crystallogr.* **2004**, *34* (8), 553–540.

(220)   Cb, R.; Hua, T.; Vemuri, K.; Pu, M.; Makriyannis, A.; Stevens, R. C.; Liu, Z. Crystal Structure of the Human Cannabinoid Receptor CB 1. *Cell* **2016**, *167*, 750–762.

(221)   Harder, E.; Damm, W.; Maple, J.; Wu, C.; Reboul, M.; Xiang, J. Y.; Wang, L.; Lupyan, D.; Dahlgren, M. K.; Knight, J. L.; Kaus, J. W.; Cerutti, D. S.; Krilov, G.; Jorgensen, W. L.; Abel, R.; Friesner, R. A. OPLS3: A Force Field Providing Broad Coverage of Drug-like Small Molecules and Proteins. *J. Chem. Theory Comput.* **2016**, *12* (1), 281–296.

Publications

- **Kellett, K**.; Broome, J.H.; Zloh, M.; Kirton, S.B.; Fergus, S.; Gerhard, U.; Stair, J. L.; Wallace, K. J. Small Molecular Recognition of Mephedrone using An Anthracene Molecular Clip, *Chem. Comm*. **2016,** *52*, 7474-7477

- Antonietta De Luca, M.; Paola Castelli, M.; Loi, B.; Porcu, A.; Martorelli, M.; Miliano, C.; **Kellett, K**.; Davidson, C.; Jacqueline Stair, L.; Schifano, F.; et al. Native CB1 Receptor Affinity, Intrisic Activity and Accumbens Shell Dopamine Stimulant Properties of Third Generation SPICE/K2 Cannabinoids: BB-22, 5F-PB-22, 5F-AKB- 48 and STS-135. *Neuropharmacology* **2016**, *105*, 630–638.

- Fergus, S.; **Kellett, K**.; Gerhard, U. The Khat and Meow Meow Tale: Teaching the Relevance of Chemistry through Novel Recreational Drugs. *J. Chem. Educ.* **2015**, *92*, 843–848.

- *In preparation* **Kellett, K**; Owen, J. D.; Stair, J. L. Determination of Molecular and Elemental Constituents in Aminoindanes 'legal high' Products. *J. Pharm. Biomed. Anal.* **2016**

Conference Presentations

- **Poster - RSC Analytical Research Forum, Hatfield 2013**
"Chemical characterisation of aminoindan 'legal high' products purchased from the Internet"

- **Poster - Novel Psychoactive Substances Conferences, Swansea 2013**
"Synthesis and characterisation of 'legal high' 5-iodo-2-aminoindan"

- **Poster - Young Modellers Forum, London 2014**
"Metadynamics Analysis of Potential Host Molecules for Detection of NPS Mephedrone"

- **Poster - EuroAnalysis International Conference, Bordeaux 2015**
"Design, Synthesis and Testing of a Selective Sensory Device for Detection of NPS Mephedrone"

- **Poster - Molecular Sensors and Molecular Logic Gates, Bath 2016**
"Detecting Mephedrone in a Simulated Street Sample using Host-Guest Chemistry"

- **Poster - Novel Psychoactive Substances Conferences, Budapest 2016**
"A Selective Sensory Device for NPS Mephedrone"

Awards

- Poster Prize RSC Analytical Research Forum 2013
- Winston Churchill Travel Fellowship, WCMT 2014 - £5000
- Poster Prize Young Modellers Forum 2014
- Santander Research Grant 2014 - £2000
- 1st Prize 3 Minute Thesis competition 2016 - £1000